PONTIFÍCIA UNIVERSIDADE CATÓLICA DO RIO GRANDE DO SUL
FACULDADE DE BIOCIÊNCIAS
PROGRAMA DE PÓS-GRADUAÇÃO EM BIOLOGIA CELULAR E MOLECULAR

THIAGO DE JESUS BORGES

**MECANISMOS DA MODULAÇÃO DA EXPRESSÃO DE MHC II E CD86 EM CÉLULAS DENDRÍTICAS PELA DNAK E A DIMINUIÇÃO DA REJEIÇÃO EM TRANSPLANTES DE PELE**

Porto Alegre
2015

PONTIFÍCIA UNIVERSIDADE CATÓLICA DO RIO GRANDE DO SUL
FACULDADE DE BIOCIÊNCIAS
PROGRAMA DE PÓS-GRADUAÇÃO EM BIOLOGIA CELULAR E MOLECULAR


THIAGO DE JESUS BORGES


**MECANISMOS DA MODULAÇÃO DA EXPRESSÃO DE MHC II E CD86 EM CÉLULAS DENDRÍTICAS PELA DNAK E A DIMINUIÇÃO DA REJEIÇÃO EM TRANSPLANTES DE PELE**

Tese apresentada ao Programa de Pós-Graduação em Biologia Celular e Molecular da Pontifícia Universidade Católica do Rio Grande do Sul como requisito para obtenção do grau de Doutor.


Orientadora
**Profª. Drª. Cristina Beatriz C Bonorino**


Co-orientadora
**Profª. Drª. Ana Paula D de Souza**


Porto Alegre
2015

PONTIFÍCIA UNIVERSIDADE CATÓLICA DO RIO GRANDE DO SUL
FACULDADE DE BIOCIÊNCIAS
PROGRAMA DE PÓS-GRADUAÇÃO EM BIOLOGIA CELULAR E MOLECULAR


THIAGO DE JESUS BORGES

Tese apresentada ao Programa de Pós-Graduação em Biologia Celular e Molecular da Pontifícia Universidade Católica do Rio Grande do Sul como requisito para obtenção do grau de Doutor.


Aprovada em:_____de_____de_____


BANCA EXAMINADORA:


_____
Profª. Drª. Silvia Boscardin – USP


_____
Prof. Dr. Roberto Manfro – UFRGS


_____
Prof. Dr. Moisés Bauer – PUCRS


Porto Alegre
2015

*Science knows no country, because knowledge belongs to humanity, and is the torch which illuminates the world.*

*Louis Pasteur*

# AGRADECIMENTOS

# RESUMO

Células dendríticas (DCs) são as principais células apresentadoras de antígenos e fornecem três sinais principais para a ativação completa das células T. O primeiro sinal consiste na apresentação do complexo peptídeo:MHC; o segundo sinal é a expressão de moléculas co-estimulatórias da família B7, como o CD80 e CD86, e o terceiro consiste no conjunto de citocinas produzidas pelas DCs que irão moldar o tipo de resposta T que será gerada. Uma vez que algum desses dois sinais é interrompido as células T não são ativadas de forma completa e, ainda, podem entrar em anergia ou apoptose. As células T estão envolvidas não apenas em respostas de defesa, mas também em uma série de patologias, e estratégias que visam sua ativação ou inibição vem sendo usadas no manejo dessas doenças. Terapias que visam a inibição do segundo sinal (*checkpoint blockade*) ou a modulação das células T pelas moléculas co-inibitórias tem sido testadas e utilizadas para tumores, autoimunidade e transplantes. Nosso grupo demonstrou que a proteína DnaK (Hsp70 procariótica) de *M. tuberculosis* tem papel imunossupressor em células dendríticas e *in vivo,* podendo diminuir a rejeição de transplantes cutâneos em camundongos. Porém, os mecanismos envolvidos nessa resposta ainda precisam ser elucidados. No presente trabalho, mostramos que a DnaK foi capaz de diminuir a expressão basal de TNF-α, IFN-γ e MCP-1 em DCs de camundongos. Essa modulação foi concomitante com a diminuição de dois fatores de transcrição – C/EBPβ e C/EBPδ – de maneira dependente da via molecular TLR2-ERK-STAT3-IL-10 nas DCs. Além do terceiro sinal, a DnaK pode modular a expressão dos níveis de MHC II (primeiro sinal) e CD86 (segundo sinal) nas DCs, através da indução de uma molécula chave chamada MARCH1. Em um modelo murino de aloenxerto cutâneo, o tratamento local com a DnaK, antes do transplante, prolongou a sobrevida do enxerto e diminuiu a aloimunidade de maneira dependente de MARCH1. A indução de MARCH1 pela DnaK foi dependente da via molecular TLR2-ERK-STAT3-IL-10 nas DCs. Além disso, demonstramos que a DnaK modula exclusivamente um subtipo de DC migratório da pele – as DCs CD103+. Também observamos que esse subtipo de DC é o principal subtipo celular envolvido na rejeição de transplantes de pele, gerando um conceito biológico novo nessa área. Mapeamos os receptores inatos nos quais a DnaK pode se ligar. Testamos dez receptores inatos e vimos que essa proteína não se liga diretamente no TLR2, mas sim nos receptores LOX-1 e Siglec-E, formando o complexo LOX-1/Siglec-E/TLR2. Finalmente, a partir dos dados obtidos nessa tese, formulamos uma composição e um método para a modulação do enxerto antes da realização do transplante, e depositamos uma patente junto ao INPI. Portanto, a DnaK pode tolerizar as células dendríticas através da modulação dos três sinais necessários para a ativação das células T. Acreditamos que essa estratégia pode ser utilizada no tratamento de patologias inflamatórias, incluindo a rejeição a transplantes.

**Palavras-chaves:** DnaK, células dendríticas, MHC II, MARCH1, transplante

# ABSTRACT

Dendritic cells (DCs) are the major antigen-presenting cells. They provide three main signals to fully activate T cells. Signal one is when the complex peptide:MHC (p:MHC) expressed by DC is recognized by T cell receptor; signal two is the expression of co-stimulatory molecules from the B7 family (CD80 and CD86). The third signal consists in the cytokines produced by DCs, which will bias the quality of T cell response. Once one of this signal is blocked/interrupted, T cells are not fully activated. T cells are involved in the eradication of pathogens, but also in the pathogenesis of several disorders and, strategies that modulate signal two are being used to treat these disorders. Novel therapies that inhibit the second signal (checkpoint blockade) or T cell modulation by these molecules have being used/tested to manage tumors, autoimmune disorders and transplant rejection. Our group demonstrated that the *M. tuberculosis* protein DnaK (prokaryote Hsp70) has an immunosuppressive role on DCs, and can suppress rejection in a murine skin allograft model. Nevertheless, the molecular mechanism involved in this response need to be further elucidated. In the present work, we demonstrated that the treatment of murine DC with DnaK could decrease the basal levels TNF-α, IFN-γ and MCP-1 produced by these cells. This modulation was concomitant with a downregulation of the transcription factors C/EBPβ and C/EBPδ in a TLR2-ERK-STAT3-IL-10-dependent way. Beyond the signal three, DnaK could also downregulate the expression of MHC II (signal one) and CD86 (signal theree) on DCs, through the induction of a molecule called MARCH1. We developed an-situ treatment of skin grafts with DnaK prior the transplant. We observed that this treatment prolongs allograft survival with a decreased alloimmunity, and this dependent on MARCH1. The molecular pathway TLR2-ERK-STAT3-IL-10 was required for MARCH1 induction by DnaK. Moreover, we found that DnaK modulates a specific skin migratory DC – the CD103+ DCs. This is the major subset involved in skin allograft rejection. We tested in which innate receptors DnaK could bind and found that DnaK could not bind directly on TLR2, but in the LOX-1 and Siglec-E receptor, in a LOX-1/Siglec-E/TLR2 complex. Finally, from the data obtained we patented a new formulation and method to treat allografts prior the transplantation. Thus, DnaK tolerizes dendritic cells through the modulation of the three signals required to activate T cells. We believe that consists an innovative strategy to treat inflammatory disorders, rejection, asthma and sepsis.

**Keywords:** DnaK, dendritic cells, MHC II, MARCH1, transplant

# LISTA DE FIGURAS

# LISTA DE TABELAS

# LISTA DE SIGLAS

**Ab –** *Antibody;* Anticorpo
**APC** – *Antigen-presenting* cell*;* Célula apresentadora de antígenos
**ASGPR –** *Asialoglycoprotein receptor*
**Batf3** - *Basic Leucine Zipper Transcription Factor, ATF-Like 3*
**BM –** *Bone marrow*; Medula óssea
**BMDC** – *Bone marrow dendritic cell*; Célula dendrítica diferenciada da medula óssea
**C/EBP -** *CCAAT/enhancer binding protein*
**CCR5 –** *C-C chemokine receptor*; Receptor de quimiocina C-C
**CD** – *Cluster of diferentiation;* Grupo de diferenciação
**CIITA** - *MHC class II transactivator*
**CTLA-4 -** *Cytotoxic T-lymphocyte antigen-4*
**CTLs** - *Cytotoxic T lymphocytes;* Linfócitos T citotóxicos
**DCs** – *Dendritic cells;* Células dendríticas
**DC-SIGN -** *Dendritic Cell-Specific Intercellular adhesion molecule-3-Grabbing Non-integrin*
**DEXA -** Dexametasona
**DNA** - *Deoxyribonucleic acid*; Ácido desoxirribonucleico
**FEEL-1** - *Fasciclin, EGF-like, laminin-type EGF-like, and link domain-containing scavenger receptor-1*
**Foxp3** – *Factor forkhead Box P3*
**GM-CSF -** *Granulocyte–macrophage colony-stimulating*
**HMGB-1** - *High mobility group box-1*
**Hsp -** *Heat shock protein;* Proteína de choque térmico
**IFN -** Interferon
**Ig -** Imunoglobulina
**IL –** Interleucina
**iNOS** - *Inducible nitric oxide synthase;* Oxido Nitrato sintase induzivel
**LCs** – *Langerhan's cells*; Células de Langerhans
**LLR –** *Lectin-like receptors*
**LOX-1 -** *Lectin-like Oxidized Low-density Lipoprotein Receptor 1*
**LPS –** Lipopolissacarídeo
**MARCH1 -** M*embrane-Associated Ring Finger 1*
**MDSC** - *Myeloid-derived Suppressor Cell*
**MFI -** *Mean Fluorescence Intensity;* Média da intensidade de fluorescência
**MHC** – *Major histocompatibility complex;* Complexo principal de histocompatibilidade
**mMGL2** - *Mouse macrophage galactose-type C-type lectin 2*
**Mt** – *Mycobacterium tuberculosis*
**MyD** - *Myeloid differentiation primary response*

**NK** – *Natural killer*

**OVA -** Ovalbumina

**PBS** – *Phosphate buffered saline;* Tampão fostato-salino

**PD-1** - *Programmed cell death 1*

**PD-L -** *Programmed death-ligand*

**PGN –** Peptidoglicano

**sHsp –** *Small heat shock protein;* Proteína de choque térmico pequena

**SIGLEC** - *Sialic acid-binding immunoglobulin-type lectins*

**SR** – *Scavenger receptor*

**SREC-I** - *Scavenger receptor expressed by endothelial cell-I*

**TCR** – *T cell receptor;* Receptor da célula T

**TGF** – *Transforming growth factor;* Fator de crescimento transformador

**Th** – *T helper cell;* Célula T h*elper*

**TLR-** *Toll like receptor*; Receptor do tipo Toll

**TNF** - *Tumor necrosis factor;* Fator de necrose tumoral

**Treg** – *Regulatory T cell;* Células T reguladora

**TRIF** - *TIR-domain-containing adapter-inducing interferon-β*

**VCA** – *Vascular composite allograft*

# SUMÁRIO

# 1. INTRODUÇÃO

## 1.1 CÉLULAS DENDRÍTICAS E A GERAÇÂO DE RESPOSTAS T

As células dendríticas (DCs) foram descobertas em 1973 por Ralph Steinman (1). Em 2011, ele recebeu o prêmio Nobel de Fisiologia e Medicina por essa descoberta. As DCs são leucócitos derivados da medula óssea e são distribuídas entre diversos tecidos. Essas células são responsáveis e especializadas em adquirir, transportar, processar e apresentar antígenos às células T, coordenando a resposta adaptativa (2, 3). Por essas características, as DCs são as principais células apresentadoras de antígenos (APCs). Nos tecidos periféricos, as DCs se encontram em um estado imaturo de desenvolvimento e estão sempre monitorando o ambiente, agindo como sentinelas. Uma vez que essas células reconhecem um microrganismo invasor ou algum sinal de dano celular, através de receptores inatos como os receptores do tipo *toll* (*toll-like receptors* – TLRs) ou *scavenger receptors*, elas adquirem esses antígenos estranhos e iniciam sua migração para os linfonodos (2, 3). Essa ligação de sinais de perigo, incluindo produtos microbianos, nos receptores inatos desencadeia a produção de citocinas pro-inflamatórias como a IL-12 e IFN-γ pelas DCs. Durante a migração para o linfonodo, as DCs sofrem um processo de maturação ou ativação. Nesse processo, essas células irão processar os antígenos adquiridos no tecido e apresenta-los em moléculas de MHC de classe I ou II na superfície, em um complexo peptídeo:MHC. Além disso, as DCs aumentam a expressão de moléculas da família B7, como o CD80 e CD86. Portanto, o aumento dos níveis do complexo peptídeo:MHC I ou II, do CD80 e CD86 são referenciados como sinais de maturação das DCs.

No linfonodo as DCs precisam fornecer três sinais para ativar as células T de forma completa. O primeiro sinal ocorre quando o receptor da célula T (TCR) reconhece os antígenos apresentados no MHC, o complexo peptídeo:MHC. O segundo sinal, também denominado co-estimulação, acontece quando o receptor CD28 expresso na célula T é engajado pelas moléculas da família B7, expresso pelas DCs – formando o complexo B7:CD28 (4). O terceiro sinal,

denominado de polarização, é fornecido pelo conjunto de citocinas que as DCs produzem e que irão determina a diferenciação das células T em seus diversos subtipos, como Th1, Th2, Th17, Treg, células CD8 citotóxicas (CTLs) (5), entre outros. Se algum desses sinais é interrompido, as células T não são ativadas de forma completa e, ainda, podem entrar em anergia ou em apoptose (4). Portanto, as DCs podem ser moduladas de acordo com o microambiente no qual estão presentes e, por isso, são consideradas a ponte entre a imunidade inata e adaptativa.

Depois das células T receberem os sinais necessários, elas sofrem uma expansão clonal e migram para os tecidos para combater os agentes invasores ou os danos. À medida que esses antígenos são erradicados, as células T sofrem uma redução em seu número e algumas delas persistem como células de memória específicas ao antígeno. Células T CD8+ são essenciais para a indução direta da morte de células infectadas com vírus e tumores. As células T CD4+ possuem um papel crucial nas respostas imunes: orquestram a resposta contra patógenos e ao dano celular, ajudam as células B a produzirem anticorpos, são responsáveis pela amplificação e manutenção das respostas T CD8+ e regulam a função de macrófagos (6). As células T CD4+ reguladoras (Tregs) regulam e suprimem outras células imunes para ajustar a amplitude e persistência de respostas efetoras, evitando o dano tecidual excessivo e a autoimunidade (7). Porém, esse controle muitas vezes não é perfeito e o desequilíbrio  de respostas mediadas por células T CD4+ do tipo Th1 está associado com varias desordens inflamatórias crônicas, como as doenças autoimunes  (8). Subtipos de células T CD4+, como Th17 e Th1, também possuem um papel crucial na rejeição de enxertos (9).

### 1.1.1 Modulação das células dendríticas para o tratamento de desordens inflamatórias

Os sinais fornecidos pelas DCs moldam o tipo e a qualidade da resposta T gerada frente a um estímulo. Dependendo do receptor inato que vai ser estimulado e engajado, as DCs irão produzir citocinas e moléculas co-estimulatórias diferentes, gerando um tipo de resposta T diferente – pro-inflamatória ou tolerância, por exemplo (10). Uma maneira de modular as

desordens mediadas por respostas T é a modulação desses sinais que as células dendríticas fornecem. O uso de moléculas que modulem o estado de ativação de DCs é uma estratégia promissora que vem utilizada de forma experimental e clinica (11). As DCs tolerizadas são caracterizadas pela baixa produção de citocinas inflamatórias e por uma alta produção de citocinas anti-inflamatórias, como a IL-10 e o TGF-β. A IL-10 produzida pelas DCs pode modular a produção de citocinas, fatores solúveis e a expressão de moléculas de superfície, com consequências na habilidade dessas células iniciarem ou manterem respostas inflamatórias (12). Por exemplo, a IL-10 pode agir de forma autócrina nas DCs, ou ainda inibindo a proliferação e a produção de citocinas inflamatórias pelas células T, além de favorecer a geração de Tregs (12).

Foi demonstrado que as DCs tolerogênicas expressam níveis baixos do MHC II e de moléculas co-estimulatórias, como o CD80 e o CD86 (13-15). Mesmo com baixos níveis de MHC II, essas células conseguem apresentar antígenos a células T específicas. Porém, com a falta dos sinais co-estimulatórios (segundo sinal) não há a ativação e proliferação de células T efetoras (4), incluindo células T aloreativas (16). Os baixos níveis da apresentação de antígeno, a diminuição da co-estimulação e produção de citocinas anti-inflamatórias pelas DCs tolerizadas podem levar à diferenciação das células T em Tregs (17-19). Com isso, as DCs tolerogênicas podem regular respostas imunes inatas e adaptativas (15), incluindo a resposta de células T CD4+ e CD8+ de memória (20, 21). Essas DCs também são mais resistentes à ativação por sinais de perigo via TLRs e podem fornecer sinais indutores de apoptose para células T efetoras (22). Nosso grupo de pesquisa vem utilizando a DnaK (nome da Hsp70 em procariotos) de *M. tuberculosis* para induzir um estado tolerogênico nas DCs (23). Para demonstrar o papel imunossupressor dessa proteína *in vivo*, utilizamos um modelo de aloenxerto cutâneo em camundongos, em que o tratamento *in-situ* com DnaK prolongou a sobrevida do enxerto [(24) – esse tópico será melhor explorado abaixo), de maneira dependente de Tregs. Esta tese investigou a hipótese de que a modulação de DCs é a fonte desse efeito, e buscou determinar os mecanismos pelos quais ocorre essa modulação.

Além disso, varias terapias que visam à inibição do segundo sinal (*checkpoint blockade*) ou a modulação das células T pelas moléculas co-inibitórias tem sido testadas e utilizadas para tumores (25), autoimunidade e transplantes (16). Essas terapias são baseadas no fato de existirem

receptores que fornecem sinais inibitiórios para as células T. Por exemplo, o CTLA-4 (*cytotoxic T lymphocyte antigen-4*) é expresso pelas células T e se liga nas moléculas da família B7, como o CD80 e CD86. Essa via CTLA-4:B7 tem como função regular negativamente a ativação de células T e manter sua homeostase (16). O PD-1 presente nas células T é engajado por seus ligantes PD-L1 ou PD-L2, presente nas APCs. A interação PD-1:PD-L mantém a tolerância periférica (26). Essas vias são utilizadas por tumores e vírus para evadir respostas imunes. O aumento ou a diminuição da sinalização de ambas as vias tem grande potencial terapêutico. Por exemplo, o microambiente tumoral é amplamente tolerizado para evitar o reconhecimento e a erradicação do tumor por células imunes efetoras (27). Foi demonstrado que o uso combinado de anticorpos que inibem essas moléculas (Ipilimumab – anti-CTLA-4 e Nivolumab – anti-PD-1) é uma estratégia muito promissora no tratamento de melanoma (28). Outro exemplo seria o Belatacept, o qual foi desenvolvido com o domínio extracelular do CTLA-4 humano fusionado com uma cauda da cadeia pesada de uma imunoglobulina [CTLA-4Ig (29)]. Essa molécula se liga ao CD80 e CD86 presente nas DCs, inibindo a geração de respostas T efetoras. Porém, testes clínicos que utilizaram esta droga em pacientes com transplantes de rim tiveram resultados inesperados como a maior taxa de rejeição aguda (29). Esse efeito foi devido ao efeito deletério dessa droga nas células Tregs (30, 31), além da falta de inibição de células T de memória específicas a antígenos do doador, as quais são menos dependentes do segundo sinal (32). Contudo, nenhuma dessas terapias explora a diminuição do primeiro sinal, o complexo peptídeo:MHC, sendo esse campo de extremo potencial terapêutico.

A modulação do MHC II pode acontecer através de um controle transcricional ou de modificações pós-translacionais. O transativador CIITA (*MHC class II transactivator*) é o principal regulador transcricional das moléculas de MHC II (33). O CIITA não se liga diretamente ao promotor dos genes do MHC II, porém coordena a atividade de vários fatores de transcrição essenciais para a transcrição do MHC II (34). A expressão do CIITA é sensível à sinalização desencadeada por receptores de interferon (IFN) e TLRs (33), os quais irão aumentar sua expressão, levando ao aumento de MHC II na superfície. Entretanto, o CIITA pode ser regulado negativamente pelo TLR2, o qual vai induzir a expressão de fatores de transcrição da família C/EBP (*CCAAT/enhancer-binding protein*) que inibem a transcrição do CIITA e a expressão de MHC II (35).

Além da regulação da transcrição pelo CIITA, a expressão de MHC II pode ser regulada por modificações pós-translacionais como a ubiquitinação (36). A apresentação de antígenos mediada pelo MHC II é dependente do transporte intracelular das moléculas de MHC. Estas são sintetizadas no reticulo endoplasmático, vão para os lisossomos onde se associam a peptídeos antigênicos fagocitados e degradados previamente e, posteriormente, o complexo peptídeo:MHC é transportado para a membrana celular (37). A ubiquitinação tem um papel crucial no controle do transporte intracelular do MHC II. A molécula de MHC II é composta por uma cadeia α e uma β, e é ubiquitinada em uma lisina citoplasmática presente na cadeia β. Essa lisina é extremamente conservada evolutivamente nos isotipos de MHC II presente em diferentes espécies de vertebrados, mostrando a importância da ubiquitinação na modulação da função do MHC II (38). Duas ligases foram identificadas como sendo capaz de ubiquitinar o MHC II: MARCH1 e MARCH8 (*membrane-associated RING-CH*), sendo MARCH1 a mais estudada. Além do MHC II, MARCH1 também pode ubiquitinar moléculas do sinal co-estimulatório CD86 (39). Quando as DCs são ativadas elas diminuem a expressão de MARCH1, através de um mecanismo regulado por CD83, levando ao aumento de MHC II e CD86 na superfície das células (40). Em contraste, a indução de MARCH1 é induzida pela citocina IL-10 (41), levando ao aumento da ubiquitinação do MHC II e CD86, direcionando essas moléculas para serem degradadas em lisossomos e diminuindo sua expressão na superfície das DCs (38). Foi observado que a expressão de MARCH1 nas DCs de camundongos regula a ativação de células T *in vitro* (39) e é essencial para a geração de Tregs *in vivo* (42). Porém, o papel dessa molécula durante uma resposta inflamatória *in vivo* precisa ser melhor estudado. Estratégias que induzem MARCH1 nas DCs podem apresentar potencial terapêutico em modelos e autoimunidade e transplante, e precisam ser exploradas.

### 1.1.2 Subtipos de células dendríticas

As células dendríticas formam uma população heterogênea de células apresentadoras de antígenos (APCs) que podem desempenhar desencadear respostas imunes deletérias ou protetoras. O melhor entendimento do papel de cada subtipo em desordens inflamatórias é crucial

para aperfeiçoar e desenvolver novas terapias que visam à modulação dessas células. A divisão de células dendríticas em subtipos foi primeiramente proposta nos anos 70, quando se observou que as células de Langerhans (LCs) eram diferentes das DCs do baço, quanto à formação de grânulos Birbeck (feitos de Langerina). Hoje sabemos que a complexidade nos subtipos de DCs é muito maior, e que esses subtipos são definidos com base na expressão diferencial de marcadores de superfície, localização anatômica e função (43). Em camundongos, podemos dividir as DCs em três grandes grupos: DCs plasmocitóides (pDCs), DCs que residem nos órgãos linfoides (DCs residentes ou DCs convencionais, cDCs) e DCs migratórias que estão presentes em tecidos periféricos não-linfoides (DCs migratórias) (44). Em condições inflamatórias, um quarto grande grupo pode surgir quando DCs são formadas a partir de monócitos (mo-DCs ou DCs inflamatórias, iDCs). As DCs residentes podem ser encontradas no baço e linfonodos e são divididas em dois subtipos, baseado na expressão de CD11b e CD8α: subtipo CD11b+ (CD11b+ CD8α-) e CD8α+ (CD11b- CD8α+) (45). Porém, na literatura as DCs residentes são referenciadas basicamente como CD8α- ou CD8α+ (43). As DCs migratórias podem ser encontradas na pele, pulmão, intestino e após serem ativadas, migram para os linfonodos drenantes para apresentarem antígenos para as células T. Podemos dividir as DCs migratórias em CD11b+ ou CD103+ e, no caso do intestino ainda podemos encontrar DCs CD11b+CD103+.

Apesar das DCs compartilharem uma série de características em comum, como o reconhecimento de patógenos e dano celular, cada subtipo possui funções especializadas (46-48). Por exemplo, as pDCs produzem IFN do tipo I em infecções virais (49), enquanto as mo-DCs possuem funções antimicrobianas, produzindo TNF e iNOS durante infecções (50). Além disso, As DCs CD8α+ e CD103+ são especializadas em fazer apresentação cruzada e ativar células T CD8+, enquanto as CD11b+ ativam células T CD4+ naive de maneira mais eficiente (51) .

Por utilizarmos um modelo de aloenxerto cutâneo, vamos nos focar nos subtipos de DCs migratórias da pele. A pele possui três subtipos principais de células dendríticas consideradas migratórias, sendo um epidérmico e dois dermais. As células dendríticas dermais podem ser CD11b$^+$CD103$^-$Langerina$^-$ (DCs CD11b) ou CD11b$^-$CD103$^+$Langerina$^+$ (DCs CD103); as DCs epidérmicas são chamadas de Células de Langerhans (LCs) e são CD11b$^+$CD103$^-$Langerina$^+$ (52) (Tabela 1 e Figura 1). Esses subtipos de DCs possuem capacidades estimulatórias diferentes,

podendo gerar respostas de células T distintas para o mesmo antígeno (46). Por exemplo, Células de Langerhans podem induzir respostas mediadas por células Tregs em um *steady state*, porém induzem células T inflamatórias em um contexto de inflamação (53). As DCs CD103+ compõem um subtipo residente de tecidos periféricos e correspondem à mesma linhagem das DCs CD8α+. Em camundongos, esses dois subtipos dependem do fator de transcrição Batf3 para seu desenvolvimento (54). As DCs dependentes de Batf3 (ou DCs CD103+) desempenham um papel na patogênese de uma série de modelos experimentais como diabetes tipo 1 (55), asma (56) e infecções virais (55). Sob um contexto não inflamatório, essas células podem exercer papéis opostos. Por exemplo, podem induzir tolerância a antígenos circulantes de OVA em linfonodos drenantes renais (57). Também foi visto que as DCs migratórias Langerina+ da pele possuem uma habilidade única em promover respostas mediadas por Tregs in vivo, quando comparadas com as DCs residentes CD8α+ e CD8α- , e com as DCs migratórias CD11b+ (58). Essas células também são especializadas em ativar células T CD8+, por uma via de apresentação cruzada (59). As DCs CD141$^{hi}$ humanas são o subtipo correspondente das DCs CD103+ murinas (60). Essas células, quando isoladas da pele, produzem IL-10 e podem inibir o desenvolvimento da doença do enxerto contra o hospedeiro em um modelo xenoenxerto (61).

**Tabela 1**. Subtipos residentes e migratórios de células dendríticas de camundongos. Baseado em Heath & Carbone, 2013. Nat Immunol.

| Subtipos/Marcadores | CD11c | CD103 | CD11b | XCR1 | B220 | CD4 | CD8 | Langerina (CD207) | DEC205 |
|---|---|---|---|---|---|---|---|---|---|
| pDCs | interm | | | | + | | | | |
| Batf3-dependente (migratórias da derme) | + | + | baixo/- | + | | | - | +/- | + |
| Batf3-dependente (Residentes de baco e linfonodos) | + | +/- | baixo/- | + | | | + | +/- | + |
| CD11b+ DCs (migratórias da derme) | + | - | + | | | | | | + |
| CD11b+ DCs (Residentes de baco e linfonodos) | + | | + | | | +/- | - | | - |
| Células de Langerhans (migratórias da epiderme) | + | - | interm | | | | | + | + |
| Mo-DCs | + | | + | | | | | | + |
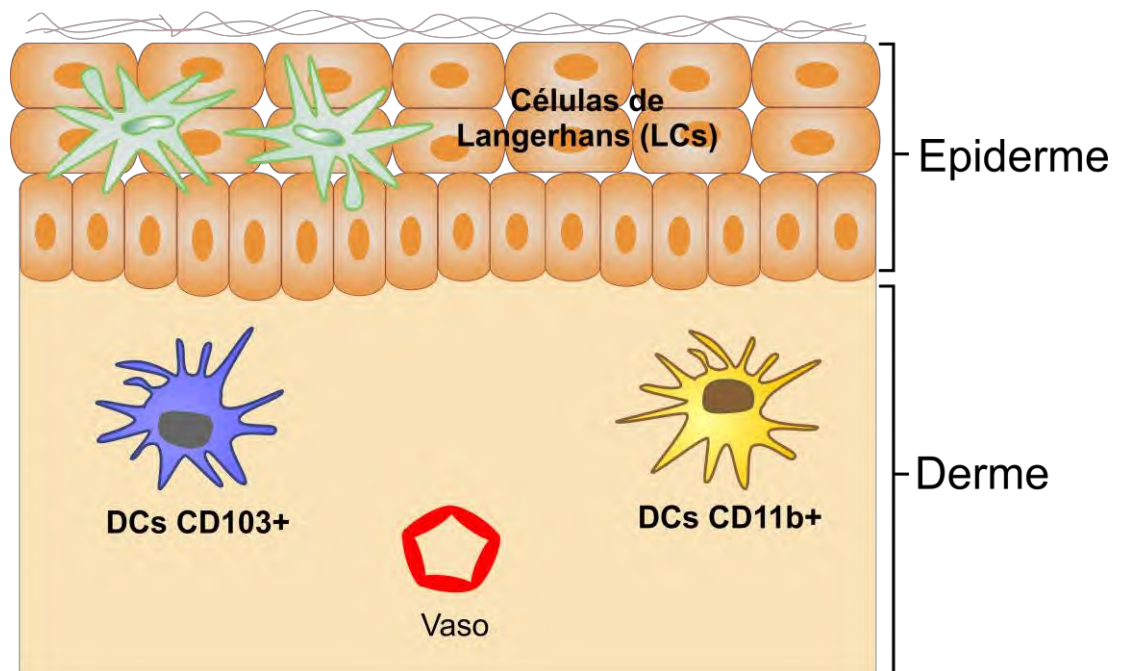
**Figura 1. Subtipos de DCs migratórias da pele.** As Células de Langerhans (LCs) são CD11b$^+$CD103$^-$ Langerina$^+$ e residem na epiderme. Enquanto as DCs CD103+ (CD11b$^-$CD103$^+$Langerina$^+$) e DCs CD11b+ (CD11b$^+$CD103$^-$Langerina$^-$) são dermais.

Flacher e colaboradores demonstraram que DCs dermais Langerina$^+$ podem ativar e induzir respostas mediadas por células T CD8+ na pele, enquanto as LCs influenciam essa resposta negativamente, induzindo tolerância (59). Um estudo demonstrou que as LCs não são necessárias para a rejeição de aloenxertos cutâneos (62), provavelmente porque elas permanecem presas na epiderme do enxerto, não migrando para o linfonodo drenante (63). Apesar de todos esses conhecimentos, os subtipos de DCs que mediam a rejeição ou a tolerância a enxertos estão apenas começando a serem identificados. O papel de cada subtipo das DCs dermais ainda precisa melhor explorado no contexto no transplante de pele. Identificar os diferentes subtipos de DCs dermais envolvidos na resposta alogênica enxertos de pele é essencial para o desenvolvimento de um imunomodulador eficiente que possa ser usado *in-situ* para a modulação das células do doador antes do transplante.

Um dos aspectos que pode determinar qual tipo de resposta cada subtipo de DC irá gerar é o conjunto de receptores inatos que está sendo engajado nessas DCs. Por exemplo, Li e colaboradores demonstraram que a entrega dos mesmos antígenos, tanto próprios como estranhos, às DCs via receptores diferentes, pode gerar respostas T CD4+ opostas. A entrega dos antígenos via o receptor LOX-1 gerou células T CD4+ que produziam IFN-γ e não IL-10. Enquanto que a entrega via um receptor chamado DC-ASGPR favoreceu a geração de células T CD4+ supressoras que eram antígeno-específicas e produziam IL-10 (64). Interessantemente, essas células T CD4+ produtoras de IL-10 eram Foxp3- e os autores sugeriram elas tinham uma origem Th1. Nesse caso, o que determinou o tipo de células T geradas não foi a origem dos antígenos (próprios ou não-próprios), mas o receptor inato que foi engajado na superfície da DC. Em condições fisiológicas, foi proposto que esses receptores inatos podem ser ativados por padrões moleculares presentes nos patógenos ou por moléculas liberadas durante o dano e rompimento celular, como HMGB-1 (*high mobility group box-1*) e as proteínas de choque térmico (Hsps). Porém, foi demonstrado que as Hsps também podem ser secretadas pelas células (65, 66) e que podem modular respostas imunes (23, 67). Esse aspecto será melhor discutido nos itens a seguir.

## 1.2 PROTEÍNAS DE CHOQUE TÉRMICO (HSPS)

A resposta ao choque térmico foi primeiramente descrita em 1962 pelo geneticista italiano Ferruccio Ritossa (68). Posteriormente descobriu-se que essa resposta era mediada por proteínas chamadas proteínas de choque térmico ou estresse [Hsps - (69)]. Elas formam um grupo de proteínas induzidas por estresses celulares como o calor e radiação ionizante, sendo distribuídas de forma ubíqua entre organismos procarióticos e eucarióticos. As Hsps de mamíferos podem ser classificadas em cinco principais famílias de acordo com seu peso molecular: Hsp100, Hsp90, Hsp70, Hsp60 e sHsp (*small heat shock proteins*) e estão presentes no citosol, membrana, núcleo, retículo endoplasmático e mitocôndria da célula (70).

Cada família de Hsps é composta por membros expressos constitutivamente e outros induzidos. Funcionam principalmente como chaperonas moleculares, transportando proteínas entre compartimentos celulares, ajudando no dobramento de proteínas que estão sendo formadas ou no redobramento de proteínas que sofreram danos, protegendo a agregação de outras proteínas, além de direcionar proteínas às rotas de degradação e auxiliar na dissolução de complexos proteicos (71).

Além das funções intracelulares, em 1989, Hightower e Guidon demonstraram que em células neurais, as Hsps poderiam ser liberadas para o meio extracelular (66). Posteriormente, demonstrou-se que as Hsps possuem um papel importante nas interações de sinalização célula-célula. As Hsps possuem um papel imunológico (23, 72), cicatrização de ferimentos (73) e na biologia e metástase de tumores (74). Foi demonstrado que as Hsps são as proteínas mais conservadas e imunogênicas compartilhadas entre mamíferos e microrganismos (75). Por exemplo, a Hsp70 de bactérias e humanos possui um grau de homologia de 50% (76). Nos mamíferos, durante a maioria das respostas inflamatórias e/ou contra doenças infecciosas, são observadas respostas imunes contra as proteínas de choque de calor, tanto do hospedeiro quanto do microrganismo infeccioso. Por exemplo, durante infecções por bactérias, membros bacterianos das famílias da Hsp60 e da Hsp70 (GroEL e DnaK, respectivamente) são alvos comuns da resposta humoral e da resposta imune mediada por células (77-79). Com a observação de que as Hsps procarióticas e eucarióticas possuem um alto grau de homologia, foi proposta a hipótese na qual as Hsps são candidatas potenciais para o mimetismo molecular e muitos de seus peptídeos podem agir, potencialmente, como auto-antígenos (80).

## 1.2.1 Membros da família Hsp70 e seus efeitos imunorreguladores

A família Hsp70 é a mais conservada e a melhor estudada entre as outras famílias de proteínas de choque de calor (81, 82). Sua expressão é induzida nas células expostas ao calor e a uma variedade de outros estímulos estressantes, como espécies reativas de oxigênio, infecção, inflamação, hipóxia e drogas antitumorais (83).

Historicamente, nosso grupo vem estudando os efeitos reguladores da DnaK (Hsp70) de *M. tuberculosis* no sistema imune (23, 24, 84, 85). Um estudo do nosso grupo demonstrou que células do líquido sinovial provenientes de pacientes com artrite foram incubadas com a DnaK por 48 horas. Após esse período, essas células apresentaram uma reversão do perfil inflamatório, uma alta produção de IL-10 e uma diminuição da produção de TNF-α e IFN-γ (84). Em outro estudo realizado pelo nosso grupo, a DnaK (Hsp70) de *M. tuberculosis* bloqueou a diferenciação de DCs diferenciadas a partir de células precursoras da medula óssea (*bone marrow* - BM). Essas BMDCs foram tratadas com DnaK e foi observada uma inibição da maturação dessas células, caracterizada pela geração em cultura de uma população celular com baixa expressão de MHC II e CD86. Além disso, essas células apresentaram uma grande produção de IL-10, principal citocina anti-inflamatória (85). Esse resultado indicou que DCs tratadas com a DnaK apresentam um fenótipo tolerogênico e, *in vivo*, poderiam favorecer a diferenciação de células Tregs. No meu trabalho de mestrado, demonstramos que a DnaK suprime a rejeição aguda em dois modelos de aloenxerto cutâneo. Quando camundongos BALB/c (H-2$^d$/I-A$^d$) são injetados via subcutânea com células do melanoma B16F10 (H-2$^b$/I-A$^b$), uma aloreação inflamatória rejeita o tumor imediatamente. Após doze dias, as células tumorais não são mais visíveis na pele do animal. Contudo, se as mesmas células forem injetadas em presença da DnaK o tumor cresce significativamente e ainda é visível após doze dias. Além disso, foi detectada uma grande infiltração de células Tregs no tecido tumoral, demonstrando que a DnaK foi capaz de induzir um microambiente tolerogênico (24).

Para excluir a possibilidade da aceitação do tumor na presença da DnaK ser devido a outros mecanismos imunossupressores apresentados pelos tumores no microambiente tumoral (27), testamos o efeito imunossupressor da DnaK em um modelo de transplante não tumoral. Foi utilizado um modelo murino bem estabelecido e estudado de aloenxerto cutâneo (86). Nesse modelo, transplantamos peles de camundongos C57Bl/6 (H-2$^b$/I-A$^b$) em receptores BALB/c (H-2$^d$/I-A$^d$). Os enxertos foram tratados com DnaK de uma maneira inovadora: foram embebidos por 1h à 4°C em uma solução contendo a proteína, mimetizando a utilização de uma solução de preservação. Esse tratamento *in-situ* foi capaz de melhorar a sobrevida dos aloenxertos cutâneos, inibindo a rejeição aguda em um mecanismo dependente de Tregs (24).

Outros grupos verificaram que membros da família da Hsp70 também eram capazes de induzir respostas anti-inflamatórias e imunossupressoras em modelos inflamatórios animais, como por exemplo, a proteção contra a artrite pode ser proporcionada através de pré-imunizações com a DnaK (Hsp70) de *M. tuberculosis* (87-89). Além disso, a Hsp70 murina foi capaz de proteger os animais contra modelos de colite experimental (90) e de fibrose pulmonar (91). Também foi observado que o aumento da expressão dessa proteína levou a uma proteção em diferentes modelos de injúria no sistema nervoso (92). Chalmin e colaboradores demonstraram, em um modelo murino, que células tumorais liberam moléculas de Hsp72 associadas à exossomos, resultando na ativação das funções supressoras das MDSCs. Os autores viram que esse efeito foi dependente de TLR2 e MyD88 e independente de TLR4 e Trif (93). Essa dependência de TLR2 é corroborada pelo fato de que vem sendo demonstrado que esse receptor é frequentemente utilizado para  induzir a produção de IL-10 (94-97), além de ser importantíssimo na indução de respostas inflamatórias contra patógenos (98, 99). O fato de membros extracelulares da família Hsp70 induzirem IL-10 em diferentes sistemas suporta a ideia de que o TLR2 pode ter um papel importante na via de sinalização desencadeada pela DnaK em DCs.

A modulação de células imunes por membros extracelulares da família da Hsp70 começa pela ligação dessas proteínas em receptores de superfície inatos. Alguns estudos analisaram a interação da Hsp70, disponível no meio extracelular ou presente na porção extracelular da membrana plasmática, com receptores presentes na superfície de células imunes. Por exemplo, foi descrito que a Hsp70 murina ou humana poderiam ligar-se a receptores como o TLR2 e 4 (100), CD14 (101), CD91 (102), LOX-1 (103) e desencadear respostas pro-inflamatórias. Para a DnaK especificamente, alguns estudos reportam que ela poderia ligar-se a receptores como o CD40 (104), CCR5 (105) e DC-SIGN (106).   Porém, pelo menos em parte, esses efeitos foram associados com a contaminação da proteína por LPS ou outros compostos microbianos (107, 108). Isso porque os efeitos inflamatórios da Hsp70 sumiram quando o LPS foi cuidadosamente removido da proteína (109, 110). Por outro lado, a Hsp70 vem sendo utilizada como vacina para o combate de tumores (111, 112). Nesses estudos, a Hsp70 não induziu uma resposta inflamatória inata nas DCs, sugerindo que as endotoxinas não estavam presentes. A Hsp70 pode facilitar o processamento e a apresentação de antígenos tumorais fusionados com ela, gerando respostas

mediadas por células T CD8+ efetoras (113, 114). A Hsp70 associada a antígenos tumorais pode ligar-se a receptores endocíticos presentes na superfície das células dendríticas, modulando essas células para um fenótipo maduro, capaz de fazer apresentação cruzada (antígenos capturados no meio extracelular são apresentados no MHC I), gerando uma resposta T CD8+ efetora e diminuindo o tamanho tumoral (115). Uma das possíveis explicações para esses efeitos dicotômicos é o fato desses trabalhos não utilizarem a mesma fonte de proteína, ou proteínas recombinantes produzidas em diferentes sistemas experimentais. Outra possível explicação seria a natureza dos receptores inatos que essas proteínas podem se ligar e os complexos que esses receptores formam entre si. Esse campo continua sendo controverso e um pouco obscuro no campo das Hsps e precisa melhor elucidado (23). Um dos objetivos dessa tese foi investigar receptores inatos aos quais a DnaK de *M. tuberculosis* poderia se ligar, e se isso estaria envolvido na resposta anti-inflamatória que ela desempenha.

A necessidade do aprofundamento no entendimento sobre a dinâmica celular e os mecanismos moleculares envolvidos no efeito imunomodulador da DnaK é essencial para a confirmação do papel imunossupressor exercido por essa proteína nas células dendríticas e na modulação da rejeição cutânea. Acreditamos que provavelmente seu efeito é local evitando que o receptor do transplante não entre em um quadro de imunossupressão sistêmica causada pelos fármacos administrados atualmente (116, 117).

## 1.3 TRANSPLANTE DE PELE

### 1.3.1 Contexto histórico

Na década de 40, vítimas com queimaduras sofridas devido a ataques aéreos na 2ª Guerra Mundial motivaram o biólogo Sir Peter Medawar (ganhador do prêmio Nobel de Fisiologia e Medicina de 1960) em seus famosos estudos sobre a imunologia de transplantes. Buscando entender os mecanismos da rejeição a transplantes cutâneos, ele observou que coelhos rejeitavam enxertos cutâneos de outros indivíduos mais rapidamente do que se os animais fossem re-transplantados com um enxerto do mesmo doador (118).

Em 1953, Billingham, Brent e Medawar descreveram, em camundongos, a tolerância imunológica adquirida a aloantígenos (119). Esse artigo é considerado um marco na história da imunologia dos transplantes. No ano seguinte, a equipe lidera por Joseph Murray (ganhador do prêmio Nobel de Fisiologia e Medicina de 1990) realizou com sucesso, no antigo Hospital Peter Bent Brigham, hoje Hospital Brigham and Women's, o primeiro transplante renal entre gêmeos idênticos (120). Nesse procedimento, Richard H., o receptor de 24 anos, recebeu enxertos cutâneos de seu irmão e doador antes do transplante renal. Depois de algum tempo, os enxertos foram biopsados e verificou-se que os tecidos de doador e receptor eram compatíveis, sendo os irmãos gêmeos monozigóticos. Portanto, podemos dizer que tanto experimentalmente como na clinica, o campo dos transplantes começou com transplantes de pele.

O transplante de pele alogênico visa o tratamento de pessoas que sofreram grandes queimaduras e perdas cutâneas (121). Além disso, esse tipo de transplante está envolvido em transplantes reconstrutivos, como transplante de membros e face. O primeiro transplante reconstrutivo tornou-se realidade em 1998, na França, com o primeiro transplante de mão bem sucedido (122). Em 2005, também na França, ocorreu o primeiro transplante de face do mundo, e até o presente um total de 28 pacientes foram submetidos a esse procedimento (123).

## 1.3.2 Base celular e molecular da rejeição de pele

O transplante reconstrutivo é chamado de *vascularized composite allograft* (VCA) e envolve o transplante de vários tecidos como pele, ossos, vasos, nervos e tecidos conjuntivos. A pele é um tecido altamente imunogênico, sendo a rejeição ao transplante de pele a mais agressiva dentre as que ocorrem em todos os transplantes, incluindo os de órgãos sólidos (124, 125). A rejeição de pele é resultado de uma série coordenada e complexa de interações envolvendo células do sistema imune inato e adaptativo (126). Essas interações levam a uma resposta inflamatória potente, a qual irá culminar na destruição das células do doador e rejeição do enxerto (125).

Células dendríticas (DCs) são responsáveis pela iniciação da resposta imune adaptativa. Na rejeição de pele, as DCs do doador [os clássicos leucócitos passageiros - (125)] são ativadas inicialmente pela inflamação e injúria isquêmica do tecido e migram da pele para o linfonodo drenante do enxerto, através de vasos linfáticos (127). No linfonodo drenante, as DCs da pele fornecem sinais suficientes para a ativação de células T. Esses sinais consistem na apresentação de aloantígenos em moléculas de MHC (complexo peptídeo:MHC) e em sinais co-estimulatórios da família B7. O complexo peptídeo:MHC ira ser reconhecido pelo receptor de célula T (TCR) e as moléculas co-estimulatórias como CD80 e CD86 irão ligar-se ao receptor CD28 presente nas células T. Após o reconhecimento desses dois sinais, as células T são ativadas e irão exercer suas funções efetoras. A base molecular da rejeição está na habilidade das células T reconhecerem versões polimórficas de uma gama de proteínas, nesse caso, aloantígenos provenientes de um organismo geneticamente diferente do receptor. No momento em que as células T específicas reconhecerem esses aloantígenos, elas irão proliferar, diferenciar-se em células efetoras, e migrar para o local do enxerto, onde irão promover a destruição do tecido (rejeição) (128). Foi observado, em um modelo de aloenxerto cutâneo em camundongos, que no sexto dia após o transplante, células T efetoras (CD4$^+$ e CD8$^+$) começam a migrar lateralmente do tecido adjacente para o enxerto (63). Finalmente, no dia 10 após o transplante, células T CD8+ destroem as células estranhas do doador, levando à necrose do tecido enxertado e aos estágios finais da rejeição.

A interação direta das células dendríticas do doador com as células T do receptor é chamada de via direta do aloreconhecimento, e ocorre nos primeiros dias após o transplante e esta associada com a rejeição aguda. Portanto, inibir o aumento da expressão de MHC e de moléculas co-estimulatórias nas células dendríticas pode afetar o desfecho da resposta aloimune e melhorar a sobrevida do enxerto. Essa estratégia inovadora precisar melhor explorada e é um dos objetivos dessa tese.

### 1.3.3 Células dendríticas e a indução de tolerância a enxertos

A tolerância a enxertos ideal seria um estado no qual o órgão do doador é aceito sem uma terapia imunossupressora crônica, enquanto o restante do sistema imune é mantido intacto. Deste modo, a falta de uma resposta patológica aos aloantígenos seria específica, e o receptor seria capaz de responder a microrganismos patogênicos e danos. A tolerância não implica na falta de respostas imunes. Na verdade, há evidencias de mecanismos imunorreguladores ativos, os quais podem operar para manter a tolerância aos enxertos (129).

Um desses mecanismos é mediado por DCs tolerogênicas. Apesar das DCs serem importantes para a geração de respostas de células T efetoras, elas também podem gerar respostas anti-inflamatórias. Uma vasta literatura demonstrou que essas DCs tem o potencial de diminuir a aloimunidade e promover a tolerância a transplantes em modelos animais (15, 130). Em transplantes, diferentes estratégias vêm sendo utilizadas, como a administração, antes do transplante, de DCs tolerizadas do doador ou DCs do receptor tolerizadas e pulsadas com antígenos do doador (131-133). O maior risco dessas estratégias é a sensibilização do receptor a antígenos do doador, levando a produção de aloanticorpos e a uma rejeição mediada por anticorpos, a qual foi documentada em estudos anteriores (134, 135). O mecanismo potencial pelo qual as DCs podem induzir tolerância envolve a diminuição direta de células T reativas a antígenos do doador, a geração de células Tregs especifica a antígenos do doador. Outro mecanismo seria a promoção de tolerância nas DCs do receptor. Isso ocorre quando DCs do receptor fagocitam DCs tolerizadas do doador e apresentam seus antígenos para as células T em um microambiente imunossupressor (136, 137).

A terapia celular utilizando DCs tolerizadas possui uma série de obstáculos como a necessidade da expansão *ex-vivo* dessas células, o risco de desenvolvimento de mutações, a falta de padronização de qual subtipo de DC, qual fonte do antígeno do doador e o tempo ideal e o sitio de injeção no paciente. A modulação *in-situ* das DCs um pouco antes do transplante tem o potencial de ser uma estratégia mais simples e efetiva para promover a tolerância aloespecífica. Por exemplo, se conseguirmos diminuir a expressão de moléculas co-estimulatórias e aumentar as moléculas co-inibitórias nas DCs do doador, iremos suprimir a ativação das células T no linfonodo drenante, podendo levar as células T a apoptose, anergia e/ou a geração de células

Tregs (13). Além disso, o desenvolvimento de moléculas que alteram o fenótipo das DCs *in-situ* e sejam clinicamente aplicáveis é muito importante para desenvolvimento desse campo. O uso de vesículas provenientes de células apoptóticas ou exossomos derivados de APCs imaturas foram propostos para a geração de DCs tolerizadas, porem se observou algumas limitações como a dificuldade de preservação e armazenamento dos leucócitos apoptóticos e o desafio de gerar quantidade suficiente de exossomos para a administração sistêmica (131). Ainda, as DCs se comunicam de forma bidirecional com outras células do sistema imune como células T e células *natural killer* (NK). Sua modulação pode ser fundamental na indução de tolerância a enxertos cutâneo e fundamental para a modulação bidirecional de outros tipos celulares imunes. Assim, os transplantes oferecem uma oportunidade para estudar a manipulação das DCs antes ou depois do início da resposta imune, e estas são consideradas alvos terapêuticos promissores no manejo da rejeição a enxertos, visando à promoção de uma tolerância específica para o doador.

Nossa hipótese de trabalho é que a DnaK consegue tolerizar células dendríticas murinas, modulando a expressão de MHC II e CD86, diminuir a produção de citocinas inflamatórias e induzir a produção de IL-10. Quando embebemos os enxertos cutâneos em uma solução com a DnaK as células dendríticas do doador vão ser moduladas, chegando no linfonodo drenante com um fenótipo tolerizando, induzindo uma resposta aloreativa mais branda e promovendo uma maior sobrevida do enxerto.

# 2. OBJETIVOS

## 2.1. OBJETIVO GERAL

Analisar os mecanismos celulares e moleculares pelos quais a DnaK de *Mycobacterium tuberculosis* diminuiu a expressão de MHC II e desempenha seu efeito imunossupressor em células dendríticas, prolongando a sobrevida de aloenxertos cutâneos.

## 2.2. OBJETIVOS ESPECÍFICOS

**2.2.1.** Verificar os mecanismos pelos quais a DnaK diminui a expressão do MHC II nas células dendríticas, via CIITA e suas moléculas relacionadas ou via MARCH1;

**2.2.2.** Elucidar a via molecular pela qual a DnaK modula as células dendríticas;

**2.2.3.** Verificar em quais subtipos de células dendríticas a DnaK exerce seus efeitos;

**2.2.4.** Testar o papel da IL-10 nos efeitos induzidos pela DnaK;

**2.2.5.** Testar o papel do TLR2 na imunossupressão mediada pela DnaK;

**2.2.6.** Analisar as vias celulares e moleculares pelas quais o tratamento *in-situ* com a DnaK pode prologar a aceitação de enxertos cutâneos;

**2.2.7.** Identificar os receptores inatos nos quais a DnaK pode se ligar.

# 3. JUSTIFICATIVA

A nova geração de terapias para transplantes e tumores visa modular a co-estimulação de células T, o segundo sinal. Porém nenhuma terapia foca hoje desenvolver moléculas que consigam modular o primeiro sinal (MHC) ou ainda os dois. Esse estudo irá consolidar nosso tratamento como uma estratégia inovadora para modular tanto o primeiro quanto o segundo sinal, os quais são necessários para a ativação de células T patogênicas. Com essa modulação poderemos utilizar essa proteína na tentativa de tratar ou amenizar a inflamação que causa doenças autoimunes ou a rejeição a enxertos. Uma vez que provavelmente seu efeito é local, isso poderá minimizar uma série de efeitos adversos causados pelos fármacos imunossupressores administrados atualmente.

Finalmente, investigar os receptores inatos aos quais a DnaK pode se ligar auxilia no melhor entendimento do papel das Hsps extracelulares e sua relação com o sistema imune. Esse campo padece de uma grande controvérsia e descrença, porém estudos bem controlados podem ser cruciais para elucidar a dinâmica de intercomunicação celular dessas proteínas tão importantes.

# CAPÍTULO 1

## Extracellular Hsp70 inhibits pro-inflammatory cytokine production by IL-10 driven down-regulation of C/EBPβ and C/EBPδ

**Autores:** Thiago J. Borges, Rafael L. Lopes, Nathana G. Pinho, Felipe D. Machado, Ana Paula D. Souza e Cristina Bonorino

**Situação:** Publicado

**Revista:** *International Journal of Hyperthermia*

**Referência:** *International Journal of Hyperthermia.* 2013 Aug;29(5):455-63.

**Website:** http://www.tandfonline.com/doi/full/10.3109/02656736.2013.798037#.Vj96bPmrTIU

**Motivação:** Esse trabalho foi realizado no Laboratório de Biologia Celular, na PUCRS. Nele exploramos por quais mecanismos a Hsp70 de *M. tuberculosis* (DnaK) diminuiu os níveis basais da produção de TNF-α, IFN-γ e MCP-1 em células dendríticas derivadas da medula de camundongos. Ele surgiu da tentativa de mapear por quais vias a DnaK diminuía a expressão de MHC II, com a análise de moléculas como o CIITA, C/EBPβ e C/EBPδ.

RESEARCH ARTICLE

# Extracellular Hsp70 inhibits pro-inflammatory cytokine production by IL-10 driven down-regulation of C/EBPβ and C/EBPδ

Thiago J. Borges, Rafael L. Lopes, Nathana G. Pinho, Felipe D. Machado, Ana Paula D. Souza and Cristina Bonorino

School of Biosciences and Biomedical Research Institute, Pontifícia Universidade Católica do Rio Grande do Sul, Av. Ipiranga, 6690, Porto Alegre, Rio Grande do Sul, Brazil

## Abstract

*Purpose*: Extracellular Hsp70 has anti-inflammatory potential, demonstrated in different models of inflammatory diseases. We investigated probable mechanisms used by Hsp70 to down-regulate pro-inflammatory cytokines.

*Materials and methods*: We analysed cytokine mRNA levels in bone marrow-derived murine dendritic cells treated with Hsp70, lipopolysaccharide (LPS) and peptidoglycan (PGN) or OVA (an irrelevant protein control), hypothesising that this was mediated by C/EBPβ and C/EBPδ transcription factors. We also tested the involvement of TLR2, IL-10, ERK and STAT3, using genetically deficient mice and pharmacological inhibitors.

*Results*: C/EBPβ and C/EBPδ levels were inhibited in bone marrow derived dendritic cells (BMDCs) treated with Hsp70, and that correlated with inhibition of TNF-α, IFN-γ and MCP-1. Such inhibition was not observed in TLR2 or IL-10 knockout mice, and was also abrogated upon pretreatment of cells with ERK and JAK2/STAT3 inhibitors.

*Conclusions*: C/EBPβ and C/EBPδ transcription factors are inhibited by Hsp70 treatment, and their inhibition occurs via the TLR2-ERK-STAT3-IL-10 pathway in BMDCs, mediating the anti-inflammatory effects of Hsp70.

## Introduction

The heat shock protein 70 (Hsp70) is a ubiquitously expressed protein in cells following exposure to heat, UV radiation and other stressors [1]. Hsp70 has been demonstrated to have anti-inflammatory and protective effects in diverse mouse models of inflammation [2]. For example, treatment with Hsp70 whole protein or Hsp70 peptides can prevent arthritis in animal models [3–6] in an IL-10-dependent manner [7]. Hsp70 can also delay acute rejection in tumour and tissue allograft models [8] and protect mice against dextran sulphate sodium (DSS)-induced colitis [9].

We have previously observed that treatment of synovial cells from arthritis patients with mycobacterial Hsp70 not only induced IL-10 production by these cells, but also led to the inhibition of both IFN-γ and TNF-α production in these cells, as well as in healthy control monocytes [10].

Dendritic cells (DCs) are the major antigen-presenting cells (APCs), playing a crucial role in immunity and tolerance [11,12]. These cells uptake antigens in peripheral tissues, migrate to draining lymph nodes (dLNs) through lymphatic vessels, and present antigens to T cell lymphocytes [13,14]. DCs can be found in synovium of arthritis patients, where

they are involved in arthritis pathogenesis [15]. These cells are involved in maintenance and progression of arthritis, presenting arthritogenic antigens to T cells and producing pro-inflammatory cytokines, such as TNF-α, IL-1 and IL-6 into the joint [16]. Hsp70 was found to inhibit maturation of murine bone marrow derived dendritic cells (BMDCs) and induce IL-10 production *in vitro* [10,17]. Nevertheless, the molecular pathways involved in this process were not elucidated.

In DCs, inflammatory cytokines are released following inflammatory stimuli [18]. NF-κB is a transcription factor that plays a key role in the induction of pro-inflammatory cytokines [19]. Under a condition without inflammation, NF-κB is maintained inactive in the cytoplasm as complex with its inhibitor IκBα (NF-κB/IκBα complex). In an inflammatory state, IκBα is degraded and NF-κB is liberated to translocate into the nucleus and direct the transcription of pro-inflammatory genes [20]. Hsp70 can prevent lipopolysaccharide (LPS)-induced production of inflammatory cytokines by interfering with the NF-κB-dependent transcription of cytokines [21]. Overexpression of Hsp70 in human mononuclear cells prevents LPS-induced NF-κB p65 nuclear translocation into the nucleus [22], potentially inhibiting the downstream induction of pro-inflammatory cytokines by LPS. It was suggested that Hsp70 stabilise the NF-κB/IκBα complex by the inhibition of IκBα degradation [23].

Correspondence: Cristina Bonorino, Cellular and Molecular Biology Department and Biomedical Research Institute. Av. Ipiranga, 6690 – 2nd floor. Porto Alegre, RS 90680-001, Brazil. Tel: 55 51 3320 3000. Fax: 55 51 3320 3312. E-mail: cbonorino@pucrs.br

Another group of transcription factors that are important for pro-inflammatory cytokines production comprise the CCAAT/enhancer-binding proteins (C/EBPs). These transcription factors compose a family involved in several aspects of cellular functions, such as proliferation, differentiation and cytokine production [24]. C/EBPβ and C/EBPδ were demonstrated to be important for induction of inflammatory cytokines, such as TNF-α and IL-6, in TLR-stimulated macrophages [25], and both C/EBPβ and C/EBPδ mRNA and protein levels have been demonstrated to be induced upon inflammatory stimuli [26]. Upon LPS stimulation, cells from C/EBPβ knockout (KO) mice can express pro-inflammatory cytokines normally, because of the compensatory expression of C/EBPδ, suggesting that these two members of C/EBP family seem to have overlapping roles [27].

In this study we investigated mechanisms by which Hsp70 can down-regulate basal levels of pro-inflammatory cytokines in BMDCs, and asked whether this is mediated by C/EBPβ or C/EBPδ transcription factors. Our results indicate that Hsp70 decreases basal levels of TNF-α, IFN-γ and MCP-1 cytokines in BMDCs concomitantly with down-regulation of C/EBPβ and C/EBPδ. Furthermore, TNF-α, IFN-γ and MCP-1 impairment, as well as C/EBPβ and C/EBPδ inhibition depend on a TLR2-ERK-STAT3-IL-10 cascade.

## Materials and methods

### Animals

Female C57Bl/6 mice were purchased from FEPPS (Rio Grande do Sul, Brazil). C57Bl/6 TLR2$^{-/-}$ mice were kindly provided by João Santana da Silva (University of São Paulo, Brazil). 129SV wild type (WT) and IL-10$^{-/-}$ mice were kindly provided by Ana M.C. Faria (Federal University of Minas Gerais, Belo Horizonte, Brazil). All mice were used between 6–10 weeks of age and housed in individual and standard mini-isolators (Tecniplast, Buguggiate, Varese, Italy) in a specific pathogen free facility (School of Biosciences, Pontifícia Universidade Católica do Rio Grande do Sul (PUCRS)) with free access to water and food. All procedures were previously reviewed and approved by the Ethics Committee for the Use of Animals of the University (CEUA-PUCRS) under protocol ID CEUA 08/00048.

### Protein purification and LPS extraction

Recombinant mycobacterial Hsp70 was produced in XL1-blue *Escherichia coli* as described previously [17]. Briefly, it was purified according to Mehlert and Young [28], and triton X-114 was used to remove LPS, according to the method described in Aida and Pabst [29]. Contaminating Triton X-114 was removed by incubating overnight with Bio-Beads® (Bio-Rad, Hercules, California, United States) at 4°C with agitation. Protein concentration was determined using a Qubit® Protein Assay Kit and the Qubit® Fluorometer (both purchased from Invitrogen, Eugene, OR).

### Bone marrow dendritic cells cultures

Dendritic cells were differentiated from bone marrow of C57Bl/6 WT mice or TLR2$^{-/-}$ and 129 WT or IL-10$^{-/-}$ mice

with GM-CSF and IL-4 (both purchased from Peprotech, Rocky Hill, NJ), as described by Inaba et al. [30]. Cells were cultured in 24-well plates in medium AIM-V® (Gibco, Grand Island, NY). On the fifth day of culture, BMDCs were incubated with either 30 μg/mL of Hsp70, 30 μg/mL of OVA (Sigma, St. Louis, MO), 500 ng/mL of LPS (Sigma) or 10 μg/mL of peptidoglycan (PGN) (Sigma) for 24 h and total RNA was extracted. The supernatant was collected and used for cytokine analysis. For ERK inhibition, BMDCs were treated with 30 μM of selective inhibitor PD98059 (Cayman, Ann Arbor, MI) for 60 min prior to Hsp70 stimulation. To inhibit the JAK2/STAT3 pathway we used 50 μM of AG490 inhibitor (Sigma) for 60 min prior to stimulation.

### Cytokine measurement

Cytokines present in BMDC supernatants were measured using a CBA mouse inflammation kit (BD Biosciences, San Diego, CA), according to manufacturer's instructions. Samples were analysed by flow cytometry using a FACSCanto II and FACSDiva software (both from BD Biosciences). Cytokine concentrations were obtained using the FCAP software (version 1.01, BD Biosciences).

### Real time qPCR

Total RNA was isolated from BMDC cultures using an RNAeasy kit (Qiagen, Germantown, MD) according to manufacturer's instructions. The concentration of the purified total RNA samples was measured using a Qubit® RNA assay kit and the Qubit® fluorometer (both purchased from Invitrogen). An aliquot of 50 ng of RNA was reverse transcribed with 100 U of Sensiscript (Qiagen). cDNA concentrations were measured using Qubit® dsDNA HS assay kit and the Qubit® fluorometer (purchased from Invitrogen). In a final volume of 10 μL, 8 ng of cDNA was amplified using the following Taqman® gene expression assays (Applied Biosystems, Foster City, CA): Cebpb (Mm00843434_s1), Cepbd (Mm00786711_s1) and β-actin (4352933E). Real-time qPCR was performed with a StepOne™ real-time PCR system (Applied Biosystems). The relative mRNA levels were calculated using the comparative $C_t$ method [31]. The housekeeping gene β-actin was used as a normaliser. Non-treated BMDCs served as a reference for Hsp70-, OVA-, PGN- or LPS-treated BMDCs.

## Results

### Hsp70 treatment results in decreased basal levels of IFN-γ, TNF-α and MCP-1 in BMDCs with concomitant C/EBPβ and C/EBPδ down-regulation

To determine whether Hsp70 treatment could modulate pro-inflammatory cytokines in BMDCs, DCs differentiated from murine bone marrow were treated with Hsp70, OVA (negative control) or LPS for 24 h. Subsequently, IFN-γ, TNF-α and MCP-1 protein levels were measured in the supernatant by flow cytometry. As expected, stimulation with LPS increased the production of IFN-γ, TNF-α and MCP-1 when compared with OVA (Figure 1A–C). Interestingly, we found that Hsp70 treatment decreased basal levels (BMDCs treated with OVA) of the analysed cytokines (Figure 1A–C).
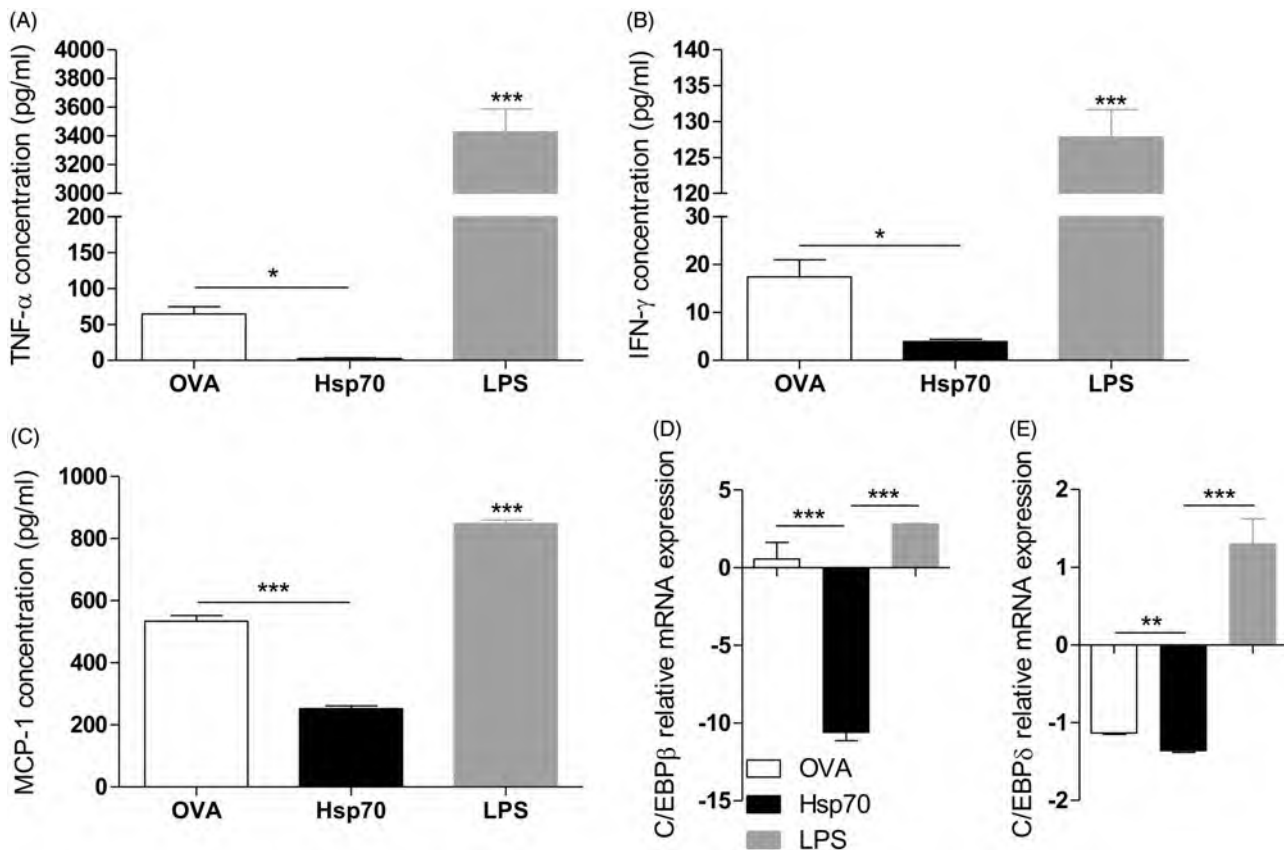
Figure 1. Hsp70 treatment decreases basal levels of TNF-$\alpha$, IFN-$\gamma$, MCP-1 and down-regulates C/EBP$\beta$ and C/EBP$\delta$. BMDCs were treated with OVA (30 $\mu$g/mL), Hsp70 (30 $\mu$g/mL) or LPS (500 ng/mL) for 24 h. Supernatants were analysed for (A) TNF-$\alpha$, (B) IFN-$\gamma$, (C) MCP-1 using a CBA mouse inflammation kit. (D) C/EBP$\beta$ and (E) C/EBP$\delta$ expression evaluation by qPCR in BMDCs treated as described in A. $\beta$-actin was used as a normaliser as described in Materials and methods. *$p < 0.05$; **$p < 0.01$; ***$p < 0.001$. Experiments were performed three times in triplicates.

Because C/EBP$\beta$ and C/EBP$\delta$ are transcription factors that are largely associated with the production of pro-inflammatory cytokines, we tested the hypothesis that C/EBP$\beta$ and C/EBP$\delta$ modulation could be involved in this effect mediated by Hsp70. mRNA levels of C/EBP$\beta$ and C/EBP$\delta$ in BMDCs treated as described above were analysed by qPCR, and while LPS treatment induced an increase in C/EBP$\beta$ and C/EBP$\delta$ expression, Hsp70 treatment led to down-regulation of C/EBP$\delta$ (Figure 1D) and C/EBP$\delta$ (Figure 1E). These data suggested that the decrease in basal levels of IFN-$\gamma$, TNF-$\alpha$ and MCP-1 was related to the down-regulation of C/EBP$\beta$ and C/EBP$\delta$ transcription factors.

### Down-regulation of C/EBP$\beta$, C/EBP$\delta$ and IFN-$\gamma$, TNF-$\alpha$ and MCP-1 inhibition by Hsp70 is dependent on TLR2 expression

TLR2 has been associated with Hsp70-induced suppressive effects in MDSCs, when Hsp70 release in tumour derived-exosomes activated STAT3 in a toll-like receptor (TLR)2-dependent manner in myeloid-derived suppressor cells (MDSCs) [32]. Zymosan, Pam3Cys and Vitamin D3, which are TLR2 ligands, have been described to have anti-inflammatory effects in DCs [33,34] and tolerance in a type 1 diabetes model [35]. In order to further investigate the molecular mechanisms involved in the observations described above, we analysed whether TLR2 was required for the anti-inflammatory Hsp70 effects.

BMDCs from WT or TLR2 KO mice were treated for 24 h with OVA, Hsp70, PGN (a TLR2 agonist), or left unstimulated. After this period, IFN-$\gamma$, TNF-$\alpha$ and MCP-1 protein levels were measured in the supernatant by flow cytometry. C/EBP$\beta$ and C/EBP$\delta$ mRNA levels were analysed by qPCR.

WT PGN-treated cells exhibited a higher production of IFN-$\gamma$, TNF-$\alpha$ and MCP-1 when compared with cells lacking TLR2 (Figure 2A–C). WT BMDCs treated with Hsp70, however, presented an inhibition of IFN-$\gamma$, TNF-$\alpha$ and MCP-1 production when compared with OVA. However, the production of TNF and IFN was only partially recovered in TLR2 KO BMDCs treated with Hsp70 (Figures 2A and 2B), while MCP-1 production in TLR2 KO BMDCs treated with Hsp70 was completely recovered and comparable to the basal levels (Figure 2C). Concomitantly, down-regulation of both C/EBP$\beta$ (Figure 2D) and C/EBP$\delta$ (Figure 2E) induced by Hsp70 was abolished by the absence of TLR2 in BMDCs.

### ERK and STAT3 are required for Hsp70-driven impaired IFN-$\gamma$, TNF-$\alpha$ and MCP-1 production and C/EBP$\beta$/$\delta$ down-regulation

Recently, Hsp70 has been demonstrated to activate ERK and STAT3 in MDSCs [32]. IL-10 production has been linked to ERK and STAT3 activation [36] and STAT3 has also been shown to mediate anti-inflammatory responses [37–39]. Thus we analysed the role of these two molecules on the inhibition

RIGHTSLINK()
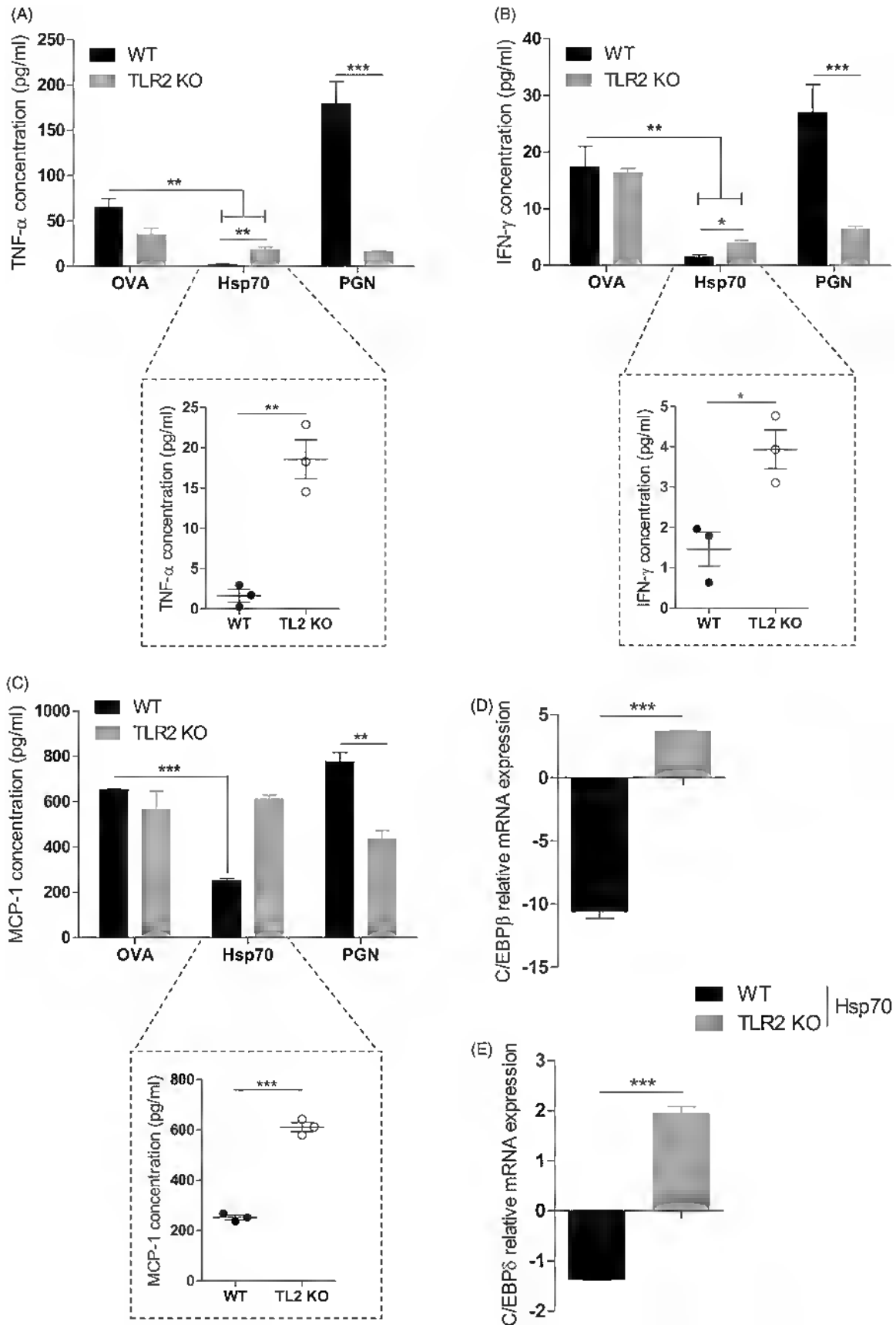
Figure 2. Pro-inflammatory cytokine inhibition and C/EBPβ and C/EBPδ down-regulation induced by Hsp70 is dependent on TLR2. WT or TLR2 KO BMDCs were treated with OVA, TBHsp70 or PGN for 24 h. Cytokines in the supernatants were analysed using a CBA mouse inflammation kit: (A) TNF-α, (B) IFN-γ and (C) MCP-1; (D) C/EBPβ and (E) C/EBPδ expression evaluation by qPCR in WT or TLR2 KO BMDCs treated with Hsp70 or left unstimulated for 24 h. β-actin was used as a normaliser as described in Materials and methods. $*p < 0.05$; $**p < 0.01$; $***p < 0.001$. Experiments were performed three times in triplicates.

RIGHTSLINK()
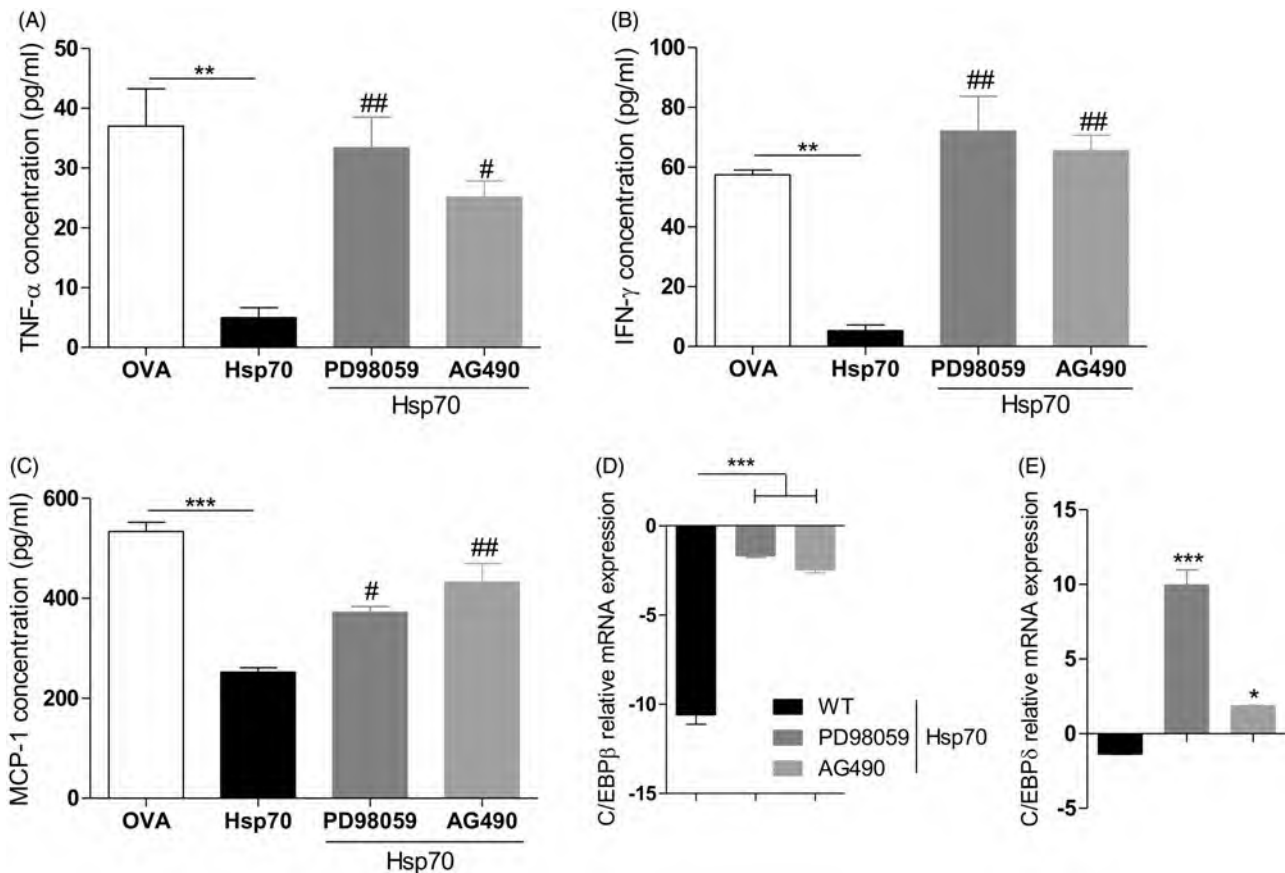
Figure 3. ERK and STAT3 are required for Hsp70-induced pro-inflammatory cytokines inhibition and C/EBPβ and C/EBPδ down-regulation. BMDCs from WT mice were treated with inhibitors of ERK PD98059 or JAK2/STAT3 AG490 for 1 h prior to stimulation. After that, cells were treated with OVA, Hsp70, LPS or left unstimulated for 24 h. Culture supernatants were analysed for the presence of (A) TNF-α, (B) IFN-γ, and (C) MCP-1 using a CBA inflammation kit, (D) C/EBPβ and (E) C/EBPδ expression evaluation by qPCR. β-actin was used as a normaliser as described in Materials and methods. $*p < 0.05$; $**p < 0.01$; $***p < 0.001$. $^{\#}p < 0.05$, $^{\#\#}p < 0.01$ when compared with Hsp70. Experiments were performed three times in triplicates.

of pro-inflammatory cytokines basal levels and down-regulation of both C/EBPβ and C/EBPδ by Hsp70. To inhibit ERK, we used the specific inhibitor PD98059. We inhibited the JAK2/STAT3 pathway using the AG490 inhibitor. Once again, Hsp70 treatment impaired IFN-γ, TNF-α and MCP-1 production when compared with OVA. However, when BMDCs were pre-treated with ERK or STAT3 inhibitors and then stimulated with Hsp70, the production of IFN-γ, TNF-α and MCP-1 observed were very similar to the basal levels (BMDCs treated with OVA) (Figure 3A–C). Both ERK and STAT3 were required for Hsp70-driven down-regulation of C/EBPβ (Figure 3D) and C/EBPδ mRNA levels (Figure 3E).

### Hsp70 down-regulation of basal levels of IFN-γ, TNF-α and MCP-1 is dependent on IL-10 production by BMDC

IL-10 is the most powerful anti-inflammatory cytokine [40] and its production can be triggered by Hsp70 [10,17]. We asked whether IL-10 is involved in Hsp70-driven down-regulation of pro-inflammatory cytokines. In order to do that, we treated WT or IL-10 KO BMDCs with either OVA, Hsp70 or PGN for 24 h. Indeed, IFN-γ and TNF-α inhibition was dependent on IL-10 expression in BMDCs treated with Hsp70 (Figure 4A–B). MCP-1 production was down-regulated in WT BMDCs treated with Hsp70 when compared with OVA.

This production was re-established in IL-10 KO BMDCs (Figure 4C). In addition, Hsp70-driven reduced expression of C/EBPβ and C/EBPδ were both dependent on IL-10 as shown in Figure 4D and Figure 4E, respectively.

### Discussion

During acute or chronic inflammatory conditions, DCs acquire a mature phenotype in which they can produce high amounts of pro-inflammatory cytokines [41]. This phenotype can be induced upon a microbial inflammatory stimulus [42]. Moreover, DCs play a crucial role in the pathogenesis of autoimmunity conditions [43]. Therewith, the modulation of DC activation has been suggested as an interesting strategy in the attempt to abrogate chronic inflammatory diseases, such as arthritis [16,44]. Indeed, one of the contributions to the powerful effect of TNF-α blockade in arthritis patients is that this treatment leads to DC impaired functions such as down-regulation of co-stimulatory signals [45]. In the present work we demonstrated that immature BMDC stimulation with Hsp70 decreased the basal expression of C/EBPβ or C/EBPδ, leading to impairment in TNF-α, IFN-γ and MCP-1 production. However, we did not analyse whether Hsp70 can exert its anti-inflammatory proprieties in mature BMDCs which had been stimulated with LPS before Hsp70 treatment, for example. Moreover, we also did not analyse whether
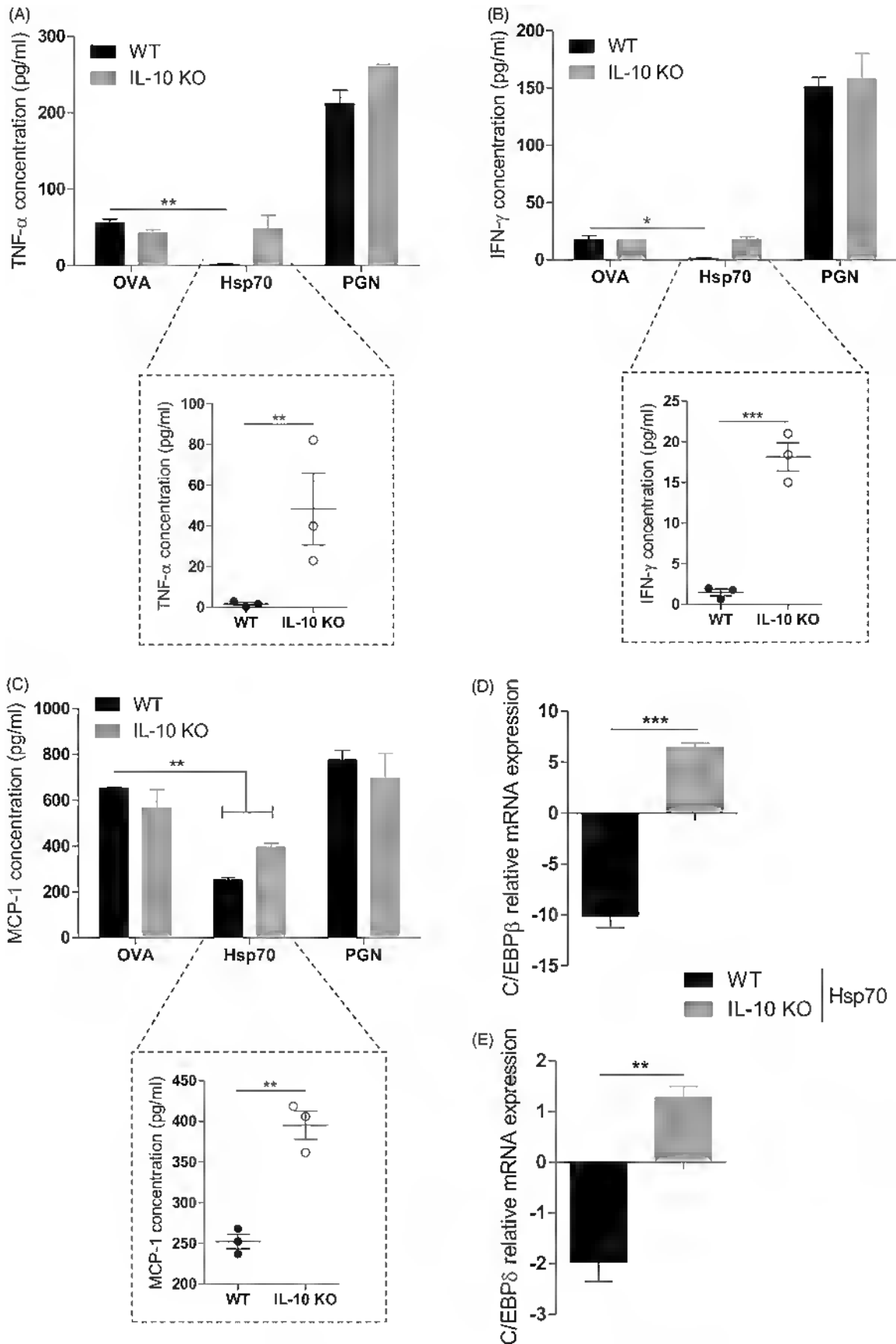
Figure 4. IL-10 is necessary for Hsp70 anti-inflammatory effects. BMDCs from WT or IL-10 KO mice were treated with OVA, Hsp70, PGN or left unstimulated for 24 h. Cytokines in the supernatants were analysed using a CBA mouse inflammation kit: (A) TNF-$\alpha$, (B) IFN-$\gamma$ and (C) MCP-1; (D) C/EBP$\beta$ and (E) C/EBP$\delta$ expression evaluation by qPCR. $\beta$-actin was used as a normaliser as described in Materials and methods. *$p < 0.05$; **$p < 0.01$; ***$p < 0.001$. #$p < 0.05$ and ##$p < 0.01$ when compared with Hsp70. Experiments were performed two or three times in triplicates.

BMDCs treated with Hsp70 can prevent the up-regulation of both C/EBPβ and C/EBPδ and pro-inflammatory cytokines induced by LPS. These questions need to be further elucidated in our system. In a different study, Spiering et al. [46] recently demonstrated that the administration of Hsp70-pulsed BMDCs can prevent proteoglycan-induced arthritis (PGIA) in mice. In the same work, the treatment of BMDCs with Hsp70 generates a semi-mature phenotype that was stable after the addition of LPS in culture.

In accordance with our findings, the treatment of synovial cells from arthritis patients with Hsp70 diminished TNF-α and IFN-γ production by these cells [10]. MCP-1 was not measured in that previous work, but this chemokine is important for cell migration in inflammatory responses [47]. We believe that MCP-1 production should be analysed in future works with human cells treated with Hsp70.

TLR2 has an interesting feature that, depending on the nature of TLR2 ligand, it can induce pro-inflammatory or anti-inflammatory responses [33,48,49]. We observed that TLR2 plays a critical role in mediating down-regulation of C/EBPβ and C/EBPδ and inhibition of pro-inflammatory cytokines (Figure 2). In contrast with our findings, macrophages treated with a *Mycobacterium tuberculosis* 19-kDa lipoprotein leads to up-regulation of both via TLR2 [50]. This is the first time that TLR2 has been associated with a down-regulation of C/EBPβ and C/EBPδ expression.

We next tried to elucidate other molecules that could be involved in Hsp70-mediated effects found in BMDCs. Tumour-associated Hsp70 can activate ERK and STAT3 in a TLR2-dependent manner [32], and both molecules can be activated downstream of TLR activation [51]. We observed that after ERK inhibition, Hsp70 tolerogenic effects on BMDCs could not be observed anymore. C/EBPβ or C/EBPδ activation via the ERK pathway has been reported in chondrocytes [52], monocytes [53] and macrophages [54]. ERK is also required for the stability of tolerogenic phenotype in DCs [55,56]. We believe that ERK interaction with C/EBPβ and C/EBPδ could be a possible explanation for our observations.

In addition, we observed that STAT3 was required for decreasing the basal expression of C/EBPβ and C/EBPδ, leading to an impairment in TNF-α, IFN-γ and MCP-1 production in Hsp70-treated BMDCs. Previous studies suggested that STAT3 could control transcription of C/EBPβ [54] and C/EBPδ [57] genes. Macrophages from STAT3 KO mice failed to induce C/EBPβ upon LPS or IL-10 stimulation [58]. This regulation was suggested to be due to STAT3 binding in the distal region of C/EBPβ promoter [59]. These findings strongly corroborate our observations that STAT3 can mediate C/EBP family members' expression.

In our system, IL-10 production by BMDCs induced by Hsp70 was necessary for C/EBPβ and C/EBPδ down-regulation and concomitant inhibition of pro-inflammatory cytokines. ERK and STAT3 have been described to be involved in IL-10 signalling [36] and Hsp70 effects were also dependent on this cytokine [60]. C/EBPβ and C/EBPδ have been associated with the production of IL-10 in macrophages [61,62]; however, the effects of IL-10 over the expression of these transcription factors in different immune cells have not

been investigated in detail. One study suggested that IL-10 treatment could either up-regulate C/EBPβ in THP-1 macrophages, or yet that it has no effect over undifferentiated monocytes, [58]. It is possible that the regulation of C/EBP transcription factors expression depends not only on a single cytokine stimulus, but rather requires a combination of signals triggered in Hsp70-treated cells.

Aside from the anti-inflammatory effects of extracellular Hsp70, elevation of intracellular Hsp70 levels by chemical agents or thermal stress also demonstrated tolerogenic properties on DCs [63], perhaps due to secretion of this protein when it is produced in elevated levels. Consequently, induction of intracellular HSPs using non-toxic chemical compounds isolated from medicinal plants [64] might constitute an alternative way to induce tolerance in inflammatory conditions.

## Conclusion

Our results indicate a probable mechanism employed by Hsp70 to down-regulate levels of IFN-γ, TNF-α and MCP-1, via inhibition of the expression of C/EBPβ and C/EBPδ transcription factors. Hsp70 was not capable to impair pro-inflammatory cytokines production and decrease C/EBPβ and C/EBPδ levels in TLR2 or IL-10 KO cells, or in BMDCs that had ERK or STAT3 signalling pathways inhibited. We suggest that extracellular Hsp70 signals via the TLR2-ERK-STAT3-IL-10 pathway in BMDCs to exert its strong anti-inflammatory effects.

## Acknowledgements

## Declaration of interest

## References

1. Fleshner M, Johnson JD. Endogenous extra-cellular heat shock protein 72: Releasing signal(s) and function. Int J Hyperthermia 2005;21:457–71.
2. Borges TJ, Wieten L, van Herwijnen MJ, Broere F, van der Zee R, Bonorino C, et al. The anti-inflammatory mechanisms of Hsp70. Front Immunol 2012;3:95.
3. Tanaka S, Kimura Y, Mitani A, Yamamoto G, Nishimura H, Spallek R, et al. Activation of T cells recognizing an epitope of heat-shock protein 70 can protect against rat adjuvant arthritis. J Immunol 1999;163:5560–5.
4. Wendling U, Paul L, van der Zee R, Prakken B, Singh M, van Eden W. A conserved mycobacterial heat shock protein (HSP) 70 sequence prevents adjuvant arthritis upon nasal administration and

induces IL-10-producing T cells that cross-react with the mammalian self-Hsp70 homologue. J Immunol 2000;164:2711–17.

5. van Eden W, van der Zee R, Prakken B. Heat-shock proteins induce T-cell regulation of chronic inflammation. Nat Rev Immunol 2005;5:318–30.

6. Broere F, Wieten L, Klein Koerkamp EI, van Roon JA, Guichelaar T, Lafeber FP, et al. Oral or nasal antigen induces regulatory T cells that suppress arthritis and proliferation of arthritogenic T cells in joint draining lymph nodes. J Immunol 2008;181:899–906.

7. Wieten L, Berlo SE, Ten Brink CB, van Kooten PJ, Singh M, van der Zee R, et al. IL-10 is critically involved in mycobacterial Hsp70 induced suppression of proteoglycan-induced arthritis. PLoS One 2009;4:e4186.

8. Borges TJ, Porto BN, Teixeira CA, Rodrigues M, Machado FD, Ornaghi AP, et al. Prolonged survival of allografts induced by mycobacterial Hsp70 is dependent on CD4+CD25+ regulatory T cells. PLoS One 2010;5:e14264.

9. Tanaka K, Namba T, Arai Y, Fujimoto M, Adachi H, Sobue G, et al. Genetic evidence for a protective role for heat shock factor 1 and heat shock protein 70 against colitis. J Biol Chem 2007;282:23240–52.

10. Detanico T, Rodrigues L, Sabritto AC, Keisermann M, Bauer ME, Zwickey H, et al. Mycobacterial heat shock protein 70 induces interleukin-10 production: Immunomodulation of synovial cell cytokine profile and dendritic cell maturation. Clin Exp Immunol 2004;135:336–42.

11. Watowich SS, Liu YJ. Mechanisms regulating dendritic cell specification and development. Immunol Rev 2010;238:76–92.

12. Heath WR, Carbone FR. Dendritic cell subsets in primary and secondary T cell responses at body surfaces. Nat Immunol 2009;10:1237–44.

13. Shortman K, Liu YJ. Mouse and human dendritic cell subtypes. Nat Rev Immunol 2002;2:151–61.

14. Liu K, Nussenzweig MC. Origin and development of dendritic cells. Immunol Rev 2010;234:45–54.

15. Sarkar S, Fox DA. Dendritic cells in rheumatoid arthritis. Front Biosci 2005;10:656–65.

16. Khan S, Greenberg JD, Bhardwaj N. Dendritic cells as targets for therapy in rheumatoid arthritis. Nat Rev Rheumatol 2009;5:566–71.

17. Motta A, Schmitz C, Rodrigues L, Ribeiro F, Teixeira C, Detanico T, et al. *Mycobacterium tuberculosis* heat-shock protein 70 impairs maturation of dendritic cells from bone marrow precursors, induces interleukin-10 production and inhibits T-cell proliferation in vitro. Immunology 2007;121:462–72.

18. Kawai T, Akira S. Toll-like receptors and their crosstalk with other innate receptors in infection and immunity. Immunity 2011;34:637–50.

19. Baldwin Jr. AS. The NF-kappa B and I kappa B proteins: New discoveries and insights. Annu Rev Immunol 1996;14:649–83.

20. Ruland J. Return to homeostasis: Downregulation of NF-kappaB responses. Nat Immunol 2011;12:709–14.

21. Shi Y, Tu Z, Tang D, Zhang H, Liu M, Wang K, et al. The inhibition of LPS-induced production of inflammatory cytokines by Hsp70 involves inactivation of the NF-kappaB pathway but not the MAPK pathways. Shock 2006;26:277–84.

22. Dokladny K, Lobb R, Wharton W, Ma TY, Moseley PL. LPS-induced cytokine levels are repressed by elevated expression of HSP70 in rats: Possible role of NF-kappaB. Cell Stress Chaperones 2010;15:153–63.

23. Malhotra V, Wong HR. Interactions between the heat shock response and the nuclear factor-kappaB signaling pathway. Crit Care Med 2002;30:S89–95.

24. Lekstrom-Himes J, Xanthopoulos KG. Biological role of the CCAAT/enhancer-binding protein family of transcription factors. J Biol Chem 1998;273:28545–8.

25. Lu YC, Kim I, Lye E, Shen F, Suzuki N, Suzuki S, et al. Differential role for c-Rel and C/EBPbeta/delta in TLR-mediated induction of proinflammatory cytokines. J Immunol 2009;182:7212–21.

26. Poli V. The role of C/EBP isoforms in the control of inflammatory and native immunity functions. J Biol Chem 1998;273:29279–82.

27. Hu HM, Baer M, Williams SC, Johnson PF, Schwartz RC. Redundancy of C/EBP-alpha, -beta, and -delta in supporting the lipopolysaccharide-induced transcription of IL-6 and monocyte chemoattractant protein-1. J Immunol 1998;160:2334–42.

28. Mehlert A, Young DB. Biochemical and antigenic characterization of the *Mycobacterium tuberculosis* 71-kD antigen, a member of the 70-kD heat-shock protein family. Mol Microbiol 1989;3:125–30.

29. Aida Y, Pabst MJ. Removal of endotoxin from protein solutions by phase-separation using triton X-114. J Immunol Methods 1990;132:191–5.

30. Inaba K, Inaba M, Romani N, Aya H, Deguchi M, Ikehara S, et al. Generation of large numbers of dendritic cells from mouse bone marrow cultures supplemented with granulocyte/macrophage colony-stimulating factor. J Exp Med 1992;176:1693–1702.

31. Schmittgen TD, Livak KJ. Analyzing real-time PCR data by the comparative C(T) method. Nat Protoc 2008;3:1101–8.

32. Chalmin F, Ladoire S, Mignot G, Vincent J, Bruchard M, Remy-Martin JP, et al. Membrane-associated Hsp72 from tumor-derived exosomes mediates STAT3-dependent immunosuppressive function of mouse and human myeloid-derived suppressor cells. J Clin Invest 2010;120:457–71.

33. Dillon S, Agrawal S, Banerjee K, Letterio J, Denning TL, Oswald-Richter K, et al. Yeast zymosan, a stimulus for TLR2 and dectin-1, induces regulatory antigen-presenting cells and immunological tolerance. J Clin Invest 2006;116:916–28.

34. Manicassamy S, Ravindran R, Deng J, Oluoch H, Denning TL, Kasturi SP, et al. Toll-like receptor 2-dependent induction of vitamin A-metabolizing enzymes in dendritic cells promotes T regulatory responses and inhibits autoimmunity. Nat Med 2009;15:401–9.

35. Filippi CM, Ehrhardt K, Estes EA, Larsson P, Oldham JE, von Herrath MG. TLR2 signaling improves immunoregulation to prevent type 1 diabetes. Eur J Immunol 2011;41:1399–409.

36. Saraiva M, O'Garra A. The regulation of IL-10 production by immune cells. Nat Rev Immunol 2010;10:170–81.

37. Cheng F, Wang HW, Cuenca A, Huang M, Ghansah T, Brayer J, et al. A critical role for STAT3 signaling in immune tolerance. Immunity 2003;19:425–36.

38. Barton BE. STAT3: A potential therapeutic target in dendritic cells for the induction of transplant tolerance. Expert Opin Ther Targets 2006;10:459–70.

39. Dhingra S, Bagchi AK, Ludke AL, Sharma AK, Singal PK. Akt regulates IL-10 mediated suppression of TNFalpha-induced cardiomyocyte apoptosis by upregulating STAT3 phosphorylation. PLoS One 2011;6:e25009.

40. Kubo M, Motomura Y. Transcriptional regulation of the anti-inflammatory cytokine IL-10 in acquired immune cells. Front Immunol 2012;3:275.

41. Banchereau J, Steinman RM. Dendritic cells and the control of immunity. Nature 1998;392:245–52.

42. Granucci F, Girolomoni G, Lutz MB, Foti M, Marconi G, Gnocchi P, et al. Modulation of cytokine expression in mouse dendritic cell clones. Eur J Immunol 1994;24:2522–6.

43. Amodio G, Gregori S. Dendritic cells a double-edge sword in autoimmune responses. Front Immunol 2012;3:233.

44. Hackstein H, Thomson AW. Dendritic cells: Emerging pharmacological targets of immunosuppressive drugs. Nat Rev Immunol 2004;4:24–34.

45. Baldwin HM, Ito-Ihara T, Isaacs JD, Hilkens CM. Tumour necrosis factor alpha blockade impairs dendritic cell survival and function in rheumatoid arthritis. Ann Rheum Dis 2010;69:1200–7.

46. Spiering R, van der Zee R, Wagenaar J, van Eden W, Broere F. Mycobacterial and mouse Hsp70 have immuno-modulatory effects on dendritic cells. Cell Stress Chaperones 2012.

47. Rossi D, Zlotnik A. The biology of chemokines and their receptors. Annu Rev Immunol 2000;18:217–42.

48. Frodermann V, Chau TA, Sayedyahossein S, Toth JM, Heinrichs DE, Madrenas J. A modulatory interleukin-10 response to staphylococcal peptidoglycan prevents Th1/Th17 adaptive immunity to *Staphylococcus aureus*. J Infect Dis 2011;204:253–62.

49. Dearman RJ, Cumberbatch M, Maxwell G, Basketter DA, Kimber I. Toll-like receptor ligand activation of murine bone marrow-derived dendritic cells. Immunology 2009;126:475–84.

50. Harding CV, Boom WH. Regulation of antigen presentation by *Mycobacterium tuberculosis*: A role for toll-like receptors. Nat Rev Microbiol 2010;8:296–307.

51. Aderem A, Ulevitch RJ. Toll-like receptors in the induction of the innate immune response. Nature 2000;406:782–7.

52. Raymond L, Eck S, Mollmark J, Hays E, Tomek I, Kantor S, et al. Interleukin-1 beta induction of matrix metalloproteinase-1 transcription in chondrocytes requires ERK-dependent activation of CCAAT enhancer-binding protein-beta. J Cell Physiol 2006;207: 683–8.

53. Zhang T, He YM, Wang JS, Shen J, Xing YY, Xi T. Ursolic acid induces HL60 monocytic differentiation and upregulates C/EBPbeta expression by ERK pathway activation. Anticancer Drugs 2011;22:158–65.

54. Niehof M, Streetz K, Rakemann T, Bischoff SC, Manns MP, Horn F, et al. Interleukin-6-induced tethering of STAT3 to the LAP/C/EBPbeta promoter suggests a new mechanism of transcriptional regulation by STAT3. J Biol Chem 2001;276:9016–27.

55. Nakahara T, Moroi Y, Uchi H, Furue M. Differential role of MAPK signaling in human dendritic cell maturation and Th1/Th2 engagement. J Dermatol Sci 2006;42:1–11.

56. Puig-Kroger A, Relloso M, Fernandez-Capetillo O, Zubiaga A, Silva A, Bernabeu C, et al. Extracellular signal-regulated protein kinase signaling pathway negatively regulates the phenotypic and functional maturation of monocyte-derived human dendritic cells. Blood 2001;98:2175–82.

57. Yamada T, Tobita K, Osada S, Nishihara T, Imagawa M. CCAAT/enhancer-binding protein delta gene expression is mediated by APRF/STAT3. J Biochem 1997;121:731–8.

58. Tanaka N, Hoshino Y, Gold J, Hoshino S, Martiniuk F, Kurata T, et al. Interleukin-10 induces inhibitory C/EBPbeta through STAT-3 and represses HIV-1 transcription in macrophages. Am J Respir Cell Mol Biol 2005;33:406–11.

59. Zhang K, Guo W, Yang Y, Wu J. JAK2/STAT3 pathway is involved in the early stage of adipogenesis through regulating C/EBPbeta transcription. J Cell Biochem 2011;112:488–97.

60. Stocki P, Dickinson AM. The immunosuppressive activity of heat shock protein 70. Autoimmune dis 2012;2012:617213.

61. Csoka B, Nemeth ZH, Virag L, Gergely P, Leibovich SJ, Pacher P, et al. A2A adenosine receptors and C/EBPbeta are crucially required for IL-10 production by macrophages exposed to *Escherichia coli*. Blood 2007;110:2685–95.

62. Ruffell D, Mourkioti F, Gambardella A, Kirstetter P, Lopez RG, Rosenthal N, et al. A CREB-C/EBPbeta cascade induces M2 macrophage-specific gene expression and promotes muscle injury repair. Proc Natl Acad Sci USA 2009;106:17475–80.

63. Spiering R, van der Zee R, Wagenaar J, Kapetis D, Zolezzi F, van Eden W, et al. Tolerogenic dendritic cells that inhibit autoimmune arthritis can be induced by a combination of carvacrol and thermal stress. PLoS One 2012;7:e46336.

64. Ahmed K, Furusawa Y, Tabuchi Y, Emam HF, Piao JL, Hassan MA, et al. Chemical inducers of heat shock proteins derived from medicinal plants and cytoprotective genes response. Int J Hyperthermia 2012;28:1–8.

# CAPÍTULO 2

MARCH1 induction in dendritic cells *in vivo* downregulates MHC II and improves the survival of skin allografts

**Autores:** Thiago J. Borges, Felipe D. Machado, Rafael L. Lopes, Ayesha Murshid, Mayuko Uehara, Gabriel Birrane, Rafael F. Zanin, Reza Abdi, Satoshi Ishido, Stuart K. Calderwood, Ana Paula D. Souza, Leonardo V. Riella[*], Cristina Bonorino[*]

[*] Co-senior author

**Situação:** Em preparação

**Revista:** *Nature Communications*

**Motivação:** Nesse trabalho apresentamos as vias moleculares pelas quais a DnaK modula a expressão de MHC II e CD86 em células dendríticas murinas. Essa modulação acontece através da indução da molécula MARCH1, que irá ubiquitinar as moléculas de MHC II direcionando-as para o lisossomo. Para testar o papel da DnaK *in vivo* utilizamos um modelo de aloenxerto cutâneo – o modelo de rejeição mais agressivo. O tratamento *in-situ* com a DnaK antes do transplante prolongou a sobrevida do enxerto, Isso aconteceu através da modulação das células dendríticas do doador que chegavam expressando menos MHC II e CD86 no linfonodo drenante, diminuindo a aloreatividade das células T CD4 e CD8 de maneira dependente de MARCH1. Além disso, a indução de MARCH1 e a diminuição da rejeição in vivo pela DnaK aconteceu de maneira dependente da via TL2-ERK-STAT3-IL-10.

# MARCH1 induction in dendritic cells in vivo downregulates MHC II and improves the survival of skin allografts

Thiago J. Borges[1], Felipe D. Machado[1], Rafael L. Lopes[1], Ayesha Murshid[2], Mayuko Uehara[3], Gabriel Birrane[2,4], Rafael F. Zanin[1], Reza Abdi[3], Satoshi Ishido[5], Stuart K. Calderwood[2], Ana Paula D. Souza[6], Leonardo V. Riella[3,7*], Cristina Bonorino[1,7*]

[1] School of Biosciences and Biomedical Research Institute, Pontifícia Universidade Católica do Rio Grande do Sul - PUCRS, Porto Alegre, RS, Brazil

[2] Department of Radiation Oncology, Beth Israel Deaconess Medical Center, Harvard Medical School, Boston, Massachusetts, USA

[3] Schuster Family Transplantation Research Center, Renal Division, Brigham and Women's Hospital, Harvard Medical School, Boston, Massachusetts, USA

[4] Department of Medicine, Beth Israel Deaconess Medical Center, Harvard Medical School, Boston, Massachusetts, USA

[5] Genetics Department and Post-Graduation Program in Genetics and Molecular Biology, Universidade Federal do Rio Grande do Sul, Porto Alegre, RS, Brazil

[5] Laboratory of Integrative Infection Immunity, Showa Pharmaceutical University, Machida, Tokyo, Japan

[6] School of Pharmacy and Centro Infant, Biomedical Research Institute, Pontifícia Universidade Católica do Rio Grande do Sul, Porto Alegre - PUCRS, RS, Brazil

[7] Co-senior author

*Address for Correspondence: Cristina Bonorino, PhD

Email: cbonorino@pucrs.br

Av. Ipiranga, 6690 - Jardim Botânico - Porto Alegre, RS, Brazil - CEP: 90610-000.

Tel +55 51-3320-3000, ext. 2725

*Address for Correspondence: Leonardo V. Riella, MD, PhD

Email: lriella@bwh.harvard.edu

221 Longwood Ave, Boston MA 02115, USA.

Tel: +1 617-732-5252; Fax: +1 617-732-5254

**Abstract (150 words – 151)**

T cell responses initiate upon interaction of the T cell receptor with MHC molecules expressed on the membrane of dendritic cells. Additional costimulatory signals must be provided for T cells to progress into effector mode, and absence of such signals results in tolerance. While inflammatory chronic diseases depend on CD4+ T cell activation, current therapies focus on blockage of co-stimulation and/or subsequent T cell proliferation, with limited success. The ubiquitin ligase MARCH1 targets MHC II and CD86 for degradation in lysosomes, downregulating their membrane expression. Complete pathways for MARCH1 induction have not been described, and it is unknown if MARCH1 induction can modulate an inflammatory response *in vivo*. In this study, we report a pathway for induction of MARCH1 by mycobacterial DnaK in DCs, leading to inhibition of allograft rejection in vivo. Our results pave the way for therapies that target the expression of MHC, in DCs minimizing T cell activation.

**Introduction**

Dendritic cells (DCs) initiate adaptive immune responses, delivering the necessary signals for specific T cell activation. DCs present peptides in MHC II and I and, when activated, provide costimulatory molecules and cytokines that shape the type of T cell response that ensues[1, 2, 3]. The activation of CD4+ T cells upon interaction with MHC II molecules on DCs is the key event to generate immunity to infection, and yet also necessary for autoimmune, allergic and alloreactive responses that harm the host. Graft rejection and autoimmunity are currently modulated with the use of drugs that inhibit non-specific T cell activation and proliferation[4]. More recent strategies involve drugs targeting costimulatory molecule blockade[5]. Both approaches target the results of an already activated, undesired T cell response and lead to a series of undesirable off-target side-effects.

The membrane-associated RING-CH 1 (MARCH1) is a membrane associated E3 ubiquitin ligase that ubiquitinates a conserved lysine the cytoplasmic tail of MHC II β chain[6, 7]. When DCs are activated, they downregulate MARCH1 by a CD83 regulated mechanism, leading to an upregulation of MHC II and the costimulatory molecule CD86[8]. In contrast, induction of MARCH1, driven by IL-10[9] leads to ubiquitination of MHC II and CD86, resulting in lysosomal degradation and a decrease in surface expression[10]. MARCH1 expression in murine DCs was demonstrated to regulate T cell activation in vitro[11], providing a tolerogenic environment, however a role for this molecule during an *in vivo* inflammatory response has not been well characterized, nor have the molecular pathways underlying MARCH1 regulation.

In this study we have mapped a complete route for MARCH1 induction, triggered in DCs upon engagement of a mycobacterial protein, DnaK, and which results in downregulation of MHC II and CD86 expression. Using an allogeneic skin transplant experimental system, we demonstrate that in-situ DnaK treatment of donor skins prior the transplant limits alloreactive proliferation of both CD4+ and CD8+ T cells. This treatment inhibits skin rejection through downregulation of MHC II and CD86 in donor DCs in a MARCH1-dependent manner. DnaK induced MARCH1 and MHC II downregulation via a TLR2-ERK-STAT3-IL-10/IL-10R molecular pathway, delaying acute rejection in the absence of any additional treatment.

Skin transplants are the most immunogenic of all. Our results unveil an innate pathway for the modulation of signal one - MHC expression – via MARCH1, that creates an organ acceptance prone environment, preventing the activation of such responses *in vivo*.

## Results

*MARCH1-dependent MHC II ubiquitination and surface downregulation is induced by mycobacterial DnaK*

We hypothesized that downregulation of MHC II and CD86 expression in the donor DCs through MARCH1 would constitute a major approach to modulate an immune response in vivo. To test that hypothesis, we chose a skin allograft experimental system. Molecules that have been reported to modulate DCs and inhibit allograft rejection - cyclosporin A (CsA)[12, 13], Rapamycin (RAPA)[14] and DnaK from *M. tuberculosis*[15, 16] – were tested for their ability to induce MARCH1 in murine LN DCs. DnaK and recombinant murine IL-10 treatments, but not CsA or RAPA, lead to the induction of MARCH1 mRNA in murine DCs (Fig. 1a). Ubiquitination of MHC II was increased in DCs treated with DnaK when compared to control (Fig 1b). To assess whether ubiquitination targeted MHC II for late lysosomal vesicles, we analyzed the localization of MHC and late endosomes/lysosomes marker LAMP-1 marker in DCs treated with DnaK using confocal microscopy. In DnaK-treated DCs, MHC II was internalized and co-localized with LAMP-1 in intracellular vesicles, while untreated DCs showed MHC II on the surface and LAMP-1 intracellularly with minimal overlap (Fig. 1c). We next treated WT or MARCH1 KO DCs with DnaK or control and assessed MHC II and CD86 expression by flow cytometry. DnaK could downregulate MHC II (Fig. 1d) and CD86 (Fig. 1e) expression in WT DCs, but not in in MARCH1 KO cells.



**Figure 1 | MARCH1 was induced by DnaK, but not cyclosporine A or Rapamycin in murine DCs.** (a) DCs isolated from mice lymph nodes (LN) were treated with Cyclosporine A (CsA),

Rapamycin (RAPA), DnaK or recombinant murine IL-10 for 24h. After that, MARCH1 mRNA levels were analyzed by real time PCR. β-actin was used as normalizer (see Methods). ** p<0.01 and *** p<0.001 when means are compared to medium by ANOVA with Tukey post-test. (b) LN DCs were treated with DnaK or left untreated for 24h at 37°C. Cells were lysed, MHC II proteins were immunoprecipitated, and analyzed for ubiquitination or total MHC II by Western Blot. (c) Isolated DCs were grown for 48h in poly-d-Lysine coated coverslips then treated with DnaK or medium for 24h and stained for MHC II and LAMP-1. Cells were then analyzed by Confocal microscopy. Spleen and LN DCs from WT or MARCH1 KO mice were isolated and treated with DnaK or control for 24h. After that, MHC II (d) and CD86 (e) levels were analyzed by flow cytometry.

*In-situ DnaK skin treatment prior to transplant inhibits alloreactive T cell proliferation via MARCH1*

We performed a fully mismatched skin transplant, with an in-situ treatment of donor skin prior the transplant. We immersed C57Bl/6 (H-2$^b$) donor tissues in a solution containing DnaK for 60 min and then transplanted into BALB/c (H-2$^d$) hosts (Supplementary Fig. 1a). Donor skin treatment with DnaK significantly prolonged allograft survival without any additional treatment (Supplementary Fig. 1b, c). DnaK-treated grafts had a median survival time (MST) of 20 days compared to 14 days of the control group (n=23 per group; p>0.0001).

In light of this powerful *in vivo* effect, we investigated whether it depended on MARCH1. WT or MARCH1 KO skins were treated with DnaK or control and transplanted into BALB/c hosts. MARCH1 KO skins were rejected in the same timeframe as WT skins whether they were treated or not with DnaK (Fig. 2a). Analysis of recipients' LN revealed a significant reduction in total cells for mice that received DnaK-treated allografts compared to those that received control allografts (Fig. 2b). LNs from DnaK group were visually smaller than controls (Fig. 2c). Because we observed a MARCH1-dependent MHC II downregulation induced by DnaK *in vitro*, we investigated whether this reduction in T cells was due to an impartment in T cell alloreactivity. DnaK treatment decreased the total numbers of CD4 and CD8 T cells (Supplementary Fig. 2a) in allografts' draining LN (Supplementary Fig 2a), in a MARCH1 dependent manner (Supplementary Fig 2b). We observed a significant reduction in both the percentage and absolute numbers of proliferating CD4 T cells (CD4$^+$Ki67$^+$ cells) in the hosts that received DnaK-treated allografts (Fig. 2d). This reduction was completely abolished when the donor skins were MARCH1 KO (Fig. 2d). Furthermore, CD8 T cells proliferated (CD8$^+$Ki67$^+$ cells) significantly less in DnaK hosts when compared to control (Fig. 2e). This phenomenon was also dependent on MARCH1 KO expression by donor cells (Fig. 2e).

We next examined if DnaK allograft treatment could alter the function of lymphocytes isolated from host allograft draining LNs. Consistently with decreased allosensization, mice

that received DnaK-treated allografts presented a MARCH1-dependent reduction in percentage and absolute number of CD8 T effector memory cells (TEM – CD8^{+}CD44^{+}CD62L^{-} cells; Fig. 3a) and CD4 TEM cells (CD4^{+}CD44^{+}CD62L^{-} cells; Fig. 3b). Because IFN-γ and IL-17-producing T cells are described to play a role during skin rejection[17, 18, 19], we investigated these cells in our experimental system. CD4 T cells from mice that that received DnaK-treated allografts showed a diminished production of IL-17 at 24h and 96h post-transplant (Fig. 3c). This effect was also dependent on MARCH1 (Fig. 3c). In addition, we found that IFN-γ was decreased in both CD4 (Fig. 3d) and CD8 T (Fig. 3e) cells at 24h post-transplant, in a MARCH1-dependent way. Thus, MARCH1 induction by DnaK is essential to decrease alloreactivity to skin transplants, modulate T cell activation and function and improve allograft survival.



**Figure 2 | MARCH1 is required for the decrease in alloreactivity induced by DnaK.** (a) Percent survival of skin allografts from WT B6 or MARCH1 KO (H-2[b]) mice treated with DnaK or control and transplanted into BALB/c (H-2[d]) recipients. *p<0.05, **p<0.01 by long-rank test. (n=5 mice per group). (b) Absolute numbers of total cells from allograft's draining lymph nodes (LN) harvested from mice that received DnaK-treated skin grafts or controls on days 1, 4, 7 and 10 post transplantation (n=3-6 mice per time-point/group). Dot graphs represent the mean ± SEM. *p<0.05 and ***p<0.001 when compare to control by t test. (c) Visual aspect of the allograft draining LN at day 7 post-transplant. Skin grafts from WT or MARCH1 KO were treated with DnaK or controls were transplanted into BALB/c mice. Percentage and absolute numbers of proliferating (d) CD4 (CD4^{+}Ki67^{+}) and (e) CD8 (CD8^{+}Ki67^{+}) T cells from allografts' draining LN harvested at 24h or 96h post-transplant. *p<0.05 and **p<0.01 when compare to control by t test. Representative results of at least two independent experiments.

**Figure 3 | Reduced alloreactive T cell responses in DnaK-treated group is impaired in MARCH1 KO mice.** Allografts' draining LN were harvested at 24h or 96h post-transplant from BALB/c mice that received skin grafts from WT or MARCH1 KO in-situ treated with DnaK or controls. Percentage and absolute numbers of (a) CD4 TEM and (b) CD8 TEM cells. *p<0.05, **p<0.01 and ***p<0.001 when compare to control by t test. (c) Representative histograms (upper panel) and IL-17A mean fluorescence intensity (MFI – lower panel) in CD4 T cells. IFN-γ MFI in CD4 (d) and CD8 (e) T cells. *p<0.05 when compare to control by t test. Representative results of at least two independent experiments.

*DnaK impairs alloimmunity through a MARCH1-dependent modulation of donor DCs*

We tracked donor DCs *in vivo* and analyzed their MHC II and CD86 expression upon in-situ DnaK treatment. Donor DCs were tracked by two different strategies – first we tracked donor cells (I-A$^b$) by their differential MHC expression in allograft draining LN (I-A$^d$). In a different set of experiments, to control the possibility that we would not detect donor cells because they would have downregulated MHC II molecules, we transplanted skins from B6-GFP (H-2$^b$) mice into a BALB/c (H-2$^d$) hosts and tracked GFP$^+$ (donor) cells in host draining LN (Supplementary Fig. 3a,b). In both approaches, the vast majority (~99%) of

the donor cells reaching the host draining LN were DCs (CD11c$^+$ cells), and could not observe differences in migrating cell numbers between DnaK and control groups (Supplementary Fig. 3c,d). Importantly, ~85% of donor DCs that reached host draining LNs were alive (Supplementary Fig. 3e). We also measured the levels of CCR7, which is necessary for the homing of migratory DCs to the secondary lymphoid tissues[20]. Surprisingly, migratory DCs from the DnaK-treated allografts expressed superior levels of CCR7 when compared to control at 24h post-transplant (Supplementary Fig. 3f). After 96h post transplantation, CCR7 mean levels in donor DCs did not differ between DnaK and control treatments. These results suggested that our in-situ treatment did not influence migration of donor DCs to graft draining LN.

To reconcile the *in vitro* effects of MARCH1 induction and MHC II downregulation in DCs with the *in vivo* findings that DnaK delays skin allograft rejection in a MARCH1-dependent way, we examined the MHC II expression of donor DCs in mice that received DnaK-treated allografts or controls. MHC II levels were significantly reduced in migrating donor DCs from DnaK group at 24h and 96h post-transplant (Fig. 4a). In both time-points, MARCH1 was required for the MHC II downregulation in donor DCs (Fig. 4a). A similar MARCH1-dependent reduction was observed in CD86 levels (Fig. 4b). Such results indicated that we could modulate donor DCs MHC II and CD86 levels through MARCH1 by performing an in-situ treatment of the allograft prior to transplant, and thus inhibit rejection.
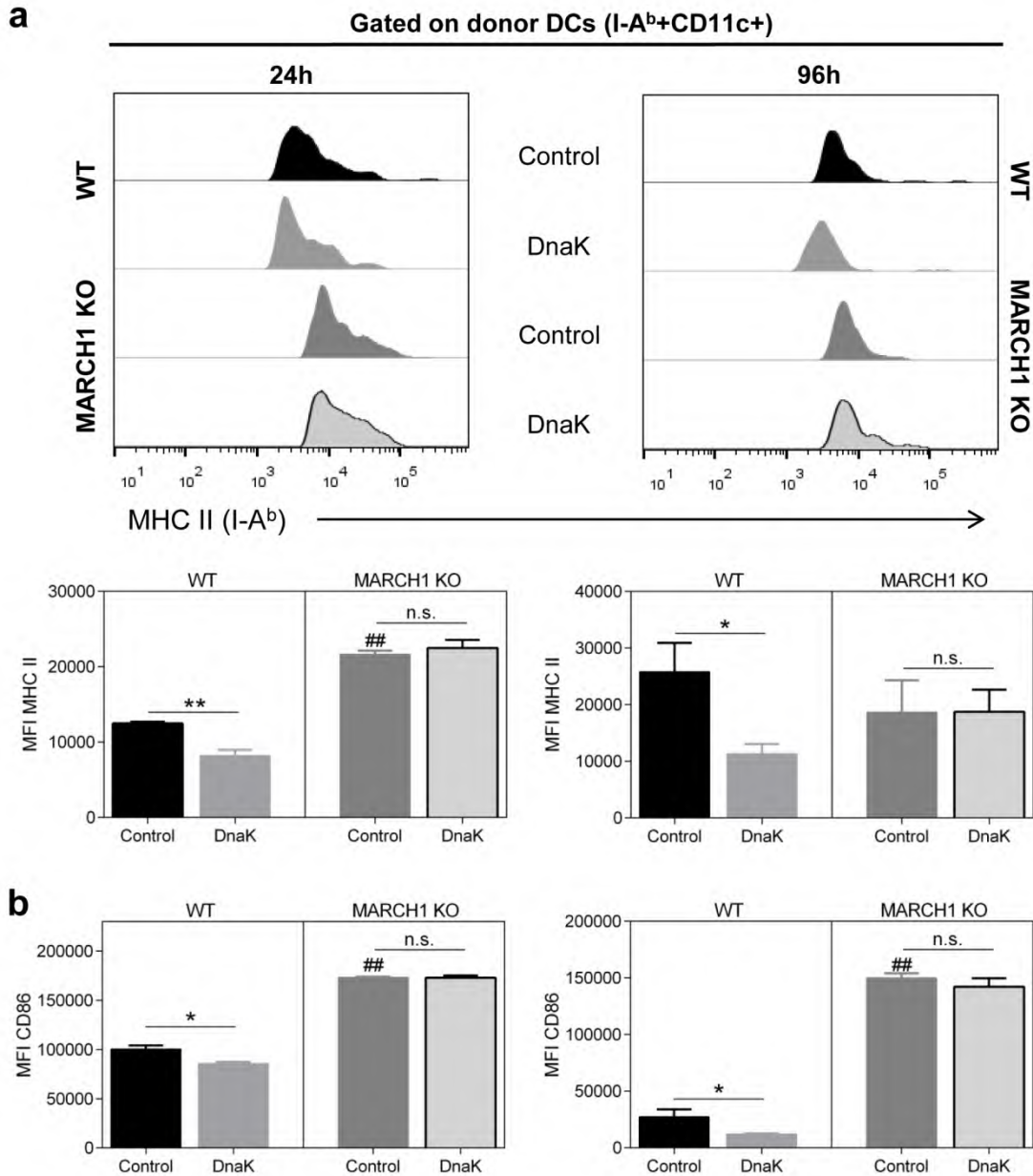
**Figure 4 | In-situ treatment downregulates MHC II and CD86 expression via MARCH1 on donor migrating DCs.** WT or MARCH1 KO (both B6) skin allografts were treated prior the transplant and MHC II (a) and CD86 (b) levels expressed by donor migrating DCs (I-A$^{b+}$CD11c$^+$ cells) were measured by flow cytometry in BALB/c recipients' draining LN at 24h or 96h post-transplant. MFI: mean fluorescence intensity. * p<0.05 and **p<0.01; #p<0.05 control MARCH1 KO compared to control WT, all by t test. Representative results of at least two independent experiments.

*MARCH1 is induced via TLR2/ERK/STAT3/IL-10 pathway in DCs*

We further investigated the underlying mechanisms by which DnaK was inducing MARCH1 and downregulating MHC II levels in DCs. IL-10 is the major anti-inflammatory cytokine[21] and it is known that IL-10 can downregulate MHC II expression[22], through the induction of MARCH1[9]. Also, DnaK has been shown to induce IL-10 expression in BMDCs[16] and its anti-inflammatory effects in murine model of arthritis depend on this cytokine[23]. We tested whether the induction of IL-10 was the mechanism driving MARCH1 induction and MHC II downregulation by DnaK. In fact, DnaK could induce both IL-10 mRNA and protein expression on DCs isolated from mice LNs (Supplementary Fig. 4a). In addition, IL-10 expression in these cells was required for DnaK-induced downregulation of MHC II (Supplementary Fig. 4b). In order to determine whether IL-10 production triggered by DnaK was responsible for MARCH1 induction, we treated WT or IL-10 KO mice DCs with DnaK and analyzed MARCH1 expression. We observed that IL-10 KO DCs treated with DnaK did not upregulate MARCH1 compared to WT DCs (Fig. 5a). The addition of recombinant murine IL-10 partially reestablished MARCH1 expression by DCs (Fig. 5a).

Once we determined that IL-10 was essential for MARCH1 induction in DnaK-treated DCs, we sought to identify the molecular pathway of IL-10-MARCH1 induction in our system. We previously demonstrated that DnaK could modulate DCs in a pathway involving TLR2, ERK and STAT3[24]. We thus investigated if DnaK-induced expression of MARCH1 was being mediated by TLR2. Indeed, TLR2 KO DCs treated with DnaK showed a significantly decreased expression of MARCH1 compared to WT DCs (Fig. 5b). Also, IL-10 production (Supplementary Fig. 5a,b) and MHC II downregulation (Supplementary Fig. 5c) by DnaK was dependent on TLR2. DnaK effects, including MARCH1 induction, were independent on TLR4 (Supplementary Fig. 5e,f,g). We further characterized downstream events in this molecular pathway. We treated BMDCs with DnaK for 15, 30, 45 minutes or left unstimulated and then analyzed the expression of p-Akt (pS473), p-STAT6 (pY641), p-ERK1/2 (pT202/pY204) and p-STAT3 (pY705). DnaK could increase p-ERK1/2 levels, peaking at 15 min post-stimulation (Fig. 5c, lane 3) and p-STAT3, peaking at 45 min. This effect was dependent on TLR2 expression by DCs (Supplementary Fig. 6a,b, respectively). To test whether these two molecules were required for MARCH1 expression induced by DnaK, we inhibited p-ERK using the MEK inhibitor – PD98059[25] and p-STAT3 with the JAK2/STAT inhibitor - AG490[26]. MARCH1 expression was completely inhibited in the PD98059- and AG490-treated LN DCs prior to DnaK stimulation (Fig. 5d). In addition, both molecular pathways were required for IL-10 production (Supplementary Fig. 6e) and MHC II downregulation (Supplementary Fig. 6f,g) in DnaK-treated LN DCs. Because p-ERK1/2 expression peaked faster than p-STAT3, we analyzed whether p-ERK was required for the increase in p-STAT3 levels. Inhibition of p-ERK by PD98059 inhibitor[25] abolished STAT3 phosphorylation upon DnaK treatment (Supplementary Fig. 6c). Because STAT3 is described to be activated by IL-10[27], we pre-

treated LN DCs with anti-IL-10R, stimulated them with DnaK and analyzed p-STAT3 levels. Blocking of IL-10R decreased p-STAT3 levels (Supplementary Fig. 6d), indicating a positive feedback loop of IL-10-induced STAT3 activation triggered by DnaK. Thus, MARCH1 induction by DnaK requires the TLR2/ERK/STAT3/IL-10 molecular pathway.

Finally, a prediction from these findings was that TLR2 and IL-10 would be required in donor cells in order to mediate the improvement in allograft survival induced by DnaK. To test that, we transplanted DnaK in-situ-treated skins from TLR2 KO mice (H-2$^b$) into BALB/c recipients (H-2$^d$). The absence of TLR2 in grafts abrogated DnaK-mediated graft protection (Fig. 5e). This result coincides with the ones obtained when we used DnaK in-situ-treated skins from IL-10 KO mice and transplanted them into BALB/c donors (H-2$^d$) hosts (Fig. 5f).

**Figure 5 | MARCH1 induction by DnaK requires the TLR2-ERK-STAT3-IL-10 pathway.** (a) LN DCs isolated from WT or IL-10 KO mice were treated with DnaK or medium. IL-10 KO DCs were also treated with DnaK + recombinant murine IL-10 for 24h. MARCH1 expression was analyzed by real time PCR. **p<0.01; ***p<0.001 by t test. (b) LN DCs isolated from WT or TLR2 KO mice were treated with DnaK or medium for 24h. MARCH1 expression was analyzed by real time PCR. ***p<0.001 compared to WT by t test. (c) BMDCs were treated with DnaK for 15, 30 and 45 min, or left unstimulated. p-Akt (pS473), p-STAT6 (pY641), p-ERK1/2 (pT202/pY204) and p-STAT3 (pY705) levels were analyzed by flow cytometry. BioHeat map generated illustrates fold change in the mean fluorescent intensity (MFI) of phosphorylated molecules. (d) WT BMDCs treated with PD98059 or AG490 were stimulated with DnaK for 24h and MARCH1 levels were analyzed by real time PCR. ***p<0.001 compared to WT by t test. In all PCRs experiments, β-actin was used as normalizer (see *Methods*). Bars are the mean ± SEM.

Experiments performed in triplicates. (e) Percent survival of skin allografts from WT B6 or IL-10 KO (H-2$^b$) mice treated with DnaK or control and transplanted into BALB/c (H-2$^d$) recipients. *p<0.05 by long-rank test. (n=6 mice per group). (f) As in (e), but donors were WT B6 or TLR2 KO (H-2$^b$). Representative results of at least two independent experiments.

## Discussion

Current therapy for transplantation, as well as autoimmunity, consists in lifelong systemic immunosuppression of the patient, leading to debilitating susceptibility to infections, tumors and metabolic disorders[28, 29]. In this study, we elucidated a molecular pathway for the induction of MARCH1, which downregulates MHC II expression in dendritic cells of a skin allograft, upon in-situ pre-treatment, significantly improving graft survival in the absence of any other immunosuppressive drugs.

Low MHC II expression not only constitutes absence of stimulation, but actively promotes tolerogenic responses[30, 31, 32]. Tolerogenic or regulatory DCs (DCregs) are characterized by the low constitutive expression of surface MHC molecules and low net expression of co-stimulatory molecules[31], which are functionally more resistant to danger signals received through TLRs, promoting apoptosis of effector T cells and generating regulatory T cells (Tregs). An extensive literature indicates the potential of DCregs to restrain the alloimmune response and promote tolerance[31]. In transplantation, different approaches have been attempted; including the administration of donor DCregs or recipients' DCregs pulsed with donor-antigen prior to transplantation[33, 34, 35]. A major risk of these approaches is of sensitizing the recipient to donor's antigens, leading to the production of alloantibodies and antibody-mediated rejection, which has been clearly documented in prior studies[36, 37].

Our *in-situ* graft pre-treatment exerts a powerful effect over rejection, through modulation of donor MHC II levels prior the transplant, leading to decreased alloreactivity. The expression of MHC II on host cells is critical for induction of rejection. Donor, but not host, MHC II expression is required for CD4 T cell-mediated rejection in a mouse model of cardiac transplant[38]Absence of surface MHC II in donor cells results in significant prolongation of primary cardiac allograft survival[39].. Nevertheless, complete eradication of donor MHC II in order to induce transplant tolerance *in vivo* has not been considered a possibility to this day[40].

Blockade of B7 ligands via CTLA4-Ig from B7 molecule family is currently being tested as a promising therapy to prevent allograft rejection[41]. However, clinical trials using this drug had unexpected results with a higher rate of acute cellular rejection[42]. This effect is thought to be due to a deleterious effect on Tregs in cardiac[43] and skin[44] transplant models. Also, memory allospecific T cells seems to be resistant to co-stimulatory blockade in a transplant context[45]. The in-situ treatment with DnaK that induces MARCH1 expression in donor APCs and leads to a downregulation of the two signals required by T cell activation – MHC II and CD86 is thus a more appealing therapeutic approach preserving co-inhibitory signals, such as B7:CTLA4, favoring long-term alloimmune regulation.

We demonstrated here that induction of MARCH1 by DnaK in DCs depends on TLR2, ERK, STAT3 and IL-10 (Supplementary Fig. 8). Although previous works have demonstrated that ERK expression could modulate IL-10 production upon signaling via TLRs[46, 47], this is the first time that ERK is implicated in the pathway of MARCH1 expression. This is also the first time that STAT3 is described to be involved in the pathway of MARCH1 expression. In our system, STAT3 activation induced by DnaK was downstream of ERK activation in this pathway. Previous studies reported STAT3 activation upon TLR2 engagement[48]. DnaK also induced MARHC1 in a IL-10-dependent manner. IL-10 is the major anti-inflammatory cytokine, and is required for early acceptance of skin allografts[49]. Co-overexpression of IL-10 and CCR7 in DCs has been linked to prolonged survival of cardiac allografts[50], and DnaK treatment led to enhanced expression of both molecules. Although it is still not clear how enhanced expression of CCR7 can promote graft acceptance. Furthermore, STAT3 has been linked to IL-10 in more than one study. In human monocyte-derived macrophages, STAT3 can bind to the *il10* promoter and induce IL-10 production[51]. In addition, IL-10 exerts its anti-inflammatory role in a STAT3 dependent manner[52]. Indeed, we saw that the signaling pathway triggered by DnaK a positive feedback loop of IL-10-induced STAT3 activation. STAT3 activators on DCs were proposed to be potential therapeutic target induction of transplant tolerance[53].

MARCH1 induction, IL-10 production, MHC II downregulation in DC and inhibition of graft rejection induced by DnaK were dependent on TLR2. Whereas MARCH1 expression is described to be downregulated upon TLR engagement[8], we could observe for the first time that signaling through TLR2 could positively induce MARCH1. Some TLR2 agonists (PGN and LTA) can lead to inflammatory responses[54], however other TLR2 ligands have been shown to be good inducers of IL-10 expression[55]. Activation of the TLR2 signaling pathway is required for induction of IL-10 in DCs stimulated with *M. tuberculosis* or with lipoproteins[56]. A recent study demonstrated that tumor-derived exosomes can express a membrane bound form of Hsp72 (mammalian counterpart of DnaK) that signals via TLR2 in MDSCs, promoting tumor evasion from immune responses[48]. We do not have evidence of TLR2 direct binding by DnaK, however our data indicate this molecule as the one mediating all the following signals that lead to the DnaK effects observed here. It is possible that DnaK binds to a membrane receptor, still unidentified, that associates with and signals through TLR2 in order to activate this pathway.

We had previously observed that inhibition of acute rejection induced by DnaK was dependent on CD4$^+$CD25$^+$ Tregs, and that subcutaneous injection of DnaK increased the percentage of Tregs in draining LN[15]. One model that would explain all these observations is that DnaK-induced MARCH1 induction, downregulation of MHC II, together with IL-10 induction, generates DCs that will favor Tregs stimulation[30, 31, 57]. Although we expected an increase in the percentage of Tregs in draining LN of mice that received DnaK-treated allografts, we did not observe it (not shown). It is possible that low amounts of antigen that

reach allograft draining LN in our system are insufficient to cause detectable Tregs proliferation. Alternatively, the activation of DnaK specific Tregs, in a number that could be below detection levels in this system, might be sufficient to promote the tolerogenic effect observed. We are currently performing experiments in which we will enrich DnaK-specific T cells with DnaKp:I-A$^b$ tetramers and try to assess their role in this response.

Although the tolerance induced by the tested in-situ treatment is not long-term, we expect that more doses of DnaK, provided locally and inducing MARCH1 in a non-invasive fashion, associated with suboptimal doses of immunosuppression represent a novel concept that is relevant for clinical management design. Furthermore, while immune checkpoint blockade inhibitors emerge as a powerful new tool for modulation in diverse conditions, not only transplants, but also tumors, autoimmunity and asthma, most therapies focus on costimulatory blockade. Prevention of signal 1, peptide:MHC, has so far been considered impractical. The molecular pathway activated by DnaK for the induction of MARCH1 has the potential to be employed in therapies for diverse chronic inflammatory diseases driven by T cells.

**Methods**

*Mice*

BALB/c (H-2[d]) and C57Bl/6 (B6, H-2[b]) mice were purchased from FEPPS (Rio Grande do Sul, BRA). MARCH1 KO[6] (H-2[b]) mice were gently provided by Dr. Jeoung-Sook Shin (University of California, San Francisco, USA). TLR2 KO and TLR4 KO (both, H-2[b]) mice were gently provided by Dr. João Santana da Silva (University of São Paulo, São Paulo, BRA). IL-10 KO (H-2[b]) mice were gently provided by Dr. Ana M. C. Faria (Federal University of Minas Gerais, Belo Horizonte, BRA). C57BL/6-GFP mice were gently provided by Dr. Gustavo B. Menezes (Federal University of Minas Gerais, Belo Horizonte, BRA). All mice used in the experiments were between females six- to ten-week old. Animals were bred and housed in individual and standard mini-isolators under specific pathogen-free conditions at School of Biosciences – PUCRS facility. All procedures were previously reviewed and approved by the Ethics Committee for the Use of Animals of Pontifícia Universidade Católica do Rio Grande do Sul (CEUA-PUCRS) under protocol ID CEUA 08/00048 and PUC-000118-15.

*Protein purification and endotoxins extraction*

Recombinant DnaK was produced with the construct pET23a(+)/MtbDnaK in BL21 *Escherichia coli* and purified according to Mehlert[58]. To remove LPS, Triton X-114 was used according to the method described in Aida *et al* [59]. Contaminating Triton X-114 was removed by incubating overnight with Bio-Beads (Bio-Rad) at 4°C with agitation. Protein concentration was determined using Qubit Protein Assay Kit (Invitrogen) and the Qubit® Fluorometer (Invitrogen). Protein integrity was analyzed by Western Blot using the anti-HSP70 antibody (clone C92F3A-5 - StressMarq, Supplementary Fig.9a). Endotoxin levels were measured during all purification processes (Supplementary Fig.9b) using a chromogenic LAL endotoxin assay kit (GenScript). Only samples with below 0.1 EU/ml were used. To check protein purity we took advantage from the fact the splenic DCs upregulates CD86 levels after 6h of intravenous injection of LPS[60]. We intravenously injected B6 mice with LPS (25µg), Bio-beads-treated PBS 1x or DnaK treated or not with Triton X-114 (both 30µg). After 6h, we sacrificed the mice and analyzed CD86 expression in splenic DCs (CD11c^{+}) by flow cytometry. LPS and not treated DnaK increased the expression of CD86 on splenic DCs. In contrast, Triton X-114-treated DnaK as well as PBS 1x could not upregulate CD86 (Supplementary Fig.9b). DnaK has an ATPase activity, so we tested our purified protein for its capacity to hydrolyse ATP. Functional DnaK (5µg) and Non Functional DnaK (5µg) were incubated in a reaction medium containing 2 mM CaCl2, 120 mM NaCl, 5 mM KCl, 10 mM glucose, 20 mM Hepes with 100µM ATP for 0, 10, 20, 60 and 120 min, pH 7.4 at 37°C. After the incubation the reaction medium was transferred to ice, followed by centrifugation for 30 min at 10,000 rpm and high-performance liquid chromatography (HPLC) analysis. HPLC analysis, 40 µl aliquots of supernatant, were applied to a reversed-phase HPLC system (Shimadzu) using C18 column

at 260 nm with a mobile phase containing 60 mM KH2PO4 (Sigma-Aldrich) and 5 mM tetrabutylammonium chloride (Sigma-Aldrich), pH 6.0, in 30% methanol. All peaks were identified by retention time compared with ATP standard curve. The control for nonenzymatic hydrolysis of nucleotides was performed by measuring the peaks present in the same reaction medium incubated without proteins. The results are expressed as total amount of the ATP (µM) in the respective incubation time (Supplementary Fig.9c).

*Skin transplant and in-situ treatment*

We performed a fully MHC-mismatched murine skin allograft model[61]. B6 WT, MARCH1 KO, IL-10 KO, TLR2 KO and TLR4 KO mice (all H-$2^b$) were used as donor. Briefly, 1 cm$^2$ sections of tail skin were removed and immersed in a PBS solution containing 60 µg/mL of purified DnaK or only PBS for 60 minutes at 4°C. BALB/c (H-$2^d$) recipients were anesthetized, and fur was shaved off the dorsal trunk. At the shaved area, 1 cm$^2$ of skin was removed in each recipient mouse and donor tail skin fragment was sutured to the exposed tissue of each recipient. Animals were kept in individual cages and observed daily, the state of graft acceptance being photographed and recorded. Graft rejection was confirmed by the observation of cyanosis, erythema, erosion, and loss of skin graft.

*Dendritic cells cultures*

CD11c+ cells were purified from spleen or LNs from B6 WT, MARCH1 KO, IL-10 KO, TLR2 KO and TLR4 KO mice. LNs were disrupted against a nylon screen and treated with Collagenase D (Roche) for 30min at 37°C. The resultant single cell suspensions were labeled with anti-CD11c (N418) magnetic beads (Miltenyi). After washing, CD11c$^+$ cells were purified by positive selection using MACS separation columns (Miltenyi). Purity of selected cells was controlled by FACS analysis. Cells were cultured in 96-well plates in serum-free medium AIM-V® (Gibco). DCs were incubated with either 30 µg/mL of DnaK or medium for 24 h and then analyzed by FACS or total RNA was extracted. The supernatant was collected and used for cytokine analysis.

DCs were grown from murine bone marrow (BMDCs) in the presence of GM-CSF and IL-4 (both from Peprotech). Cells were cultured in 24-well plates in serum-free medium AIM-V® (Gibco). On the sixth day of culture, the non-adherents cells (DCs) were separated from adherent cells. BMDCs were incubated with 30 µg/mL of DnaK, medium, 10 µg/ml of PGN (Sigma) or DnaK + recombinant murine IL-10 (20 ng; R&D System) for 24 h and then analyzed by FACS or total RNA was extracted. The supernatant was collected and used for cytokine analysis.

*Real time PCR*

Total RNA was isolated from murine dendritic cells cultures using RNAeasy kit (Qiagen). The concentration of the purified total RNA samples was measured using a Qubit RNA

Assay Kit (Invitrogen) and read in Qubit Fluorometer (Invitrogen). 50 ng of RNA was reverse transcribed with 100 U of Sensiscript (Qiagen). cDNA concentrations were measured using Qubit dsDNA HS Assay Kit (Invitrogen) and the read in Qubit Fluorometer (Invitrogen). In a final volume of 10 μL, 8 ng of cDNA was amplified using the following Taqman Gene Expression assays (Applied Biosystems): *Il10* (Mm00439614_m1), *March1* (Mm00613524_m1) and β-actin (4352933E). Quantitative real-time PCR was performed with a StepOn Real-Time PCR System (Applied Biosystems). The relative mRNA levels were calculated using the comparative $C_t$ method[62], using the house keeping gene β-actin as a normalizer. Non-treated DCs served as a reference for treated DCs.

*Immunofluorescence*

*MHC II immunoprecipitation*

*Flow cytometry*
Following antibodies were used: CD4 (GK1.5), CD8a (53-6.7), Foxp3 (MF23), Ki67 (B56), I-A$^b$ (AF6-120.1), CD11c (HL3), CD45R/B220 (RA3-6B2), CCR7 (CD197 - 4B12), p-Akt (pS473; M89-61), p-STAT6 (pY641; 18/P-Stat6), p-ERK1/2 (pT202/pY204; 20A) and p-STAT3 (pY705; 4/P-STAT3), CD44, CD62L, IL-17, IFN-γ, from BD Biosciences and from eBioscience. Cell suspensions were Fc blocked for 20 min on ice, and then surface markers were stained by incubation for 30 min with antibodies in 1% FCS in PBS on ice. Staining of Ki67 and Foxp3 was performed by using Fixation/Permeabilization kit (eBioscience). For cytokine detection, cell suspensions were pre-incubated for 4 h with 50 ng/ml of PMA (phorbol 12-myristate 13-acetate), 500 ng/ml ionomycin and GolgiStop (BD Biosciences) in complete medium before Fc blocking, followed by surface staining, permeabilization and intracellular staining of IFN-γ, and IL-17. Cells were analyzed using FACSCanto II (BD Biosciences) and BD FACSDiva software (BD Biosciences). Data obtained were analyzed using Flowjo software (version X, Tree Star).

*Phosphorylated molecules analysis*
For signaling experiments, WT or TLR2 KO BMDCs were treated with 30 μM of selective MEK inhibitor PD98059 (Cayman Chemical) for 30 minutes, or 50 μM of JAK2/STAT pathway inhibitor AG490 (Sigma) for 60 minutes or left untreated prior DnaK stimulation. Cells were stimulated with 30μg/ml of DnaK for 15, 30 or 45 min. Cells were fixed with Cytofix Buffer (BD Biosciences) for 10 minutes at 37°C and permeabilized with Phosflow Perm Buffer III (BD Biosciences) for 30 minutes on ice. Then, cells were stained for p-Akt, p-STAT6, p-ERK, and p-STAT3. Cells were analyzed using FACSCanto II (BD Biosciences) and BD FACSDiva software (BD Biosciences). BioHeat maps were generated with the web-based software Cytobank (www.cytobank.org).

*IL-10 measurement*

Supernatants of WT, TLR2 KO or TLR4 KO DCs cultures treated with DnaK or medium for 24h were analyzed for the presence of IL-10 with the CBA Mouse Inflammation kit (BD Biosciences), according to manufacturer's instructions. Cells were analyzed using FACSCanto II (BD Biosciences) and BD FACSDiva software (BD Biosciences). Data obtained were analyzed using FCAP Array software (version 3.0, BD Biosciences) and expressed in pg/ml.

*Statistical analysis*

Statistical analysis was performed using the software Prism5 (Graphpad Software Inc.). Differences between specific points were determined by the Student's *t*-test, or when appropriated, the non-parametric Mann-Whitney. The one-way ANOVA test was used to determine differences between groups. Multiple comparisons among levels were checked with Tukey post hoc tests. To analyze graft survival and determine the median survival time (MST), the Kaplan-Meier/long-rank test was used. The level of significance was set at $p < 0.05$.

**References (70)**

1.  Young JW, Koulova L, Soergel SA, Clark EA, Steinman RM, Dupont B. The B7/BB1 antigen provides one of several costimulatory signals for the activation of CD4+ T lymphocytes by human blood dendritic cells in vitro. *J Clin Invest* **90**, 229-237 (1992).

2.  Kalinski P, Hilkens CM, Wierenga EA, Kapsenberg ML. T-cell priming by type-1 and type-2 polarized dendritic cells: the concept of a third signal. *Immunol Today* **20**, 561-567 (1999).

3.  Celli S, Garcia Z, Bousso P. CD4 T cells integrate signals delivered during successive DC encounters in vivo. *The Journal of experimental medicine* **202**, 1271-1278 (2005).

4.  Safa K, Riella LV, Chandraker A. Beyond calcineurin inhibitors: emerging agents in kidney transplantation. *Curr Opin Nephrol Hypertens* **22**, 689-697 (2013).

5.  Ford ML, Adams AB, Pearson TC. Targeting co-stimulatory pathways: transplantation and autoimmunity. *Nat Rev Nephrol* **10**, 14-24 (2014).

6.  Matsuki Y*, et al.* Novel regulation of MHC class II function in B cells. *EMBO J* **26**, 846-854 (2007).

7.  De Gassart A*, et al.* MHC class II stabilization at the surface of human dendritic cells is the result of maturation-dependent MARCH I down-regulation. *Proc Natl Acad Sci U S A* **105**, 3491-3496 (2008).

8.  Tze LE*, et al.* CD83 increases MHC II and CD86 on dendritic cells by opposing IL-10-driven MARCH1-mediated ubiquitination and degradation. *The Journal of experimental medicine* **208**, 149-165 (2011).

9.  Thibodeau J*, et al.* Interleukin-10-induced MARCH1 mediates intracellular sequestration of MHC class II in monocytes. *Eur J Immunol* **38**, 1225-1230 (2008).

10. Oh J, Shin JS. Molecular mechanism and cellular function of MHCII ubiquitination. *Immunol Rev* **266**, 134-144 (2015).

11. Baravalle G*, et al.* Ubiquitination of CD86 is a key mechanism in regulating antigen presentation by dendritic cells. *J Immunol* **187**, 2966-2973 (2011).

12. Lagodzinski Z, Gorski A, Wasik M. Effect of FK506 and cyclosporine on primary and secondary skin allograft survival in mice. *Immunology* **71**, 148-150 (1990).

13. Turnquist HR, Fischer RT, Thomson AW. Pharmacological modification of dendritic cells to promote their tolerogenicity in transplantation. *Methods Mol Biol* **595**, 135-148 (2010).

14.     Turnquist HR, Raimondi G, Zahorchak AF, Fischer RT, Wang Z, Thomson AW. Rapamycin-conditioned dendritic cells are poor stimulators of allogeneic CD4+ T cells, but enrich for antigen-specific Foxp3+ T regulatory cells and promote organ transplant tolerance. *J Immunol* **178**, 7018-7031 (2007).

15.     Borges TJ, *et al.* Prolonged survival of allografts induced by mycobacterial Hsp70 is dependent on CD4+CD25+ regulatory T cells. *PLoS One* **5**, e14264 (2010).

16.     Motta A, *et al.* Mycobacterium tuberculosis heat-shock protein 70 impairs maturation of dendritic cells from bone marrow precursors, induces interleukin-10 production and inhibits T-cell proliferation in vitro. *Immunology* **121**, 462-472 (2007).

17.     Ring GH, *et al.* Interferon-gamma is necessary for initiating the acute rejection of major histocompatibility complex class II-disparate skin allografts. *Transplantation* **67**, 1362-1365 (1999).

18.     de Oliveira VL, *et al.* Humanized mouse model of skin inflammation is characterized by disturbed keratinocyte differentiation and influx of IL-17A producing T cells. *PLoS One* **7**, e45509 (2012).

19.     Chen L, *et al.* TLR signals promote IL-6/IL-17-dependent transplant rejection. *J Immunol* **182**, 6217-6225 (2009).

20.     Ohl L, *et al.* CCR7 governs skin dendritic cell migration under inflammatory and steady-state conditions. *Immunity* **21**, 279-288 (2004).

21.     Moore KW, de Waal Malefyt R, Coffman RL, O'Garra A. Interleukin-10 and the interleukin-10 receptor. *Annu Rev Immunol* **19**, 683-765 (2001).

22.     Koppelman B, Neefjes JJ, de Vries JE, de Waal Malefyt R. Interleukin-10 down-regulates MHC class II alphabeta peptide complexes at the plasma membrane of monocytes by affecting arrival and recycling. *Immunity* **7**, 861-871 (1997).

23.     Wieten L, *et al.* IL-10 is critically involved in mycobacterial HSP70 induced suppression of proteoglycan-induced arthritis. *PLoS One* **4**, e4186 (2009).

24.     Borges TJ, Lopes RL, Pinho NG, Machado FD, Souza AP, Bonorino C. Extracellular Hsp70 inhibits pro-inflammatory cytokine production by IL-10 driven down-regulation of C/EBPbeta and C/EBPdelta. *Int J Hyperthermia*, (2013).

25.     Crews CM, Alessandrini A, Erikson RL. The primary structure of MEK, a protein kinase that phosphorylates the ERK gene product. *Science* **258**, 478-480 (1992).

26. Dadi H, Ke S, Roifman CM. Activation of phosphatidylinositol-3 kinase by ligation of the interleukin-7 receptor is dependent on protein tyrosine kinase activity. *Blood* **84**, 1579-1586 (1994).

27. Niemand C*, et al.* Activation of STAT3 by IL-6 and IL-10 in primary human macrophages is differentially modulated by suppressor of cytokine signaling 3. *J Immunol* **170**, 3263-3272 (2003).

28. Page EK, Dar WA, Knechtle SJ. Tolerogenic therapies in transplantation. *Front Immunol* **3**, 198 (2012).

29. Halloran PF. Immunosuppressive drugs for kidney transplantation. *N Engl J Med* **351**, 2715-2729 (2004).

30. Steinman RM, Hawiger D, Nussenzweig MC. Tolerogenic dendritic cells. *Annu Rev Immunol* **21**, 685-711 (2003).

31. Morelli AE, Thomson AW. Tolerogenic dendritic cells and the quest for transplant tolerance. *Nature reviews Immunology* **7**, 610-621 (2007).

32. van Kooten C*, et al.* Dendritic cells as a tool to induce transplantation tolerance: obstacles and opportunities. *Transplantation* **91**, 2-7 (2011).

33. Moreau A*, et al.* Tolerogenic dendritic cells and negative vaccination in transplantation: from rodents to clinical trials. *Front Immunol* **3**, 218 (2012).

34. Vassalli G. Dendritic cell-based approaches for therapeutic immune regulation in solid-organ transplantation. *J Transplant* **2013**, 761429 (2013).

35. Svajger U, Rozman P. Tolerogenic dendritic cells: molecular and cellular mechanisms in transplantation. *J Leukoc Biol* **95**, 53-69 (2014).

36. Smyth LA*, et al.* Tolerogenic Donor-Derived Dendritic Cells Risk Sensitization In Vivo owing to Processing and Presentation by Recipient APCs. *J Immunol* **190**, 4848-4860 (2013).

37. de Kort H*, et al.* Accelerated antibody-mediated graft loss of rodent pancreatic islets after pretreatment with dexamethasone-treated immature donor dendritic cells. *Transplantation* **94**, 903-910 (2012).

38. Pietra BA, Wiseman A, Bolwerk A, Rizeq M, Gill RG. CD4 T cell-mediated cardiac allograft rejection requires donor but not host MHC class II. *J Clin Invest* **106**, 1003-1010 (2000).

39. Qian S*, et al.* Impact of donor MHC class I or class II antigen deficiency on first- and second-set rejection of mouse heart or liver allografts. *Immunology* **88**, 124-129 (1996).

40. Umemura A, Monaco AP, Maki T. Donor MHC class II antigen is essential for induction of transplantation tolerance by bone marrow cells. *J Immunol* **164**, 4452-4457 (2000).

41. Sayegh MH, Carpenter CB. Transplantation 50 years later--progress, challenges, and promises. *N Engl J Med* **351**, 2761-2766 (2004).

42. Riella LV, Sayegh MH. T-cell co-stimulatory blockade in transplantation: two steps forward one step back! *Expert Opin Biol Ther* **13**, 1557-1568 (2013).

43. Riella LV, *et al.* Deleterious effect of CTLA4-Ig on a Treg-dependent transplant model. *Am J Transplant* **12**, 846-855 (2012).

44. Charbonnier LM, Vokaer B, Lemaitre PH, Field KA, Leo O, Le Moine A. CTLA4-Ig restores rejection of MHC class-II mismatched allografts by disabling IL-2-expanded regulatory T cells. *Am J Transplant* **12**, 2313-2321 (2012).

45. Valujskikh A, Pantenburg B, Heeger PS. Primed allospecific T cells prevent the effects of costimulatory blockade on prolonged cardiac allograft survival in mice. *Am J Transplant* **2**, 501-509 (2002).

46. Kaiser F, *et al.* TPL-2 negatively regulates interferon-beta production in macrophages and myeloid dendritic cells. *The Journal of experimental medicine* **206**, 1863-1871 (2009).

47. Agrawal A, Dillon S, Denning TL, Pulendran B. ERK1-/- mice exhibit Th1 cell polarization and increased susceptibility to experimental autoimmune encephalomyelitis. *J Immunol* **176**, 5788-5796 (2006).

48. Chalmin F, *et al.* Membrane-associated Hsp72 from tumor-derived exosomes mediates STAT3-dependent immunosuppressive function of mouse and human myeloid-derived suppressor cells. *J Clin Invest* **120**, 457-471 (2010).

49. Takiishi T, Tadokoro CE, Rizzo LV, de Moraes LV. Early IL-10 production is essential for syngeneic graft acceptance. *J Leukoc Biol* **92**, 259-264 (2012).

50. Garrod KR, Chang CK, Liu FC, Brennan TV, Foster RD, Kang SM. Targeted lymphoid homing of dendritic cells is required for prolongation of allograft survival. *J Immunol* **177**, 863-868 (2006).

51. Staples KJ, *et al.* IL-10 induces IL-10 in primary human monocyte-derived macrophages via the transcription factor Stat3. *J Immunol* **178**, 4779-4785 (2007).

52. Williams L, Bradley L, Smith A, Foxwell B. Signal transducer and activator of transcription 3 is the dominant mediator of the anti-inflammatory effects of IL-10 in human macrophages. *J Immunol* **172**, 567-576 (2004).

53.     Barton BE. STAT3: a potential therapeutic target in dendritic cells for the induction of transplant tolerance. *Expert Opin Ther Targets* **10**, 459-470 (2006).

54.     Schwandner R, Dziarski R, Wesche H, Rothe M, Kirschning CJ. Peptidoglycan- and lipoteichoic acid-induced cell activation is mediated by toll-like receptor 2. *J Biol Chem* **274**, 17406-17409 (1999).

55.     Saraiva M, O'Garra A. The regulation of IL-10 production by immune cells. *Nature reviews Immunology* **10**, 170-181 (2010).

56.     Jang S, Uematsu S, Akira S, Salgame P. IL-6 and IL-10 induction from dendritic cells in response to Mycobacterium tuberculosis is predominantly dependent on TLR2-mediated recognition. *J Immunol* **173**, 3392-3397 (2004).

57.     Oh J*, et al.* MARCH1-mediated MHCII ubiquitination promotes dendritic cell selection of natural regulatory T cells. *The Journal of experimental medicine* **210**, 1069-1077 (2013).

58.     Mehlert A, Young DB. Biochemical and Antigenic Characterization of the Mycobacterium-Tuberculosis 71-Kd Antigen, a Member of the 70-Kd Heat-Shock Protein Family. *Molecular Microbiology* **3**, 125-130 (1989).

59.     Aida Y, Pabst MJ. Removal of Endotoxin from Protein Solutions by Phase-Separation Using Triton X-114. *Journal of Immunological Methods* **132**, 191-195 (1990).

60.     Khoruts A, Osness RE, Jenkins MK. IL-1 acts on antigen-presenting cells to enhance the in vivo proliferation of antigen-stimulated naive CD4 T cells via a CD28-dependent mechanism that does not involve increased expression of CD28 ligands. *Eur J Immunol* **34**, 1085-1090 (2004).

61.     Billingham RE, Medawar PB. The Technique of Free Skin Grafting in Mammals. *Journal of Experimental Biology* **28**, 385-402 (1951).

62.     Schmittgen TD, Livak KJ. Analyzing real-time PCR data by the comparative C(T) method. *Nat Protoc* **3**, 1101-1108 (2008).

63.     Murphy DB*, et al.* Monoclonal antibody detection of a major self peptide. MHC class II complex. *J Immunol* **148**, 3483-3491 (1992).

## Acknowledgements

## Author Contributions

T.J.B. helped design the study, performed experiments and helped in the manuscript. R.L.L. and R.F.Z. assisted T.J.B in the experiments. F.D.M. and M.U. transplanted the animals. A.M. performed immunofluorescence and IP experiments. G.B. assisted T.J.B in the protein purification. S.K.C. and A-P.D.S. helped interpret the results and helped in the manuscripts. L.V.R and C.B. conceived and designed the study, helped interpret the results and edited he manuscript.

## Competing Financial Interests

The authors have declared that no conflict of interest exists.

## Figure Legends

**Figure 1 | MARCH1 was induced by DnaK, but not cyclosporine A or Rapamycin in murine DCs.** (a) DCs isolated from mice lymph nodes (LN) were treated with Cyclosporine A (CsA), Rapamycin (RAPA), DnaK or recombinant murine IL-10 for 24h. After that, MARCH1 mRNA levels were analyzed by real time PCR. β-actin was used as normalizer (see Methods). ** $p<0.01$ and *** $p<0.001$ when means are compared to medium by ANOVA with Tukey post-test. (b) LN DCs were treated with DnaK or left untreated for 24h at 37°C. Cells were lysed, MHC II proteins were immunoprecipitated, and analyzed for ubiquitination or total MHC II by Western Blot. (c) Isolated DCs were grown for 48h in poly-d-Lysine coated coverslips then treated with DnaK or medium for 24h and stained for MHC II and LAMP-1. Cells were then analyzed by Confocal

microscopy. Spleen and LN DCs from WT or MARCH1 KO mice were isolated and treated with DnaK or control for 24h. After that, MHC II (d) and CD86 (e) levels were analyzed by flow cytometry.

**Figure 2 | MARCH1 is required for the decrease in alloreactivity induced by DnaK.** (a) Percent survival of skin allografts from WT B6 or MARCH1 KO (H-2$^b$) mice treated with DnaK or control and transplanted into BALB/c (H-2$^d$) recipients. *p<0.05, **p<0.01 by long-rank test. (n=5 mice per group). (b) Absolute numbers of total cells from allograft's draining lymph nodes (LN) harvested from mice that received DnaK-treated skin grafts or controls on days 1, 4, 7 and 10 post transplantation (n=3-6 mice per time-point/group). Dot graphs represent the mean ± SEM. *p<0.05 and ***p<0.001 when compare to control by t test. (c) Visual aspect of the allograft draining LN at day 7 post-transplant. Skin grafts from WT or MARCH1 KO were treated with DnaK or controls were transplanted into BALB/c mice. Percentage and absolute numbers of proliferating (d) CD4 (CD4$^+$Ki67$^+$) and (e) CD8 (CD8$^+$Ki67$^+$) T cells from allografts' draining LN harvested at 24h or 96h post-transplant. *p<0.05 and **p<0.01 when compare to control by t test. Representative results of at least two independent experiments.

**Figure 3 | Reduced alloreactive T cell responses in DnaK-treated group is impaired in MARCH1 KO mice.** Allografts' draining LN were harvested at 24h or 96h post-transplant from BALB/c mice that received skin grafts from WT or MARCH1 KO in-situ treated with DnaK or controls. Percentage and absolute numbers of (a) CD4 TEM and (b) CD8 TEM cells. *p<0.05, **p<0.01 and ***p<0.001 when compare to control by t test. (c) Representative histograms (upper panel) and IL-17A mean fluorescence intensity (MFI – lower panel) in CD4 T cells. IFN-γ MFI in CD4 (d) and CD8 (e) T cells. *p<0.05 when compare to control by t test. Representative results of at least two independent experiments.

**Figure 4 | In-situ treatment downregulates MHC II and CD86 expression via MARCH1 on donor migrating DCs.** WT or MARCH1 KO (both B6) skin allografts were treated prior the transplant and MHC II (a) and CD86 (b) levels expressed by donor migrating DCs (I-A$^{b+}$CD11c$^+$ cells) were measured by flow cytometry in BALB/c recipients' draining LN at 24h or 96h post-transplant. MFI: mean fluorescence intensity. * p<0.05 and **p<0.01; #p<0.05 control MARCH1 KO compared to control WT, all by t test. Representative results of at least two independent experiments.

**Figure 5 | MARCH1 induction by DnaK requires the TLR2-ERK-STAT3-IL-10 pathway.** (a) LN DCs isolated from WT or IL-10 KO mice were treated with DnaK or medium. IL-10 KO DCs were also treated with DnaK + recombinant murine IL-10 for 24h. MARCH1 expression was analyzed by real time PCR. **p<0.01; ***p<0.001 by t test. (b) LN DCs isolated from WT or TLR2 KO mice were treated with DnaK or medium for 24h. MARCH1 expression was analyzed by real time PCR. ***p<0.001 compared to WT by t test. (c) BMDCs were treated with DnaK for 15, 30 and 45 min, or left unstimulated. p-Akt (pS473), p-STAT6 (pY641), p-ERK1/2 (pT202/pY204) and p-STAT3 (pY705) levels were analyzed by flow cytometry. BioHeat map generated illustrates fold change in the mean fluorescent intensity (MFI) of phosphorylated molecules. (d) WT BMDCs treated with PD98059 or AG490 were stimulated with DnaK for 24h and MARCH1 levels were analyzed by real time PCR. ***p<0.001 compared to WT by t test. In all PCRs experiments, β-actin was used as normalizer (see *Methods*). Bars are the mean ± SEM. Experiments performed in triplicates. (e) Percent survival of skin allografts from WT B6 or IL-10

KO (H-2$^b$) mice treated with DnaK or control and transplanted into BALB/c (H-2$^d$) recipients. *p<0.05 by long-rank test. (n=6 mice per group). (f) As in (e), but donors were WT B6 or TLR2 KO (H-2$^b$). Representative results of at least two independent experiments.

# Supplementary Information for

# MARCH1 induction in donor DCs downregulates MHC II suppressing T cell alloreactivity and alloimmunity

Thiago J. Borges[1], Felipe D. Machado[1], Rafael L. Lopes[1], Ayesha Murshid[2], Mayuko Uehara[3], Gabriel Birrane[2,4], Rafael F. Zanin[1], Reza Abdi[3], Satoshi Ishido[5], Stuart K. Calderwood[2], Ana Paula D. Souza[6], Leonardo V. Riella[3,7*], Cristina Bonorino[1,7*]
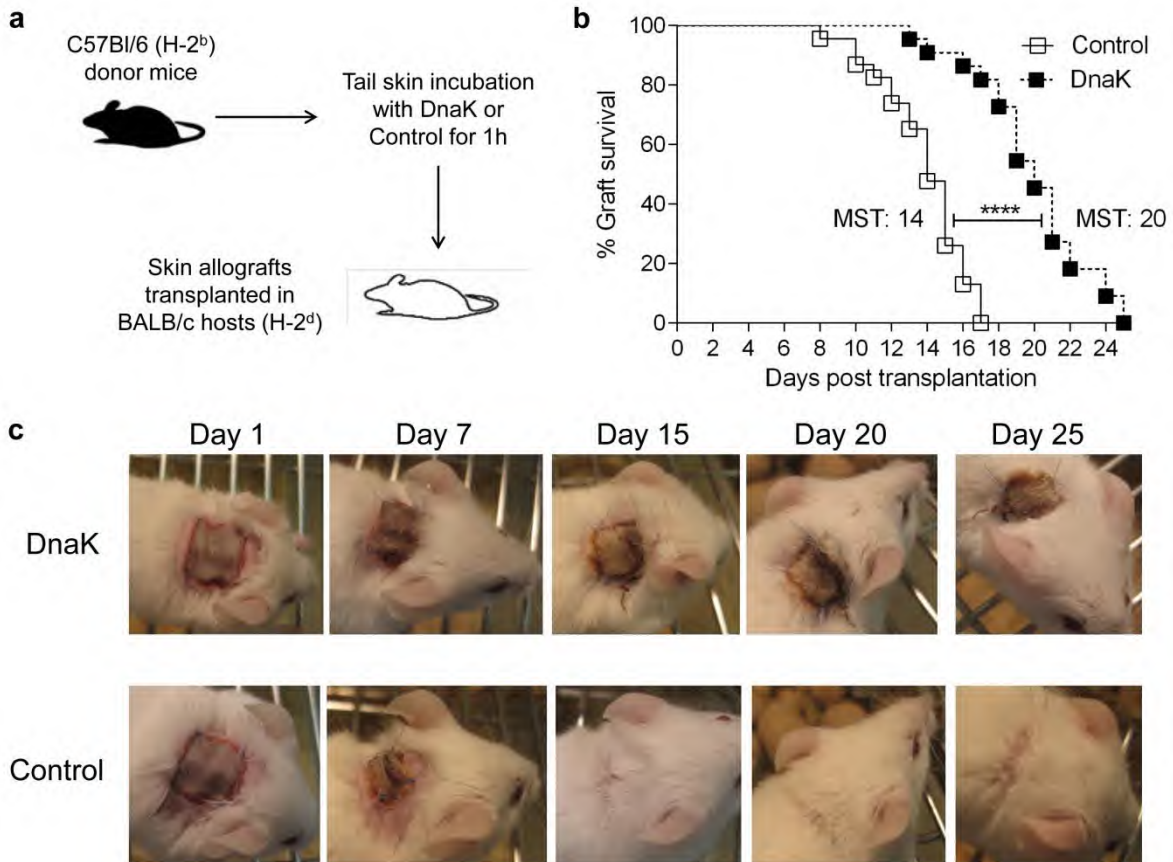
**Supplementary Figure 1 | Donor skin in-situ treatment with DnaK prior the transplant improves allograft survival.** Skin allografts from B6 mice (H-2[b]) mice were immersed in a PBS solution containing DnaK or nothing for 1h. After this period, treated skin allografts were transplanted into BALB/ hosts (H-2[d]). (a) Schematic view of the experimental design. (b) Percent of graft survival after DnaK treatment (n= 23 mice each group). ****, p>0.0001 by long-rank test. Results are pooled from three experiments (c) Aspect view of the allografts overtime.
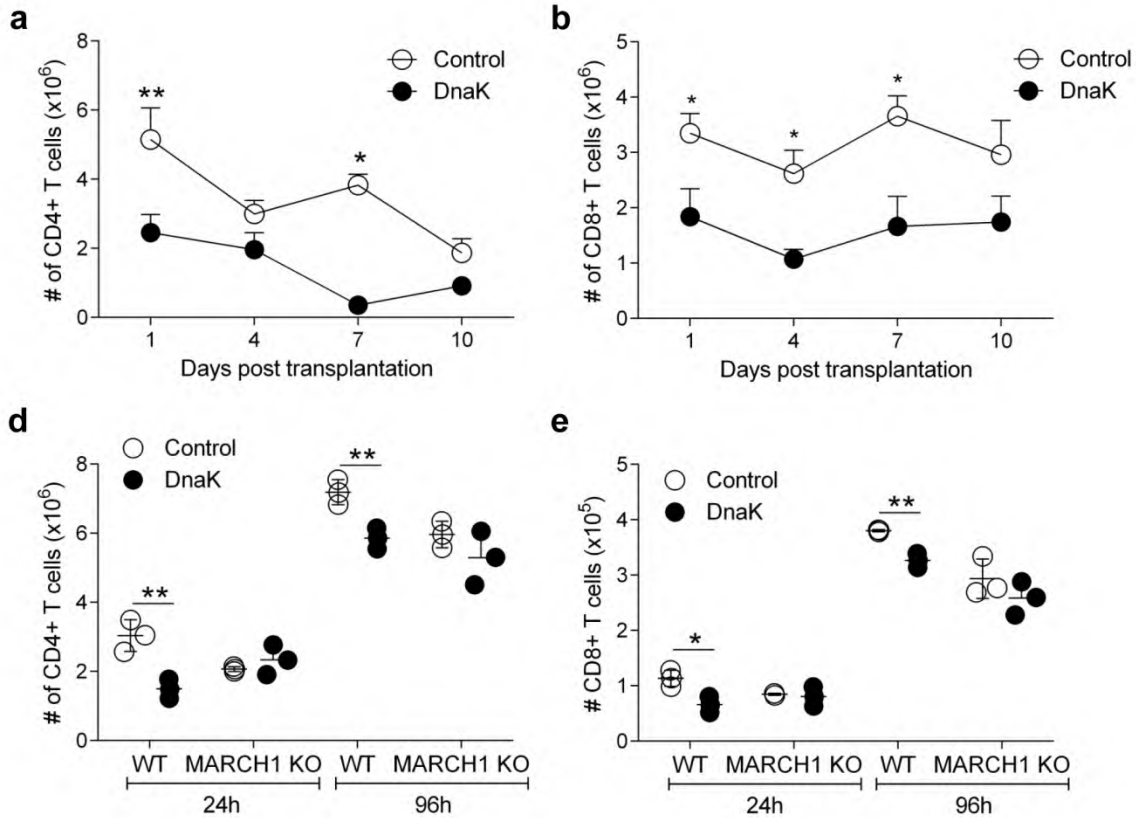
**Supplementary Figure 2 | MARCH1-dependent decrease in total numbers of draining LN CD4 and CD8 T cells in mice that received DnaK-treated allografts.** Absolute numbers of CD4 (a) and CD8 (b) T cells from allograft draining lymph nodes (LN) harvested from mice that received DnaK-treated skin grafts or controls on days 1, 4, 7 and 10 post transplantation (n=3-6 mice per time-point/group). Dot graphs represent the mean ± SEM. *p<0.05 and **p<0.01 when compare to control by t test. Skin grafts from WT or MARCH1 KO were treated with DnaK or control were transplanted into BALB/c mice. Absolute numbers of (d) CD4 and (e) CD8 T cells from allografts' draining LN harvested at 24h or 96h post-transplant. p<0.05 and **p<0.01 when compare to control by t test. Representative results of at least two independent experiments.
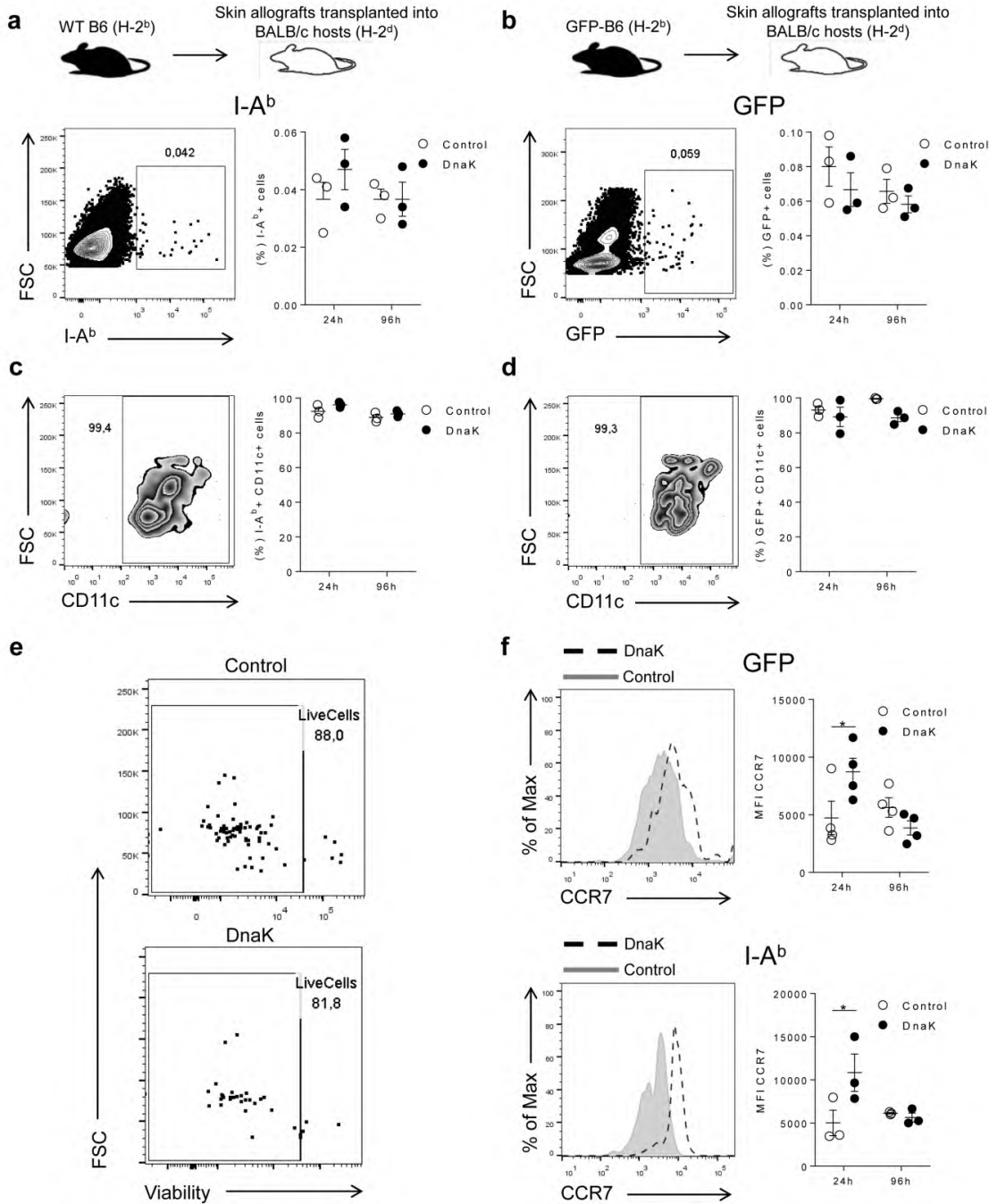
**Supplementary Figure 3 | DCs from DnaK-treated allografts skins migrate efficiently to recipient's draining LN.** Skin allografts from B6 WT or B6-GFP (H-2^b/I-A^b) mice were in-situ treated with DnaK or control prior the transplant and transplanted into BALB/c (H-2^d/I-A^d). Donor cells were tracked in allografts' draining LN, 24h or 96h post-transplantation, by (a) I-A^b or (b) GFP expression. Representative dot plots and percentages of CD11c+ cells that were I-A^{b+} (c) or GFP^+ (d) allografts' draining LN. (f) CCR7 expression on I-A^{b+} (upper panel) or GFP^+ population (lower panel) tracked in hosts' draining LN of transplanted mice. Dot graphs represent the mean ± SEM. *p<0.05. Representative results of at least two independent experiments.
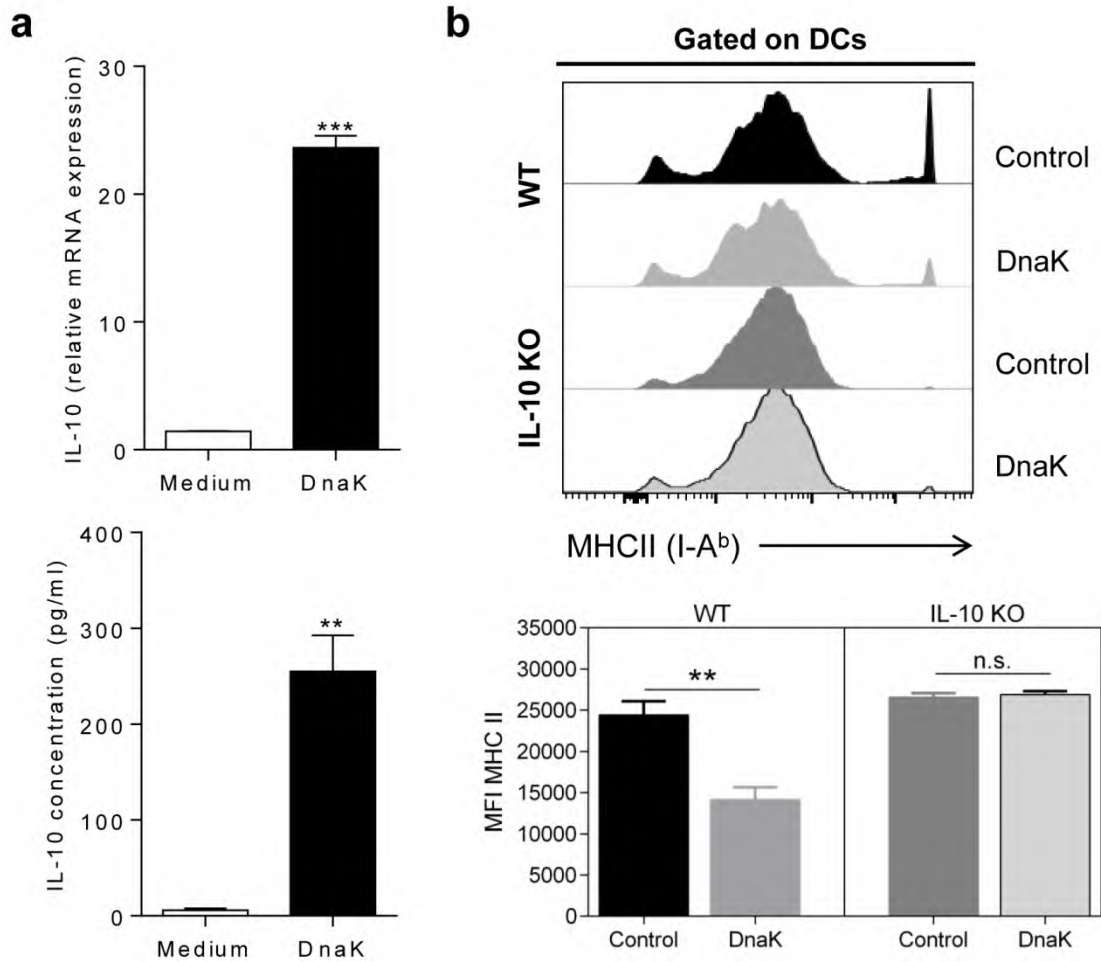
**Supplementary Figure 4 | IL-10 induction by DnaK is crucial MHC II downregulation in DCs.**
(a) DCs isolated from mice lymph nodes (LN) were treated with DnaK or control for 24h. After that, IL-10 mRNA levels were analyzed by real time PCR. β-actin was used as normalizer (see *Methods* – upper panel). IL-10 concentration was also measured in the supernatant by flow cytometry (lower panel). (b) Representative histograms (upper panel) and MHC II (I-A$^b$) mean fluorescence intensity (MFI – right panel) of DCs isolated from LN of WT or IL-10 KO mice and treated with DnaK or control for 24h. Data are presented as the mean ± SEM. ** p<0.01 and *** p<0.001 when compare to medium/control by t test. Representative results from at least two independent experiments.
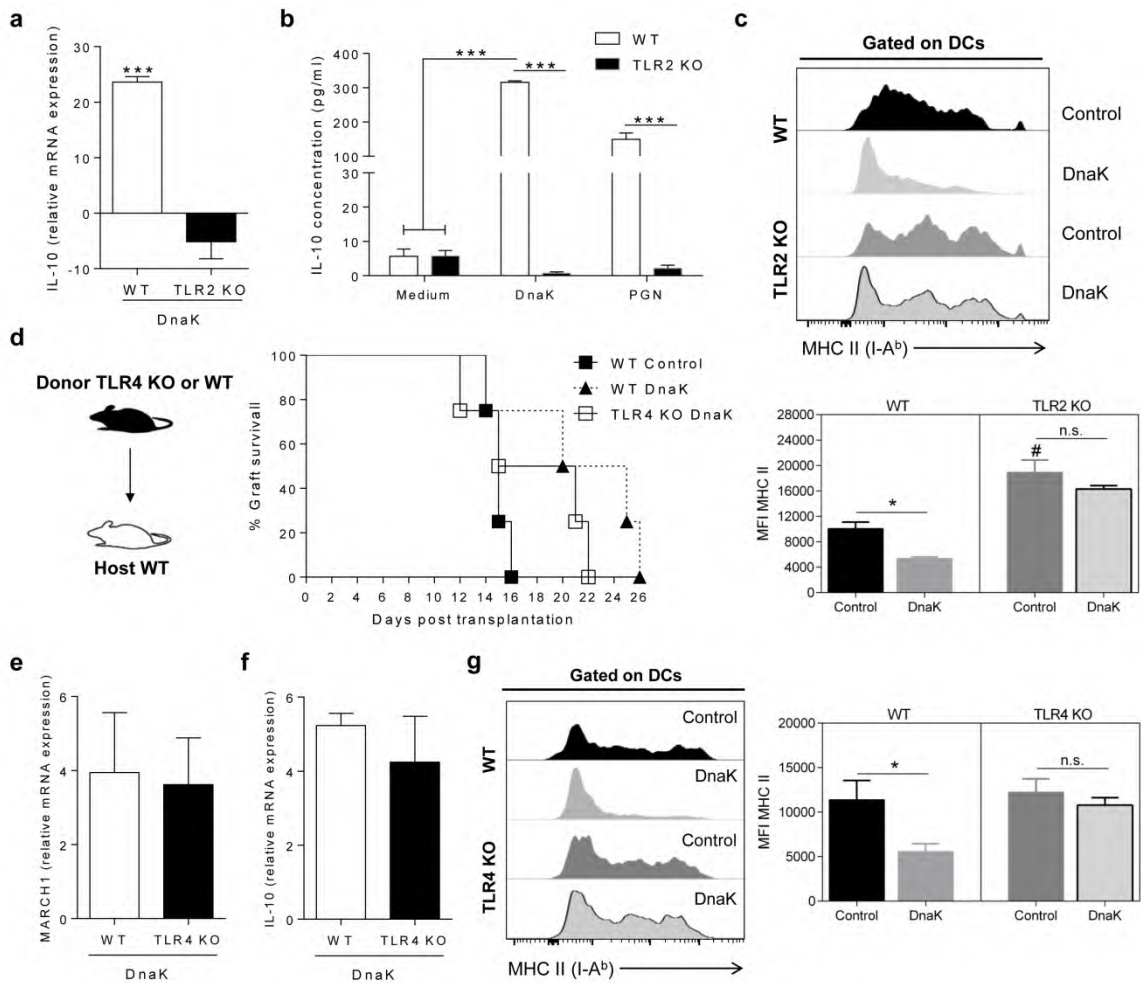
**Supplementary Figure 5 | TLR2, but not TLR4, is required for IL-10 production and MHC II downregulation induced by DnaK.** (a) DCs isolated from lymph nodes (LN) of WT or TLR2 KO mice were treated with DnaK or control for 24h, and IL-10 mRNA levels were analyzed by real time PCR. β-actin was used as normalizer (see Methods). *** $p<0.001$ when compare to WT by t test. (b) LN DCs from WT or TLR2 KO mice were treated with DnaK, PGN or control for 24h and IL-10 concentration was also measured in culture supernatants. ***$p<0.001$ when compare to WT/medium by t test. (c) Representative histograms (upper panel) and MHC II (I-A$^b$) mean fluorescence intensity (MFI – lower panel) of DCs isolated from LN of WT or TLR2 KO mice and treated with DnaK or control for 24h. *$p<0.05$ DnaK compare with control; #, $p<0.05$ control TLR2 KO compared with control WT, all by t test. (d) Skin allografts from WT or TLR4 KO (H-2$^b$) mice were immersed in a solution containing DnaK or control for 1h and transplanted into BALB/C (H-2$^d$). Data represented as the percent of graft survival after DnaK treatment (n= 4 mice each group). DCs isolated from lymph nodes (LN) of WT or TLR4 KO mice were treated with DnaK or control for 24h, and MARCH1 (e) or IL-10 (f) mRNA levels were analyzed by real time PCR. β-actin was used as normalizer. (g) Representative histograms (left panel) and MHC II (I-A$^b$) mean fluorescence intensity (MFI – right panel) of DCs isolated from LN of WT or TLR4 KO mice and treated with DnaK or control for 24h. *$p<0.05$ when compare to control by t test. All data are presented as the mean ± SEM. Representative results from at least two independent experiments.

78
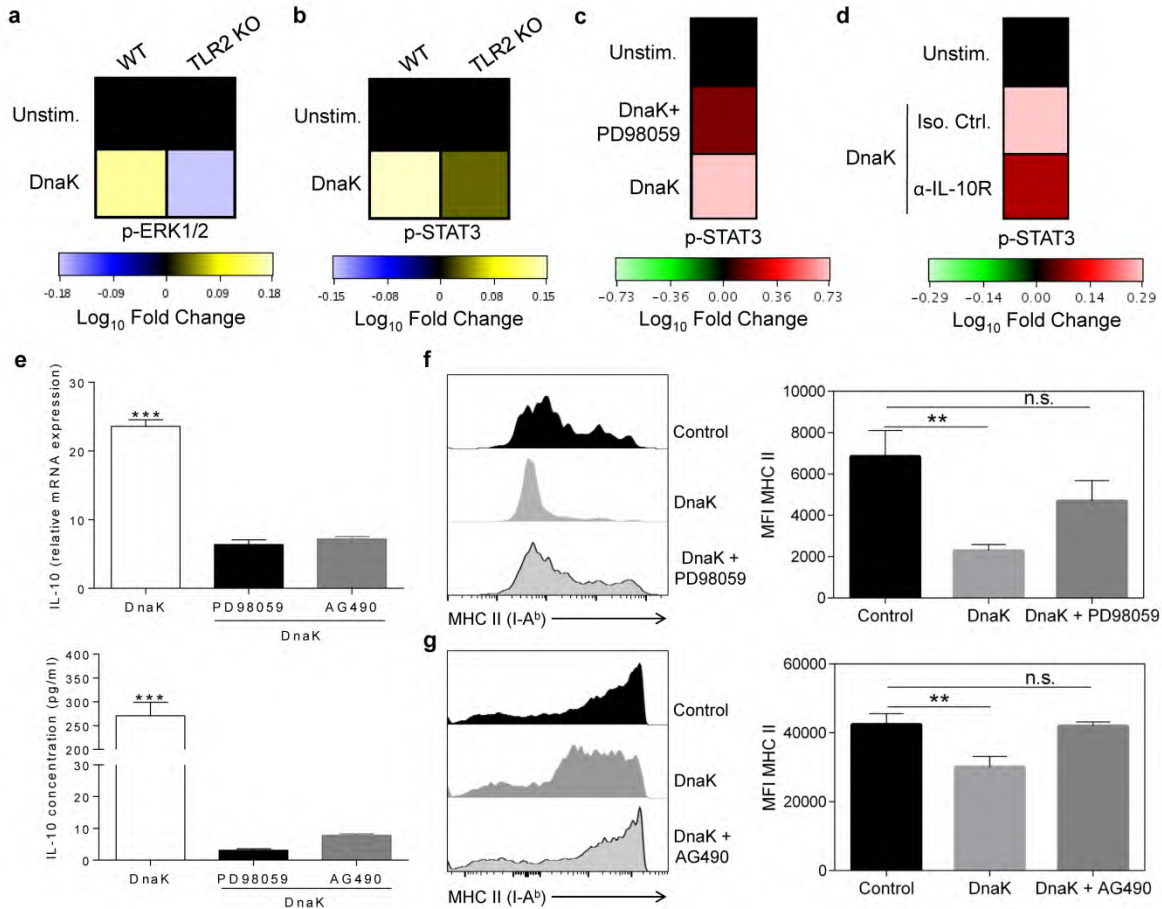
**Supplementary Figure 6 | ERK1/2-dependent STAT3 activation is required for IL-10 production and MHC II downregulation induced by DnaK.** BMDCs from WT or TLR2 KO mice were treated with DnaK or control for 24h, and (a) p-ERK1/2 (pT202/pY204) and (b) p-STAT3 (pY705) levels were analyzed by flow cytometry. WT BMDCs treated with (c) PD98059 or α-IL-10R and then stimulated with DnaK for 24h. After that, p-STAT3 (pY705) levels were analyzed by flow cytometry. WT BMDCs treated with PD98059 or AG490 were stimulated with DnaK or control for 24h and (e, upper) IL-10 mRNA, (e, lower) IL-10 production or (f, g) MHC II levels were analyzed. **p>0.01 and ***p>0.001 by t test. In PCRs experiments, β-actin was used as normalizer (see *Methods*). Bars are the mean ± SEM. Experiments performed in triplicates.
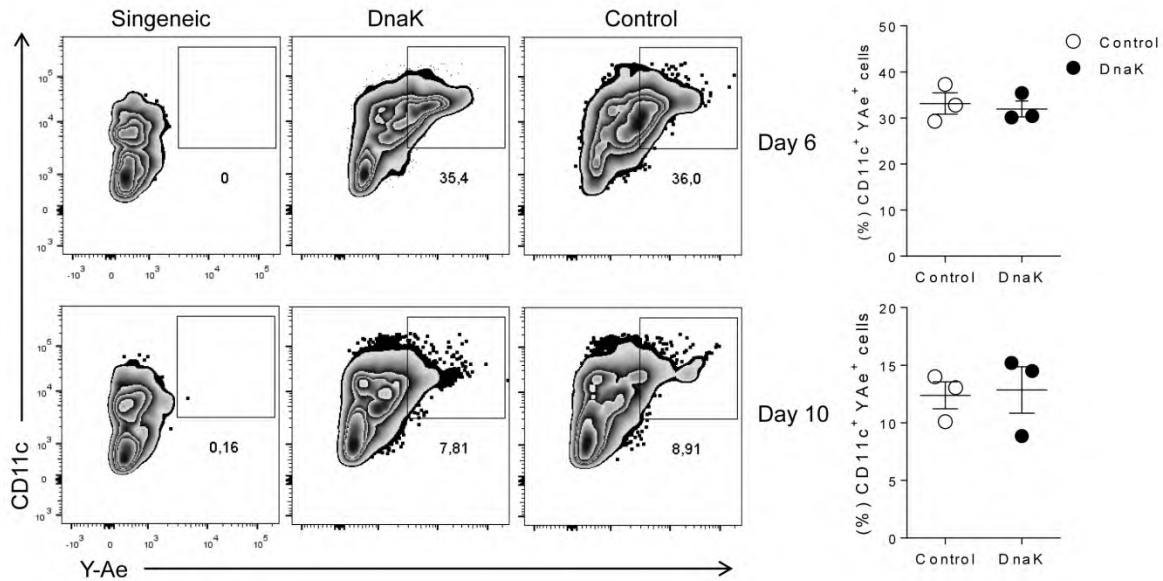
**Supplementary Figure 7 | In-situ DnaK treatment does not affect the p:MHC levels of recipients' cells that acquires an allograft's antigen.** We performed skin transplants of BALB/c donor skin into C57Bl/6 hosts, and analyzed antigen presentation using the Y-Ae antibody at day 6 and day 10 post-transplant. This antibody recognizes a peptide the 52–68 fragment of the α-chain of I-E MHC II molecules (the Eα$_{52-68}$ peptide) bound on the I-A$^b$ MHC II molecule[63].
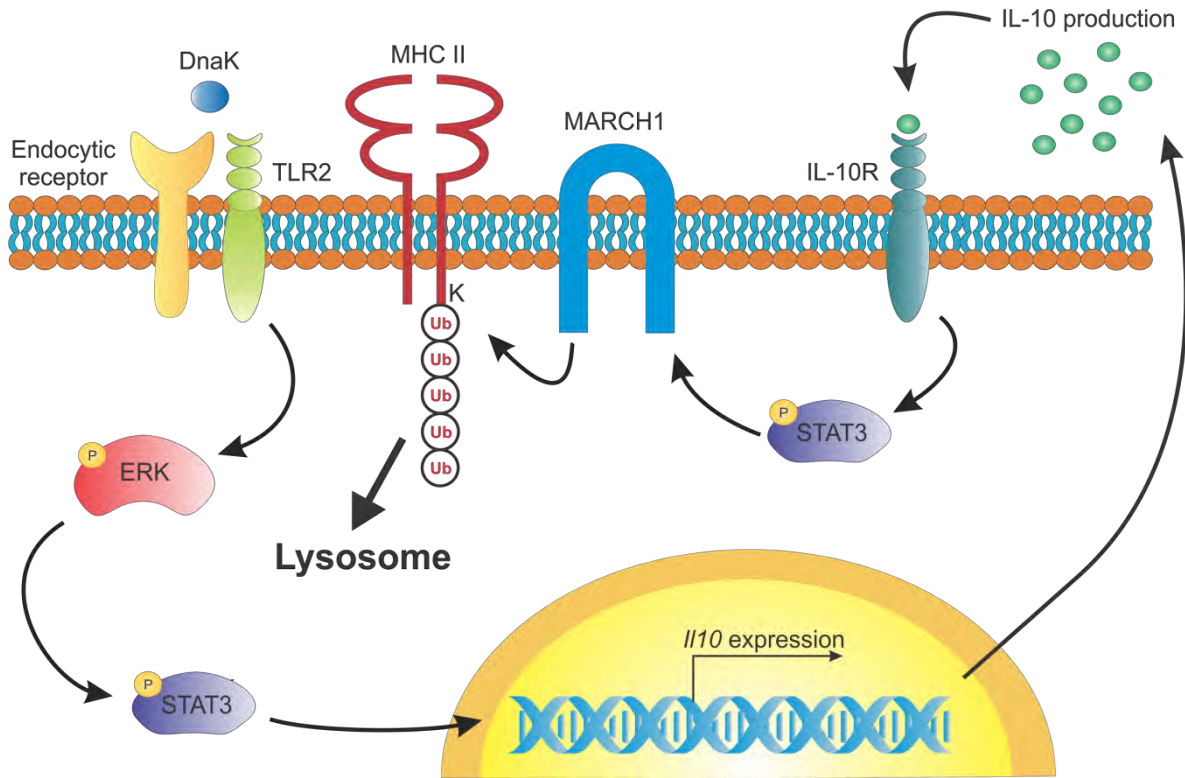
**Supplementary Figure 8 | DnaK induced IL-10-driven MARCH1 expression in DCs via ERK and STAT3 upon TLR2 engagement, causing MHC II ubiquitination and surface downregulation.** Schematic representation of the model pathway described in this study. DnaK can signal through TLR2 in DCs, or an endocytic receptor, that cooperates with TLR2. This triggers ERK and STAT3 activation, enhancing the expression of the *il10* gene and IL-10 production. IL-10 production leads to a positive feedback activation of STAT3 via IL-10R with a subsequent increase in MARCH1 expression, increase in MHC II ubiquitination and downregulating MHC II expression on the membrane surface.
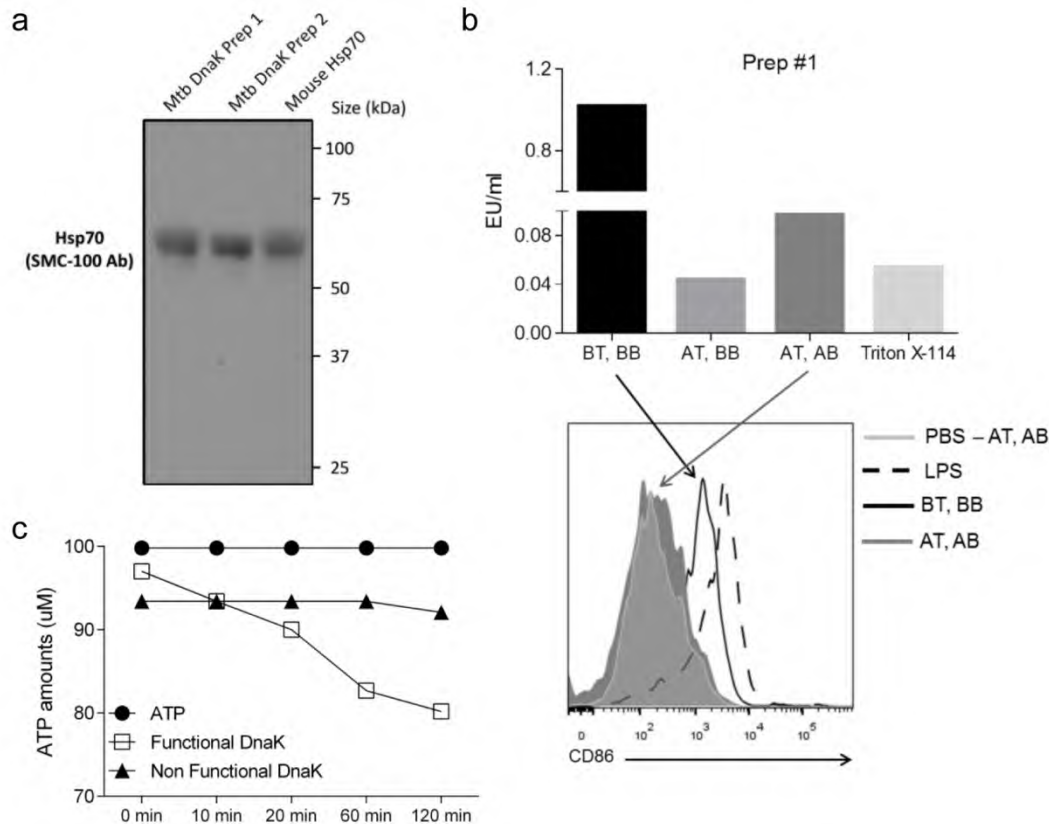
**Supplementary Figure 9 | DnaK purification controls.** Purified DnaK was Western blotted using SMC-100 antibody. (b, upper) Endotoxin levels of DnaK preparation at all purification stages: BT, BB (before Triton, before beads); AT, BB (after Triton, before beads); AT, AB (after Triton and after beads incubation) or only Triton X-114 as a control. (b, lower) B6 mice were intravenously injected with LPS (25µg), Bio-beads-treated PBS 1x or DnaK treated or not with Triton X-114 (both 30µg). After 6h, mice were sacrificed and CD86 expression was analyzed in splenic CD11c+ cells by flow cytometry. (c) Evaluation of ATP hydrolysis by functional DnaK or non-functional DnaK. Proteins (5µg) were incubated with 100µM ATP and were analyzed by HPLC after treatment times 0, 10, 20, 60 and 120 min. The results are expressed as total amount of the ATP (µM) in the respective incubation time.

# CAPÍTULO 3

Lack of Donor Batf3-dependent DCs Dampens Skin Allograft Rejection due to Impaired Activation of CD8 T cells

**Autores:** Thiago J. Borges, Mayuko Uehara, Felipe D. Machado, Rafael L. Lopes, Priscilla Vianna, José Artur Bogo Chies, Reza Abdi, Cristina Bonorino[*], Leonardo V. Riella[*]

[*] Co-senior author

**Motivação:** Esses dados surgiram quando estávamos mapeando qual subtipo de célula dendrítica da pele a DnaK modulava. Nessa busca, observamos que tanto em controles como animais tratados, a migração de um subtipo de DCs do doador predominava em relação aos outros – as DCs CD103+ migratórias. Com isso, exploramos mais esses achados utilizando animais que não possuem o fator de transcrição Batf3 e, portanto não desenvolvem células dendríticas dos subtipos CD8α+ (residentes) e CD103+ (migratórias). Como a pele não possui células CD8α+, quando utilizamos animais Batf3 nocautes como doadores, utilizamos um tecido que continha todos os subtipos de DCs da pele, menos o CD103+. Portanto, conseguimos estudar especificamente seu papel na resposta de rejeição de pele.

# Lack of Donor Batf3-dependent DCs Dampens Skin Allograft Rejection due to an Impaired Activation of CD8 T cells

Thiago J. Borges[1,2], Mayuko Uehara[2], Felipe D. Machado[1], Rafael L. Lopes[1], Priscilla Vianna[3], José Artur Bogo Chies[3], Reza Abdi[2], Cristina Bonorino[1,4*], Leonardo V. Riella[2,4*]

[1] School of Biosciences and Biomedical Research Institute, Pontifícia Universidade Católica do Rio Grande do Sul - PUCRS, Porto Alegre, RS, Brazil

[2] Schuster Family Transplantation Research Center, Renal Division, Brigham and Women's Hospital, Harvard Medical School, Boston, Massachusetts, USA

[3] Genetics Department and Post-Graduation Program in Genetics and Molecular Biology, Universidade Federal do Rio Grande do Sul, Porto Alegre, RS, Brazil

[4] Co-senior author


*Address for Correspondence: Leonardo V. Riella, MD, PhD

Email: lriella@bwh.harvard.edu

221 Longwood Ave, Boston MA 02115, USA.

Tel: +1 617-732-5252; Fax: +1 617-732-5254


*Address for Correspondence: Cristina Bonorino, PhD

Email: cbonorino@pucrs.br

Av. Ipiranga, 6690 - Jardim Botânico - Porto Alegre, RS, Brazil - CEP: 90610-000.

Tel +55 51-3320-3000, ext. 2725

**Abstract (200)**

Skin transplants are the most immunogenic of all transplants and donor DCs play a crucial role in activating effector alloreactive T cells and initiating rejection. However, the role of specific donor DC subsets in the alloimmune response requires further investigation. Strategies to modulate donor DC subsets prior the transplant may yield a new therapeutic approach in skin and vascular composite allograft (VCAs).

We found that donor skins lacking Batf3-dependent DCs were less immunogenic when transplanted into fully mismatched recipients. This effect was due to an impaired priming, activation and differentiation of alloreactive T cells, mainly CD8+ T cells. We also found that donor tissue-memory T cells could migrate to draining lymph node in the transplant context and the absence of Baf3-dependent DCs in donor skins led to decreased alloproliferation of these cells. Finally, *in-situ* treatment of donor skins with mycobacterial protein DnaK delayed rejection by inducing MARCH1 and decreasing MHC II expression exclusively on donor CD103+ DCs.

In sum, we found that Batf3-dependent DCs are crucial for initiation of skin rejection and have established a immune modulatory in-situ therapeutic strategy that targets donor CD103+ DCs and could be translated to VCA organs prior to transplantation, minimizing the need for systemic immunosuppression.

**Introduction**

Skin is the most immunogenic of all transplants and its high immunogenicity is related to the numerous APCs contained in both epidermis and dermis (1, 2). In particular, dendritic cells (DCs) are responsible for the initiation of adaptive immune responses, delivering the required signals for specific T cell activation in secondary lymphoid organs. In this process, donor DCs (the classic passenger leukocytes) are initially activated in the setting of inflammation and tissue ischemic injury, and then migrate from the graft to the recipient's draining lymph node (dLN) to induce direct activation of alloreactive T cells (1, 3, 4).

DCs are a heterogeneous population of antigen-presenting cells (APCs) that may have either protective or deleterious role in the immune response. In skin, three major distinct subsets of DCs have been described two dermal and one epidermal subset. Dermal DCs are typically either CD11b+CD103-Langerin- or CD11b-CD103+Langerin+; epidermal DCs are Langerhan's cells (LCs), which are CD11b+ CD103-Langerin+ (5). These skin-resident DC subsets have distinct stimulatory capacities, promoting different T cell polarization for the same antigen (6). The CD103+ DC subset is a tissue-resident DC and corresponds to the same lineage of the CD8α+ DC subset in secondary lymphoid organs, and both require the transcription factor Batf3 for their development in mice (7). Batf3-dependent or CD103+ DCs were reported to have a role in the pathogenesis of several disorders such as type 1 diabetes (8), asthma (9) and viral infections (10). However, in a steady-state, Batf3-dependent DCs can exert opposite roles. Murine Batf3-dependent DCs can induce tolerance to circulating OVA antigens in renal draining lymph nodes (11). One study (12) reported that LCs are not necessary for allograft rejection, probably because they remain stuck in the graft epidermis (13). Nonetheless, the precise role for each subset of dermal DCs in transplant rejection has not been fully determined. Identifying the different donor subsets involved in the skin alloimmune responses is crucial in order to optimize therapeutic interventions.

We found that donor CD103+CD207+ DCs was the predominant subset capable to migrate into host dLN early after skin transplant. Also, donor skins lacking Batf3-dependent DCs could survive more in fully MHC-mismatched hosts. In addition, hosts that received skins from Batf3 KO mice presented a decreased T cell alloreactivity. An in-situ treatment that

targets and modulates donor dermal CD103+ DCs prolonged graft acceptance in a similar fashion as Batf3 KO donor skins. Thus, our findings suggest that Batf3-dependent DCs play a critical role in the initiation of acute rejection and its modulation could be a novel strategy to improve graft acceptance.

**Materials and Methods**

*Mice*

C57BL/6 (H-$2^b$, B6) and BALB/c (H-$2^d$) mice were purchased from Jackson Laboratory. Batf3 $^{-/-}$ (KO) mice on the B6 background were maintained as a breeding colony in our animal facility. All mice were 8–12 weeks of age and housed in accordance with Institutional and National Institutes of Health guidelines.

*Skin grafting*

Skin transplantation was performed as previously described in (14). Briefly, full-thickness donor tail-skin pieces (~1 cm$^2$ – H-$2^b$) were grafted on the flank of the recipients (BALB/c, H-$2^d$). For *in-situ* DnaK treatment donor skins were removed and immersed in a PBS solution containing 60 µg/mL of purified DnaK or only PBS for 60 minutes at 4°C, prior the transplant. The time point of rejection was defined as the complete necrosis of the graft.

*Flow cytometry*

We used the following antibodies: CD4 (GK1.5), CD8a (53-6.7), Ki67 (B56), I-A$^b$ (AF6-120.1), CD11c (HL3), CD45R/B220 (RA3-6B2), CD11b, CD103 (M290), CD44, CD62L, IL-17, IFN-g, Granzyme B, KLRG1 from BD Biosciences; Cell suspensions were Fc blocked for 20 min on ice, and then surface markers were stained by incubation for 30 min with antibodies in 1% FCS in PBS on ice. Staining of Ki67 and Foxp3 was performed by using Fixation/Permeabilization kit (eBioscience). For cytokine detection, cell suspensions were pre-incubated for 4 h with 50 ng/ml of PMA (phorbol 12-myristate 13-acetate), 500 ng/ml ionomycin and GolgiStop (BD Biosciences) in complete medium before Fc blocking, followed by surface staining, permeabilization and intracellular staining of IFN-γ, and IL-17. Cells were analyzed using FACSCanto II (BD Biosciences) and BD FACSDiva software (BD Biosciences). Data obtained were analyzed using Flowjo software (version X, Tree Star).

*DnaK purification and endotoxins extraction*

Recombinant DnaK was produced with the construct pET23a(+)/MtbDnaK in XL1-blue *Escherichia coli* and purified according to Mehlert (15). To remove LPS, Triton X-114 was used according to the method described in Aida *et al* (16). Contaminating Triton X-114 was removed by incubating overnight with Bio-Beads (Bio-Rad) at $4^o$C with agitation. Protein concentration was determined using Qubit Protein Assay Kit (Invitrogen) and the Qubit® Fluorometer (Invitrogen). Protein integrity was analyzed by Western Blot using the anti-HSP70 antibody (clone C92F3A-5 - StressMarq. Endotoxin levels were measured using a chromogenic LAL endotoxin assay kit (GenScript). Only samples with below 0.1 EU/ml were used.

*Cell sorting*

Dendritic cells were purified from skin draining lymph node; organs were disrupted against a nylon screen and treated with Collagenase D (Roche) for 30min at 37°C. The resultant single cell suspensions were FcR blocked and labeled with anti-CD11c (N418) magnetic beads (Miltenyi Biotech). After washing, CD11c$^+$ cells were purified by positive selection using MACS separation columns (Miltenyi). After that, cells were stained for viability, CD11c, CD11b, CD103 and Langerin. CD11c+CD11b+CD103-Langerin- or CD11c+CD11b-CD103+Langerin+ live cells were isolated by flow cell sorting with greater than 90% purity, using a FACS Aria II (BD Biosciences) and BD FACSDiva software (BD Biosciences).

*MARCH1 real time PCR*

Total RNA was isolated from murine dendritic cells cultures using RNAeasy kit (Qiagen). 50 ng of RNA was reverse transcribed with 100 U of Sensiscript (Qiagen). In a final volume of 10 µL, 8 ng of cDNA was amplified using the following Taqman Gene

Expression assays (Applied Biosystems): *March1* (Mm00613524_m1) and β-actin (4352933E). Quantitative real-time PCR was performed with a StepOn Real-Time PCR System (Applied Biosystems). The relative mRNA levels were calculated using the comparative $C_t$ method (17), using the house keeping gene β-actin as a normalizer. Non-treated DCs of each subset served as a reference for treated DCs.

*Statistical methods*

Graft survival was expressed graphically using the Kaplan–Meier method, and statistical differences in survival between the groups were assessed by the log-rank test. A $p<0.05$ was considered statistically significant. Student *t test* was used for comparison of means. The one-way ANOVA test was used to determine differences between groups. Multiple comparisons among levels were checked with Tukey post hoc tests. Statistical analysis was performed using the software Prism5 (Graphpad Software Inc.).

## Results

*CD207+CD103+ DCs are the main donor DC subsets found in hosts' dLN*

We first characterized donor migratory DCs that reach hosts' draining LNs (dLN). So, we initialy performed fully MHC-mismatched skin transplants from B6 donors (H-2$^b$) into BALB/c hosts (H-2$^d$). We then tracked the presence of donor cells by analyzing the expression of I-A$^b$ in hosts' dLNs at 24 hours post-transplant. We found that CD103+ DC subset was the prominent donor skin subset (Fig. 1A, B). Donor DCs were CD11c+CD207(Langerin)+CD11b-CD103+ (Figure 1C). To evaluate the role of donor dermal CD103+CD207+ DCs in skin transplant, we transplanted skins from Batf3 KO mice (H-2$^b$), which lacks peripheral CD103+ DCs (7), into BALB/c hosts (H-2$^d$). There was no donor CD103+CD207+ DCs in dLN of mice that received Batf3 KO skins (Figure 1, B and C). We also observed a reduced percentage of total donor cells (I-A$^b$+) and donor DCs (I-A$^b$+CD11c+) in hosts' dLN received skins from Batf3 KO donors (Figure 1D). Thus, these data indicate that donor Batf3-dependent DCs is the major DC subset reaching hosts' dLN after skin transplant.
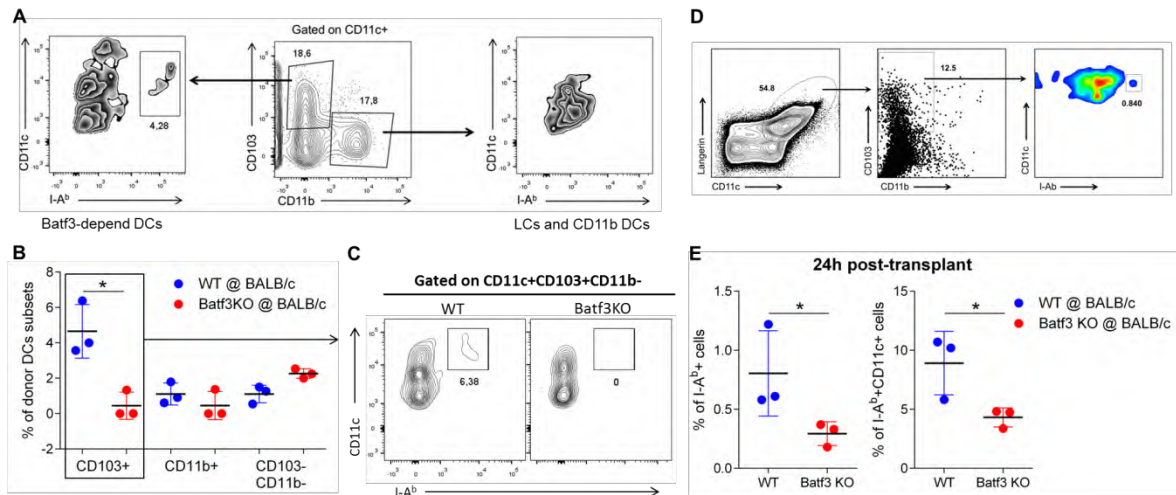


**Figure 1. CD207+CD11b-CD103+ cells are the predominant donor migrating DC subset reaching allografts' draining lymph nodes after skin transplant.** Skin allografts from WT B6 or Batf3KO (I-A$^b$) mice were transplanted into BALB/c (I-A$^d$) recipients. (**A**) Gating strategy for tracking donor DC subsets in recipients' draining lymph nodes, based on I-A$^b$ expression at 24h post-transplant. (B) Quantification of DCs subsets gated as in (**A**). *p<0.05 when compare to WT by ANOVA with Tukey post-test. (n=3 mice per group). (**C**) Representative dot plots of I-A$^b$

expression gated on CD103+ DCs from draining lymph nodes of mice that received WT or Batf3 KO skins, 24h post-transplant. (**D**) Gating strategy confirming the phenotype of donor DCs as CD11c+Langerin+CD103+CD11b-. (**E**) Percentage of I-A$^b$+ (left) and I-A$^b$+CD11c+ cells (right) isolated from draining lymph nodes of mice that received WT or Batf3 KO skins, 24h post-transplant. *p<0.05 when compare to WT by t test. (n=3 mice per group).

*Donors Batf3-dependent DCs initiate acute skin rejection*

In light of these interesting findings, we then investigated the requirement of Batf3-dependent donor DCs in initiating rejection responses early after skin transplant. We transplanted WT or Batf3 KO skins (H-2$^b$) into BALB/c hosts (H-2$^d$). We observed that mice that received Batf3 KO skins presented an increased allograft survival compared to WT skins, with a median survival time (MST) of 19 days compared with 11 days, respectively (n=5 per group; *p=0.0019*) (Figure 2, A and B). To elucidate the mechanism underlying the delayed rejection with Batf3 KO skin, we immunophenotyped lymphocytes isolated from allografts' dLNs at day 1, 7 or 25 post-transplant. Analysis of the LNs of recipients that received Batf3 KO skins revealed a significant reduction in the percentage of proliferating CD8 T cells (CD8$^+$Ki67$^+$ cells) at all time-points compared to WT (Figure 2C). Furthermore, there was a decrease in the CD8 effector memory T cells (CD8 TEM – CD8$^+$CD62L$^-$CD44$^+$ cells) at day 1 and 7, with no change at day 25 post-transplant, in allografts' dLN from mice that received Batf3 KO skin compared to WT (Figure 2D). Interestingly, in the recipients of Batf3 KO skins, we observed a significant, but less prominent, decrease in proliferating-CD4 T cells at day 7 post-transplant (Suppl. Figure 1A). We observed a reduction in CD4 TEM cells at day 7 post-transplant, but no changes at day 1 and 25 (Suppl. Figure 1B). These findings led us to investigate whether T cells were being less primed due to the lack of CD103$^+$ DCs in the skin. To confirm that, we analyzed the expression of CD69 – an early T cell activation marker – in CD8 T cells. We found that at day 7 post-transplant the percentage of CD4$^+$CD69$^+$ and CD8$^+$CD69$^+$ cells were significantly decreased in the allografts' dLNs of mice that received Batf3 KO skins (Suppl. Figure 2). In sum, both alloreactive CD8 and CD4 T cells are being less primed, however, CD8 T cells seem to be most susceptible to the lack of Batf3-dependent DCs in donor skin allografts. This could be explained due the fact that Batf3-dependent DCs are described the main cross-presenting subset (18), including in the skin (19).

Next, we investigated the cytokine production by T cells from WT or Batf3 KO skin allografts' dLNs. Recipients of Batf3 KO skins presented a reduced percentage of CD8$^+$IFN-γ$^+$ cells at day 1, 7 and 25 post-transplant (Figure 2D), along with a decrease of CD8$^+$IL-17$^+$ cells at day 7 post-transplant compared to WT skins (Figure 2E). The CD4 T cells had a similar pattern of IFN-γ and IL-17 production (Suppl. Figure 3). The CD8$^+$GranzymeB (GrB)$^+$ cells were significantly decreased at day 1, 7 and 25 post-transplant in mice that received Batf3 KO skin allografts compared to WT (Figure 2F). Altogether, our data suggest that the lack of Batf3-dependent DCs in donor skins leads to an impaired in the prime, proliferation and function of alloreactive T cells, mainly in the CD8+ T cell pool.

**A** B6 WT → BALB/c

Batf3 KO → BALB/c

Day 11 post-transplant

**B**
- B6 WT --> BALB/c
- Batf3 KO --> BALB/c

% Graft survival

** p = 0.0019

Days post transplantation

**C** Day7 post-transplantation

WT    Batf3KO

CD8

Ki67

6,07    4,77

% CD8+Ki67+ cells

WT  Batf3KO  WT  Batf3KO  WT  Batf3KO
Day1        Day7        Day25

**D** Day7 post-transplantation
(Gated on CD8+ T cells)

WT    Batf3KO

CD62L

CD44

13,4  76,5    12,5  80,1
0,95  9,13    0,54  6,93

% CD8+ TEM cells

- WT @ BALB/c
- Batf3KO @ BALB/c

WT  Batf3KO  WT  Batf3KO  WT  Batf3KO
Day1        Day7        Day25

**E**

WT    Batf3KO

CD8

IFN-γ

Day1   13,4    8,86
Day7   0,41    0,27

% of CD8+IFN-γ+ cells

WT  Batf3KO  WT  Batf3KO  WT  Batf3KO
Day1        Day7        Day25

**F**

WT    Batf3KO

CD8

IL-17

Day1   0,11    0,14
Day7   39,6    19,1

- WT @ BALB/c
- Batf3KO @ BALB/c

% of CD8+IL-17+ cells

WT  Batf3KO  WT  Batf3KO  WT  Batf3KO
Day1        Day7        Day25

**G**

WT    Batf3KO

CD8

GrB

Day1   0,55    0,21
Day7   0,68    0,36

% of CD8+GrB+ cells

WT  Batf3KO  WT  Batf3KO  WT  Batf3KO
Day1        Day7        Day25

94

**Figure 2. Increased allograft survival and attenuated alloimmunity of recipients of Batf3 KO skins.** Skin allografts from WT B6 or Batf3 KO (H-2$^b$) mice were transplanted into BALB/c (H-2$^d$) recipients. (**A**) Visual aspects of skin grafts. (**B**) Percent of graft survival. **p<0.01 by long-rank test. (n=5 mice per group). (**C**) Representative dot plots (upper panels) and percentages (lower panels) of CD8+Ki67+ cells from allograft's draining lymph nodes (LN) harvested from mice that received WT or Batf3 KO skin grafts or controls on 1, 7 and 25 post transplantation (n=3-5 mice per time-point/group). Dot graphs represent the mean ± SEM. *p<0.05 when compare to WT by t test. (**D**) Representative dot plots (upper panels) and percentages (lower panels) of CD8+ effector memory T cells (TEM – CD8+CD44+CD62L- cells) as in (**C**). *p<0.05 and **p<0.01 when compare to WT by t test. (**E**) Representative dot plots (upper panels) and percentages (lower panels) of CD8+IFN-γ+ cells as in (**C**). *p<0.05, **p<0.01 and ***p<0.001 when compare to WT by t test. (**F**) Representative dot plots (upper panels) and percentages (lower panels) of CD8+IL-17+ cells as in (**C**). *p<0.05 when compare to WT by t test. (**G**) Representative dot plots (upper panels) and percentages (lower panels) of CD8+GranzymeB (GrB)+ cells as in (**C**). *p<0.05 and **p<0.01 when compare to WT by t test.

*Lack of Batf3-dependent DCs in donor skins reduces tissue-resident memory alloproliferation*

Tissue-resident memory T cells (TRMs) compose a lymphocyte subset that resides in various barrier tissues such as skin, lung and GI (20). In the skin, after their formation, they persist long-term and can respond rapidly to an antigen re-challenge (21). They are associated with several skin diseases (22), and are characterize by the absence of CD62L and the expression of  CD69 and CD103 (23, 24). Despite to be consider non-circulating, we could found both CD8+ and CD4+CD62L-CD69+CD103+ cells in skin draining lymph nodes seven days, but not in the day one, after transplant (Figure 3). We found that both CD4 and CD8 TRMs were reduced in recipients that received Batf3 KO skins compared to WT, at day 1 and 7 post-transplant (Figure 3, A and B). Furthermore, these TRMs proliferated significantly less than those isolated from mice transplanted with WT skins, which was determined by expression of the intracellular marker Ki67 (Figure 3, C and D). Thus, TRMs could migrate to draining lymph node in a transplant context and the absence of Baf3-dependent DCs on donor skins leads to a decreased alloproliferation by these cells.
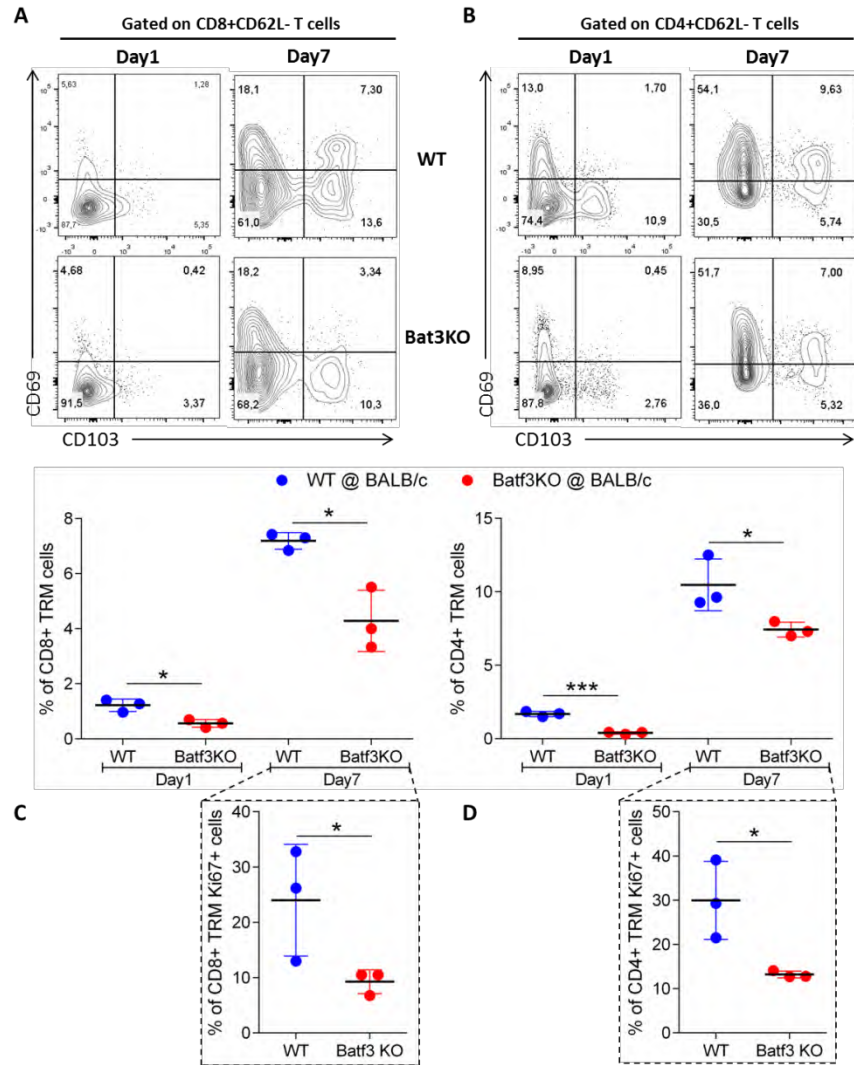
**Figure 3. Recipients of Batf3 KO skins presented decreased percentage of tissue-resident memory T cells with an impaired proliferation.** Skin allografts from WT B6 or Batf3 KO (H-2$^b$) mice were transplanted into BALB/c (H-2$^d$) recipients. (**A**) Representative dot plots (upper panels) and percentages (lower panels) of CD8 tissue-resident memory T cells (TRMs, CD8+CD62L-CD103+CD69+ cells) from allograft's draining lymph nodes (LN) harvested from mice that received WT or Batf3 KO skin grafts or controls on 1 and 7 post transplantation (n=3 mice per time-point/group). Dot graphs represent the mean ± SEM. *p<0.05 when compare to WT by t test. (**B**) Representative dot plots (upper panels) and percentages (lower panels) of CD4 TRMs (CD4+CD62L-CD103+CD69+ cells) as in (**A**). (n=3 mice per time-point/group). Dot graphs represent the mean ± SEM. *p<0.05 and ***p<0.001 when compare to WT by t test. Percentages of proliferating (Ki67+) CD8 (**C**) and CD4 (**D**) TRMs, as in (**A**). (n=3 mice per time-point/group). Dot graphs represent the mean ± SEM. *p<0.05 when compare to WT by t test.

*In-situ treatment that targets donor skin CD103+ DCs delays skin rejection*

We recently demonstrated that an *in-situ* treatment prior the transplant using the mycobacterial protein DnaK, could modulate donor DCs, prolongs graft survival and attenuates alloimmunity (Borges et al, *in preparation* – Capitulo 1). This modulation of DCs was characterized by a downregulation of MHC II and it was dependent on the ubiquitin ligase MARCH1. We initially analyzed which skin migratory DC subset DnaK could modulate. So, we isolated DCs from skin-draining lymph nodes, treated them with DnaK and measured MHC II levels after 24h by flow cytometry. We found that DnaK treatment could decrease MHC II levels in CD103+CD11b- DCs, with less cells expressing high levels and more cells expressing low levels of MHC II (Figure 4A). MHC II levels did not change in CD103-CD11b+ DCs upon DnaK treatment (Figure 4B). To exclude the effect of other lymph node DCs subsets, we sorted the CD103 and CD11b DCs (Figure 4C) and treated them with DnaK. After 24h, DnaK could modulate MHC II levels only in the CD103 DCs, but not in CD11b (Figure 4D). Moreover, MARCH1 was induced by DnaK on CD103+ DCs, but not CD11b+ or CD103-CD11b- (Figure 4E).

Next, we analyzed whether DnaK could modulate donor migrating CD103+ DCs. We transplanted C57Bl/6 (I-A$^b$) skins, previously immersed in a solution containing DnaK for 60 min, into BALB/c (I-A$^d$) hosts. We then tracked donor CD103 DCs (as in Figure 1A) and assessed MHC II expression by flow cytometry. We observed that about 50% of donor migrating CD103 DCs from DnaK-treated skin grafts reached the draining lymph nodes expressing diminished levels of MHC II, compared to about 100% of controls was expressing high levels of MHC II. Altogether, our data suggest that DnaK can exclusively modulate skin migratory CD103+CD207+ dendritic cells *in vitro* and *in vivo*.
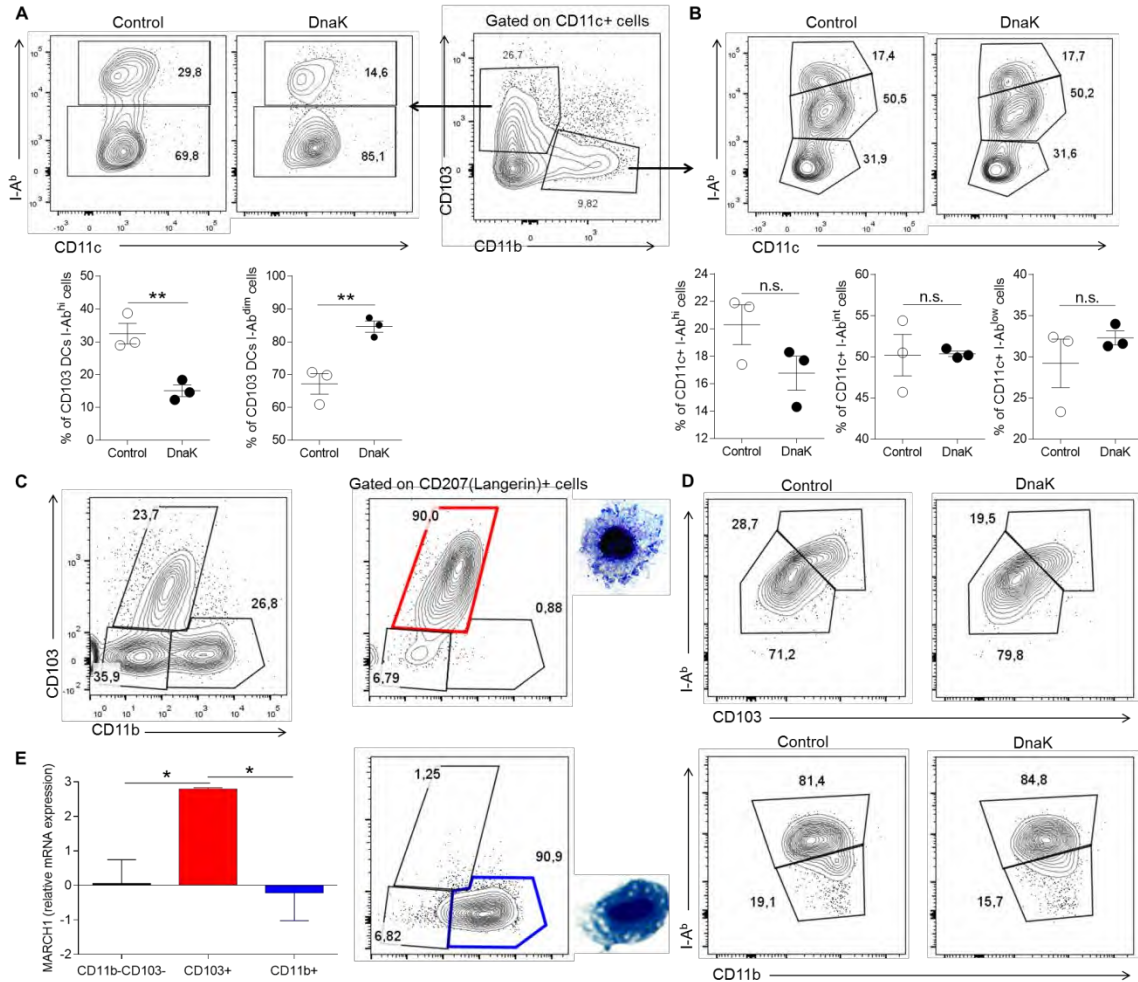
**Figure 4. DnaK modulates MHC II levels and induces MARCH1 on CD103+CD207+ DCs.** Dendritic cells from skin-draining lymph nodes were treated with DnaK or control for 24h and MHC II expression was analyzed in CD103+CD11b- (CD103 DCs) or CD103-CD11b+ (CD11b DCs) cells. Representative dot plots (upper) and percentages (lower) of I-A$^b$ expression on CD103 (**A**) or CD11b DCs (**B**). (**C**) Gating strategy of flow sorted DCs - CD11c+CD11b-CD103+CD207+(Langerin)+ (CD103 DCs) and CD11c+CD11b+CD103- (CD11b DCs) (**D**) Representative dot plots of MHC II expression by flow sorted CD103 (upper) and CD11b (lower) DCs treated with DnaK. (**E**) Flow sorted CD103, CD11b or CD103-CD11b- DCs as in (**C**) were treated with DnaK and MARCH1 expression was assessed by real-time PCR. Bars represent the mean ± SEM. *p<0.05 by t test.
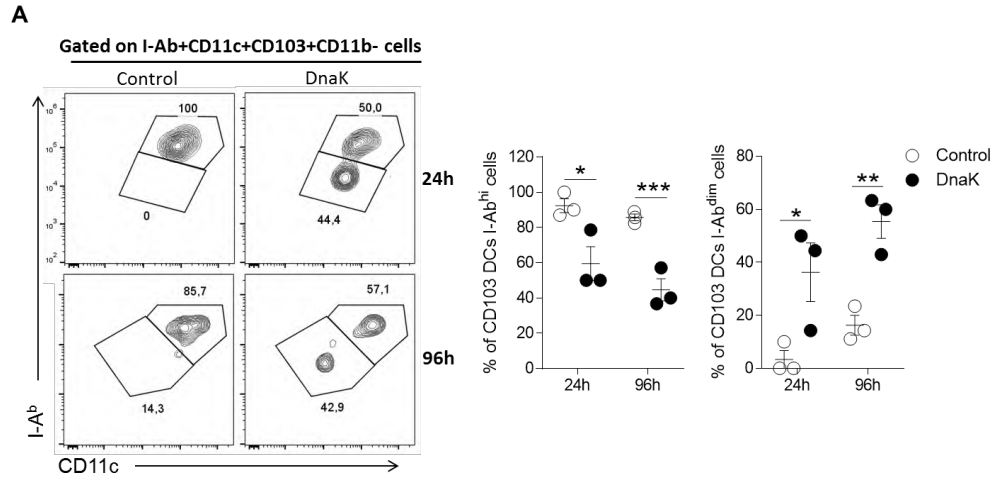
**Figure 5. In-situ treatment prior the transplant with DnaK targets donor migrating CD103 DCs and modulates its MHC II expression.** (**A**) Representative dot plots of I-A$^b$ expression on donor CD103+ DCs (gated as in Figure 1A - left) and percentage of CD103+ DCs expressing high or diminished levels of I-A$^b$ in allografts' draining lymph nodes of mice transplanted with DnaK-treated allografts or control, 24h or 96h after transplantation. Dot graphs represent the mean ± SEM. *p<0.05, **p<0.01 and ***p<0.001 when compare to control by t test. n= 3 mice per group.

**Discussion**

In the present study, we reported that Batf3-dependent DCs (CD103) are the major migrating DC subset upon skin transplant. Its absence in donor tissues leads to decreased immunogenicity and prolonged graft survival. In the skin transplant context, it was reported that LCs are not required for the completely rejection of major or minor MHC-mismatched allografts (12). Using intravital microscopy, Celli et al. reported that donor dermal DCs rapidly migrated from the skin to hosts' draining lymph nodes, 24h after the transplant, whereas LCs persisted stuck in donor tissue (13). In that study, they did not distinguish between CD103 or CD11b dermal DCs subsets, and they also suggested that donor dermal DCs dies once they reached the lymph nodes, however this conclusion was based exclusively on the cells' morphology, since they did not use cell viability markers or dyes. Using specific viability dyes, we recently found that donor DCs could reach skin draining lymph node 24 and 96h after the transplant, an also that these migrating cells were alive at those same time-points, (Borges et al, *in preparation* – Capitulo 1). One feasible explanation is that this DC subset is more resistant to NK-mediated killing of allogeneic DCs in draining lymph nodes (25). However, this hypothesis needs to be further explored.

Batf3-dependent DCs are involved in the pathology of several animal immune disorders. For example, nonobese diabetic (NOD) mice lacking CD103+ DCs had no incidence of disease with an absence of autoreactive T cells (8). Recently, donor CD103+ DCs were shown to have a major role in amplifying the pathology of graft-versus-host disease (GVHD) in a model of gastrointestinal (GI) tract transplant (26). Moreover, Batf3-dependent DCs were associated to have an important role in the rejection of minor mismatched grafts (27). Our data is the first report demonstrating the crucial role of donor Batf3-dependent DCs in initiating skin rejection in a fully MHC mismatched model. We saw that T cell alloimmunity was impaired in hosts of Batf3 KO skins due to a primary effect on CD8+ alloreactive T cells. This is in accordance with prior data indicating that Batf3-dependent DCs are the major cross-presenting cells (18), and that CD207+CD103+ DCs have the unique capability to cross-present keratinocytes antigens (28). Thus, direct interaction of activated donor CD103+ DCs with host CD8 T cells could elicit a strong donor-specific cytotoxic response. We also observed a decreased percentage of both CD4

and CD8 TRM cells at day 7 after transplant in mice that received Batf3 KO skins, along with a diminished proliferation by these cells. Recently, it was reported that CD8 TRM cells from a donor origin were increased in the graft during rejection of full face transplant patients (29). This underlies that the role of these cells in skin transplantation needs to be further explored.

Interestingly, under non-inflamed conditions, Batf3-dependent DCs can mediate tolerance to circulating antigens in renal draining lymph nodes (11). These DCs presented concentrated antigens in the kidney and used PD-L1 to induce apoptosis of reactive CD8 T cells (11). Also, CD103+ DCs mediate the development of Tregs in the intestine (30). In the skin, migratory CD207+ DCs have a superior ability to generate antigen-specific Tregs *in vivo* (31). Human CD141$^{hi}$ DCs are the human counterpart of murine CD103+ DCs (32), and they can produce IL-10 and inhibit graft versus host disease in a xenograft model (33). In transplant setting, donor DC cells are activated by released factors in the setting of inflammation and tissue injury (34). Thus, minimizing the upregulation of MHC molecules and costimulatory ligands and modulating donor CD103+ DCs upon transplantation may significantly affect the fate of the alloimmune response. We previously developed a method by which we treat the skin tissue in a solution containing a protein called DnaK prior the transplant. In-situ DnaK treatment downregulated MHC II expression in donor migrating CD103+ DCs, significantly improving graft survival in the absence of any other immunosuppressive drugs. Thus, we have established a regulatory in-situ therapeutic strategy that targets donor CD103+ DCs and could be translated to VCA organs prior to transplantation, minimizing the need for systemic immunosuppression.

## Acknowledgments

## Disclosure

The authors have declared that no conflict of interest exists.

# References

1. Rosenberg AS, Singer A. Cellular basis of skin allograft rejection: an in vivo model of immune-mediated tissue destruction. Annu Rev Immunol 1992;10:333-358.

2. Jones ND, Turvey SE, Van Maurik A, Hara M, Kingsley CI, Smith CH et al. Differential susceptibility of heart, skin, and islet allografts to T cell-mediated rejection. J Immunol 2001;166(4):2824-2830.

3. Ingulli E. Mechanism of cellular rejection in transplantation. Pediatr Nephrol 2010;25(1):61-74.

4. Benichou G, Yamada Y, Yun SH, Lin C, Fray M, Tocco G. Immune recognition and rejection of allogeneic skin grafts. Immunotherapy 2011;3(6):757-770.

5. Heath WR, Carbone FR. The skin-resident and migratory immune system in steady state and memory: innate lymphocytes, dendritic cells and T cells. Nat Immunol 2013;14(10):978-985.

6. Igyarto BZ, Haley K, Ortner D, Bobr A, Gerami-Nejad M, Edelson BT et al. Skin-resident murine dendritic cell subsets promote distinct and opposing antigen-specific T helper cell responses. Immunity 2011;35(2):260-272.

7. Edelson BT, Kc W, Juang R, Kohyama M, Benoit LA, Klekotka PA et al. Peripheral CD103+ dendritic cells form a unified subset developmentally related to CD8alpha+ conventional dendritic cells. The Journal of experimental medicine 2010;207(4):823-836.

8. Ferris ST, Carrero JA, Mohan JF, Calderon B, Murphy KM, Unanue ER. A minor subset of Batf3-dependent antigen-presenting cells in islets of Langerhans is essential for the development of autoimmune diabetes. Immunity 2014;41(4):657-669.

9. Nakano H, Free ME, Whitehead GS, Maruoka S, Wilson RH, Nakano K et al. Pulmonary CD103(+) dendritic cells prime Th2 responses to inhaled allergens. Mucosal immunology 2012;5(1):53-65.

10. Helft J, Manicassamy B, Guermonprez P, Hashimoto D, Silvin A, Agudo J et al. Cross-presenting CD103+ dendritic cells are protected from influenza virus infection. J Clin Invest 2012;122(11):4037-4047.

11. Gottschalk C, Damuzzo V, Gotot J, Kroczek RA, Yagita H, Murphy KM et al. Batf3-dependent dendritic cells in the renal lymph node induce tolerance against circulating antigens. Journal of the American Society of Nephrology : JASN 2013;24(4):543-549.

12. Obhrai JS, Oberbarnscheidt M, Zhang N, Mueller DL, Shlomchik WD, Lakkis FG et al. Langerhans cells are not required for efficient skin graft rejection. J Invest Dermatol 2008;128(8):1950-1955.

13. Celli S, Albert ML, Bousso P. Visualizing the innate and adaptive immune responses underlying allograft rejection by two-photon microscopy. Nat Med 2011;17(6):744-749.

14.     Billingham RE, Medawar PB. The Technique of Free Skin Grafting in Mammals. Journal of Experimental Biology 1951;28(3):385-402.

15.     Mehlert A, Young DB. Biochemical and Antigenic Characterization of the Mycobacterium-Tuberculosis 71-Kd Antigen, a Member of the 70-Kd Heat-Shock Protein Family. Molecular Microbiology 1989;3(2):125-130.

16.     Aida Y, Pabst MJ. Removal of Endotoxin from Protein Solutions by Phase-Separation Using Triton X-114. Journal of Immunological Methods 1990;132(2):191-195.

17.     Schmittgen TD, Livak KJ. Analyzing real-time PCR data by the comparative C(T) method. Nat Protoc 2008;3(6):1101-1108.

18.     Hildner K, Edelson BT, Purtha WE, Diamond M, Matsushita H, Kohyama M et al. Batf3 deficiency reveals a critical role for CD8alpha+ dendritic cells in cytotoxic T cell immunity. Science 2008;322(5904):1097-1100.

19.     Bedoui S, Whitney PG, Waithman J, Eidsmo L, Wakim L, Caminschi I et al. Cross-presentation of viral and self antigens by skin-derived CD103+ dendritic cells. Nature immunology 2009;10(5):488-495.

20.     Park CO, Kupper TS. The emerging role of resident memory T cells in protective immunity and inflammatory disease. Nat Med 2015;21(7):688-697.

21.     Jiang X, Clark RA, Liu L, Wagers AJ, Fuhlbrigge RC, Kupper TS. Skin infection generates non-migratory memory CD8+ T(RM) cells providing global skin immunity. Nature 2012;483(7388):227-231.

22.     Clark RA. Resident memory T cells in human health and disease. Sci Transl Med 2015;7(269):269rv261.

23.     Mackay LK, Rahimpour A, Ma JZ, Collins N, Stock AT, Hafon ML et al. The developmental pathway for CD103(+)CD8+ tissue-resident memory T cells of skin. Nature immunology 2013;14(12):1294-1301.

24.     Mueller SN, Zaid A, Carbone FR. Tissue-resident T cells: dynamic players in skin immunity. Front Immunol 2014;5:332.

25.     Garrod KR, Liu FC, Forrest LE, Parker I, Kang SM, Cahalan MD. NK cell patrolling and elimination of donor-derived dendritic cells favor indirect alloreactivity. J Immunol 2010;184(5):2329-2336.

26.     Koyama M, Cheong M, Markey KA, Gartlan KH, Kuns RD, Locke KR et al. Donor colonic CD103+ dendritic cells determine the severity of acute graft-versus-host disease. The Journal of experimental medicine 2015;212(8):1303-1321.

27.     Atif SM, Nelsen MK, Gibbings SL, Desch AN, Kedl RM, Gill RG et al. Cutting Edge: Roles for Batf3-Dependent APCs in the Rejection of Minor Histocompatibility Antigen-Mismatched Grafts. J Immunol 2015;195(1):46-50.

28.     Henri S, Poulin LF, Tamoutounour S, Ardouin L, Guilliams M, de Bovis B et al. CD207+ CD103+ dermal dendritic cells cross-present keratinocyte-derived antigens irrespective of the presence of Langerhans cells. The Journal of experimental medicine 2010;207(1):189-206.

29.     Lian CG, Bueno EM, Granter SR, Laga AC, Saavedra AP, Lin WM et al. Biomarker evaluation of face transplant rejection: association of donor T cells with target cell injury. Mod Pathol 2014;27(6):788-799.

30.     Ruane DT, Lavelle EC. The role of CD103(+) dendritic cells in the intestinal mucosal immune system. Front Immunol 2011;2:25.

31.     Idoyaga J, Fiorese C, Zbytnuik L, Lubkin A, Miller J, Malissen B et al. Specialized role of migratory dendritic cells in peripheral tolerance induction. J Clin Invest 2013;123(2):844-854.

32.     Haniffa M, Shin A, Bigley V, McGovern N, Teo P, See P et al. Human tissues contain CD141hi cross-presenting dendritic cells with functional homology to mouse CD103+ nonlymphoid dendritic cells. Immunity 2012;37(1):60-73.

33.     Chu CC, Ali N, Karagiannis P, Di Meglio P, Skowera A, Napolitano L et al. Resident CD141 (BDCA3)+ dendritic cells in human skin produce IL-10 and induce regulatory T cells that suppress skin inflammation. The Journal of experimental medicine 2012;209(5):935-945.

34.     Solhjou Z, Athar H, Xu Q, Abdi R. Emerging therapies targeting intra-organ inflammation in transplantation. Am J Transplant 2015;15(2):305-311.

# Supplementary Materials for

# Lack of Donor Batf3-dependent DCs Dampens Skin Allograft Rejection due to an Impaired Activation of CD8 T cells

**Authors:** Thiago J. Borges[1], Mayuko Uehara[2], Felipe D. Machado[1], Rafael L. Lopes[1], Priscilla Vianna[3], José Artur Bogo Chies[3], Reza Abdi[2], Cristina Bonorino[1,4*], Leonardo V. Riella[2,4**]

*Corresponding authors: lriella@bwh.harvard.edu and cbonorino@pucrs.br
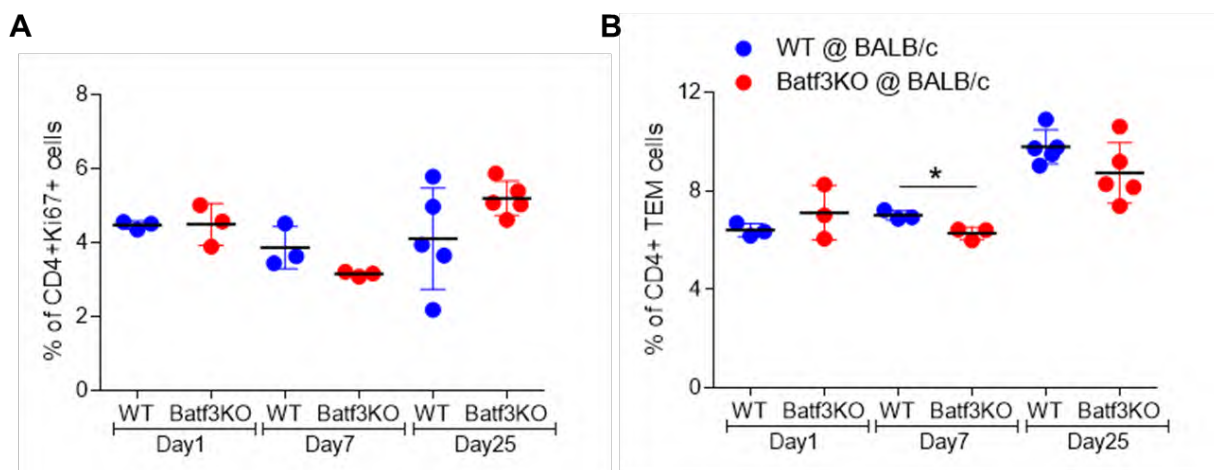
**Supplemental Figure 1. Recipients of Batf3 KO skins presented minimal changes in CD4 T cells.** Skin allografts from WT B6 or Batf3 KO (H-2$^b$) mice were transplanted into BALB/c (H-2$^d$) recipients. (**A**) Percentages of CD4+Ki67+ cells from allograft's draining lymph nodes (LN) harvested from mice that received WT or Batf3 KO skin grafts or controls on 1, 7 and 25 post transplantation (n=3-5 mice per time-point/group). Dot graphs represent the mean ± SEM. *p<0.05 when compare to WT by t test. (**B**) Percentages of CD4+ effector memory T cells (TEM – CD4+CD44+CD62L- cells) as in (**A**). *p<0.05 when compare to WT by t test.
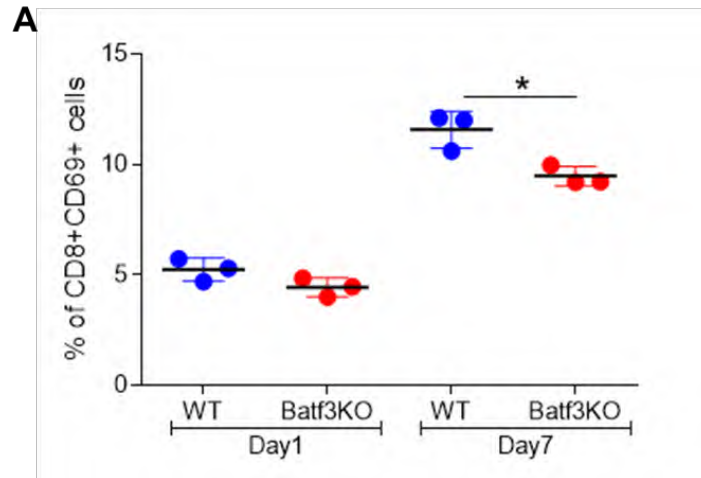
**Supplemental Figure 2. Recipients of Batf3 KO skins presented decreased priming of CD8 T cells.** Skin allografts from WT B6 or Batf3 KO (H-2$^b$) mice were transplanted into BALB/c (H-2$^d$) recipients. (**A**) Percentages of CD8+CD69+ cells from allograft's draining lymph nodes (LN) harvested from mice that received WT or Batf3 KO skin grafts or controls on 1 and 7 post transplantation (n=3 mice per time-point/group). Dot graphs represent the mean ± SEM. *p<0.05 when compare to WT by t test.
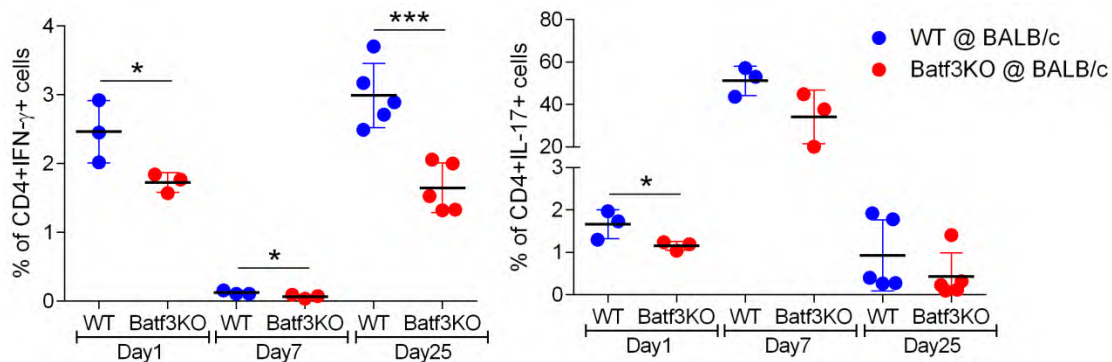


**Supplemental Figure 3. IFN-γ and IL-17 production by recipients' CD4 T cells.** Skin allografts from WT B6 or Batf3 KO (H-2$^b$) mice were transplanted into BALB/c (H-2$^d$) recipients. Percentages of CD4+ IFN-γ+ (left) and CD4+IL-17+ (right) cells from allograft's draining lymph nodes (LN) harvested from mice that received WT or Batf3 KO skin grafts or controls on 1 and 7 post transplantation (n=3 mice per time-point/group). Dot graphs represent the mean ± SEM. *p<0.05 and ***p<0.001 when compare to WT by t test.

# CAPÍTULO 4

## A DnaK extracelular co-localiza com o complexo Siglec-E/TLR2/LOX-1 em células dendríticas de camundongos

**Autores:** Thiago J. Borges*, Ayesha Murshid*, Leonardo Riella, Cristina Bonorino[#], Stuart K. Calderwood[#]

* Contribuíram igualmente para o trabalho

# Co-senior authors

**Situação:** Em preparação - Dados complementares que quando finalizados serão submetidos à eLife

**Motivação:** Trabalho foi realizado durante o período sanduiche realizado no Hospital Beth Israel Deaconess Medical Center, no laboratório do Dr. Stuart Calderwood. O objetivo desse trabalho foi utilizar um sistema que esta bem estabelecido no laboratório e que consiste em usar células CHO transfectadas com uma variedade de receptores inatos para mapear os receptores nos quais a DnaK pode se ligar.

Os resultados apresentados a seguir foram obtidos durante o período de Doutorado Sanduiche e futuramente, quando complementados com dados novos, farão parte de um artigo científico que será submetido à revista *eLife*.

**Materiais e métodos**

### Purificação da proteína e extração do LPS

Para a produção da DnaK recombinante, o gene da DnaK de *M. tuberculosis* foi inserido em um vetor pET-23a(+) (o plasmídeo foi montado pela empresa Genscript, EUA), a proteína foi produzida na cepa BL21 de Escherichia coli e purificada de acordo com Mehlert & Young (21). Para a remoção do LPS, foi utilizado o Triton X-114 (Sigma), como descrito em Aida e Pabst (22). O Triton contaminante foi removido através da incubação da proteína com Biobeads (Bio-Rad) à 4ºC em agitação durante 12h. Para determinar a concentração da proteína foi utilizado o teste fluorimétrico Quant-iT™ Protein Assay Kit (Invitrogen) e as amostras foram lidas no Qubit® fluorometer (Invitrogen). A proteína foi produzida com o auxilio do Dr. Gabriel Birrane, BIDMC, Harvard Medical School.

### Marcação da DnaK purificada com fluorescência

A DnaK purificada foi marcada com os fluorocromos Alexa 488 ou Alexa 594, utilizando os kits Microscale Protein Labeling da Thermo Fischer Scientific (Molecular Probes), de acordo com as instruções do fabricante.

### Animais

Fêmeas de camundongos C57Bl/6 foram adquiridas dos laboratórios Jackson (Estados Unidos) com idades entre seis e oito semanas e foram mantidos no vivário do *Center for Life Sciences* (Boston, Estados Unidos). Os camundongos LOX-1 KO (em *background* C57Bl/6) foram gentilmente cedidos pelo Dr. Jawahar L Mehta (Universidade de Ciências Medicas do Arkansas). Os animais foram mantidos em condições livre patógenos e de acordo com as normas de uso e cuidados de animais da Instituição.

### Células e condições da cultura

Células CHO-K1 foram transfectadas de maneira estável com o gene que codifica para os receptores LOX-1, SREC-1, DC-SIGN ou FEEL-1 todos inseridos em plasmídeos pcDNA3. Células CHO-K1 também foram transfectadas de maneira transiente para os receptores mMGL2 ou Dectin-1 inseridos em plasmídeos pcDNA3.Todas as linhagens foram mantidas em meio Ham's F12K (Gibco) suplementado com 10% de soro fetal bovino inativado por calor, 100 U/ml de penicilina e 100 g/ml de estreptomicina. Todas as linhagens foram selecionadas e mantidas no meio com 400 ng/ml do antibiótico G418.

Células HEK293 foram transfectadas de maneira estável com o gene que codifica para os receptores TLR2 ou TLR4 inseridos em plasmídeos pcDNA3. As linhagens foram mantidas em meio DMEM (Gibco) suplementado com 10% de soro fetal bovino inativado por calor, 100 U/ml de penicilina e 100 g/ml de estreptomicina. Todas as linhagens foram selecionadas e mantidas no meio com 400 ng/ml do antibiótico G418.

### Cultura de células dendríticas

As células dendríticas murinas foram geradas a partir da medula óssea (BMDCs), proveniente de animais selvagens ou LOX-1 KO, juntamente com 40 ng/mL GM-CSF, como descrito no trabalho de Inaba e colaboradores (138). Juntamente com o GM-CSF, adicionamos 40 ng/mL de IL-4 nas culturas. As células foram cultivadas em meio DMEM complementado com 10% de soro fetal bovino inativado por calor, 100 U/ml de penicilina e 100 g/ml de estreptomicina.  O meio e as citocinas foram substituídos a cada dois dias de cultura. As células foram utilizadas no sexto dia de cultura.

### Imunofluorescência e analises de microscopia

As células CHO-K1 (controle), CHO-LOX-1, CHO-SREC-1, CHO-DC-SIGN, CHO-FEEL-1, CHO-mMGL2, CHO-Dectin-1, HEK293 (controle), HEK293-TLR2 ou HEK293-TLR4 foram colocadas para crescer em lamínulas por 12h. As DCs dos linfonodos foram colocadas para aderir em lamínulas revestidas com poli-L-lisina, por 48h. Posteriormente, todas as células foram marcadas com 10 µg/ml da DnaK fluorescente por 20 minutos no gelo. Em alguns casos, para

analises de internalização da proteína, o meio gelado foi substituído por meio previamente aquecido a 37°C e as células incubadas a 37°C por 20 min. No fim das incubações, as células foram lavadas com PBS para remover as moléculas DnaK as quais não se ligaram nas células. Depois disso, as células foram fixadas com 4% de paraformaldeído e permeabilizadas ou não com 0,1% de Triton X-100. As DCs tiveram seus receptores Fc bloqueados com um anticorpo anti-FcR por 10 min, no gelo em uma concentração de 1mg/ml/milhão de células. Posteriormente, as DCs foram marcadas com anticorpos para LOX-1 (10 µg/ml - Abcam), TLR2 (Abcam), Siglec-E (R&D Systems) e SR-A (Abcam), seguido da marcação com seus respectivos anticorpos secundários. As células também foram marcadas com DAPI por uma hora a temperatura ambiente. As células foram analisadas em um microscópio Zeiss LSM 510 (Carl Zeiss, Alemanha) e processadas no programa ZEN (Blue Edition, Carl Zeiss).

### Citometria de fluxo

As DCs de LNs ou BMDCs selvagens ou dos animais LOX-1 KO foram estimuladas com 30 µg/ml de DnaK ou apenas com meio por 24 horas em meio AIM-V (Gibco – livre de soro). Após isso, as células tiveram os receptores Fc bloqueados e foram marcadas para CD11c, B220, CD11b, CD103, MHC II (I-A$^{b}$), CD80 e Viabilidade (eBioscience) por 30 min, no gelo. As amostras foram lavadas e analisadas no citômetro de fluxo FACSCanto II (BD Biosciences) com o software FACSDiva. Todos os dados foram analisados com o programa FlowJo (versão X, Tree Star Inc., Ashland, US).

### Análise estatística

As análises estatísticas foram realizadas com o auxílio do software Prism (versão 5.00, Graphpad Software Inc., San Diego, US). As comparações de parâmetros entre diferentes grupos experimentais foram realizadas por teste t de Student ou análise de variância de uma via (ANOVA), seguida de testes post-hoc adequados quando a ANOVA revelou diferenças significativas entre grupos, conforme descrito em estudos anteriores. Os resultados foram expressos em média e desvio padrão da média e valores de P menores do que 0,05 indicaram diferenças significativas.

## Resultados

Com base em dados obtidos anteriormente em nosso laboratório e publicações de outros grupos, construímos a hipótese de que a DnaK estaria se ligando a um receptor da família dos *scavenger receptors ou C-type lection receptors* e, estaria utilizando o TLR2 como um co-receptor, para a transmissão do sinal intracelular. Com isso, começamos um *screening* para ver em qual receptor a DnaK poderia se ligar. Para isso, pegamos células CHO-K1 ou HEK293 que não expressam nenhum receptor de superfície (139) e as transfectamos com plasmídeos que codificam para diversos receptores. Depois disso, tratamos as células com a DnaK fluorescente e as analisamos por microscopia Confocal. No total, foram testados 10 receptores (Tabela 1).

**Tabela 1**. Receptores testados para a Hsp70 de *M. tuberculosis* (DnaK)

| Receptor | Tipo | Expresso em | DnaK |
|---|---|---|---|
| TLR2 | Sinalização | DCs, Monócitos, Mɸs, Mastócitos | - |
| TLR4 | Sinalização | DCs, Monócitos, Mɸs, Mastócitos | - |
| DC-SIGN | C-type lectin | DCs | - |
| mMGL2 | C-type lectin | DCs, Mɸs | + |
| Dectin-1 | C-type lectin | DCs, Monócitos, Mɸs, células B | + |
| Siglec-E | I-type lectin | Nɸs, Mɸs, DCs, NK | +++ |
| LOX-1 | Scavenger | DCs, Mɸs, células B | +++ |
| SREC-I | Scavenger | DCs, Monócitos, Mɸs | + |
| SR-A | Scavenger | DCs, Mɸs | - |
| FEEL-1 | Scavenger | Monócitos, Mɸs | - |

A Figura 1 mostra que a DnaK foi capaz de se ligar, nas células que expressam LOX-1, provavelmente com alta afinidade. A DnaK também se ligou, de forma mais fraca e provavelmente com menor afinidade, as células que expressavam SREC-I. Nenhuma ligação da DnaK foi visualizada nas células que expressavam DC-SIGN ou FEEL-1, nem nas células controle – transfectadas com o plasmídeo vazio (CHO-pcDNA).
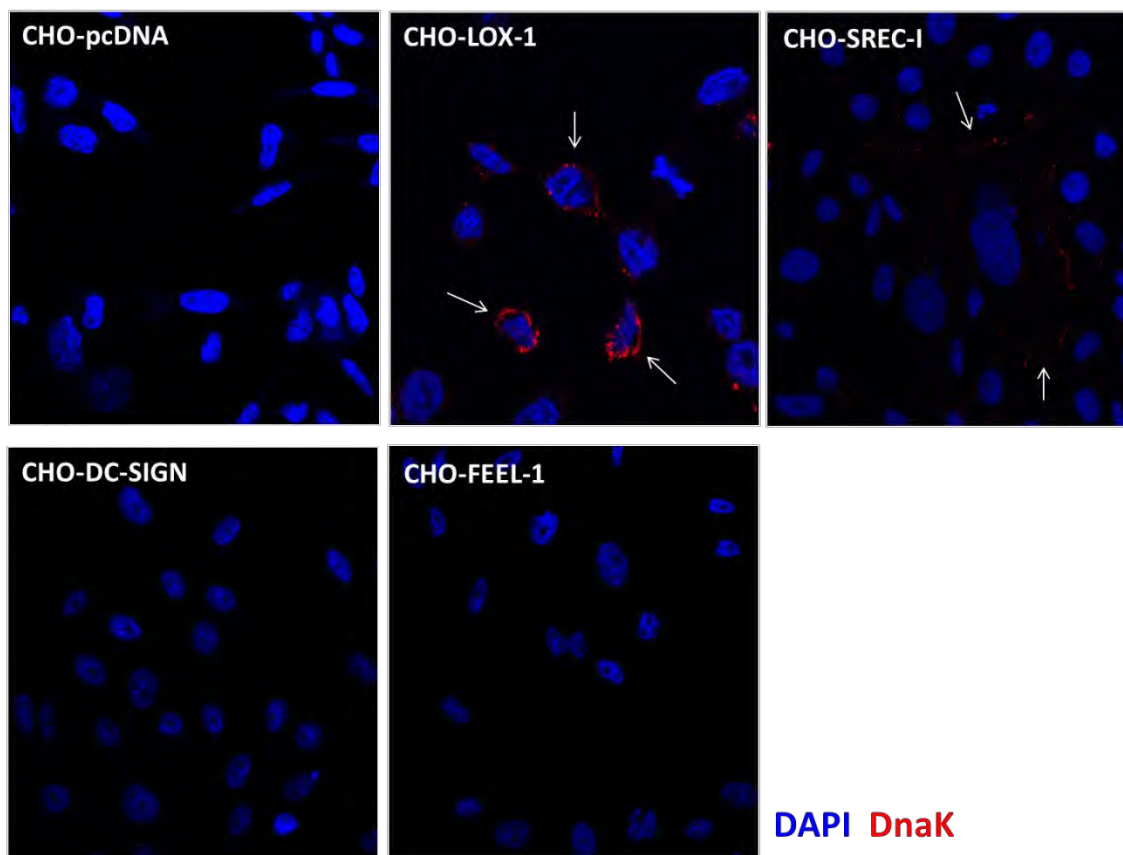


**Figura 1. A DnaK de *M. tuberculosis* (Hsp70) se liga a células CHO expressando o receptor LOX-1.** Células CHO-pcDNA, CHO-SREC-1, CHO-LOX-1, CHO-DC-SIGN e CHO-FEEL-1 foram tratadas com 10 μg/ml de DnaK marcada com o corante Alexa 594 por 20 min, no gelo. Posteriormente, as células foram fixadas, coradas com DAPI e analisadas por microscopia Confocal.

A ligação da DnaK nas células expressando o LOX-1 e o SREC-I foi confirmada utilizando-se a técnica de citometria de fluxo (Figura 2).
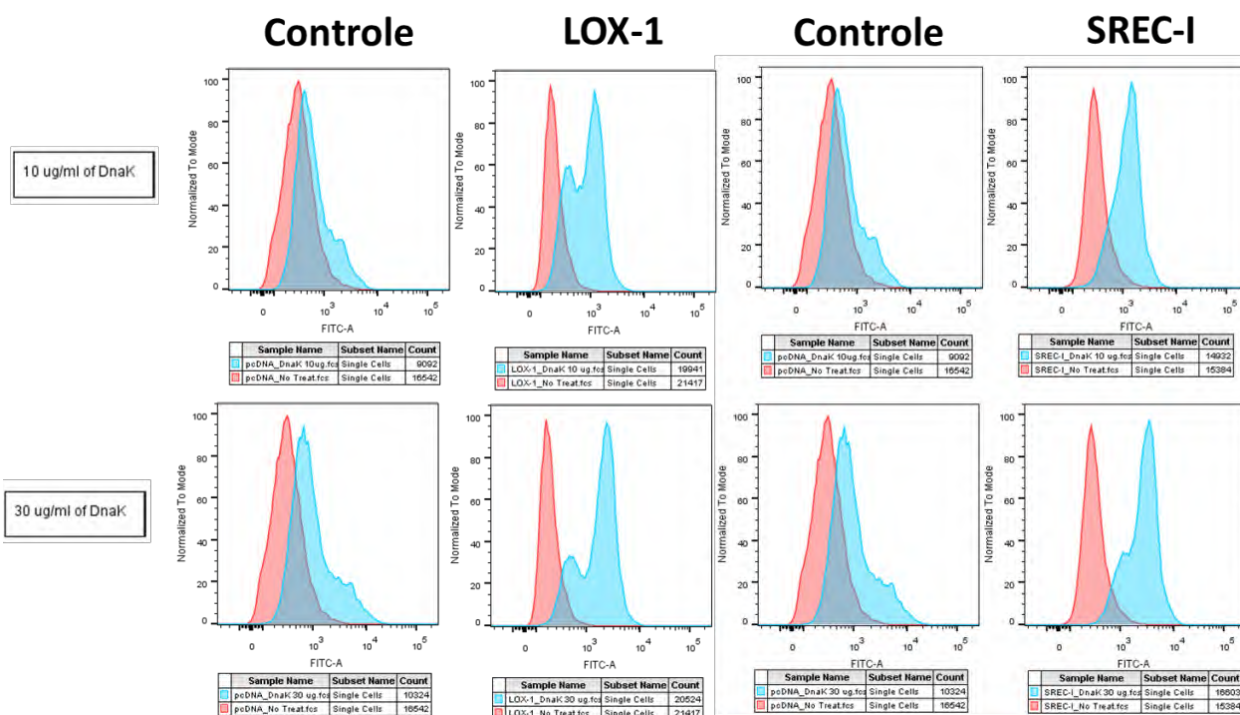


**Figura 2. A DnaK de *M. tuberculosis* (Hsp70) se liga a células CHO expressando o receptor LOX-1 e SREC-I.** Células CHO-pcDNA (controle), CHO-SREC-1 ou CHO-LOX-1 foram tratadas com 10 µg/ml de DnaK marcada com o corante Alexa 488 por 20 min, no gelo. Posteriormente, as células foram fixadas e analisadas por citometria de fluxo.

Os receptores LOX-1 e SREC-I são receptores que desencadeiam respostas pro-inflamatórias (103, 140). Porém, os efeitos reportados por nos pela DnaK são anti-inflamatórios. Com isso, testamos se a DnaK estaria se ligando em dois receptores previamente descritos como anti-inflamatórios – Dectin-1 (141) e mMGL2 (142). Contudo, vimos que a DnaK não foi capaz de se ligar em células CHO expressando os receptores Dectin-1 e mMGL2 (Figura 3).
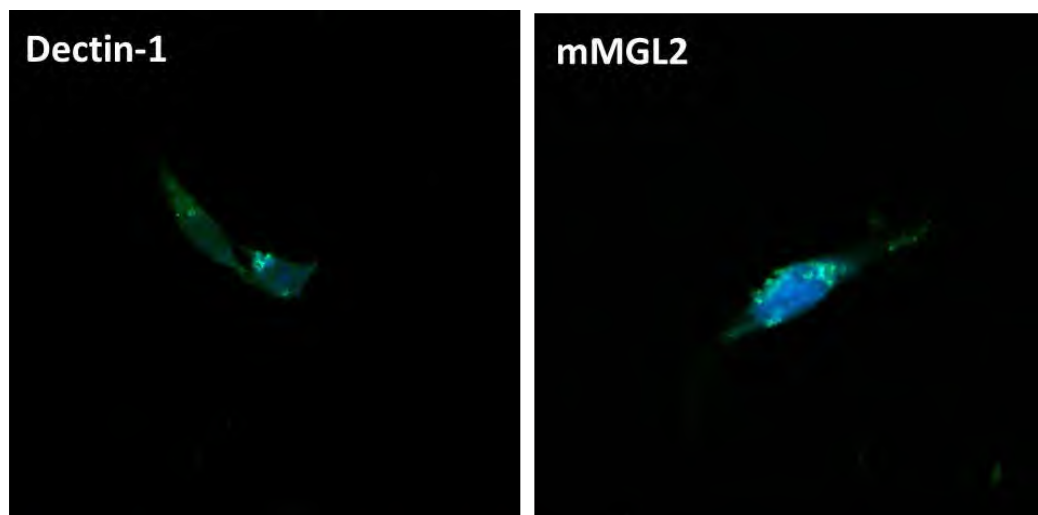


**DAPI Receptor DnaK**

**Figura 3. A DnaK não se liga diretamente aos receptores Dectin-1 e mMGL2.** Células CHO foram transfectadas com os plasmídeos Dectin-1-YFP ou mMGL2-YFP (ambos verdes) e posteriormente tratadas com 10 µg/ml de DnaK marcada com o corante Alexa 594 por 20 min, no gelo. Posteriormente, as células foram fixadas, coradas com DAPI e analisadas por microscopia Confocal.

Os efeitos da DnaK em células dendríticas foram demonstrados ao longo dos anos pelo nosso grupo (20, 21). Esse efeito foi dependente do TLR2 (22) e independente do TLR4 (não publicado ainda – Capitulo 3). Portanto, verificamos se a DnaK poderia se ligar ao TLR2 diretamente ou usa-lo como um co-receptor para enviar os sinais intracelulares. Na Figura 4 mostramos que a DnaK não foi capaz de se ligar em células CHO expressando o receptor TLR2. O mesmo aconteceu para o receptor TLR4 (não mostrado).
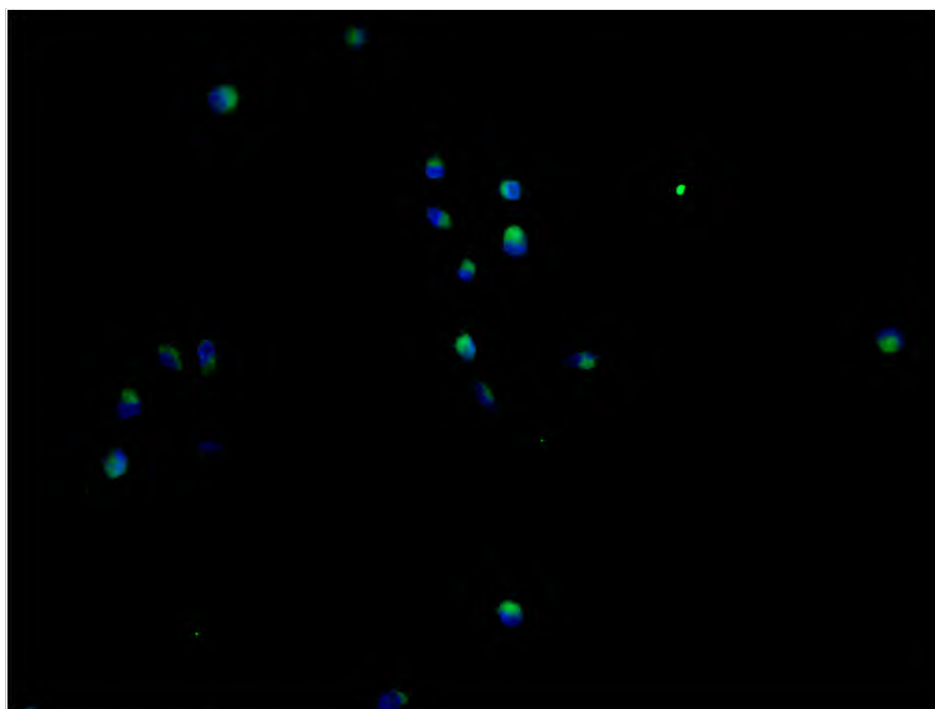


**DAPI TLR2 DnaK**

**Figura 4. A DnaK não se liga diretamente no TLR2.** Células CHO foram transfectadas com o plasmídeo TLR2-YFP (verde) e posteriormente tratadas com 10 µg/ml de DnaK marcada com o corante Alexa 594 por 20 min, no gelo. Posteriormente, as células foram fixadas, coradas com DAPI e analisadas por microscopia Confocal.

Após a analise de receptores em células CHO, verificamos se a DnaK poderia se ligar aos mesmo receptores em células dendríticas isoladas de linfonodos e bacos camundongos, em condições mais fisiológicas. Verificamos que a DnaK foi capaz de se ligar na superfície (tratamento feito a 4°C) dessas células e que esta co-localizada com a expressão de LOX-1 na superfície (Figura 5). Os receptores testados tem a característica de serem receptores endocíticos, mediando endocitose após sua ligação. Para testar se a DnaK seria endocitada via LOX-1, tratamos as células com a DnaK a 4°C e posteriormente colocamos as células a 37°C. A figura 5 mostra que a DnaK esta co-localizada com o LOX-1 em vesículas intracelulares, o que sugere que ela pode ser endocitada via esse receptor.



**Figura 5. A DnaK co-localiza com o LOX-1 na membrana de células dendríticas de camundongos.** Células dendríticas de camundongos foram isoladas do baço e linfonodos e colocadas para aderir em lamínulas por 48h. Após isso, as células foram tratadas com 10 µg/ml de DnaK marcada com o corante Alexa 488 por 20 min, no gelo. Posteriormente, as células foram fixadas, coradas com DAPI e anticorpos para LOX-1 e analisadas por microscopia Confocal. Para a analise de internalização, depois da marcação no gelo, as células foram deixadas 37°C por 20 min, fixadas, coradas com DAPI e anticorpos para LOX-1 e analisadas por microscopia Confocal.

Recentemente, a Hsp70 humana foi descrita como ligante de receptores Siglecs (72), uma família de receptores anti-inflamatórios que inibem as respostas via TLRs (143). Testamos se a DnaK se liga no Siglec-E - isoforma expressa por células dendríticas em camundongos (144). Verificamos que a DnaK foi capaz de co-localizar com o Siglec-E na membrana de células dendríticas de camundongos (Figura 6). Além disso, quando essas células foram deixadas a 37°C, a DnaK se co-localizou com o Siglec-E em vesículas intracelulares.
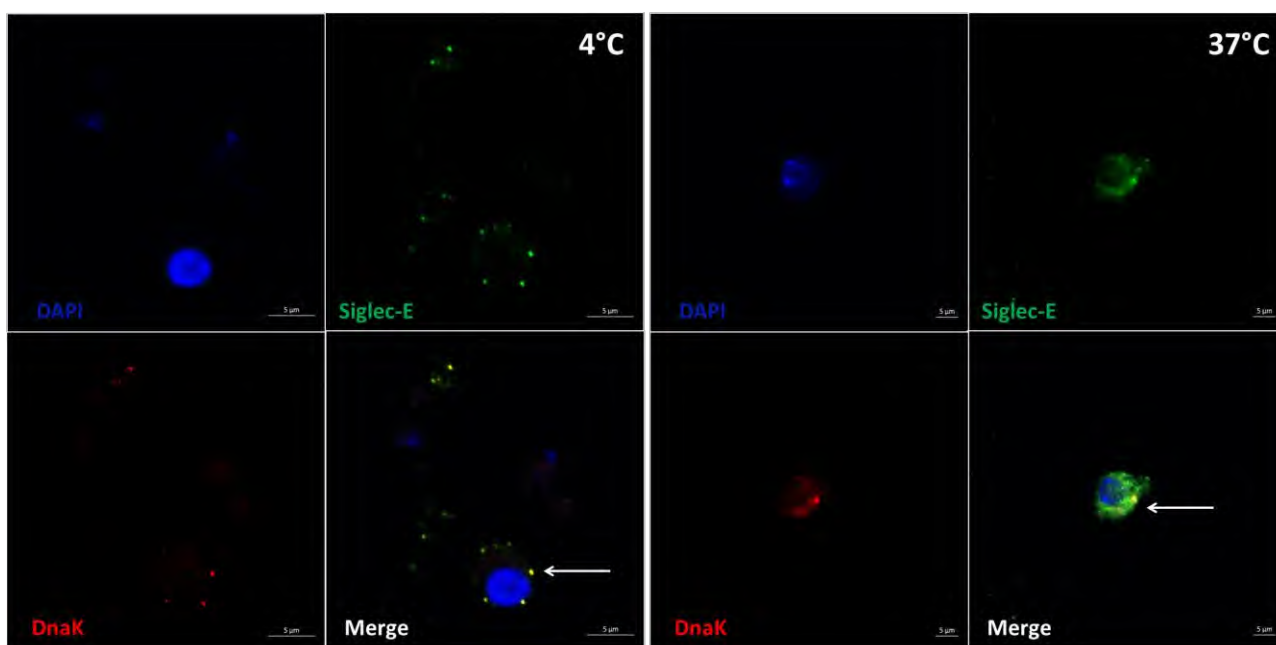


**Figura 6. A DnaK co-localiza com o Siglec-E na membrana de células dendríticas de camundongos.** Células dendríticas de camundongos foram isoladas do baço e linfonodos e colocadas para aderir em lamínulas por 48h. Após isso, as células foram tratadas com 10 µg/ml de DnaK marcada com o corante Alexa 594 por 20 min, no gelo. Posteriormente, as células foram fixadas, coradas com DAPI e anticorpos para o Siglec-E e analisadas por microscopia Confocal. Para a analise de internalização, depois da marcação no gelo, as células foram deixadas 37°C por 20 min, fixadas, coradas com DAPI e anticorpos para Siglec-E e analisadas por microscopia Confocal.

Posteriormente, nos perguntamos se o LOX-1 estava fazendo um complexo com o Siglec-E. Vimos que a DnaK co-localizava com o LOX-1 e Siglec-E, formando um grande complexo na membrana das DCs (Figura 7). Além disso, quando as células foram colocadas a 37°C, esse complexo foi todo internalizado, formando uma grande vesícula intracelular (seta branca - Figura 8).
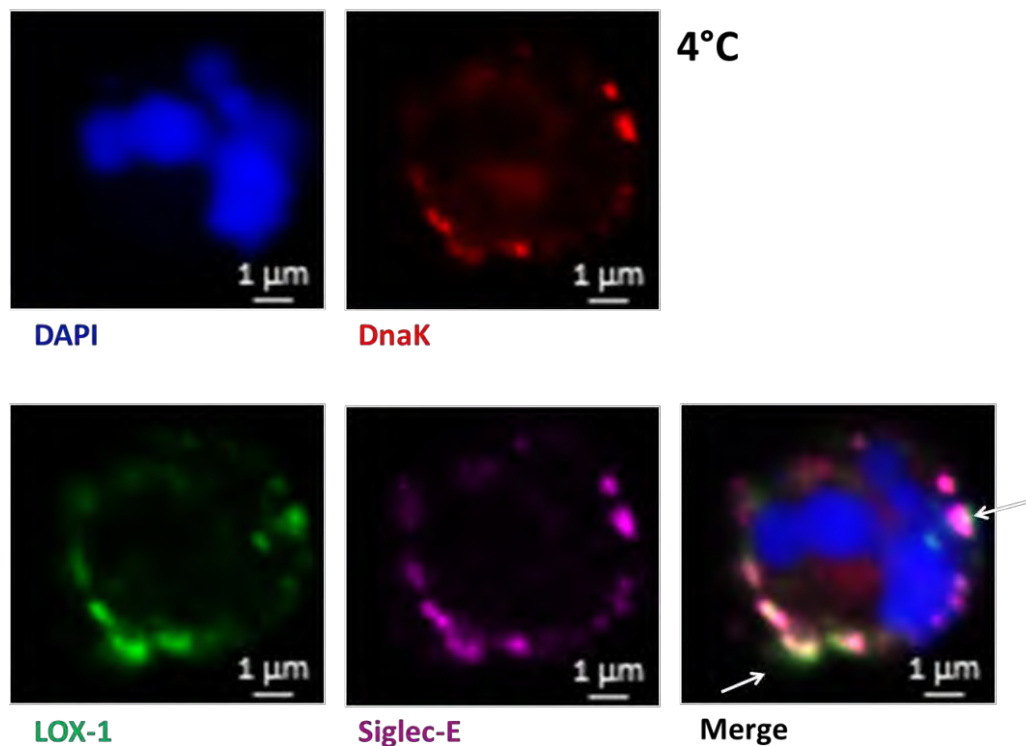


**Figura 7. A DnaK co-localiza com o complexo LOX-1/Siglec-E na membrana de células dendríticas de camundongos.** Células dendríticas de camundongos foram isoladas do baço e linfonodos e colocadas para aderir em lamínulas por 48h. Após isso, as células foram tratadas com 10 μg/ml de DnaK marcada com o corante Alexa 594 por 20 min, no gelo. Posteriormente, as células foram fixadas, coradas com DAPI e anticorpos para o Siglec-E e LOX-1 e, analisadas por microscopia Confocal.
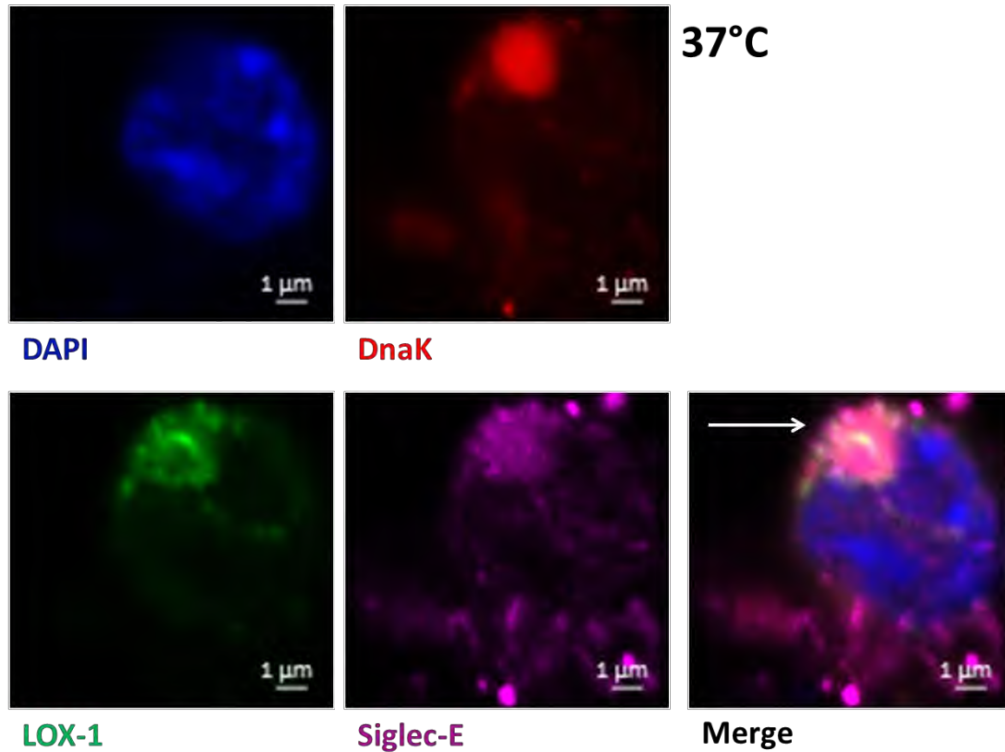
**Figura 8. A DnaK co-localiza com o complexo LOX-1/Siglec-E em vesículas intracelulares em células dendríticas de camundongos.** Células dendríticas de camundongos foram isoladas do baço e linfonodos e colocadas para aderir em lamínulas por 48h. Após isso, as células foram tratadas com 10 µg/ml de DnaK marcada com o corante Alexa 594 por 20 min, no gelo. Posteriormente, as células foram deixadas 37°C por 20 min, fixadas, coradas com DAPI e anticorpos para o Siglec-E e LOX-1 e, analisadas por microscopia Confocal.

Também observamos que o TLR2 estava no complexo com a DnaK e o Siglec-E (Figura 9) e o mesmo foi endocitado (Figura 10). Assim como o Siglec-E, o TLR2 também estava co-localizado com o LOX-1 e a DnaK nas células dendríticas (Figura 11).
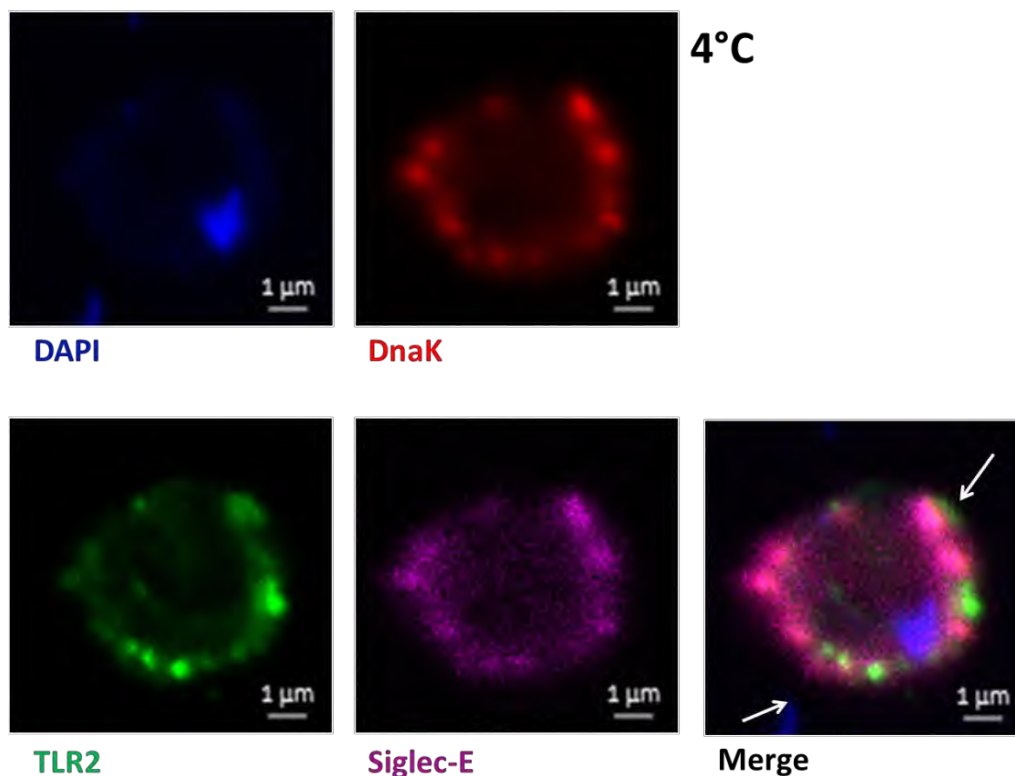


**Figura 9. A DnaK co-localiza com o complexo Siglec-E/TLR2 na membrana de células dendríticas de camundongos.** Células dendríticas de camundongos foram isoladas do baço e linfonodos e colocadas para aderir em lamínulas por 48h. Após isso, as células foram tratadas com 10 µg/ml de DnaK marcada com o corante Alexa 594 por 20 min, no gelo. Posteriormente, as células foram fixadas, coradas com DAPI e anticorpos para o Siglec-E e TLR2 e, analisadas por microscopia Confocal.
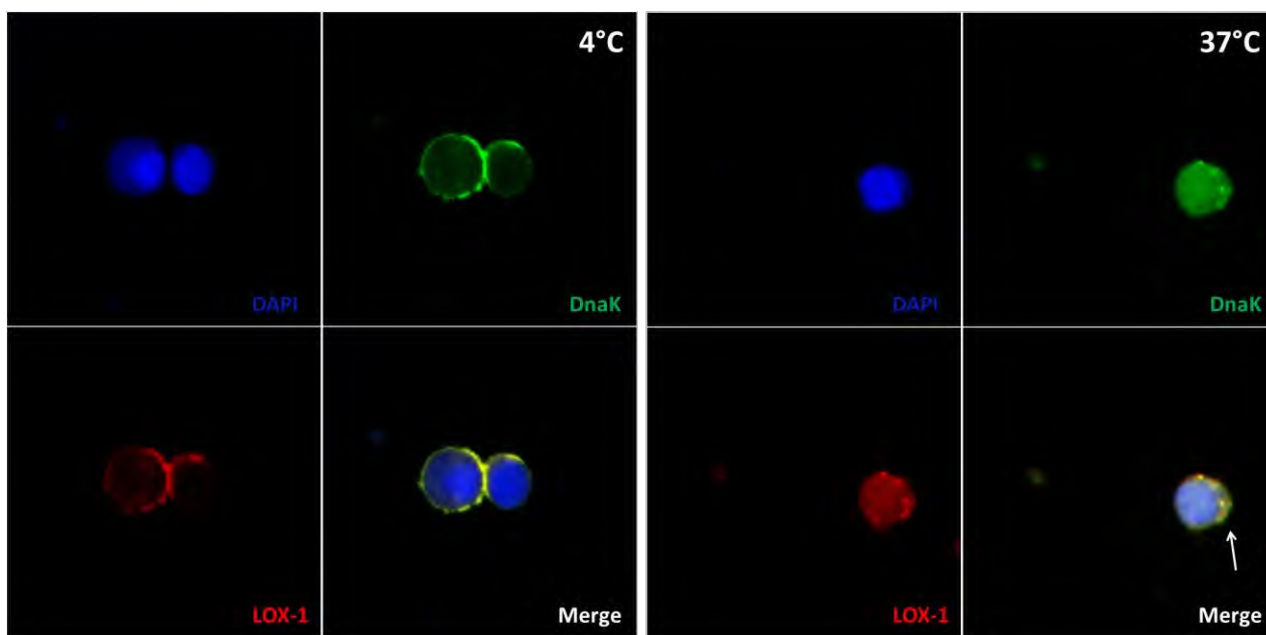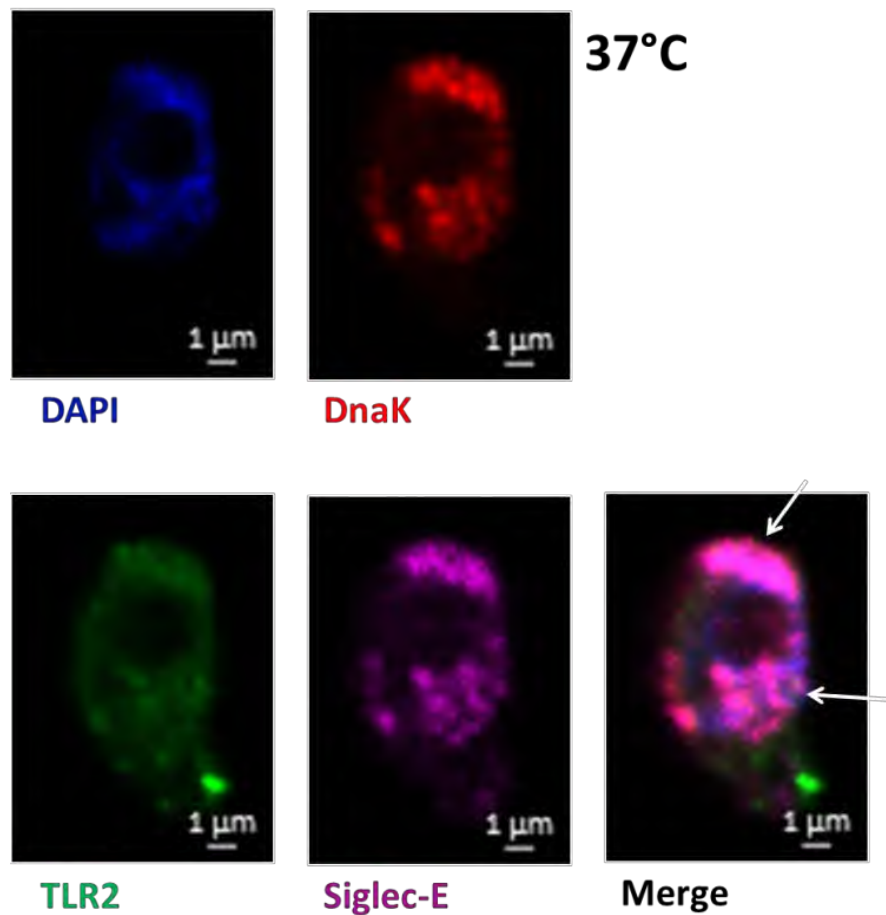
**Figura 10. A DnaK co-localiza com o complexo Siglec-E/TLR2 em vesículas intracelulares em células dendríticas de camundongos.** Células dendríticas de camundongos foram isoladas do baço e linfonodos e colocadas para aderir em lamínulas por 48h. Após isso, as células foram tratadas com 10 µg/ml de DnaK marcada com o corante Alexa 594 por 20 min, no gelo. Posteriormente, as células foram deixadas 37°C por 20 min, fixadas, coradas com DAPI e anticorpos para o Siglec-E e TLR2 e, analisadas por microscopia Confocal.
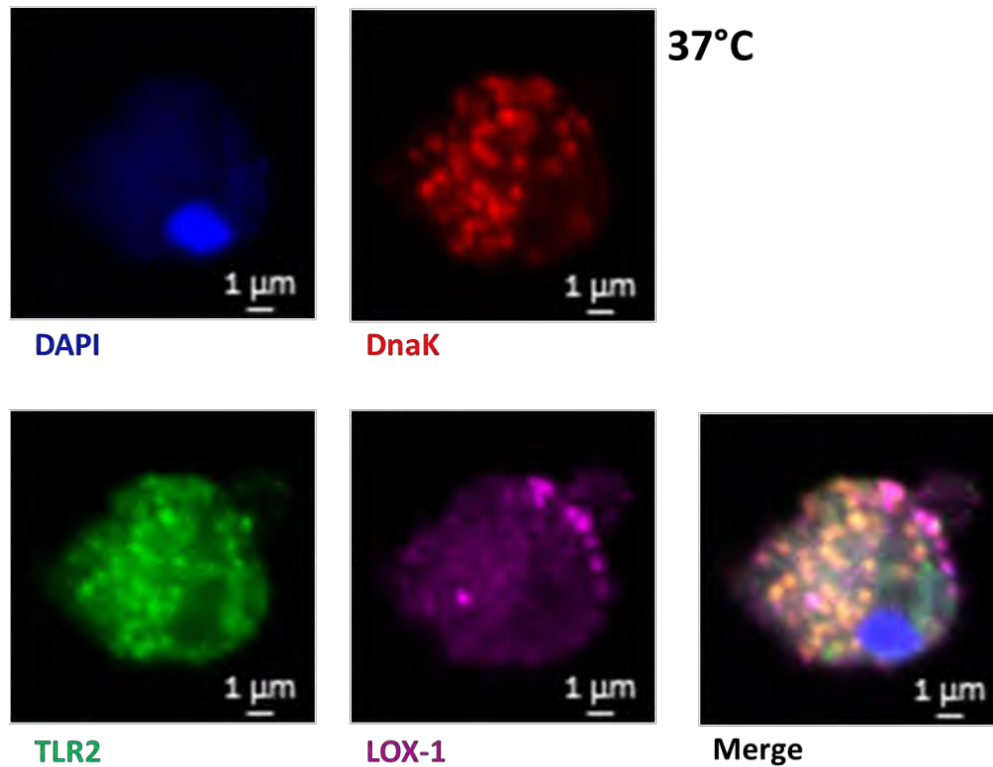
**Figura 11. A DnaK co-localiza com o complexo LOX-1/TLR2 em vesículas intracelulares em células dendríticas de camundongos.** Células dendríticas de camundongos foram isoladas do baço e linfonodos e colocadas para aderir em lamínulas por 48h. Após isso, as células foram tratadas com 10 μg/ml de DnaK marcada com o corante Alexa 594 por 20 min, no gelo. Posteriormente, as células foram deixadas 37°C por 20 min, fixadas, coradas com DAPI e anticorpos para o LOX-1 e TLR2 e, analisadas por microscopia Confocal.

O receptor SR-A foi descrito como um receptor para Hsps e possui um efeito supressor das respostas inflamatórias desencadeadas pelo TLR4 (145). Portanto, testamos a co-localização da DnaK com SR-A em DCs de camundongos. Na Figura 12 demonstramos que a DnaK não co-localiza com células expressando SR-A.
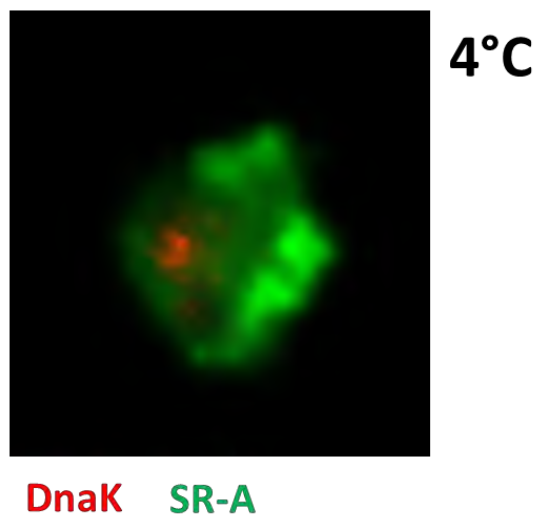


**Figura 12. A DnaK não co-localiza com o receptor SR-A em células dendríticas de camundongos.** Células dendríticas de camundongos foram isoladas do baço e linfonodos e colocadas para aderir em lamínulas por 48h. Após isso, as células foram tratadas com 10 μg/ml de DnaK marcada com o corante Alexa 594 por 20 min, no gelo. Posteriormente, as células foram fixadas, coradas com DAPI, marcadas com anticorpos para o SR-A e analisadas por microscopia Confocal.

Portanto, nossos dados indicam que a DnaK esta co-localizando com o complexo Siglec-E/LOX-1/TLR2, o qual pode ser todo endocitado por células dendríticas de camundongos.

A DnaK pode tolerizar células dendríticas de camundongos através da diminuição do MHC II e do CD80. Testamos se esse efeito é dependente do LOX-1. Para isso, tratamos células dendríticas (DCs) de animais WT ou LOX-1 KO com a DnaK ou controle por 24h. Depois analisamos os níveis de MHC II e CD80 por citometria de fluxo. Vimos que os efeitos da DnaK nas DCs foi independente do LOX-1 (Figura 13).
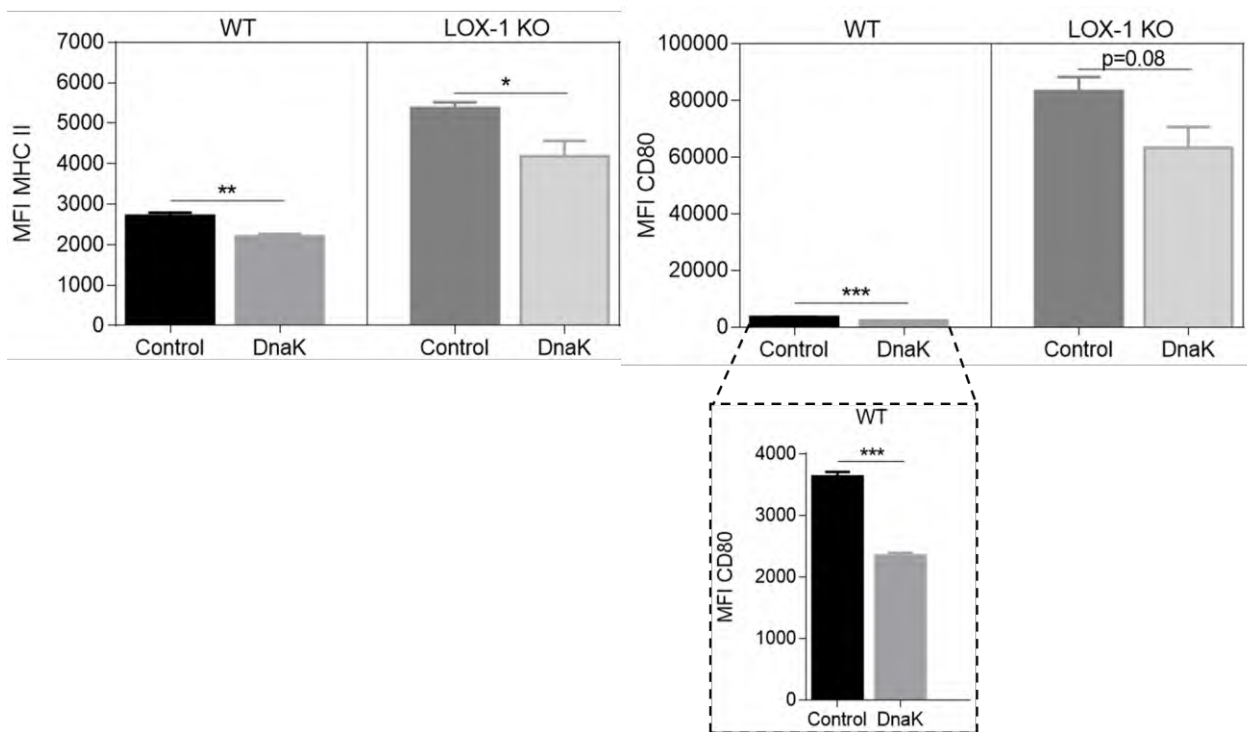


**Figura 13. Os efeitos da DnaK são independentes da expressão de LOX-1 pelas células dendríticas.** Células dendríticas foram isoladas de linfonodos e baco de animais selvagens (WT) ou LOX-1 KO e tratadas com a DnaK ou controle por 24h. Após isso, os níveis de MHC II e CD80 foram avaliados por citometria de fluxo.

Não conseguimos analisar o papel do Siglec-E nos efeitos anti-inflamatórios da DnaK, antes do termino do período de Doutorado sanduiche. Porém, isso será feito posteriormente por outro pesquisador.

**Discussão**

Alguns trabalhos têm demonstrado que membros da família Hsp70 tem um papel anti-inflamatório e protetor em modelos animais experimentais como artrite (87, 88, 146, 147), colite (90), fibrose pulmonar (91) e danos cerebrais (148). Por outro lado, a Hsp70 vem sendo utilizada como vacina para o combate de tumores (111, 112). Nesses estudos, a Hsp70 pode facilitar o processamento e a apresentação de antígenos tumorais fusionados com ela, gerando respostas mediadas por células T CD8+ efetoras (113, 114). A Hsp70 com antígenos tumorais pode se ligar a receptores endocíticos presentes na superfície das células dendríticas, modulando essas células para um fenótipo maduro capaz de fazer apresentação cruzada (antígenos capturados no meio extracelular são apresentados no MHC I), gerando uma resposta T CD8+ efetora e diminuindo o tamanho tumoral. Uma das possíveis explicações para esses efeitos dicotômicos é o fato desses trabalhos não utilizarem a mesma fonte de proteína, ou proteínas recombinantes produzidas em diferentes sistemas experimentais. Outra possível explicação seria a natureza dos receptores inatos que essas proteínas podem se ligar e os complexos que esses receptores formam entre si.

Demonstramos que a DnaK de *M. tuberculosis* (Hsp70) co-localiza com um complexo formado por Siglec-E/LOX-1/TLR2 em DCs de camundongos. Além disso, vimos que esse complexo pode ser todo internalizado. Porém, a DnaK não foi capaz de se ligar no TLR2 diretamente, quando expresso em células CHO-K1. Observamos que a diminuição de MHC II e CD80 induzida pela DnaK foi independente do LOX-1 KO, mas não tivemos a oportunidade ainda de testar nas DCs Siglec-E KO. Mesmo sem esses dados, estipulamos a hipótese de que dependendo do receptor no qual a DnaK se liga, ela ira gerar uma resposta oposta – anti ou pro-inflamatória (Figura 14). Nela, quando ligada ao Siglec-E e ao LOX-1, o Siglec-E inibe a resposta inflamatória do LOX-1 e sinaliza via TLR2 para uma resposta anti-inflamatória. Caso, a DnaK se ligue apenas ao LOX-1, quando o Siglec-E não esteja presente no complexo e/ou célula ou ainda sua expressão seja muito baixa, a resposta gerada por essa Hsp será inflamatória. Essa hipótese ainda precisa testada para Hsp70s de outras fontes, como humanos e camundongos, por exemplo. Outro ponto chave será descobrir os níveis e em quais subtipos celulares esses receptores são expressos, além de como sua expressão é modula em microambientes diferentes.
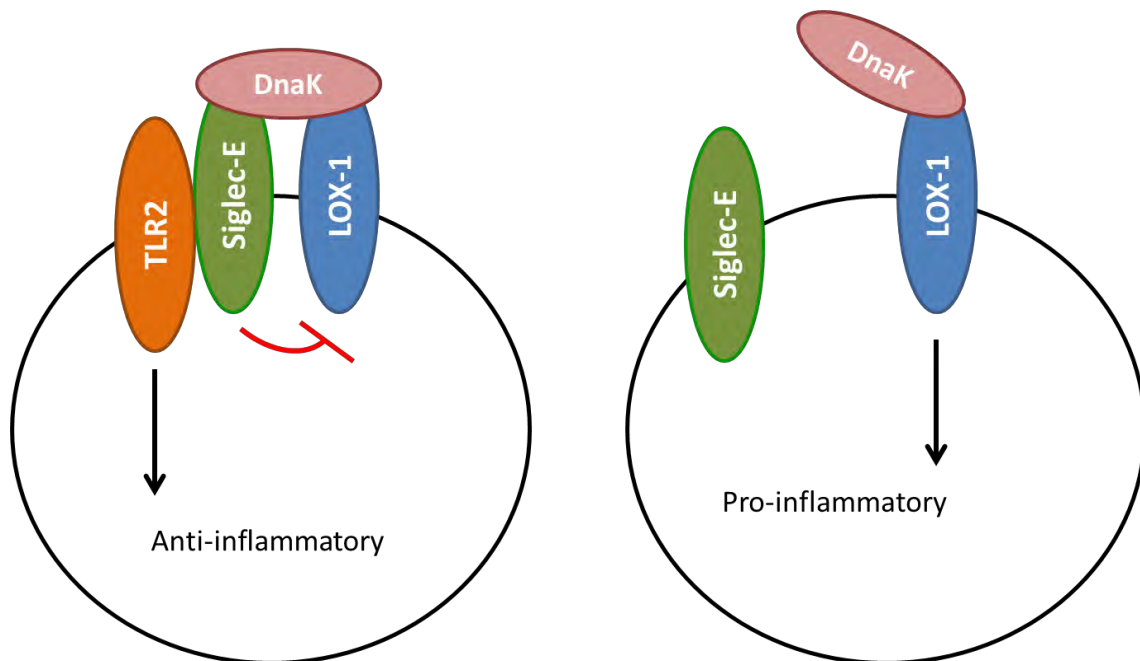
**Figura 14.** DnaK se liga ao complexo Siglec-E/TLR2/LOX-1 e modula respostas imunes.

A ligação da DnaK ao Siglec-E e ao LOX-1 parece ser evolutivamente conservada. Recentemente, foi mostrado que a Hsp70 humana pode se ligar diretamente Siglec-5 e Siglec-14, de maneira independente do ácido siálico (72). Os receptores Siglecs foram uma ampla família e compartilham a capacidade de se ligar ao ácido siálico e suprimir respostas inflamatórias. Os domínios intracelulares dos Siglecs podem inibir respostas inflamatórias desencadeadas por TLRs (149). Recentemente, nanopartículas que ligam a receptores Siglecs foram utilizadas para tratar e diminuir a inflamação em um modelo animal de sepse, demonstrando o potente efeito anti-inflamatório desses receptores (150). No trabalho de Fong e colaboradores (72), a Hsp70 humana desencadeou uma resposta pro-inflamatória quando ligada ao Siglec-14 e anti-inflamatória quando se ligou ao Siglec-5. Esse efeito dicotômico foi devido ao fato desses receptores compartilharem sítios extracelulares de ligação do ligante idênticos, porém a porção intracelular envia sinais opostos após seu engajamento.

Também foi observado que a Hsp70 humana pode se ligar ao receptor LOX-1 expresso em DCs e promover a apresentação cruzada de antígenos (103). Essa ligação foi confirmada em outro sistema por um grupo independente (151). Nesse trabalho, além do LOX-1, a Hsp70 foi

capaz de se ligar nos receptores FEEL-1, SREC-1, NGK2A e NGK2D (151). Nossos dados indicam que a DnaK não foi capaz de se ligar no FEEL-1 e se ligou de maneira fraco ao SREC-1 (Figura 1). Os receptores NGK2A e NGK2D não foram testados nesse estudo (Tabela 1). Levando em consideração que a DnaK se ligou de maneira proeminente no LOX-1 e que a Hsp70 humana também pode se ligar no mesmo receptor, acreditamos que essa ligação acontece em um região estruturalmente conservada entre a DnaK de *M. tuberculosis* e a Hsp70 humana.

O fato de observarmos a presença do TLR2 no complexo Siglec-E/LOX-1/TLR2 e a incapacidade da DnaK se ligar diretamente nesse receptor, hipotetizamos que o TLR2 esta sendo usado como um co-receptor no complexo para o envio de sinais intracelulares. De fato, tanto os Siglecs (143, 149), quanto o LOX-1, de maneira não tão clara (152), são capazes de interagir com TLRs. Também observamos que os efeitos da DnaK sobre as DCs é dependente do TLR2 (Capitulo 1 e 2). Corroborando com nossos achados, tem sido sugerido que ligantes do TLR2 são ótimos indutores de IL-10 em diferentes trabalhos (94-96). Por exemplo, a sinalização via TLR2 é crucial para indução de IL-10 por DCs estimuladas com *Mycobacterium tuberculosis* ou com lipoproteínas, e também está relacionada com a modulação do MHC II pelo microrganismo (153). O mesmo efeito foi visto em DCs estimuladas com antígenos de *Yersinia pestis* (154).

No futuro, realizaremos experimentos utilizando células Siglec-E KO para confirmar todas essas hipóteses.

# DISCUSSÃO GERAL E CONSIDERAÇÕES FINAIS

No presente trabalho, demonstramos os mecanismos pelos quais a DnaK (Hsp70) de *M. tuberculosis* pode modular células dendríticas e como podemos utilizar isso para modular respostas inflamatórias *in vivo* com o objetivo de tratar patologias. A DnaK diminuiu a expressão de MHC II e CD86 por intermédio da molécula MARCH1, através da via TLR2-ERK-STAT3-IL-10. Essa foi a primeira vez que uma via molecular completa foi descrita para a ativação de MARCH1. Pretendemos explorar se a DnaK pode induzir outros membros da família MARCH, como MARCH8 e se essa proteína é capaz de modular moléculas de MHC I. Apesar disso, acreditamos que criamos um conceito novo no qual a indução de MARCH1 e a diminuição do MHC (primeiro sinal) pode ser uma estratégia inovadora na tentativa de tratar desordens inflamatórias, como a rejeição de pele, sepse, autoimunidade e asma.

Na tentativa de mapear qual subtipo de célula dendrítica a DnaK modulava, realizamos outra descoberta relevante: em transplantes de pele, as DCs dependentes de Batf3 da pele são o principal subtipo migratório que chega ao linfonodo drenante do receptor (os clássicos leucócitos passageiros), desencadeando respostas T CD8+ aloreativas. A modulação *in-situ* dessas células pela DnaK abre uma janela para o desenvolvimento de novas terapias que modulam especificamente essas células antes do transplante, causando uma imunossupressão local. Isso pode diminuir a necessidade dos pacientes receberem drogas imunossupressoras as quais causam uma série de efeitos adversos. Será importante no futuro determinar se a DnaK extracelular pode interagir com essas células em outros tipos de transplante, vascularizados; ou se em outras patologias, como doenças autoimunes ou asma, a DnaK continua interagindo com essas DCs, ou se modula uma subpopulação diferente.

Além disso, nossos resultados apóiam a hipótese de que a via TLR2-ERK-STAT3-IL-10 é uma rota utilizada por membros da família Hsp70 para desempenharem seus papéis anti-inflamatórios. Foi demonstrado por outros trabalhos que essas moléculas estão envolvidas em rotas que integram ainda as moléculas AHR, c-Maf, CD39 e IL-27 (155, 156). Pretendemos explorar futuramente o envolvimento dessas moléculas nas respostas desencadeadas pela DnaK.

Também demonstramos que a DnaK pode diminuir níveis basais da expressão de IFN-γ, TNF-α e MCP-1 em BMDCs através da diminuição da expressão dos fatores de transcrição C/EBPβ e C/EBPδ (157). Apesar do NF-κB ser o principal fator de transcrição na indução de citocinas inflamatórias (158), o efeito da DnaK no nosso sistema foi independente dele. Em outro trabalho, a Hsp70 intracelular inibiu a produção de citocinas inflamatórias induzida por LPS, através da interferência na transcrição dos genes dessas citocinas via NF-κB (159). Em outro estudo, o aumento da expressão da Hsp70 em células mononucleares humanas, inibiu a translocação (induzida por LPS) do NF-κB para o núcleo, e a consequente a produção das citocinas inflamatórias (160). Foi sugerido, portanto, que a Hsp70 estabiliza o complexo NF-κB/ IκBα pela inibição da degradação do IκBα (161). Nosso artigo foi o primeiro trabalho o qual associou os efeitos da DnaK (ou qualquer membro da família da Hsp70) extracelular com a modulação de moléculas da família C/EBP.

Uma explicação para essa diferença pode estar na localização da Hsp70 – extracelular *versus* intracelular – a qual pode desencadear vias totalmente diferentes ou exercer funções diferentes. Outra possibilidade é a fonte da Hsp70 – sendo os mecanismos desencadeados da procariótica diferentes das de mamíferos. Para isso, estamos produzindo outros membros da família da Hsp70, como a Hsp70 murina e HSPA1A humana, em nosso sistema experimental para verificar o quanto seus efeitos diferem ou se igualam aos da DnaK, incluindo a ligação no complexo LOX-1/Siglec-E/TLR2. Também enviamos amostras dessas diferentes isoformas para um colaborador nos Estados Unidos para a análise de modificações pós-translacionais. Acreditamos essas modificações representam um ponto chave na tentativa de entender os efeitos opostos das Hsps no sistema imune.

A elucidação dos mecanismos celulares e moleculares pelos quais a DnaK age permite otimizar o seu uso  como uma terapia inovadora, *in-situ,* na prevenção da rejeição aguda a enxertos cutâneos, e também possivelmente para outras doenças inflamatórias. A partir desses conhecimentos, depositamos uma patente na qual formulamos uma composição para ser utilizada como, ou em conjunto, com uma solução de preservação de órgãos. Essa composição além de preservar o órgão, modula as células do doador, através da diminuição da expressão de MHC II e CD86. Através de uma consultoria internacional externa, a nossa patente foi indicada como uma

das mais fortes da PUCRS. Sob incentivo da Universidade, eu e a Prof. Cristina fundamos uma empresa *start-up* denominada 2BScience. Nela pretendemos explorar o potencial anti-inflamatório de moléculas baseadas na DnaK, desenvolvendo uma plataforma para o uso em patologias como a sepse, asma, transplantes e autoimunidade.

# REFERÊNCIAS

1.      Steinman RM, Cohn ZA. Identification of a novel cell type in peripheral lymphoid organs of mice. I. Morphology, quantitation, tissue distribution. The Journal of experimental medicine. 1973;137(5):1142-62. Epub 1973/05/01.

2.      Liu K, Nussenzweig MC. Origin and development of dendritic cells. Immunol Rev. 2010;234(1):45-54. Epub 2010/03/03.

3.      Shortman K, Liu YJ. Mouse and human dendritic cell subtypes. Nature reviews Immunology. 2002;2(3):151-61. Epub 2002/03/27.

4.      Chen L, Flies DB. Molecular mechanisms of T cell co-stimulation and co-inhibition. Nature reviews Immunology. 2013;13(4):227-42. Epub 2013/03/09.

5.      Curtsinger JM, Lins DC, Mescher MF. Signal 3 determines tolerance versus full activation of naive CD8 T cells: dissociating proliferation and development of effector function. The Journal of experimental medicine. 2003;197(9):1141-51. Epub 2003/05/07.

6.      Swain SL, McKinstry KK, Strutt TM. Expanding roles for CD4(+) T cells in immunity to viruses. Nature reviews Immunology. 2012;12(2):136-48. Epub 2012/01/24.

7.      Vignali DA, Collison LW, Workman CJ. How regulatory T cells work. Nature reviews Immunology. 2008;8(7):523-32. Epub 2008/06/21.

8.      Skapenko A, Leipe J, Lipsky PE, Schulze-Koops H. The role of the T cell in autoimmune inflammation. Arthritis Res Ther. 2005;7 Suppl 2:S4-14. Epub 2005/04/19.

9.      Liu Z, Fan H, Jiang S. CD4(+) T-cell subsets in transplantation. Immunol Rev. 2013;252(1):183-91. Epub 2013/02/15.

10.     Corthay A. A three-cell model for activation of naive T helper cells. Scand J Immunol. 2006;64(2):93-6. Epub 2006/07/27.

11.     Turnquist HR, Fischer RT, Thomson AW. Pharmacological modification of dendritic cells to promote their tolerogenicity in transplantation. Methods Mol Biol. 2010;595:135-48. Epub 2009/11/27.

12.     Moore KW, de Waal Malefyt R, Coffman RL, O'Garra A. Interleukin-10 and the interleukin-10 receptor. Annu Rev Immunol. 2001;19:683-765. Epub 2001/03/13.

13.     Steinman RM, Hawiger D, Nussenzweig MC. Tolerogenic dendritic cells. Annu Rev Immunol. 2003;21:685-711. Epub 2003/03/05.

14.     Rutella S, Danese S, Leone G. Tolerogenic dendritic cells: cytokine modulation comes of age. Blood. 2006;108(5):1435-40. Epub 2006/05/11.

15.     Morelli AE, Thomson AW. Tolerogenic dendritic cells and the quest for transplant tolerance. Nature reviews Immunology. 2007;7(8):610-21. Epub 2007/07/14.

16.     Ford ML, Adams AB, Pearson TC. Targeting co-stimulatory pathways: transplantation and autoimmunity. Nat Rev Nephrol. 2014;10(1):14-24. Epub 2013/10/09.

17.     Jenkins MK, Chen CA, Jung G, Mueller DL, Schwartz RH. Inhibition of antigen-specific proliferation of type 1 murine T cell clones after stimulation with immobilized anti-CD3 monoclonal antibody. J Immunol. 1990;144(1):16-22. Epub 1990/01/01.

18.     Steinman RM, Turley S, Mellman I, Inaba K. The induction of tolerance by dendritic cells that have captured apoptotic cells. The Journal of experimental medicine. 2000;191(3):411-6. Epub 2000/02/09.

19.     Long SA, Rieck M, Tatum M, Bollyky PL, Wu RP, Muller I, et al. Low-dose antigen promotes induction of FOXP3 in human CD4+ T cells. J Immunol. 2011;187(7):3511-20. Epub 2011/08/26.

20.     Kenna TJ, Thomas R, Steptoe RJ. Steady-state dendritic cells expressing cognate antigen terminate memory CD8+ T-cell responses. Blood. 2008;111(4):2091-100. Epub 2007/11/16.

21.     Anderson AE, Sayers BL, Haniffa MA, Swan DJ, Diboll J, Wang XN, et al. Differential regulation of naive and memory CD4+ T cells by alternatively activated dendritic cells. J Leukoc Biol. 2008;84(1):124-33. Epub 2008/04/24.

22.     Beriou G, Moreau A, Cuturi MC. Tolerogenic dendritic cells: applications for solid organ transplantation. Curr Opin Organ Transplant. 2012;17(1):42-7. Epub 2012/01/10.

23.     Borges TJ, Wieten L, van Herwijnen MJ, Broere F, van der Zee R, Bonorino C, et al. The anti-inflammatory mechanisms of Hsp70. Front Immunol. 2012;3:95. Epub 2012/05/09.

24.     Borges TJ, Porto BN, Teixeira CA, Rodrigues M, Machado FD, Ornaghi AP, et al. Prolonged survival of allografts induced by mycobacterial Hsp70 is dependent on CD4+CD25+ regulatory T cells. PLoS One. 2010;5(12):e14264. Epub 2010/12/21.

25.     Pardoll DM. The blockade of immune checkpoints in cancer immunotherapy. Nat Rev Cancer. 2012;12(4):252-64. Epub 2012/03/23.

26.     Riella LV, Paterson AM, Sharpe AH, Chandraker A. Role of the PD-1 pathway in the immune response. Am J Transplant. 2012;12(10):2575-87. Epub 2012/08/21.

27.     de Souza AP, Bonorino C. Tumor immunosuppressive environment: effects on tumor-specific and nontumor antigen immune responses. Expert Rev Anticancer Ther. 2009;9(9):1317-32. Epub 2009/09/19.

28.     Larkin J, Chiarion-Sileni V, Gonzalez R, Grob JJ, Cowey CL, Lao CD, et al. Combined Nivolumab and Ipilimumab or Monotherapy in Untreated Melanoma. N Engl J Med. 2015;373(1):23-34. Epub 2015/06/02.

29.     Riella LV, Sayegh MH. T-cell co-stimulatory blockade in transplantation: two steps forward one step back! Expert Opin Biol Ther. 2013;13(11):1557-68. Epub 2013/10/03.

30.     Riella LV, Liu T, Yang J, Chock S, Shimizu T, Mfarrej B, et al. Deleterious effect of CTLA4-Ig on a Treg-dependent transplant model. Am J Transplant. 2012;12(4):846-55. Epub 2012/02/04.

31.     Charbonnier LM, Vokaer B, Lemaitre PH, Field KA, Leo O, Le Moine A. CTLA4-Ig restores rejection of MHC class-II mismatched allografts by disabling IL-2-expanded regulatory T cells. Am J Transplant. 2012;12(9):2313-21. Epub 2012/07/05.

32.     Valujskikh A, Pantenburg B, Heeger PS. Primed allospecific T cells prevent the effects of costimulatory blockade on prolonged cardiac allograft survival in mice. Am J Transplant. 2002;2(6):501-9. Epub 2002/07/18.

33.     Steimle V, Siegrist CA, Mottet A, Lisowska-Grospierre B, Mach B. Regulation of MHC class II expression by interferon-gamma mediated by the transactivator gene CIITA. Science. 1994;265(5168):106-9. Epub 1994/07/01.

34.     Reith W, Boss JM. New dimensions of CIITA. Nature immunology. 2008;9(7):713-4. Epub 2008/06/20.

35.     Pennini ME, Liu Y, Yang J, Croniger CM, Boom WH, Harding CV. CCAAT/enhancer-binding protein beta and delta binding to CIITA promoters is associated with the inhibition of CIITA expression in response to Mycobacterium tuberculosis 19-kDa lipoprotein. J Immunol. 2007;179(10):6910-8. Epub 2007/11/06.

36.     Moffat JM, Mintern JD, Villadangos JA. Control of MHC II antigen presentation by ubiquitination. Current opinion in immunology. 2013;25(1):109-14. Epub 2012/11/28.

37.     Roche PA, Furuta K. The ins and outs of MHC class II-mediated antigen processing and presentation. Nature reviews Immunology. 2015;15(4):203-16. Epub 2015/02/28.

38.     Oh J, Shin JS. Molecular mechanism and cellular function of MHCII ubiquitination. Immunol Rev. 2015;266(1):134-44. Epub 2015/06/19.

39.     Baravalle G, Park H, McSweeney M, Ohmura-Hoshino M, Matsuki Y, Ishido S, et al. Ubiquitination of CD86 is a key mechanism in regulating antigen presentation by dendritic cells. J Immunol. 2011;187(6):2966-73. Epub 2011/08/19.

40.     Tze LE, Horikawa K, Domaschenz H, Howard DR, Roots CM, Rigby RJ, et al. CD83 increases MHC II and CD86 on dendritic cells by opposing IL-10-driven MARCH1-mediated ubiquitination and degradation. The Journal of experimental medicine. 2011;208(1):149-65. Epub 2011/01/12.

41.     Thibodeau J, Bourgeois-Daigneault MC, Huppe G, Tremblay J, Aumont A, Houde M, et al. Interleukin-10-induced MARCH1 mediates intracellular sequestration of MHC class II in monocytes. Eur J Immunol. 2008;38(5):1225-30. Epub 2008/04/05.

42.     Oh J, Wu N, Baravalle G, Cohn B, Ma J, Lo B, et al. MARCH1-mediated MHCII ubiquitination promotes dendritic cell selection of natural regulatory T cells. The Journal of experimental medicine. 2013;210(6):1069-77. Epub 2013/05/29.

43.     Heath WR, Carbone FR. Dendritic cell subsets in primary and secondary T cell responses at body surfaces. Nature immunology. 2009;10(12):1237-44. Epub 2009/11/17.

44.     Watowich SS, Liu YJ. Mechanisms regulating dendritic cell specification and development. Immunol Rev. 2010;238(1):76-92. Epub 2010/10/26.

45.     Merad M, Sathe P, Helft J, Miller J, Mortha A. The Dendritic Cell Lineage: Ontogeny and Function of Dendritic Cells and Their Subsets in the Steady State and the Inflamed Setting. Annual Review of Immunology, Vol 31. 2013;31:563-604.

46.     Igyarto BZ, Haley K, Ortner D, Bobr A, Gerami-Nejad M, Edelson BT, et al. Skin-resident murine dendritic cell subsets promote distinct and opposing antigen-specific T helper cell responses. Immunity. 2011;35(2):260-72. Epub 2011/07/26.

47.     Lewis KL, Reizis B. Dendritic cells: arbiters of immunity and immunological tolerance. Cold Spring Harb Perspect Biol. 2012;4(8):a007401. Epub 2012/08/03.

48.     Guery L, Hugues S. Tolerogenic and activatory plasmacytoid dendritic cells in autoimmunity. Front Immunol. 2013;4:59. Epub 2013/03/20.

49.     Fuchsberger M, Hochrein H, O'Keeffe M. Activation of plasmacytoid dendritic cells. Immunol Cell Biol. 2005;83(5):571-7. Epub 2005/09/22.

50.     Shi C, Pamer EG. Monocyte recruitment during infection and inflammation. Nature reviews Immunology. 2011;11(11):762-74. Epub 2011/10/11.

51.	Caminschi I, Maraskovsky E, Heath WR. Targeting Dendritic Cells in vivo for Cancer Therapy. Front Immunol. 2012;3:13. Epub 2012/05/09.

52.	Heath WR, Carbone FR. The skin-resident and migratory immune system in steady state and memory: innate lymphocytes, dendritic cells and T cells. Nat Immunol. 2013;14(10):978-85. Epub 2013/09/21.

53.	Seneschal J, Clark RA, Gehad A, Baecher-Allan CM, Kupper TS. Human epidermal Langerhans cells maintain immune homeostasis in skin by activating skin resident regulatory T cells. Immunity. 2012;36(5):873-84. Epub 2012/05/09.

54.	Edelson BT, Kc W, Juang R, Kohyama M, Benoit LA, Klekotka PA, et al. Peripheral CD103+ dendritic cells form a unified subset developmentally related to CD8alpha+ conventional dendritic cells. The Journal of experimental medicine. 2010;207(4):823-36.

55.	Ferris ST, Carrero JA, Mohan JF, Calderon B, Murphy KM, Unanue ER. A minor subset of Batf3-dependent antigen-presenting cells in islets of Langerhans is essential for the development of autoimmune diabetes. Immunity. 2014;41(4):657-69.

56.	Nakano H, Free ME, Whitehead GS, Maruoka S, Wilson RH, Nakano K, et al. Pulmonary CD103(+) dendritic cells prime Th2 responses to inhaled allergens. Mucosal immunology. 2012;5(1):53-65.

57.	Gottschalk C, Damuzzo V, Gotot J, Kroczek RA, Yagita H, Murphy KM, et al. Batf3-dependent dendritic cells in the renal lymph node induce tolerance against circulating antigens. Journal of the American Society of Nephrology : JASN. 2013;24(4):543-9.

58.	Idoyaga J, Fiorese C, Zbytnuik L, Lubkin A, Miller J, Malissen B, et al. Specialized role of migratory dendritic cells in peripheral tolerance induction. J Clin Invest. 2013;123(2):844-54. Epub 2013/01/10.

59.	Flacher V, Tripp CH, Mairhofer DG, Steinman RM, Stoitzner P, Idoyaga J, et al. Murine Langerin+ dermal dendritic cells prime CD8+ T cells while Langerhans cells induce cross-tolerance. EMBO molecular medicine. 2014;6(12):1638.

60.	Haniffa M, Shin A, Bigley V, McGovern N, Teo P, See P, et al. Human tissues contain CD141hi cross-presenting dendritic cells with functional homology to mouse CD103+ nonlymphoid dendritic cells. Immunity. 2012;37(1):60-73. Epub 2012/07/17.

61.	Chu CC, Ali N, Karagiannis P, Di Meglio P, Skowera A, Napolitano L, et al. Resident CD141 (BDCA3)+ dendritic cells in human skin produce IL-10 and induce regulatory T cells that suppress skin inflammation. The Journal of experimental medicine. 2012;209(5):935-45. Epub 2012/05/02.

62.	Obhrai JS, Oberbarnscheidt M, Zhang N, Mueller DL, Shlomchik WD, Lakkis FG, et al. Langerhans cells are not required for efficient skin graft rejection. J Invest Dermatol. 2008;128(8):1950-5. Epub 2008/03/14.

63.	Celli S, Albert ML, Bousso P. Visualizing the innate and adaptive immune responses underlying allograft rejection by two-photon microscopy. Nat Med. 2011;17(6):744-9. Epub 2011/05/17.

64.	Li D, Romain G, Flamar AL, Duluc D, Dullaers M, Li XH, et al. Targeting self- and foreign antigens to dendritic cells via DC-ASGPR generates IL-10-producing suppressive CD4+ T cells. The Journal of experimental medicine. 2012;209(1):109-21. Epub 2012/01/04.

65.	Mambula SS, Calderwood SK. Heat shock protein 70 is secreted from tumor cells by a nonclassical pathway involving lysosomal endosomes. J Immunol. 2006;177(11):7849-57. Epub 2006/11/23.

66.	Hightower LE, Guidon PT, Jr. Selective release from cultured mammalian cells of heat-shock (stress) proteins that resemble glia-axon transfer proteins. J Cell Physiol. 1989;138(2):257-66. Epub 1989/02/01.

67.     Pockley AG, Muthana M, Calderwood SK. The dual immunoregulatory roles of stress proteins. Trends Biochem Sci. 2008;33(2):71-9. Epub 2008/01/10.

68.     Ritossa F. New Puffing Pattern Induced by Temperature Shock and Dnp in Drosophila. Experientia. 1962;18(12):571-&.

69.     Tissieres A, Mitchell HK, Tracy UM. Protein synthesis in salivary glands of Drosophila melanogaster: relation to chromosome puffs. J Mol Biol. 1974;84(3):389-98. Epub 1974/04/15.

70.     Jolly C, Morimoto RI. Role of the heat shock response and molecular chaperones in oncogenesis and cell death. J Natl Cancer Inst. 2000;92(19):1564-72. Epub 2000/10/06.

71.     Jaattela M. Heat shock proteins as cellular lifeguards. Ann Med. 1999;31(4):261-71. Epub 1999/09/10.

72.     Fong JJ, Sreedhara K, Deng L, Varki NM, Angata T, Liu Q, et al. Immunomodulatory activity of extracellular Hsp70 mediated via paired receptors Siglec-5 and Siglec-14. EMBO J. 2015. Epub 2015/10/16.

73.     Jayaprakash P, Dong H, Zou M, Bhatia A, O'Brien K, Chen M, et al. Hsp90alpha and Hsp90beta together operate a hypoxia and nutrient paucity stress-response mechanism during wound healing. Journal of cell science. 2015;128(8):1475-80. Epub 2015/03/05.

74.     Weng D, Song B, Koido S, Calderwood SK, Gong J. Immunotherapy of radioresistant mammary tumors with early metastasis using molecular chaperone vaccines combined with ionizing radiation. J Immunol. 2013;191(2):755-63. Epub 2013/06/19.

75.     Kaufmann SH. Heat shock proteins and autoimmunity: facts or fiction? Curr Biol. 1991;1(6):359-61. Epub 1991/12/01.

76.     Daugaard M, Rohde M, Jaattela M. The heat shock protein 70 family: Highly homologous proteins with overlapping and distinct functions. Febs Letters. 2007;581(19):3702-10.

77.     Kaufmann SH, Flesch IE, Gatrill A, Gulle H, Koga T, Munk ME, et al. Function and antigen specificity of T-cells against mycobacteria. Trop Med Parasitol. 1990;41(3):319-20. Epub 1990/09/01.

78.     Zugel U, Kaufmann SH. Immune response against heat shock proteins in infectious diseases. Immunobiology. 1999;201(1):22-35. Epub 1999/10/26.

79.     Lydyard PM, van Eden W. Heat shock proteins: immunity and immunopathology. Immunol Today. 1990;11(7):228-9. Epub 1990/07/01.

80.     Hauet-Broere F, Wieten L, Guichelaar T, Berlo S, van der Zee R, Van Eden W. Heat shock proteins induce T cell regulation of chronic inflammation. Ann Rheum Dis. 2006;65 Suppl 3:iii65-8. Epub 2006/10/14.

81.     Garrido C, Gurbuxani S, Ravagnan L, Kroemer G. Heat shock proteins: endogenous modulators of apoptotic cell death. Biochem Biophys Res Commun. 2001;286(3):433-42. Epub 2001/08/21.

82.     Daugaard M, Jaattela M, Rohde M. Hsp70-2 is required for tumor cell growth and survival. Cell Cycle. 2005;4(7):877-80. Epub 2005/06/23.

83.     Morimoto RI. Regulation of the heat shock transcriptional response: cross talk between a family of heat shock factors, molecular chaperones, and negative regulators. Genes Dev. 1998;12(24):3788-96. Epub 1998/12/31.

84.     Detanico T, Rodrigues L, Sabritto AC, Keisermann M, Bauer ME, Zwickey H, et al. Mycobacterial heat shock protein 70 induces interleukin-10 production: immunomodulation of synovial cell cytokine profile and dendritic cell maturation. Clin Exp Immunol. 2004;135(2):336-42. Epub 2004/01/24.

85.     Motta A, Schmitz C, Rodrigues L, Ribeiro F, Teixeira C, Detanico T, et al. Mycobacterium tuberculosis heat-shock protein 70 impairs maturation of dendritic cells from bone marrow precursors, induces interleukin-10 production and inhibits T-cell proliferation in vitro. Immunology. 2007;121(4):462-72. Epub 2007/03/10.

86.     Billingham RE, Medawar PB. The Technique of Free Skin Grafting in Mammals. Journal of Experimental Biology. 1951;28(3):385-402.

87.     Wieten L, Berlo SE, Ten Brink CB, van Kooten PJ, Singh M, van der Zee R, et al. IL-10 is critically involved in mycobacterial HSP70 induced suppression of proteoglycan-induced arthritis. PLoS One. 2009;4(1):e4186. Epub 2009/01/15.

88.     Tanaka S, Kimura Y, Mitani A, Yamamoto G, Nishimura H, Spallek R, et al. Activation of T cells recognizing an epitope of heat-shock protein 70 can protect against rat adjuvant arthritis. J Immunol. 1999;163(10):5560-5. Epub 1999/11/24.

89.     Kingston AE, Hicks CA, Colston MJ, Billingham ME. A 71-kD heat shock protein (hsp) from Mycobacterium tuberculosis has modulatory effects on experimental rat arthritis. Clin Exp Immunol. 1996;103(1):77-82. Epub 1996/01/01.

90.     Tanaka K, Namba T, Arai Y, Fujimoto M, Adachi H, Sobue G, et al. Genetic evidence for a protective role for heat shock factor 1 and heat shock protein 70 against colitis. J Biol Chem. 2007;282(32):23240-52. Epub 2007/06/09.

91.     Tanaka K, Tanaka Y, Namba T, Azuma A, Mizushima T. Heat shock protein 70 protects against bleomycin-induced pulmonary fibrosis in mice. Biochem Pharmacol. 2010;80(6):920-31. Epub 2010/06/02.

92.     Yenari MA, Giffard RG, Sapolsky RM, Steinberg GK. The neuroprotective potential of heat shock protein 70 (HSP70). Mol Med Today. 1999;5(12):525-31. Epub 1999/11/24.

93.     Chalmin F, Ladoire S, Mignot G, Vincent J, Bruchard M, Remy-Martin JP, et al. Membrane-associated Hsp72 from tumor-derived exosomes mediates STAT3-dependent immunosuppressive function of mouse and human myeloid-derived suppressor cells. J Clin Invest. 2010;120(2):457-71. Epub 2010/01/23.

94.     Dillon S, Agrawal S, Banerjee K, Letterio J, Denning TL, Oswald-Richter K, et al. Yeast zymosan, a stimulus for TLR2 and dectin-1, induces regulatory antigen-presenting cells and immunological tolerance. J Clin Invest. 2006;116(4):916-28. Epub 2006/03/18.

95.     Manicassamy S, Ravindran R, Deng J, Oluoch H, Denning TL, Kasturi SP, et al. Toll-like receptor 2-dependent induction of vitamin A-metabolizing enzymes in dendritic cells promotes T regulatory responses and inhibits autoimmunity. Nat Med. 2009;15(4):401-9. Epub 2009/03/03.

96.     Saraiva M, O'Garra A. The regulation of IL-10 production by immune cells. Nature reviews Immunology. 2010;10(3):170-81. Epub 2010/02/16.

97.     Yamazaki S, Okada K, Maruyama A, Matsumoto M, Yagita H, Seya T. TLR2-dependent induction of IL-10 and Foxp3+ CD25+ CD4+ regulatory T cells prevents effective anti-tumor immunity induced by Pam2 lipopeptides in vivo. PLoS One. 2011;6(4):e18833. Epub 2011/05/03.

98.     Kawai T, Akira S. Toll-like receptors and their crosstalk with other innate receptors in infection and immunity. Immunity. 2011;34(5):637-50. Epub 2011/05/28.

99.     Akira S, Sato S. Toll-like receptors and their signaling mechanisms. Scand J Infect Dis. 2003;35(9):555-62. Epub 2003/11/19.

100.     Asea A, Rehli M, Kabingu E, Boch JA, Bare O, Auron PE, et al. Novel signal transduction pathway utilized by extracellular HSP70: role of toll-like receptor (TLR) 2 and TLR4. J Biol Chem. 2002;277(17):15028-34. Epub 2002/02/12.

101.     Asea A, Kraeft SK, Kurt-Jones EA, Stevenson MA, Chen LB, Finberg RW, et al. HSP70 stimulates cytokine production through a CD14-dependant pathway, demonstrating its dual role as a chaperone and cytokine. Nat Med. 2000;6(4):435-42. Epub 2000/03/31.

102.     Basu S, Binder RJ, Ramalingam T, Srivastava PK. CD91 is a common receptor for heat shock proteins gp96, hsp90, hsp70, and calreticulin. Immunity. 2001;14(3):303-13. Epub 2001/04/06.

103.     Delneste Y, Magistrelli G, Gauchat J, Haeuw J, Aubry J, Nakamura K, et al. Involvement of LOX-1 in dendritic cell-mediated antigen cross-presentation. Immunity. 2002;17(3):353-62. Epub 2002/10/02.

104.     Wang Y, Kelly CG, Karttunen JT, Whittall T, Lehner PJ, Duncan L, et al. CD40 is a cellular receptor mediating mycobacterial heat shock protein 70 stimulation of CC-chemokines. Immunity. 2001;15(6):971-83. Epub 2002/01/05.

105.     Floto RA, MacAry PA, Boname JM, Mien TS, Kampmann B, Hair JR, et al. Dendritic cell stimulation by mycobacterial Hsp70 is mediated through CCR5. Science. 2006;314(5798):454-8. Epub 2006/10/21.

106.     Carroll MV, Sim RB, Bigi F, Jakel A, Antrobus R, Mitchell DA. Identification of four novel DC-SIGN ligands on Mycobacterium bovis BCG. Protein Cell. 2010;1(9):859-70. Epub 2011/01/05.

107.     Bausinger H, Lipsker D, Ziylan U, Manie S, Briand JP, Cazenave JP, et al. Endotoxin-free heat-shock protein 70 fails to induce APC activation. Eur J Immunol. 2002;32(12):3708-13. Epub 2003/01/09.

108.     Henderson B, Calderwood SK, Coates AR, Cohen I, van Eden W, Lehner T, et al. Caught with their PAMPs down? The extracellular signalling actions of molecular chaperones are not due to microbial contaminants. Cell Stress Chaperones. 2010;15(2):123-41. Epub 2009/09/05.

109.     Gao B, Tsan MF. Endotoxin contamination in recombinant human heat shock protein 70 (Hsp70) preparation is responsible for the induction of tumor necrosis factor alpha release by murine macrophages. J Biol Chem. 2003;278(1):174-9. Epub 2002/10/31.

110.     Gao BC, Tsan MF. Induction of cytokines by heat shock proteins and endotoxin in murine macrophages. Biochemical and Biophysical Research Communications. 2004;317(4):1149-54.

111.     Kottke T, Pulido J, Thompson J, Sanchez-Perez L, Chong H, Calderwood SK, et al. Antitumor immunity can be uncoupled from autoimmunity following heat shock protein 70-mediated inflammatory killing of normal pancreas. Cancer Res. 2009;69(19):7767-74. Epub 2009/09/10.

112.     Gong J, Zhang Y, Durfee J, Weng D, Liu C, Koido S, et al. A heat shock protein 70-based vaccine with enhanced immunogenicity for clinical use. J Immunol. 2010;184(1):488-96. Epub 2009/12/02.

113.     Murshid A, Gong J, Calderwood SK. The role of heat shock proteins in antigen cross presentation. Front Immunol. 2012;3:63. Epub 2012/05/09.

114.     Noessner E, Gastpar R, Milani V, Brandl A, Hutzler PJ, Kuppner MC, et al. Tumor-derived heat shock protein 70 peptide complexes are cross-presented by human dendritic cells. J Immunol. 2002;169(10):5424-32. Epub 2002/11/08.

115.     Calderwood SK, Stevenson MA, Murshid A. Heat shock proteins, autoimmunity, and cancer treatment. Autoimmune Dis. 2012;2012:486069. Epub 2012/10/12.

116.     Halloran PF. Immunosuppressive drugs for kidney transplantation. N Engl J Med. 2004;351(26):2715-29. Epub 2004/12/24.

117.     Murakami N, Riella LV, Funakoshi T. Risk of metabolic complications in kidney transplantation after conversion to mTOR inhibitor: a systematic review and meta-analysis. Am J Transplant. 2014;14(10):2317-27. Epub 2014/08/26.

118.     Medawar PB. The behaviour and fate of skin autografts and skin homografts in rabbits: A report to the War Wounds Committee of the Medical Research Council. J Anat. 1944;78(Pt 5):176-99. Epub 1944/10/01.

119.     Billingham RE, Brent L, Medawar PB. Actively acquired tolerance of foreign cells. Nature. 1953;172(4379):603-6. Epub 1953/10/03.

120.     Murray JE, Merrill JP, Harrison JH. Renal homotransplantation in identical twins. 1955. Journal of the American Society of Nephrology : JASN. 2001;12(1):201-4. Epub 2001/04/25.

121.     Leon-Villapalos J, Eldardiri M, Dziewulski P. The use of human deceased donor skin allograft in burn care. Cell and Tissue Banking. 2010;11(1):99-104.

122.     Dubernard JM, Owen E, Herzberg G, Lanzetta M, Martin X, Kapila H, et al. Human hand allograft: report on first 6 months. Lancet. 1999;353(9161):1315-20. Epub 1999/04/28.

123.     Khalifian S, Brazio PS, Mohan R, Shaffer C, Brandacher G, Barth RN, et al. Facial transplantation: the first 9 years. Lancet. 2014;384(9960):2153-63. Epub 2014/05/03.

124.     Jones ND, Turvey SE, Van Maurik A, Hara M, Kingsley CI, Smith CH, et al. Differential susceptibility of heart, skin, and islet allografts to T cell-mediated rejection. J Immunol. 2001;166(4):2824-30. Epub 2001/02/13.

125.     Rosenberg AS, Singer A. Cellular basis of skin allograft rejection: an in vivo model of immune-mediated tissue destruction. Annu Rev Immunol. 1992;10:333-58. Epub 1992/01/01.

126.     Ingulli E. Mechanism of cellular rejection in transplantation. Pediatr Nephrol. 2010;25(1):61-74. Epub 2010/01/01.

127.     Chong AS, Alegre ML. The impact of infection and tissue damage in solid-organ transplantation. Nature reviews Immunology. 2012;12(6):459-71. Epub 2012/05/26.

128.     Benichou G, Yamada Y, Yun SH, Lin C, Fray M, Tocco G. Immune recognition and rejection of allogeneic skin grafts. Immunotherapy. 2011;3(6):757-70. Epub 2011/06/15.

129.     Lechler RI, Sykes M, Thomson AW, Turka LA. Organ transplantation--how much of the promise has been realized? Nat Med. 2005;11(6):605-13. Epub 2005/06/07.

130.     Thomson AW, Turnquist HR, Zahorchak AF, Raimondi G. Tolerogenic dendritic cell-regulatory T-cell interaction and the promotion of transplant tolerance. Transplantation. 2009;87(9 Suppl):S86-90. Epub 2009/05/14.

131.     Moreau A, Varey E, Beriou G, Hill M, Bouchet-Delbos L, Segovia M, et al. Tolerogenic dendritic cells and negative vaccination in transplantation: from rodents to clinical trials. Front Immunol. 2012;3:218. Epub 2012/08/22.

132.     Svajger U, Rozman P. Tolerogenic dendritic cells: molecular and cellular mechanisms in transplantation. J Leukoc Biol. 2014;95(1):53-69. Epub 2013/10/11.

133.     Vassalli G. Dendritic cell-based approaches for therapeutic immune regulation in solid-organ transplantation. J Transplant. 2013;2013:761429. Epub 2013/12/07.

134.     Smyth LA, Ratnasothy K, Moreau A, Alcock S, Sagoo P, Meader L, et al. Tolerogenic Donor-Derived Dendritic Cells Risk Sensitization In Vivo owing to Processing and Presentation by Recipient APCs. J Immunol. 2013;190(9):4848-60. Epub 2013/03/29.

135.     de Kort H, Crul C, van der Wal AM, Schlagwein N, Stax AM, Bruijn JA, et al. Accelerated antibody-mediated graft loss of rodent pancreatic islets after pretreatment with dexamethasone-treated immature donor dendritic cells. Transplantation. 2012;94(9):903-10. Epub 2012/10/11.

136.     Divito SJ, Wang Z, Shufesky WJ, Liu Q, Tkacheva OA, Montecalvo A, et al. Endogenous dendritic cells mediate the effects of intravenously injected therapeutic immunosuppressive dendritic cells in transplantation. Blood. 2010;116(15):2694-705. Epub 2010/06/26.

137.     Wang Z, Divito SJ, Shufesky WJ, Sumpter T, Wang H, Tkacheva OA, et al. Dendritic cell therapies in transplantation revisited: deletion of recipient DCs deters the effect of therapeutic DCs. Am J Transplant. 2012;12(6):1398-408. Epub 2012/04/17.

138.     Inaba K, Inaba M, Romani N, Aya H, Deguchi M, Ikehara S, et al. Generation of large numbers of dendritic cells from mouse bone marrow cultures supplemented with granulocyte/macrophage colony-stimulating factor. The Journal of experimental medicine. 1992;176(6):1693-702. Epub 1992/12/01.

139.     Murshid A, Theriault J, Gong J, Calderwood SK. Investigating receptors for extracellular heat shock proteins. Methods Mol Biol. 2011;787:289-302. Epub 2011/09/08.

140.     Murshid A, Borges TJ, Calderwood SK. Emerging roles for scavenger receptor SREC-I in immunity. Cytokine. 2015;75(2):256-60. Epub 2015/03/15.

141.     Brown GD. Dectin-1: a signalling non-TLR pattern-recognition receptor. Nature reviews Immunology. 2006;6(1):33-43. Epub 2005/12/13.

142.     van Vliet SJ, Saeland E, van Kooyk Y. Sweet preferences of MGL: carbohydrate specificity and function. Trends in immunology. 2008;29(2):83-90. Epub 2008/02/06.

143.     Macauley MS, Crocker PR, Paulson JC. Siglec-mediated regulation of immune cell function in disease. Nature reviews Immunology. 2014;14(10):653-66. Epub 2014/09/23.

144.     Pillai S, Netravali IA, Cariappa A, Mattoo H. Siglecs and immune regulation. Annu Rev Immunol. 2012;30:357-92. Epub 2012/01/10.

145.     Wang XY, Facciponte J, Chen X, Subjeck JR, Repasky EA. Scavenger receptor-A negatively regulates antitumor immunity. Cancer Res. 2007;67(10):4996-5002. Epub 2007/05/19.

146.     Wendling U, Paul L, van der Zee R, Prakken B, Singh M, van Eden W. A conserved mycobacterial heat shock protein (HSP) 70 sequence prevents adjuvant arthritis upon nasal administration and induces IL-10-producing T cells that cross-react with the mammalian self-HSP70 homologue. Journal of Immunology. 2000;164(5):2711-7.

147.     Luo X, Zuo X, Mo X, Zhou Y, Xiao X. Treatment with recombinant Hsp72 suppresses collagen-induced arthritis in mice. Inflammation. 2011;34(5):432-9. Epub 2010/09/21.

148.     Kim N, Kim JY, Yenari MA. Anti-inflammatory properties and pharmacological induction of Hsp70 after brain injury. Inflammopharmacology. 2012. Epub 2012/01/17.

149.     Chen GY, Brown NK, Wu W, Khedri Z, Yu H, Chen X, et al. Broad and direct interaction between TLR and Siglec families of pattern recognition receptors and its regulation by Neu1. Elife. 2014;3:e04066. Epub 2014/09/05.

150.     Spence S, Greene MK, Fay F, Hams E, Saunders SP, Hamid U, et al. Targeting Siglecs with a sialic acid-decorated nanoparticle abrogates inflammation. Sci Transl Med. 2015;7(303):303ra140. Epub 2015/09/04.

151.     Theriault JR, Adachi H, Calderwood SK. Role of scavenger receptors in the binding and internalization of heat shock protein 70. J Immunol. 2006;177(12):8604-11. Epub 2006/12/05.

152.     Ding Z, Liu S, Wang X, Khaidakov M, Dai Y, Deng X, et al. Lectin-like ox-LDL receptor-1 (LOX-1)-Toll-like receptor 4 (TLR4) interaction and autophagy in CATH.a differentiated cells exposed to angiotensin II. Mol Neurobiol. 2015;51(2):623-32. Epub 2014/06/07.

153.     Jang S, Uematsu S, Akira S, Salgame P. IL-6 and IL-10 induction from dendritic cells in response to Mycobacterium tuberculosis is predominantly dependent on TLR2-mediated recognition. J Immunol. 2004;173(5):3392-7. Epub 2004/08/24.

154.     Sing A, Rost D, Tvardovskaia N, Roggenkamp A, Wiedemann A, Kirschning CJ, et al. Yersinia V-antigen exploits toll-like receptor 2 and CD14 for interleukin 10-mediated immunosuppression. The Journal of experimental medicine. 2002;196(8):1017-24. Epub 2002/10/23.

155.     Apetoh L, Quintana FJ, Pot C, Joller N, Xiao S, Kumar D, et al. The aryl hydrocarbon receptor interacts with c-Maf to promote the differentiation of type 1 regulatory T cells induced by IL-27. Nature immunology. 2010;11(9):854-61. Epub 2010/08/03.

156.     Quintana FJ. The aryl hydrocarbon receptor: a molecular pathway for the environmental control of the immune response. Immunology. 2013;138(3):183-9. Epub 2012/11/30.

157.     Borges TJ, Lopes RL, Pinho NG, Machado FD, Souza AP, Bonorino C. Extracellular Hsp70 inhibits pro-inflammatory cytokine production by IL-10 driven down-regulation of C/EBPbeta and C/EBPdelta. Int J Hyperthermia. 2013. Epub 2013/07/03.

158.     Baldwin AS, Jr. The NF-kappa B and I kappa B proteins: new discoveries and insights. Annu Rev Immunol. 1996;14:649-83. Epub 1996/01/01.

159.     Shi Y, Tu Z, Tang D, Zhang H, Liu M, Wang K, et al. The inhibition of LPS-induced production of inflammatory cytokines by HSP70 involves inactivation of the NF-kappaB pathway but not the MAPK pathways. Shock. 2006;26(3):277-84. Epub 2006/08/17.

160.     Dokladny K, Lobb R, Wharton W, Ma TY, Moseley PL. LPS-induced cytokine levels are repressed by elevated expression of HSP70 in rats: possible role of NF-kappaB. Cell Stress Chaperones. 2010;15(2):153-63. Epub 2009/06/25.

161.     Malhotra V, Wong HR. Interactions between the heat shock response and the nuclear factor-kappaB signaling pathway. Crit Care Med. 2002;30(1 Supp):S89-S95. Epub 2002/03/14.

# ANEXOS

Anexo A – Parecer de aprovação da Comissão de Experimentação e Uso de Animais –CEUA da PUCRS

**Pontifícia Universidade Católica do Rio Grande do Sul**
PRÓ-REITORIA DE PESQUISA, INOVAÇÃO E DESENVOLVIMENTO
COMISSÃO DE ÉTICA NO USO DE ANIMAIS

Ofício 013/13 – CEUA                                    Porto Alegre, 13 de março de 2013.

Senhora Pesquisadora:

A Comissão de Ética no Uso de Animais da PUCRS apreciou e aprovou seu Protocolo de Pesquisa, registro CEUA 12/00316, **"Mecanismos da inibição da Rejeição aguda induzida pela Hsp70"**.

Sua investigação está autorizada a partir da presente data.

Lembramos que é necessário o encaminhamento de relatório final quando finalizar esta investigação.

Atenciosamente,
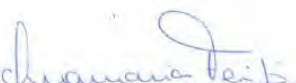
Profa. Dra. Anamaria Gonçalves Feijó
Coordenadora da CEUA/PUCRS

Ilma. Sra.
Profª. Cristina Bonorino
FABIO
Nesta Universidade

**PUCRS** | **Campus Central**
Av. Ipiranga, 6690 – Prédio 60, sala 314
CEP: 90610-000
Fone/Fax: (51) 3320-3345
E-mail: ceua@pucrs.br

**Motivação:** A partir dos conhecimentos obtidos na presente Tese, depositamos uma patente na qual formulamos uma composição para ser utilizada como, ou em conjunto, com uma solução de preservação de órgãos. Essa composição além de preservar o órgão, imunossuprime as células do doador, através da diminuição da expressão de MHC II e CD86. Através de uma consultoria internacional externa, a nossa patente foi indicada como uma das mais fortes da PUCRS.

**INSTITUTO NACIONAL DA PROPRIEDADE INDUSTRIAL**
Diretoria de Patentes
Sistema e-Patentes/Depósito

**INPI** INSTITUTO NACIONAL DA PROPRIEDADE INDUSTRIAL

**DIRPA** **@PATENTES**

| Tipo de Documento: Recibo de Peticionamento Eletrônico | DIRPA | Página: 1 / 2 |
|---|---|---|

| Título do Documento: | Código: RECIBO | Versão: 01 |
|---|---|---|
| **Recibo** | | |
| DIRPA-FQ001 - Depósito de Pedido de Patente ou de Certificado de Adição | Modo: Produção | |

## O Instituto Nacional da Propriedade Industrial informa:

Este é um documento acusando o recebimento de sua petição conforme especificado abaixo:

### Dados do INPI:

| | |
|---|---|
| Número de processo: | BR 10 2014 002362 3 |
| Número da GRU principal: | 00.000.2.2.14.0055520.0 (serviço 200) |
| Número do protocolo: | 860140010412 |
| Data do protocolo: | 30 de Janeiro de 2014, 16:05 (BRST) |
| Número de referência do envio: | 19221 |

### Dados do requerente ou interessado:

| | |
|---|---|
| Tipo de formulário enviado: | DIRPA-FQ001 v.005 |
| Referência interna: | Solução Preserv |
| Primeiro requerente ou interessado: | União Brasileira de Educação e Assistencia |
| CNPJ do primeiro requerente ou interessado: | 88.630.413/0001-09 |
| Número de requerentes ou interessados: | 1 |
| Título do pedido: | MÉTODO DE IMUNOMODULAÇÃO E/OU PRESERVAÇÃO DE ÓRGÃOS EX-VIVO, COMPOSIÇÕES, PROCESSO E USOS |

### Arquivos enviados:

| Arquivo enviado | Documento representado pelo arquivo | Número de páginas |
|---|---|---|
| *[package-data.xml]* | Arquivo com informações do pacote em XML | --- |
| *[brf101-request.xml]* | Formulário de depósito de pedido de patente ou de certificado de adição em XML | --- |
| *[application-body.xml]* | Arquivo com dados do corpo do conteúdo patentário em XML | --- |
| *[brf101-request.pdf]* | Formulário de depósito de pedido de patente ou de certificado de adição em PDF | |
| PUCRS-A0001-12-Depósito de PI.pdf *[PRIORIDADE-INTERNA-1.pdf]* | Documento de prioridade em formato eletrônico PDF *[Número da prioridade: BR 10 2013 002420 1]* | 14 |
| PUCRS-Solucao Preservacao(A0001-12)-Minuta Final - 30Jan2014.pdf *[DOCUMENTO.pdf]* | Arquivo com conteúdo técnico-patentário da petição<br>- *Relatório descritivo em formato eletrônico PDF*      *páginas 1 a 44*<br>- *Reivindicações em formato eletrônico PDF*      *páginas 45 a 46*<br>- *Resumo em formato eletrônico PDF*      *página 47*<br>- *Desenhos em formato eletrônico PDF*      *páginas 48 a 65*<br>  *[Número de desenhos: 29, Desenho para resumo: 1, Cor dos desenhos: Preto e Branco]* | 65 |
| Relatório Descritivo.txt *[RELATDESCTXT.txt]* | Relatório descritivo em formato eletrônico texto | --- |
| Reivindicações.txt *[REIVINDTXT.txt]* | Reivindicações em formato eletrônico texto | --- |
| Resumo.txt *[RESUMOTXT.txt]* | Resumo em formato eletrônico texto | --- |
| ND01490 - Solução Preservação 2 - PUCRS.pdf *[GRU-1.pdf]* | Guia de Recolhimento da União (GRU) paga com comprovante de pagamento em formato eletrônico PDF *[Código de serviço: 200, Número: 00.000.2.2.14.0055520.0, Nome do sacado: União Brasileira de Educação e Assistencia ]* | 1 |
| Listagem de Sequencia.pdf *[OUTROS-2.pdf]* | Documentos de qualquer outra natureza em formato eletrônico PDF | 7 |

| DIRPA ⊖PATENTES | Tipo de Documento:<br>Recibo de Peticionamento Eletrônico | | DIRPA | Página:<br>2 / 2 |
|---|---|---|---|---|
| **Título do Documento:**<br>**Recibo**<br>DIRPA-FQ001 - Depósito de Pedido de Patente ou de Certificado de Adição | | | Código:<br>**RECIBO** | Versão:<br>**01** |
| | | | Modo:<br>**Produção** | |

| Arquivo enviado | Documento representado pelo arquivo | Número de páginas |
|---|---|---|
| PUCRS_Procuração_Remer Villaça&Nogueira_25-07-2013.pdf<br>[INDEXADO-1.pdf] | Procuração em formato eletrônico PDF | 6 |
| Comprovante Soluções Preservação 02.pdf<br>[OUTROS-1.pdf] | Documentos de qualquer outra natureza em formato eletrônico PDF | 1 |
| PUCRS-SolucaoPreservacao(A0001-12)_ST25.txt.pdf<br>[CCSEQBIO.pdf] | Código de controle de listagem de sequência biológica em formato eletrônico PDF | 2 |
| PUCRS-SolucaoPreservacao(A0001-12)_ST25.txt<br>[SEQBIOTXT.txt] | Listagem de sequência biológica em formato eletrônico texto | --- |
| PUCRS-SolucaoPreservacao(A0001-12)_ST25.txt.xml<br>[CCSEQBIOXML.xml] | Código de controle de listagem de sequência biológica em formato eletrônico XML | --- |
| CB_20140130_111909.pdf<br>[DECLIST.pdf] | Declaração de acordo com a Resolução INPI nº 228/09 em formato eletrônico PDF | 1 |

**Dados sobre o envio:**

| | |
|---|---|
| Responsável pelo envio: | Ricardo Amaral Remer:2053a74256cd0a3b05dabb3323d134d4 |
| Assinatura (Requerente, Interessado ou Procurador): | REMER VILLACA E NOGUEIRA ASSESSORIA CONSULTORIA D:07336918000155,ST=RJ,L=RIO DE JANEIRO,OU=RFB e-CNPJ A1,OU=ARPRONOVA,OU=PRONOVA,OU=Secretaria da Receita Federal do Brasil - RFB,O=ICP-Brasil,C=BR |
| Método de envio: | Eletrônico pela Internet |
| Código de segurança: | 70:F8:62:32:F0:5B:61:08:1A:33:04:CC:3C:20:4F:29:A9:32:71:5C |

## Anexo C - Co-Dominant Role of IFN-γ- and IL-17-Producing T Cells During Rejection in Full Facial Transplant Recipients

**Autores:** Borges, T.J., Smith, B., Wo, L., Azzi, J., Tripathi, S., Lane, J.D., Bueno, E.M., O'Malley, J.T., Clark, R.A., Tullius, S.G., Chandraker, A., Lian, C.G., Murphy, G.F., Strom, T.B., Pomahac, B., Najafian, N., Riella L.V.

**Situação:** Submetido

**Revista:** *American Journal of Transplantation*

**Website:** http://onlinelibrary.wiley.com/journal/10.1111/(ISSN)1600-6143

**Motivação:** Esse trabalho foi realizado durante o período sanduiche realizado no Hospital Brigham and Women's, no laboratório do Prof. Leonardo Riella. Com esse trabalho o aluno pode aprender varias aspectos da Imunologia humana, além de aspectos translacionais sobre transplantes, principalmente o de pele.

**Title:**  Co-Dominant Role of IFN-γ- and IL-17-Producing T Cells During Rejection in Full Facial Transplant Recipients

**Authors:**  Borges, T.J.[1], Smith, B.[1], Wo, L.[2], Azzi, J.[1], Tripathi, S.[1], Lane, J.D.[2], Bueno, E.M.[2], O'Malley, J.T.[3], Clark, R.A.[3], Tullius, S.G.[4], Chandraker, A.[1], Lian, C.G.[5], Murphy, G.F.[5], Strom, T.B.[6], Pomahac, B.[2], Najafian, N.[1,7], Riella L.V.[1,*]

**Affiliations:**

[1]Schuster Transplantation Research Center, Brigham & Women's Hospital, Harvard Medical School, Boston, MA.

[2]Division of Plastic Surgery, Department of Surgery, Brigham & Women's Hospital, Harvard Medical School.

[3]Department of Dermatology, Brigham and Women's Hospital, Harvard Medical School

[4]Division of Transplant Surgery, Department of Surgery, Brigham & Women's Hospital, Harvard Medical School.

[5]Program in Dermatopathology, Department of Pathology, Brigham & Women's Hospital, Harvard Medical School.

[6]Transplant Institute, Beth Israel Deaconess Medical Center, Harvard Medical School.

[7]Department of Nephrology, Cleveland Clinic Florida, Weston, FL

\***Address for Correspondence:** Leonardo V. Riella, MD, PhD

Email: lriella@bwh.harvard.edu

Transplantation Research Center, Brigham and Women's Hospital, Harvard Medical School

221 Longwood Ave, Boston MA 02115, USA.

Tel: 617-732-5252; Fax: 617-732-5254

**Running Title:** Immune Characterization of Face Transplant

**Abbreviations:**

ANOVA - Analysis of variance
APC - Antigen-presenting cell
CMV – Cytomegalovirus
DAMPs - Damage-Associated Molecular Pattern Molecules
DAPI - 4',6-diamidino-2-phenylindole
DC – Dendritic Cells
DMSO – Dimethylsulfoxide
DSA – Donor Specific Antibodies
H&E - Hematoxylin and Eosin
HSV - Herpes Simplex Virus
IFN – Interferon
IVIG - Intravenous Immunoglobulin
MCP-1 - monocyte chemotactic protein-1
MFI - Mean Fluorescence Intensity
MICA - major histocompatibility complex class I chain-related molecule A
PBMC – Peripheral Blood Mononuclear Cells
PHA - Phytohemagglutinin
PMA - Phorbol Myristate Acetate
PRA – Panel Reactive Antibody
SCID - Severe Combined Immunodeficiency Disease
TCM – Central Memory T cells
TEM - Effector Memory T cells
TEMRA - Effector Memory RA T cells
Tfh - T follicular helper cells
Th – T helper cells
Tregs – Regulatory T cells
VCA - Vascularized Composite Allotransplantation

**Abstract**

Facial transplantation is a life-changing procedure for patients with severe composite facial defects. However, skin is the most immunogenic of all transplants and better understanding of the immunological processes after facial transplantation is of paramount importance. Here, we describe six patients that underwent full facial transplantation in our institution, with a mean follow-up of 2.7 years. Serum, PBMCs and skin biopsies were collected prospectively and a detailed characterization of their immune response (51 time-points) was performed, defining 47 immune cell subsets, 24 cytokines, anti-HLA antibodies, and donor alloreactivity on each sample, producing 4,269 data points. In a non-rejecting state, patients had a predominant Th2 phenotype in the blood. All patients developed at least one episode of acute cellular rejection, which was characterized by increases in IFN-γ/IL-17-producing cells in peripheral blood and in the allograft's skin. At 1 year post-transplant, Tregs were significantly expanded. None of the patients developed de novo donor-specific antibodies, despite significant expansion of B cells and T follicular helper cells (11-fold and 4-fold, respectively) post-transplant. There were no face graft losses in any of the patients. These findings indicate a co-dominant IFN-γ/IL-17-mediated rejection in face transplantation with the development of a unique regulatory phenotype over time.

**Trial registration:** ClinicalTrials.gov number, NCT01281267

**Introduction**

Facial deformities significantly affect the quality of life, function and social interactions of patients, predisposing them to permanent disability, depression and social isolation. Conventional reconstructive surgeries are frequently unable to appropriately correct complex deformities. Face transplantation has emerged as a viable and successful strategy to restore the appearance and function of patients with severe facial injuries (1-4).

Face transplantation involves multiple tissues with different degrees of immunogenicity and for many years was considered an unsurpassable immunological barrier. Among the components of facial allografts, the skin is the most immunogenic and the main target of rejection based on its rich content of antigen-presenting cells (5-8). Unlike other solid organ transplants that are life-saving, facial transplantation aims to improve the quality of life rather than to save the patient's life. Therefore, the consequences of applying life-long immunosuppression regimens available for solid organ transplantation in this unique patient population must be carefully balanced to minimize risks of malignancies, infections and metabolic disorders. Understanding the alloimmune response of face transplant recipients is of paramount importance to optimize their immunosuppressive regimen, increase the understanding of the immune system and further determine differences with respect to solid organ transplants.

Since the first face transplant performed in 2005, more than 30 face transplants have been performed worldwide, with 7 of those performed in our institution (1, 2, 9). Herein, we report the outcomes of six patients in this unique cohort of face transplantation, in which we collected serum, skin and peripheral blood mononuclear cells prospectively since 2009. We believe that this is the largest cohort with prospectively collected samples in the world and a rich resource to

better understand the immunological response upon full face transplant when compared with solid organ transplants.

**Methods**

*Face transplant subjects*

All patients provided written informed consent to participate in the clinical trial (ClinicalTrials.gov number, NCT01281267) for face transplantation, as approved by the human research committee at Brigham and Women's Hospital (2008BP00055). All patients were evaluated by our multidisciplinary team before participation. Donors and recipients were matched according to sex, skin color and ABO compatibility, in addition to a negative T- and B-cell cytotoxic crossmatch. The only exception was a highly sensitized patient with a high PRA (98%), in which transplant occurred across a weakly positive cytotoxic T-cell crossmatch (20%). Further demographic details are on Table 1. Patients were followed on a weekly basis during first 4-6 weeks after transplant and if stable, clinical visits were further spaced to every 2 weeks, every month and then every 3 months.

*Immunosuppression*

All patients received mycophenolate mofetil (1,000 mg), methylprednisolone (500 mg), and rabbit antithymocyte globulin (1.5 mg/kg/day × 4 days) for induction therapy starting at the time of transplant. Maintenance immunosuppression consisted of mycophenolate mofetil (1,000 mg twice daily), tacrolimus (adjusted to achieve target levels of 10-12 ng/mL) and prednisone taper (down to 20 mg on day 5) (Table 1). Prednisone withdrawal was attempted in all patients post-transplant (9). Perioperative antibacterial prophylaxis consisted of vancomycin and cefazolin and was modified according to perioperative findings. All patients received trimethoprim–sulfamethoxazole and valganciclovir prophylaxis against *Pneumocystis jirovecii*

and cytomegalovirus, respectively, for at least 6 months. In the presence of clinical acute cellular rejection, patients were treated with pulse solumedrol 500 mg daily for 3 days and maintenance immunosuppression was increased. In case of no response, thymoglobulin 3-6 mg/kg was administered. Topical steroids or tacrolimus was also used in few patients as adjuvant therapy. For antibody-mediated rejection, solumedrol and plasmapheresis with IVIG were initially attempted. For refractory cases, Eculizumab, Bortezomib and further T-cell depletion therapy (Thymoglobulin, Alemtuxumab) were considered.

*Recipient peripheral blood mononuclear cells (PBMC) and serum isolation*

Peripheral blood samples were obtained from recipients at different time points: pre-transplantation, at 24 hours, 1 week, 3, 6, 12 months post-transplant and during suspected rejection. Some samples of rejection episodes were missed due to the emergent treatment of rejection and inability to collect samples before. At the Immunological Core Facility at the Transplant Research Center, PBMCs were then isolated by density gradient centrifugation using Ficoll-Paque solution (GE Healthcare) and were cryopreserved in heat-inactivated Human AB serum (Gemini) with 10% dimethylsulfoxide (DMSO) in liquid nitrogen. Serum was isolated from each blood sample of and stored at -80°C until cytokine analysis. Anti-HLA antibody testing, cytokine measurement, flow cytometry and cell culture experiments are detailed on Supplementary methods.

*Allograft skin samples*

We obtained skin-biopsy samples from facial allografts prospectively at pre-transplantation and post-transplantation at 24 hours, 1 week, 3, 6, 12 months and during suspected rejection. Histopathological assessment of rejection was rendered using the BANFF system for grading skin-containing composite tissue allografts (10) as follows: grade 0 = 'no or rare inflammatory infiltrates'; grade I (mild) = 'mild perivascular infiltration' (with no epidermal involvement); grade II (moderate) = 'moderate-to-severe perivascular inflammation with or without mild epidermal and/or adnexal involvement'; grade III (severe) = 'dense inflammation and epidermal involvement with epithelial apoptosis, dyskeratosis, and/or keratinolysis'; grade IV (necrotizing acute rejection) = 'frank necrosis of epidermis or other skin structures'. Processing of skin samples are detailed on Supplementary methods.

*Statistical analysis*

Statistical analyses were performed using the Prism software (version 6.01, Graphpad Software Inc.). All data are represented as mean±SEM. Percentages and absolute numbers of cells at the different time points were analyzes as non-parametric using *Mann-Whitney* test. Significance was defined as a p-value <0.05.

*Immunostaining:* Percentages and absolute numbers of cells at the different time points were compared using Mann-Whitney test and significance was defined as a p-value <0.05. Percentage of double positive cells compared to total T cells was compared using a one-way ANOVA analysis followed by a Bonferroni multiple comparison test and significance was defined as a p-value <0.05.

**Results**

*Acute cellular rejection is highly prevalent upon full facial transplantation*

Between April 2009 and February 2014, six patients received face transplants in our institution and were included in this analysis. Mean follow-up was 2.7 years. Clinical characteristics of these patients are detailed on Table 1 and pre- and post-operative appearances are shown on Supplemental Figure 1. Induction therapy consisted of thymoglobulin and high-dose steroids followed by maintenance immunosuppression with tacrolimus, mycophenolate mofetil and prednisone taper (further details on Materials and Methods). All patients developed at least one episode of acute cellular rejection (total of 15 episodes) with a bimodal pattern (Figure 1, A-C) – two thirds occurred during the first 3 post-operative months, while the remaining occurred later (>1 year after transplant). Acute cellular rejection was assessed using the BANFF grading of skin-containing composite tissue (10), and the majority of clinical rejections were classified between grades II and III (Figure 1, A and C). One highly sensitized patient (#4) with preformed donor-specific antibodies developed an early acute antibody-mediated rejection with neutrophil vascular margination and positive C4d staining (Figure 1, D and E). Early surgical site infections occurred in three patients, while two patients developed pneumonia and one developed line-associated bacteremia post-transplant. Opportunistic infections included CMV infection (in two patients with negative CMV sero-status prior to transplant; POD 176 and 420), HSV infection of face allograft (POD 420) and shingles (POD 502). There were no graft failures or patient deaths.

*Effector memory T cells is the predominant subset after transplant with a dominant Th2 phenotype*

Allospecific T cells are activated primarily in secondary lymphoid organs and then migrate to target tissue to elicit injury (11). In our cohort, we characterized circulating T cell subsets overtime post-transplant. All face transplant recipients received thymoglobulin as induction therapy. As expected, both CD4 and CD8 T cells were significantly depleted at 24 hours post-transplant with progressive recovery at 3 and 6 months post-transplant (Figure 2, A and B). Analyses of the effector and memory T cell subsets (Supplemental Figure 2) revealed a dominant depletion of effector memory T cells (TEM: CD45RA-CCR7-) early after transplant with recovery to initial level by 3 months post-transplant (Figure 2, C and D). We also observed a predominance of TEM within the pool of CD4+ T cells (Figure 2E), while CD8+ T cells were characterized by TEM and TEMRA (Figure 2F). Next, we assessed the T helper (Th) phenotypes based on surface markers profile (Supplemental Figure 2 and Supplemental Table 1 for phenotype details), according to the Human Immunology Project (12). Circulating Th2 cells were the predominant phenotype in most patients post-transplant (Figure 2, G and H), followed by Th17 and Th1 cells. The only exception was on highly-sensitized patient #4 who had a predominant Th17 phenotype (Figure 2, I and J). This Th17 skewing was confirmed with intracellular cytokine staining (Figure 2K). Lastly, we evaluated donor T cell alloreactivity using the frequency of IFN-γ-producing donor-reactive PBMCs by a standardized and cross-validated ELISPOT assay (13) (Supplemental Figure 3, A-C). This assay has been proposed as an important tool to quantify cellular donor reactivity in kidney transplantation and determine subsequent risk of rejection (14-18). Pre-transplant, none of the patients had positivity to either direct or indirect T cell alloreactivity against their respective donors (Supplemental Figure 3B).

Among the 51 time-points analyzed post-transplant, only one time-point exhibited positivity at 6 months post-transplant and there was no correlation with rejection occurrence. In sum, T cell subsets are recovered by three months following thymoglobulin induction and Th2 cells are the dominant phenotype post-transplant in the non-rejection state of face recipients. Quantifying the frequency of IFN-γ-producing donor reactive PBMCs by ELISPOT did not predict rejection in face recipients.

*Tregs remarkably expand after full face transplantation*

In solid organ transplantation, an increase in Foxp3+ regulatory T cells has been associated with better long-term graft survival (19-21). In our face transplant cohort, when compared with pre-transplant levels, the percentage of circulating Tregs (CD4+Foxp3+) initially decreased at 24h after the transplant, and expanded 2-fold at 1 year post-transplant (Figure 3, A and B). The absolute number of circulating Tregs also progressively increased after initial reduction early after transplant (Figure 3C). Foxp3 expression in CD4+ by MFI increased in a similar pattern overtime (Figure 3D). Compared to conventional T cells (CD4+Foxp3-), Tregs had a faster recovery after depletion by thymoglobulin with a significant higher ratio of Treg to conventional T cells at 1-week post-transplant (Figure 3E). Since Foxp3 expression may be a consequence of activation and not as specific for T cells with a regulatory phenotype in humans when compared with mice (22), we also analyzed the frequency of Tregs using CD127 (IL-7 receptor) surface expression (CD4+CD25+CD127-/low) (Figure 3, F and G), which has shown excellence as a marker of Tregs in human peripheral blood and a high correlation with Tregs suppressive function (23). Importantly, CD127 marker was absent in the majority of the Foxp3+ cells in our samples (mean 71.76%; SD 16.16%; range 53.5-94.8%) (Figure 3F). Also, the percentage and

absolute number of CD4+CD25+CD127-/low cells in PBMCs overtime had a very similar kinetics as CD4+Foxp3+ cells (Figure 3, H and I). In sum, the proportion of Tregs characterized by either Foxp3+ or CD25+CD127-/low expression significantly increased overtime in the non-rejection state of face transplant recipients.

*Despite B and Tfh cells expansion, development of de novo DSA is uncommon*

The development of donor-specific antibodies (DSA) and consequent endothelial injury is considered one of the major causes of late allograft loss in solid organ transplantation (24). However, different organ transplants seem to have diverse susceptibility to antibody-mediated injury (25). Based on the high immunogenicity of the skin (7, 8), one would expect a high rate of de novo anti-HLA antibody generation post-transplantation. First, we analyzed the kinetics of T follicular helper cells (Tfh) and B cells post-transplantation. Though thymoglobulin presumably depletes all T cells, we observed an unexpected sparing of Tfh cells (Figure 4, A-C). Similarly, B cells were not significantly affected by thymoglobulin and increased progressively after transplantation (Figure 4, B and C). Of note, the ratio of Tfh/CD4 T cells peaked at ~40 at 1 week post-transplant and decreased progressively as other CD4 subsets recovered (Figure 4D). At 12 months post-transplant, Tfh and B cells cells were increased 11-fold and 4-fold compared to pre-transplant, respectively (Figure 4E). When we analyzed the highly sensitized patient #4 separately, we observed that the Tfh peak persisted until 3 months after initial antibody-mediated rejection (Figure 4F).

To our surprise, no patient developed persistent de novo DSA post-transplantation and panel reactive antibodies (PRA) remained stable post-transplant (Figure 4G). The highly sensitized patient #4 who had three DSAs at the time of transplant (against HLA-A2, A32 and B57) and a

positive CDC T-cell crossmatch, had progressive reduction of her PRA and of the DSA numbers over time (Figure 4H) after active treatment for antibody-mediated rejection with plasmapheresis, bortezomib, alemtuzumab and IVIG (26). Patient #5 developed CMV infection at 5 months post-transplant, which led to reduction of immunosuppression. During that time, his PRA increased from 13% (3 months) to 79% (6 months post-transplant) with concomitant detection of circulating *de novo* DSA (against HLA-A2). Repeated analysis at 7 months revealed disappearance of the DSA. Patient #1 also had a transient detection of DSA at 1-week post-transplant and patient #6 had a pre-transplant DSA against HLA-A1 with negative CDC crossmatch, which disappeared by 6 months post-transplant without any specific intervention.

Since the complement-binding capacities of DSA have been considered a useful marker for the risk of graft loss (27), we measured the C1q binding of the DSAs and observed that only the highly sensitized patient #4 had three C1q positive DSAs at 1 week post-transplant, though analyses of pre-transplant serum and at 3, 6 and 12 months did not reveal any C1q positivity (Figure 4H). Lastly, non-HLA antigens have also been suggested as important targets of alloantibodies, in particular the highly polymorphic major histocompatibility complex class I chain-related molecule A (MICA), which is expressed by endothelial cells and keratinocytes (28). Antibodies against MICA have been associated with increased kidney graft loss (29). Despite the abundance of keratinocytes on skin, we did not detect any circulating anti-MICA antibody post-transplantation in our cohort. In sum, despite the high alloimmunogenicity of the skin and the rise in B cells and Tfh cells overtime, there was no evidence of de novo DSA development or increase in PRA post-transplant.

*CD4+, CD8+ and CD14+ cells are the predominant cells during face transplant rejection*

After characterizing the kinetics of circulating immune cells overtime, we analyzed these cells in relation to the rejection events both in the allograft and in the periphery in order to better characterize the rejection process in full face transplant recipients.

Rejection episodes were characterized by accumulation of CD4+ and CD8+ cells in the allograft, though both percentage and absolute numbers of total circulating CD4+ and CD8+ cells were not significantly different compared to pre- and post-rejection time-points (Figure 5, A-D). When we analyzed circulating CD4+ and CD8+ T cell subsets during rejection episodes (naive, TCM, TEM and TEMRA), we observed a slight reduction in TEM (CD45RA-CCR7-; Figure 5, G and H) and an increase in both CD4+ and CD8+ TEMRA (CD45RA+CCR7-; Figure 5, G and I). CD14+ cells also accumulated in the allograft during rejection (Figure 5E) and were associated with a concomitant increase in the absolute numbers of CD14+ cells in peripheral blood (Figure 5F). Among 24 relevant cytokines/chemokines evaluated in the serum of rejecting recipients, monocyte chemotactic protein-1 (MCP-1) was the only cytokine that was clearly increased in average 2.5-fold during rejection when compared to pre-rejection time-points (951 $\pm$ 338 vs 387 $\pm$ 69, p=0.01) (Supplemental Figure 3D). Although high chemokine levels such as CXCL10 have been associated with rejection episodes in kidney transplantation (30-32), serum CXCL10 levels were no different during rejection or pre-rejection time-points (Supplemental Figure 3E). Other serum cytokines such as IL-6, IL-8, IP-10 and GRO also did not correlate with rejection episodes (Supplemental Table 2). In sum, acute cellular rejection after full face transplantation is characterized by CD4+, CD8+ and CD14+ infiltrates and a slight increase in circulating effector T cells. Serum MCP-1 was the only biomarker to be significantly associated with face cellular rejection.

*IFN-γ- and IL-17-producing T cells co-dominate in acute cellular rejection both in the periphery and in the face allograft*

Diverse T helper cell subtypes may emerge after transplantation depending on the microenvironment and additional signals provided by APCs upon T cell activation (33). Among alloantigen-specific CD4+ T cells, Th1 cells are the predominant Th subset during acute cellular rejection in kidney transplantation (34, 35). Little is known about the Th phenotype during rejection in human face transplantation. We observed that IL-17-producing T cells infiltrated the face allograft during rejection (Figure 6, A-C) with a concomitant increase in IFN-γ-producing T cells compared to pre-rejection time points (Figure 6, D-F). In the peripheral blood, similar increases in Th1, Th17 and IFN-γ producing CD8 T cells were seen during rejection episodes (Figure 6, G-J), with a reduction of Th2 cells (Supplemental Figure 4A). Tregs also accumulated in the graft during rejection (Figure 7A), while both percentage and absolute number of circulating Tregs were reduced at rejection time-points compared to pre-rejection (Figure 7B). Among regulatory markers, we also observed a reduction in PD-1 and CTLA4 expression on CD4 cells at the time of rejection compared to pre-rejection (Figure 7, C and D). Together, the rejection process of face allografts was characterized by a co-dominant IFN-γ and IL-17 driven immune response with simultaneous infiltration of Tregs into the allograft and a decrease of Th2 and Tregs in the blood.

**Discussion**

Here, we characterize the immune response in a cohort of full facial transplant recipients. Face allografts are unique in their composition since they contain skin, muscle, bone, vessels and lymph nodes. Each compartment has differing immunogenicity, though the predominant target and the most immunogenic component is the skin (5-8). Although there is vast data on the characterization of the immune response in murine skin transplant models (7, 36), little information is available in human face transplants. Moreover, results from animal studies are not necessarily translatable to humans due to the greater immunological diversity and environmental exposure in humans (37). Our study demonstrates that face recipients with a stable graft are characterized by predominance of Th2 cells in the periphery, while cellular rejection is associated with a shift towards Th1 and Th17 cells. The predominance of IL-4-secreting T helper cells has been previously shown to be associated with graft stability in kidney recipients (38). While Th1 cells are well accepted as dominant players during solid organ allograft rejection, the role of Th17 cells is less well defined (39). Few studies reported the presence of IL-17 in rejecting kidneys by immunofluorescence staining and RT-PCR (40, 41) as well as in the bronchoalveolar lavage fluid of rejecting lung transplant recipients (42). However, neutralization of IL-17 in murine transplant models only modestly delayed acute rejection (43, 44). Interestingly, in a humanized mouse skin model in which human skin was transplanted into SCID mice followed by infusion of human peripheral blood mononuclear cells, skin rejection was clearly associated with infiltration of IL-17-producing T cells (45). Similarly, certain inflammatory skin conditions such as psoriasis shared similar pattern of Th1/Th17 dominance, indicating that possibly signals derived from dermal DCs may be important in favoring this phenotype (46, 47). The importance in identifying T-helper phenotypes that lead to rejection is

related to variable resistance of subsets such as Th17 cells to certain immunosuppressive drugs. As an example, Th17 cells were shown to be resistant to B7:CD28 blockade with belatacept *in vitro* and acute rejection episodes in kidney transplant recipients treated with belatacept were associated with expansion of Th17 cells (48). Therefore, determination of functional pathological T cell subsets during face rejection will allow better personalization and wiser choice of potential agents to modulate the alloimmune response.

Our findings also demonstrate that acute cellular rejection in face allografts is characterized by graft infiltration of monocytes/macrophages, CD4+ and CD8+ T cells that starts in the dermal perivascular space with progressive involvement of skin adnexal structures and epidermis in the absence of treatment. This pattern of cellular rejection is similar to that observed in other solid transplant organs such as kidneys with differences pertaining to the specific targeted antigenic cells on specific organs such as tubular cells in the kidney and epithelial cells in the face (49). Analogous to our findings, an analysis of hand biopsies during rejection revealed predominance of CD3+ lymphocytes and CD68+ cells (histiocytic/macrophage lineage) (50). Monocyte chemotactic protein-1 (MCP-1) was the predominant cytokine that peaked during rejection, confirming the important role of macrophages in cellular rejection. This is in agreement with prior studies that also detected high MCP-1 levels in the serum and urine of patients at the time of kidney allograft rejection (51, 52). The lack of rejection signal among other relevant chemokines such as CXCL10 may suggest that either rejections are being caught earlier (compared to kidneys, in which creatinine elevation is a late biomarker), and therefore not allowing the full blown presentation and/or that a more local immune response is occurring that not necessarily reflects the status on peripheral blood. Our findings with donor alloreactivity

using ELISPOT indicates similar discrepancy between local and systemic responses, in particular since this assay has been clearly validated in multiple cohorts of solid organ transplants to accurately prognosticate rejection episodes (14, 53-55).

A major difference between face transplant and other solid organ transplants was the frequency of acute cellular rejections, which was present in 100% of face recipients in this cohort while it occurs in only 10-15% of kidney or heart recipients using similar immunosuppressive regimen during the first year post-transplant (56). This high rate of rejection has been documented by other groups performing VCA transplants, including hand and face (2, 57, 58). The higher rate of rejection after face transplant when compared with kidneys could be primarily related to the higher immunogenicity of the skin based on the high content of antigen-presenting cells (7). Early after transplant, the migration of donor-derived dendritic cells to secondary lymphoid organs is the main mechanism responsible for early activation of naïve T cells (36). For certain, ischemia and reperfusion injury may potentiate the immune response with the release of DAMPS and chemokines that activate further dendritic cells soon after transplant (59). One main difference between face and other solid organ transplants is that skin and mucosa are colonized by microorganisms and there is accumulating literature suggesting an important crosstalk of the commensal microbiota with epithelial immunity, with evidence of microbiota tuning the function of resident T lymphocytes (60-62). Whether microbial dysbiosis may lower the threshold for rejection in face recipients remains to be determined. Additional factors that may have contributed to the high rate of rejection include our immunosuppression protocol with early steroid withdrawal and the younger age of the recipients with a mean of 37 years old and therefore a stronger immunity (63). Despite that, all cellular rejections were successfully treated

and did not lead to graft loss. One of the advantages of skin grafts compared to other transplants is the capability of earlier detection of rejection based on its prompt visual findings, which may permit timely intervention and prevention of chronic changes. Indeed, we did not observe any chronic rejection in our cohort. In the literature, only one case of face transplant developing chronic rejection has been reported and this occurred in the setting of significant reduction of immunosuppression due to concomitant malignancy (64).

Development of de novo DSA occurs in about 5% of unsensitized transplant recipients and is significantly associated with long-term graft loss (65, 66). However, different transplanted organs may have diverse sensitivities to antibody-mediated injury. As an example, the liver appears to be remarkably resistant to DSA-mediated injury, in particular of antibodies against HLA class I (25, 67-69). In fact, the liver may even protect other organs such as kidneys from DSA-mediated injury if they are from the same donor and transplanted at the same time (68, 70). The exact mechanisms is unclear though it is hypothesized that immunoadsorption of the DSA on the extensive sinusoidal endothelial cells may be an important factor (71). Based on the high immunogenicity of the skin, one would expect a high rate of de novo donor-specific antibody (DSA) development after full facial transplantation. However, we did not observe any de novo DSA in our cohort despite the expansion of B cell and T follicular cells overtime. There are three potential explanations: (1) similar to liver, de novo DSA formed could be completely absorbed in the skin and is therefore undetectable in the serum. This is unlikely since we have no evidence of active antibody deposition in the surveillance biopsies using C4d staining; (2) de novo DSA may develop later after transplant and longer follow-up of this cohort would be required; (3) the unique composition of full face graft may promote immune regulation and prevent DSA

formation in combination with immunosuppressive drugs. Actually, the skeletal component of the face allograft may contain some bone marrow, which could confer some immunomodulatory effect (72). The rich content of lymph nodes in face grafts have also been proposed to promote donor chimerism in animal models of face transplantation and potentially protect the allograft long-term (73, 74). Whether a similar phenomenon occurs in humans is unknown. Furthermore, expansion of both the percentage and absolute numbers of B cells have been identified in tolerant transplanted patients (75-78), suggesting a potential role of B cells in regulating alloimmunity. Additional analysis of B cell subsets would be needed to assess this hypothesis in our cohort.

Regulatory T cells that express the transcription factor forkhead box P3 (FOXP3) have potent immunomodulatory properties (79, 80) and the adoptive transfer of Tregs was shown to suppress kidney allograft rejection (81, 82) in primates and promote graft survival in a humanized mouse transplant model (83). Furthermore, graft infiltrating Tregs have also been associated with favorable outcomes in patients with subclinical rejection (84). Nonetheless, the greatest increase in graft infiltrating Tregs is frequently observed during rejection (85, 86) and our cohort showed similar peak infiltration of Tregs during face rejection, probably as a counter response to the cellular rejection. Thymoglobulin has been proposed to have a favorable Treg profile with evidence that it may expand Tregs *in vitro* (87, 88) and induce or spare Tregs *in vivo* (89, 90). We demonstrated that face recipients have a greater expansion of Tregs overtime, possibly contributing to the lack of DSA generation post-transplant. Though we have to acknowledge that, despite the expansion of Tregs, cellular rejection still occurred later after transplant. This suggests that not all components of the effector immune response may respond equally to regulatory cells and currently used immunosuppressive drugs.

Our study has few limitations, including the small number of patients and the single-center nature. This reflects in part the novelty of this procedure and limited number of face transplants performed worldwide since 2005. Validation of our rejection phenotype in other face transplant cohorts will be important as well ass assessment of current findings in a cohort receiving a different regimen of immunosuppression. Despite that, we believe our unique biobank with 51 time-points involving both surveillance and rejection episodes has permitted a thorough evaluation of the effector immune function of face recipients. Lastly, the skin contains a large resident pool of lymphocytes (91, 92) and the presence of donor T cells during rejection has been previously documented during face rejection (93). Additional studies will be required to elucidate the role of donor T cells in the rejection process and differentiation of pathological infiltrates from non-pathological ones.

Overall, face transplantation is now a clinically feasible strategy for patients with facial deformities and the use of an immunosuppressive regimen similar to those used in solid organ transplants has yielded good short- and medium-term graft outcomes. Nonetheless, the high frequency of cellular rejection is concerning and the development of novel biomarkers and organ-specific immunosuppression strategies based on the known difference between transplanted organs will be critical to further advance the field.

## Acknowledgments

## Disclosure

The authors have declared that no conflict of interest exists.

**Figure Legends**

**Figure. 1**. **Clinical and histopathological findings in facial allograft rejection.** (**A**) Photographs and corresponding H&E graft stainings of representative patient (#5) during clinical cellular rejection episodes with graft erythema and edema (Grade II and III) compared to mild rejection on surveillance biopsy (Grade I) without significant erythema or edema. Grade I rejection shows normal epithelium, mild dermal edema, and a sparse perivascular lymphocytic infiltrate (arrow and higher magnification). Grade II rejection shows normal epithelium, development of superficial dermal edema, and associated lymphocytic vasculopathy (arrow and higher magnification) characterized by a brisk angiocentric lymphocytic infiltrate, endothelial prominence and sloughing. Grade III rejection retains lymphocytic vasculopathy (lower arrow) but also shows epithelial apoptosis associated with lymphoid exocytosis (higher arrow and magnification). (**B**) Timing of rejection in days and (**C**) grade of rejection according to time after transplant. Highly sensitized patient #4 who developed early acute humoral rejection characterized by neutrophil margination on H&E (arrow) (**D**) and positive C4d staining on endothelium by immunofluorescence, indicating local complement activation (**E**). Patient          had provided written consent for publication of his photographs.

**Figure. 2**. **Analysis of CD4+ and CD8+ T cell phenotypes from face recipients overtime.** Percentages (**A**) and absolute numbers (**B**) of CD4+ and CD8+ T cells from face recipients at following time-points: pre-transplant, 24h, 1 week, 3 months, 6 months and 12 months after transplant. Percentages of naïve (CCR7+CD45RA+), central memory (TCM: CCR7+CD45RA-), effector memory (TEM: CCR7-CD45RA-) and effector memory RA (TEMRA: CCR7-CD45RA+) CD4+ (**C**) and CD8+ T cells (**D**) over time. Pie charts of the mean CD4+ (**E**) and CD8+ (**F**) naïve, TCM, TEM and TEMRA at pre-transplant, 6 and 12 months post-transplant. (**G**) Representative contour plots of Th1 (CD4+CXCR3+CCR6-), Th2 (CD4+CXCR3-CCR6-) and Th17 (CD4+CXCR3-CCR6+) cells from patient #3. (**H**) Percentages of Th1, Th2 and Th17 cells from patients #1, # 2, #3, #5 and #6 overtime. (**I**) Representative contour plots of Th1, Th2 and Th17 cells from patient #4. (**J**) Percentages of Th1, Th2 and Th17 cells from patient #4 overtime. (**K**) IL-17A, IFN-γ and IL-4 production by CD4+ T cells from patient #4 at 6 months post-transplant after stimulation *in vitro* with PMA+Ionomycin. Graphs displayed as mean ±SEM at each time point examined.

**Figure 3**. **Tregs expansion in face transplant patients.** (**A**) Representative contour plots of CD4+Foxp3+ T cells (Tregs) pre-transplant and 12 months post-transplant. Percentages (**B**) and absolute numbers (**C**) of CD4+Foxp3+ cells from face recipients at following time-points: pre-transplant, 24h, 1 week, 3 months, 6 months and 12 months after transplant. (**D**) Foxp3 MFI in CD4+ T cells overtime. (**E**) Ratio of Tregs to conventional T cells pre-transplant and at 24h, 1 week and 3 months post-transplant. (**F**) Representative contour plots on CD4+-gated T cells demonstrating that the Foxp3+ cells are not expressing CD127. (**G**) Representative contour plots of CD4+CD25+CD127$^{-/low}$ cells (Tregs) pre-transplant and 12 months post-transplant. Percentages (**H**) and absolute numbers (**I**) of CD4+CD25+CD127$^{-/low}$ cells from face transplant patients overtime. Graphs displayed as mean ±SEM at each time point examined.

**Figure 4**. **Dynamics of B cells, Tfh cells and anti-HLA antibodies post-face transplant**. (**A**) Representative contour plots of CD4+PD-1+CXCR5+ cells (Tfh) pre-transplant (upper panel) and 1 week post-transplant (lower panel). Percentages (**B**) and absolute numbers (**C**) of B cells (CD19+) and Tfh cells from face recipients at following time-points: pre-transplant, 24h, 1 week, 3 months, 6 months and 12 months post-transplant  *=p<0.05 compared to pre-rejection (*Mann-Whitney* test). (**D**) Ratio of Tfh to

CD4+ T cells pre-transplant and at 24h, 1 week and 3 months post-transplant. (**E**) Fold change of absolute numbers of B cells and Tfh at 12 months compared to pre-transplant. (**F**) Percentages of B cells and Tfh from highly sensitized patient 4. (**G**) Panel-reactive antibodies (PRA) for class I and class II anti-HLA antibodies overtime. (**H**) Number of circulating donor-specific antibodies and C1q-positivity of patient #4 at different time-points post-transplant. Graphs displayed as mean ±SEM at each time point examined.

**Figure 5**. **Predominance of CD4+, CD8+ and CD14+ cells in skin grafts during face transplant rejection**. (**A**) Representative immunofluorescence of CD4 staining (green) of skin biopsy specimens from pre-rejection, rejection and post-rejection time-points (DAPI in blue) (400x). (**B**) Percentages (upper graph) and absolute numbers (lower graph) of CD4+ cells from PBMCs at pre-rejection, rejection and post-rejection time-points. (**C**) Representative immunofluorescence of CD8 staining (pink) on skin grafts as in (A) (400x). (**D**) Percentages (upper graph) and absolute numbers (lower graph) of CD8+ cells from PBMC at pre-rejection, rejection and post-rejection time-points. (**E**) Representative immunofluorescence of CD14 staining (red) on skin grafts as in (A). (400x). (**F**) Percentages (upper graph) and absolute numbers (lower graph) of CD14+ cells from PBMC at pre-rejection, rejection and post-rejection time-points. (**G**) Representative contour plots of the gating strategy for effector memory (CCR7-CD45RA-) and effector memory RA (CCR7-CD45RA+) CD4+ or CD8+ T cells. (**H**) Percentages of effector memory CD4+ (upper graph) and CD8+ (lower graph) T cells at pre-rejection, rejection and post-rejection time-points. (**I**) Percentages of effector CD4+ (upper graph) and CD8+ (lower graph) T cells at pre-rejection, rejection and post-rejection time-points. Graphs displayed as mean ±SEM at each time point examined.

**Figure 6**. **Increased infiltration of IL-17 and IFN-γ- producing T cells in skin grafts during face transplant rejection.** (**A**) Representative triple color immunofluorescence images taken from skin biopsy specimens at pre-rejection, rejection and post-rejection time-points stained for CD3 (red), IL-17 (green) and nuclear stain DAPI (blue) (200x). (**B**) Total CD3+ and CD3+IL-17+ cells were counted using 8-10 high-powered fields (200x) from patient 3 and 4, and the absolute number of CD3+ and CD3+IL-17+ cells are shown with the mean (horizontal bar). *=$p<0.05$ (*Mann-Whitney* test). (**C**) Percentage of CD3+IL-17+ T cells was calculated from the total number of CD3+ T cells from each high power field. *=$p<0.05$ compared to the pre-rejection time point. (**D**) Representative triple color immunofluorescence of skin grafts stained for CD3 (red), IFN-γ (green) and nuclear stain DAPI (blue) (200x). (**E**) Total CD3+ and CD3+ IFN-γ+ cells were counted and displayed as described in (B). *=$p<0.05$ compared to the pre-rejection time point. (**F**) Percentage of CD3+IFN-γ+ T-cells were calculated and displayed as described in (C). (**G**) Representative contour plot of IL-17A production in blood CD4+ T cells at pre-rejection and rejection time-points (upper panels). Percentages of PBMC CD4+ IL-17A+ cells (bottom left graph) and IL-17 MFI in CD4+ T cells (bottom right graph) at pre-rejection, rejection and post-rejection time-points (**H**) Flow contour plots of IFN-γ producing CD4+ T cells as in (G). (**I**) Percentages of IFN-γ-producing CD8+ T cells (left graph) and IFN-γ MFI (right graph) at pre-rejection, rejection and post-rejection time-points. (**J**) Percentages of IL-17A-producing CD8+ T cells and IL-17A MFI as in (I). Graphs displayed as mean ±SEM at each time point examined. *=$p<0.05$ compared to pre-rejection (*Mann-Whitney* test).

**Figure 7. Characterization of circulating and graft infiltrating Tregs post-transplant.** (**A**) Representative immunofluorescence of CD4 (green) and Foxp3 (red) stainings of skin biopsy specimens from pre-rejection, rejection and post-rejection time-points (DAPI in blue) (400x). (**B**) Percentages (left graph) and absolute number (right graph) of CD4+Foxp3+ cells from patients' PBMCs at pre-rejection, rejection and post-rejection. (**C**) Representative contour plots, percentages (lower left) and absolute numbers (lower right) of CD4+PD-1+ cells from patients' PBMCs at pre-rejection, rejection and post-rejection. (**D**) Representative contour plots, percentages (lower left) and absolute numbers (lower right) of

CD4+CTLA-4+ cells from patients' PBMCs at pre-rejection, rejection and post-rejection. Graphs displayed as mean ±SEM at each time point examined.

**Description of Supporting Information**

"Additional Supporting Information may be found in the online version of this article"

Supplementary Methods

Supplemental Figure 1. Photographs of the six patients before transplantation and several months after surgery.

Supplemental Figure 2. Gating strategy of the cell populations from peripheral blood analyzed in this study.

Supplemental Figure 3. Direct and indirect donor-specific T cell alloreactivity and serum cytokines post-transplant.

Supplemental Figure 4. Cytokine characterization of CD4 and CD8 T cells at rejection episode.

Supplemental Table 1. Cell phenotypes analyzed in this study.

Supplemental Table 2. Serum cytokine levels measured by Luminex assay according to rejection or pre-rejection time-points (n=8; *Mann–Whitney* nonparametric test).
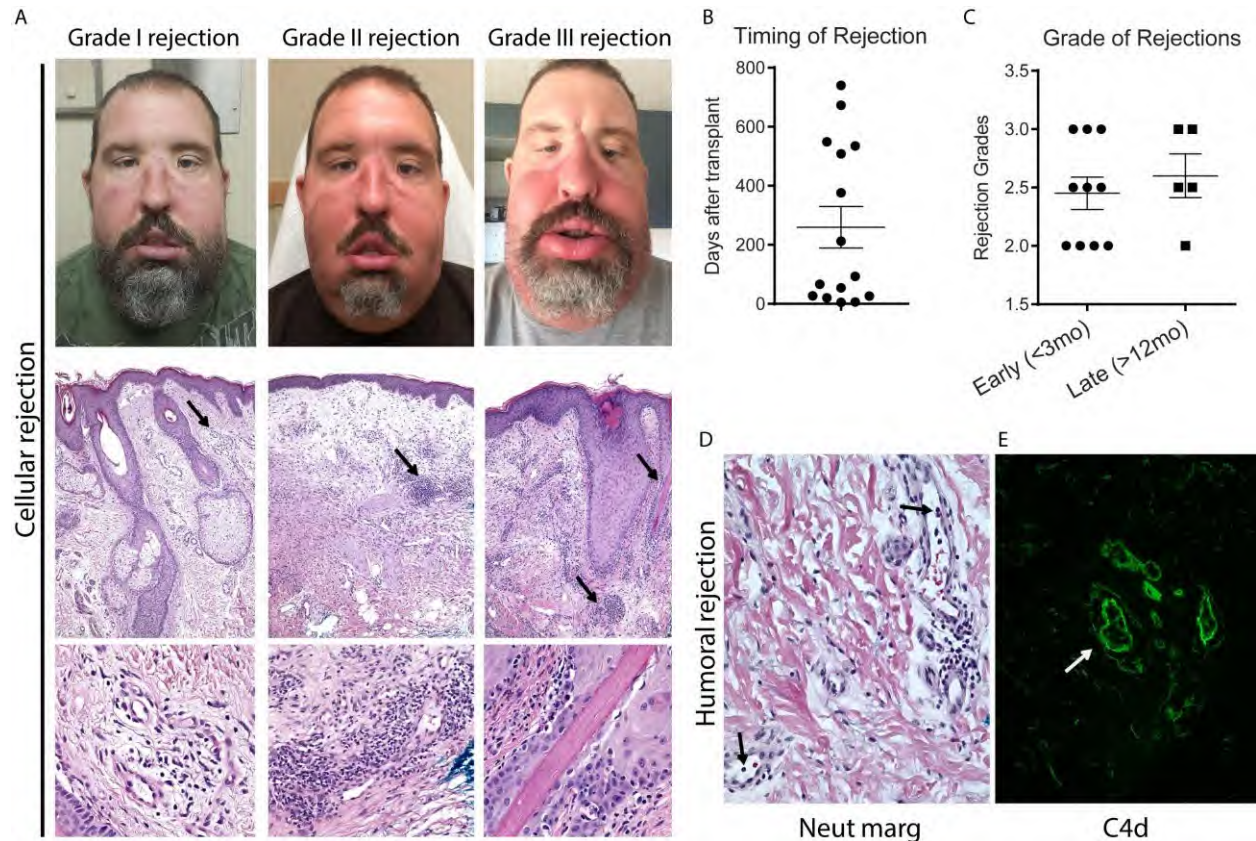
**References:**

1.　Pomahac B, Pribaz J, Eriksson E, Bueno EM, Diaz-Siso JR, Rybicki FJ, et al. Three patients with full facial transplantation. N Engl J Med. 2012;366(8):715-22. Epub 2011/12/30.

2.　Khalifian S, Brazio PS, Mohan R, Shaffer C, Brandacher G, Barth RN, et al. Facial transplantation: the first 9 years. Lancet. 2014;384(9960):2153-63. Epub 2014/05/03.

3.　Dubernard JM, Lengele B, Morelon E, Testelin S, Badet L, Moure C, et al. Outcomes 18 months after the first human partial face transplantation. N Engl J Med. 2007;357(24):2451-60. Epub 2007/12/14.

4.　Barret JP, Gavalda J, Bueno J, Nuvials X, Pont T, Masnou N, et al. Full face transplant: the first case report. Ann Surg. 2011;254(2):252-6. Epub 2011/07/21.

5.　Zhang Z, Zhu L, Quan D, Garcia B, Ozcay N, Duff J, et al. Pattern of liver, kidney, heart, and intestine allograft rejection in different mouse strain combinations. Transplantation. 1996;62(9):1267-72. Epub 1996/11/15.

6.　Jones ND, Turvey SE, Van Maurik A, Hara M, Kingsley CI, Smith CH, et al. Differential susceptibility of heart, skin, and islet allografts to T cell-mediated rejection. J Immunol. 2001;166(4):2824-30. Epub 2001/02/13.

7.　Rosenberg AS, Singer A. Cellular basis of skin allograft rejection: an in vivo model of immune-mediated tissue destruction. Annu Rev Immunol. 1992;10:333-58. Epub 1992/01/01.

8.　Bergstresser PR, Fletcher CR, Streilein JW. Surface densities of Langerhans cells in relation to rodent epidermal sites with special immunologic properties. J Invest Dermatol. 1980;74(2):77-80. Epub 1980/02/01.

9.　Diaz-Siso JR, Fischer S, Sisk GC, Bueno E, Kueckelhaus M, Talbot S, et al. Initial Experience of Dual Maintenance Immunosuppression With Steroid Withdrawal in Vascular Composite Tissue Allotransplantation. Am J Transplant. 2015. Epub 2015/03/18.

10.　Cendales LC, Kanitakis J, Schneeberger S, Burns C, Ruiz P, Landin L, et al. The Banff 2007 working classification of skin-containing composite tissue allograft pathology. Am J Transplant. 2008;8(7):1396-400. Epub 2008/05/01.

11.　Wood KJ, Goto R. Mechanisms of rejection: current perspectives. Transplantation. 2012;93(1):1-10. Epub 2011/12/06.

12.　Maecker HT, McCoy JP, Nussenblatt R. Standardizing immunophenotyping for the Human Immunology Project. Nature reviews Immunology. 2012;12(3):191-200. Epub 2012/02/22.

13.　Ashoor I, Najafian N, Korin Y, Reed EF, Mohanakumar T, Ikle D, et al. Standardization and cross validation of alloreactive IFNgamma ELISPOT assays within the clinical trials in organ transplantation consortium. Am J Transplant. 2013;13(7):1871-9. Epub 2013/05/29.

14.　Nickel P, Presber F, Bold G, Biti D, Schonemann C, Tullius SG, et al. Enzyme-linked immunosorbent spot assay for donor-reactive interferon-gamma-producing cells identifies T-cell presensitization and correlates with graft function at 6 and 12 months in renal-transplant recipients. Transplantation. 2004;78(11):1640-6. Epub 2004/12/14.

15.　van den Boogaardt DE, van Miert PP, de Vaal YJ, de Fijter JW, Claas FH, Roelen DL. The ratio of interferon-gamma and interleukin-10 producing donor-specific cells as an in vitro monitoring tool for renal transplant patients. Transplantation. 2006;82(6):844-8. Epub 2006/09/29.

16.　Andree H, Nickel P, Nasiadko C, Hammer MH, Schonemann C, Pruss A, et al. Identification of dialysis patients with panel-reactive memory T cells before kidney transplantation using an allogeneic cell bank. Journal of the American Society of Nephrology : JASN. 2006;17(2):573-80. Epub 2006/01/07.

17.　Poggio ED, Augustine JJ, Clemente M, Danzig JM, Volokh N, Zand MS, et al. Pretransplant cellular alloimmunity as assessed by a panel of reactive T cells assay correlates with acute renal graft rejection. Transplantation. 2007;83(7):847-52. Epub 2007/04/27.

18.　Tary-Lehmann M, Hricik DE, Justice AC, Potter NS, Heeger PS. Enzyme-linked immunosorbent assay spot detection of interferon-gamma and interleukin 5-producing cells as a predictive marker for renal allograft failure. Transplantation. 1998;66(2):219-24. Epub 1998/08/13.

19.　Joffre O, Santolaria T, Calise D, Al Saati T, Hudrisier D, Romagnoli P, et al. Prevention of acute and chronic allograft rejection with CD4+CD25+Foxp3+ regulatory T lymphocytes. Nat Med. 2008;14(1):88-92. Epub 2007/12/11.

20.　Kingsley CI, Karim M, Bushell AR, Wood KJ. CD25+CD4+ regulatory T cells prevent graft rejection: CTLA-4- and IL-10-dependent immunoregulation of alloresponses. J Immunol. 2002;168(3):1080-6. Epub 2002/01/22.

21.　Issa F, Wood KJ. The potential role for regulatory T-cell therapy in vascularized composite allograft transplantation. Curr Opin Organ Transplant. 2014;19(6):558-65. Epub 2014/10/22.

22.     Morgan ME, van Bilsen JH, Bakker AM, Heemskerk B, Schilham MW, Hartgers FC, et al. Expression of FOXP3 mRNA is not confined to CD4+CD25+ T regulatory cells in humans. Hum Immunol. 2005;66(1):13-20. Epub 2004/12/29.

23.     Liu W, Putnam AL, Xu-Yu Z, Szot GL, Lee MR, Zhu S, et al. CD127 expression inversely correlates with FoxP3 and suppressive function of human CD4+ T reg cells. The Journal of experimental medicine. 2006;203(7):1701-11. Epub 2006/07/05.

24.     Einecke G, Sis B, Reeve J, Mengel M, Campbell PM, Hidalgo LG, et al. Antibody-mediated microcirculation injury is the major cause of late kidney transplant failure. Am J Transplant. 2009;9(11):2520-31. Epub 2009/10/22.

25.     O'Leary JG, Demetris AJ, Friedman LS, Gebel HM, Halloran PF, Kirk AD, et al. The role of donor-specific HLA alloantibodies in liver transplantation. Am J Transplant. 2014;14(4):779-87. Epub 2014/03/04.

26.     Chandraker A, Arscott R, Murphy GF, Lian CG, Bueno EM, Marty FM, et al. The management of antibody-mediated rejection in the first presensitized recipient of a full-face allotransplant. Am J Transplant. 2014;14(6):1446-52. Epub 2014/05/07.

27.     Loupy A, Lefaucheur C, Vernerey D, Prugger C, Duong van Huyen JP, Mooney N, et al. Complement-binding anti-HLA antibodies and kidney-allograft survival. N Engl J Med. 2013;369(13):1215-26. Epub 2013/09/27.

28.     Zwirner NW, Fernandez-Vina MA, Stastny P. MICA, a new polymorphic HLA-related antigen, is expressed mainly by keratinocytes, endothelial cells, and monocytes. Immunogenetics. 1998;47(2):139-48. Epub 1998/01/31.

29.     Zou Y, Stastny P, Susal C, Dohler B, Opelz G. Antibodies against MICA antigens and kidney-transplant rejection. N Engl J Med. 2007;357(13):1293-300. Epub 2007/09/28.

30.     Lazzeri E, Rotondi M, Mazzinghi B, Lasagni L, Buonamano A, Rosati A, et al. High CXCL10 expression in rejected kidneys and predictive role of pretransplant serum CXCL10 for acute rejection and chronic allograft nephropathy. Transplantation. 2005;79(9):1215-20. Epub 2005/05/10.

31.     Rotondi M, Rosati A, Buonamano A, Lasagni L, Lazzeri E, Pradella F, et al. High pretransplant serum levels of CXCL10/IP-10 are related to increased risk of renal allograft failure. Am J Transplant. 2004;4(9):1466-74. Epub 2004/08/17.

32.     Lo DJ, Kaplan B, Kirk AD. Biomarkers for kidney transplant rejection. Nat Rev Nephrol. 2014;10(4):215-25. Epub 2014/01/22.

33.     Kapsenberg ML. Dendritic-cell control of pathogen-driven T-cell polarization. Nature reviews Immunology. 2003;3(12):984-93. Epub 2003/12/04.

34.     D'Elios MM, Josien R, Manghetti M, Amedei A, de Carli M, Cuturi MC, et al. Predominant Th1 cell infiltration in acute rejection episodes of human kidney grafts. Kidney Int. 1997;51(6):1876-84. Epub 1997/06/01.

35.     Strom TB, Koulmanda M. Recently discovered T cell subsets cannot keep their commitments. Journal of the American Society of Nephrology : JASN. 2009;20(8):1677-80. Epub 2009/08/04.

36.     Benichou G, Yamada Y, Yun SH, Lin C, Fray M, Tocco G. Immune recognition and rejection of allogeneic skin grafts. Immunotherapy. 2011;3(6):757-70. Epub 2011/06/15.

37.     Mestas J, Hughes CC. Of mice and not men: differences between mouse and human immunology. J Immunol. 2004;172(5):2731-8. Epub 2004/02/24.

38.     Tsaur I, Gasser M, Aviles B, Lutz J, Lutz L, Grimm M, et al. Donor antigen-specific regulatory T-cell function affects outcome in kidney transplant recipients. Kidney Int. 2011;79(9):1005-12. Epub 2011/01/29.

39.     Chadha R, Heidt S, Jones ND, Wood KJ. Th17: contributors to allograft rejection and a barrier to the induction of transplantation tolerance? Transplantation. 2011;91(9):939-45. Epub 2011/03/08.

40.     Strehlau J, Pavlakis M, Lipman M, Shapiro M, Vasconcellos L, Harmon W, et al. Quantitative detection of immune activation transcripts as a diagnostic tool in kidney transplantation. Proc Natl Acad Sci U S A. 1997;94(2):695-700. Epub 1997/01/21.

41.     Van Kooten C, Boonstra JG, Paape ME, Fossiez F, Banchereau J, Lebecque S, et al. Interleukin-17 activates human renal epithelial cells in vitro and is expressed during renal allograft rejection. Journal of the American Society of Nephrology : JASN. 1998;9(8):1526-34. Epub 1998/08/11.

42.     Vanaudenaerde BM, Dupont LJ, Wuyts WA, Verbeken EK, Meyts I, Bullens DM, et al. The role of interleukin-17 during acute rejection after lung transplantation. Eur Respir J. 2006;27(4):779-87. Epub 2006/04/06.

43.     Tang JL, Subbotin VM, Antonysamy MA, Troutt AB, Rao AS, Thomson AW. Interleukin-17 antagonism inhibits acute but not chronic vascular rejection. Transplantation. 2001;72(2):348-50. Epub 2001/07/31.

44.     Antonysamy MA, Fanslow WC, Fu F, Li W, Qian S, Troutt AB, et al. Evidence for a role of IL-17 in organ allograft rejection: IL-17 promotes the functional differentiation of dendritic cell progenitors. J Immunol. 1999;162(1):577-84. Epub 1999/01/14.
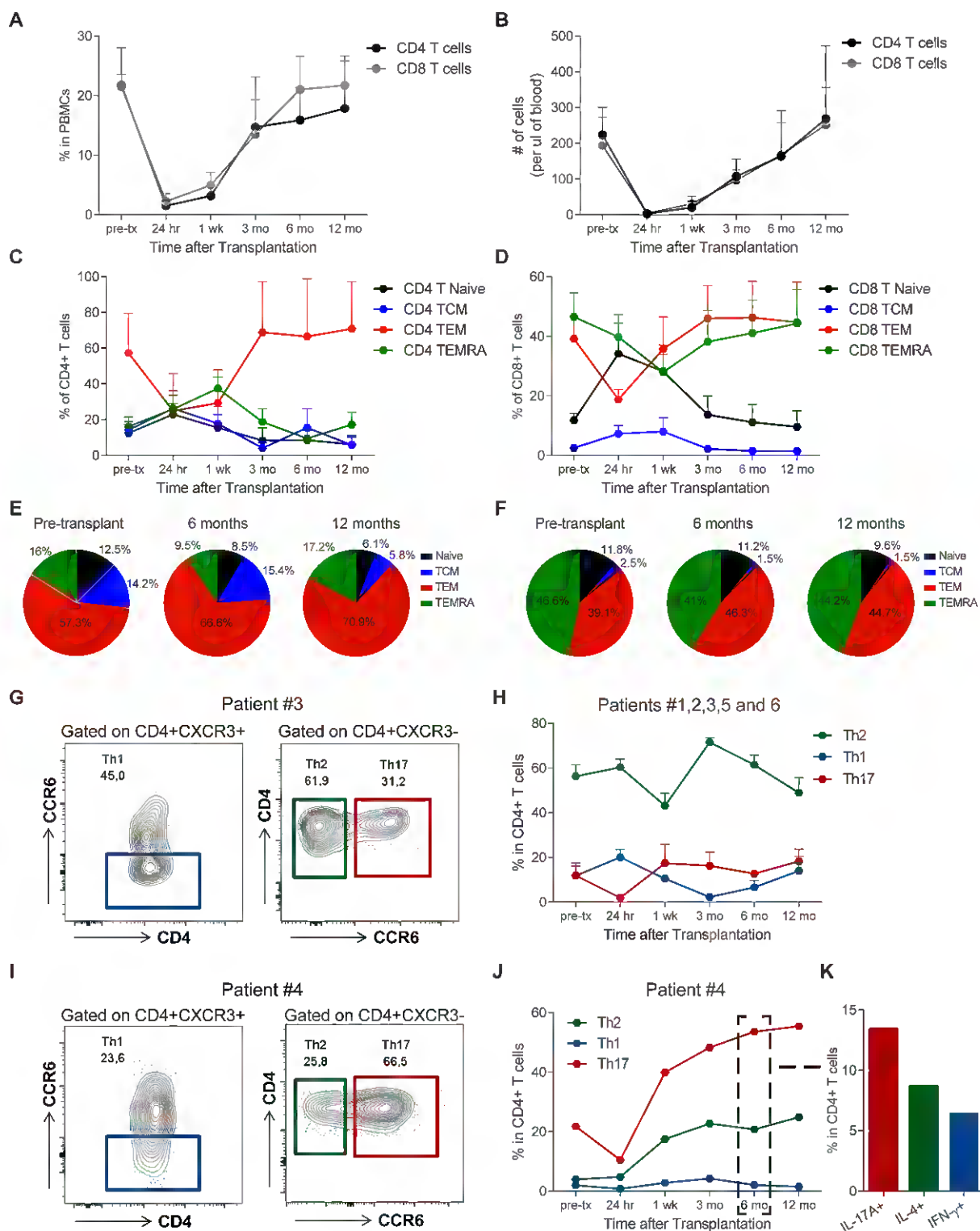
45.     de Oliveira VL, Keijsers RR, van de Kerkhof PC, Seyger MM, Fasse E, Svensson L, et al. Humanized mouse model of skin inflammation is characterized by disturbed keratinocyte differentiation and influx of IL-17A producing T cells. PLoS One. 2012;7(10):e45509. Epub 2012/10/25.

46.     Eyerich S, Onken AT, Weidinger S, Franke A, Nasorri F, Pennino D, et al. Mutual antagonism of T cells causing psoriasis and atopic eczema. N Engl J Med. 2011;365(3):231-8. Epub 2011/07/22.

47.     Pasparakis M, Haase I, Nestle FO. Mechanisms regulating skin immunity and inflammation. Nature reviews Immunology. 2014;14(5):289-301. Epub 2014/04/12.

48.     Krummey SM, Cheeseman JA, Conger JA, Jang PS, Mehta AK, Kirk AD, et al. High CTLA-4 expression on Th17 cells results in increased sensitivity to CTLA-4 coinhibition and resistance to belatacept. Am J Transplant. 2014;14(3):607-14. Epub 2014/04/15.

49.     Cornell LD, Smith RN, Colvin RB. Kidney transplantation: mechanisms of rejection and acceptance. Annu Rev Pathol. 2008;3:189-220. Epub 2007/11/28.

50.     Hautz T, Zelger B, Grahammer J, Krapf C, Amberger A, Brandacher G, et al. Molecular markers and targeted therapy of skin rejection in composite tissue allotransplantation. Am J Transplant. 2010;10(5):1200-9. Epub 2010/04/01.

51.     Corsi MM, Leone G, Fulgenzi A, Wasserman K, Leone F, Ferrero ME. RANTES and MCP-1 chemokine plasma levels in chronic renal transplant dysfunction and chronic renal failure. Clin Biochem. 1999;32(6):455-60. Epub 2000/02/10.

52.     Prodjosudjadi W, Daha MR, Gerritsma JS, Florijn KW, Barendregt JN, Bruijn JA, et al. Increased urinary excretion of monocyte chemoattractant protein-1 during acute renal allograft rejection. Nephrol Dial Transplant. 1996;11(6):1096-103. Epub 1996/06/01.

53.     Kim SH, Oh EJ, Kim MJ, Park YJ, Han K, Yang HJ, et al. Pretransplant donor-specific interferon-gamma ELISPOT assay predicts acute rejection episodes in renal transplant recipients. Transplant Proc. 2007;39(10):3057-60. Epub 2007/12/20.

54.     Nather BJ, Nickel P, Bold G, Presber F, Schonemann C, Pratschke J, et al. Modified ELISPOT technique--highly significant inverse correlation of post-Tx donor-reactive IFNgamma-producing cell frequencies with 6 and 12 months graft function in kidney transplant recipients. Transpl Immunol. 2006;16(3-4):232-7. Epub 2006/12/02.

55.     Bestard O, Crespo E, Stein M, Lucia M, Roelen DL, de Vaal YJ, et al. Cross-validation of IFN-gamma Elispot assay for measuring alloreactive memory/effector T cell responses in renal transplant recipients. Am J Transplant. 2013;13(7):1880-90. Epub 2013/06/15.

56.     Brennan DC, Daller JA, Lake KD, Cibrik D, Del Castillo D. Rabbit antithymocyte globulin versus basiliximab in renal transplantation. N Engl J Med. 2006;355(19):1967-77. Epub 2006/11/10.

57.     Petruzzo P, Dubernard JM. The International Registry on Hand and Composite Tissue allotransplantation. Clin Transpl. 2011:247-53. Epub 2011/01/01.

58.     Fischer S, Lian CG, Kueckelhaus M, Strom TB, Edelman ER, Clark RA, et al. Acute rejection in vascularized composite allotransplantation. Curr Opin Organ Transplant. 2014;19(6):531-44. Epub 2014/10/22.

59.     Iwasaki A, Medzhitov R. Control of adaptive immunity by the innate immune system. Nature immunology. 2015;16(4):343-53. Epub 2015/03/20.

60.     Naik S, Bouladoux N, Wilhelm C, Molloy MJ, Salcedo R, Kastenmuller W, et al. Compartmentalized control of skin immunity by resident commensals. Science. 2012;337(6098):1115-9. Epub 2012/07/28.

61.     Fahlen A, Engstrand L, Baker BS, Powles A, Fry L. Comparison of bacterial microbiota in skin biopsies from normal and psoriatic skin. Arch Dermatol Res. 2012;304(1):15-22. Epub 2011/11/09.

62.     Alegre ML, Mannon RB, Mannon PJ. The microbiota, the immune system and the allograft. Am J Transplant. 2014;14(6):1236-48. Epub 2014/05/21.

63.     Martins PN, Tullius SG, Markmann JF. Immunosenescence and immune response in organ transplantation. Int Rev Immunol. 2014;33(3):162-73. Epub 2013/10/17.

64.     Petruzzo P, Kanitakis J, Testelin S, Pialat JB, Buron F, Badet L, et al. Clinicopathological Findings of Chronic Rejection in a Face Grafted Patient. Transplantation. 2015. Epub 2015/05/20.

65.     Sis B, Campbell PM, Mueller T, Hunter C, Cockfield SM, Cruz J, et al. Transplant glomerulopathy, late antibody-mediated rejection and the ABCD tetrad in kidney allograft biopsies for cause. Am J Transplant. 2007;7(7):1743-52. Epub 2007/06/15.

66.     Wiebe C, Gibson IW, Blydt-Hansen TD, Karpinski M, Ho J, Storsley LJ, et al. Evolution and clinical pathologic correlations of de novo donor-specific HLA antibody post kidney transplant. Am J Transplant. 2012;12(5):1157-67. Epub 2012/03/21.

67.     Gordon RD, Fung JJ, Markus B, Fox I, Iwatsuki S, Esquivel CO, et al. The antibody crossmatch in liver transplantation. Surgery. 1986;100(4):705-15. Epub 1986/10/01.

68.    Hanish SI, Samaniego M, Mezrich JD, Foley DP, Leverson GE, Lorentzen DF, et al. Outcomes of simultaneous liver/kidney transplants are equivalent to kidney transplant alone: a preliminary report. Transplantation. 2010;90(1):52-60. Epub 2010/07/14.

69.    O'Leary JG, Gebel HM, Ruiz R, Bray RA, Marr JD, Zhou XJ, et al. Class II alloantibody and mortality in simultaneous liver-kidney transplantation. Am J Transplant. 2013;13(4):954-60. Epub 2013/02/26.

70.    Fung J, Makowka L, Tzakis A, Klintmalm G, Duquesnoy R, Gordon R, et al. Combined liver-kidney transplantation: analysis of patients with preformed lymphocytotoxic antibodies. Transplant Proc. 1988;20(1 Suppl 1):88-91. Epub 1988/02/01.

71.    Gugenheim J, Amorosa L, Gigou M, Fabiani B, Rouger P, Gane P, et al. Specific absorption of lymphocytotoxic alloantibodies by the liver in inbred rats. Transplantation. 1990;50(2):309-13. Epub 1990/08/01.

72.    Siemionow M, Nasir S. Impact of donor bone marrow on survival of composite tissue allografts. Ann Plast Surg. 2008;60(4):455-62. Epub 2008/03/26.

73.    Kulahci Y, Klimczak A, Madajka M, Altuntas S, Siemionow M. Long-term survival of composite hemiface/mandible/tongue allografts correlates with multilineage chimerism development in the lymphoid and myeloid compartments of recipients. Transplantation. 2010;90(8):843-52. Epub 2010/08/11.

74.    Siemionow M, Klimczak A. Chimerism-based experimental models for tolerance induction in vascularized composite allografts: Cleveland clinic research experience. Clin Dev Immunol. 2013;2013:831410. Epub 2013/04/11.

75.    Newell KA, Asare A, Kirk AD, Gisler TD, Bourcier K, Suthanthiran M, et al. Identification of a B cell signature associated with renal transplant tolerance in humans. J Clin Invest. 2010;120(6):1836-47. Epub 2010/05/27.

76.    Sagoo P, Perucha E, Sawitzki B, Tomiuk S, Stephens DA, Miqueu P, et al. Development of a cross-platform biomarker signature to detect renal transplant tolerance in humans. J Clin Invest. 2010;120(6):1848-61. Epub 2010/05/27.

77.    Baron D, Ramstein G, Chesneau M, Echasseriau Y, Pallier A, Paul C, et al. A common gene signature across multiple studies relate biomarkers and functional regulation in tolerance to renal allograft. Kidney Int. 2015;87(5):984-95. Epub 2015/01/30.

78.    Pallier A, Hillion S, Danger R, Giral M, Racape M, Degauque N, et al. Patients with drug-free long-term graft function display increased numbers of peripheral B cells with a memory and inhibitory phenotype. Kidney Int. 2010;78(5):503-13. Epub 2010/06/10.

79.    Wood KJ, Bushell A, Hester J. Regulatory immune cells in transplantation. Nature reviews Immunology. 2012;12(6):417-30. Epub 2012/05/26.

80.    Sakaguchi S, Powrie F, Ransohoff RM. Re-establishing immunological self-tolerance in autoimmune disease. Nat Med. 2012;18(1):54-8. Epub 2012/01/10.

81.    Bashuda H, Kimikawa M, Seino K, Kato Y, Ono F, Shimizu A, et al. Renal allograft rejection is prevented by adoptive transfer of anergic T cells in nonhuman primates. J Clin Invest. 2005;115(7):1896-902. Epub 2005/06/14.

82.    Ma A, Qi S, Song L, Hu Y, Dun H, Massicotte E, et al. Adoptive transfer of CD4+CD25+ regulatory cells combined with low-dose sirolimus and anti-thymocyte globulin delays acute rejection of renal allografts in Cynomolgus monkeys. Int Immunopharmacol. 2011;11(5):618-29. Epub 2010/11/26.

83.    Feng G, Nadig SN, Backdahl L, Beck S, Francis RS, Schiopu A, et al. Functional regulatory T cells produced by inhibiting cyclic nucleotide phosphodiesterase type 3 prevent allograft rejection. Sci Transl Med. 2011;3(83):83ra40. Epub 2011/05/20.

84.    Bestard O, Cruzado JM, Rama I, Torras J, Goma M, Seron D, et al. Presence of FoxP3+ regulatory T Cells predicts outcome of subclinical rejection of renal allografts. Journal of the American Society of Nephrology : JASN. 2008;19(10):2020-6. Epub 2008/05/23.

85.    Muthukumar T, Dadhania D, Ding R, Snopkowski C, Naqvi R, Lee JB, et al. Messenger RNA for FOXP3 in the urine of renal-allograft recipients. N Engl J Med. 2005;353(22):2342-51. Epub 2005/12/02.

86.    Taflin C, Nochy D, Hill G, Frouget T, Rioux N, Verine J, et al. Regulatory T cells in kidney allograft infiltrates correlate with initial inflammation and graft function. Transplantation. 2010;89(2):194-9. Epub 2010/01/26.

87.    Feng X, Kajigaya S, Solomou EE, Keyvanfar K, Xu X, Raghavachari N, et al. Rabbit ATG but not horse ATG promotes expansion of functional CD4+CD25highFOXP3+ regulatory T cells in vitro. Blood. 2008;111(7):3675-83. Epub 2008/02/06.

88.	Boenisch O, Lopez M, Elyaman W, Magee CN, Ahmad U, Najafian N. Ex vivo expansion of human Tregs by rabbit ATG is dependent on intact STAT3-signaling in CD4(+) T cells and requires the presence of monocytes. Am J Transplant. 2012;12(4):856-66. Epub 2012/03/07.

89.	Tang Q, Leung J, Melli K, Lay K, Chuu EL, Liu W, et al. Altered balance between effector T cells and FOXP3+ HELIOS+ regulatory T cells after thymoglobulin induction in kidney transplant recipients. Transpl Int. 2012;25(12):1257-67. Epub 2012/09/22.

90.	Gurkan S, Luan Y, Dhillon N, Allam SR, Montague T, Bromberg JS, et al. Immune reconstitution following rabbit antithymocyte globulin. Am J Transplant. 2010;10(9):2132-41. Epub 2010/10/05.

91.	Clark RA, Chong B, Mirchandani N, Brinster NK, Yamanaka K, Dowgiert RK, et al. The vast majority of CLA+ T cells are resident in normal skin. J Immunol. 2006;176(7):4431-9. Epub 2006/03/21.

92.	Clark RA. Resident memory T cells in human health and disease. Sci Transl Med. 2015;7(269):269rv1. Epub 2015/01/09.

93.	Lian CG, Bueno EM, Granter SR, Laga AC, Saavedra AP, Lin WM, et al. Biomarker evaluation of face transplant rejection: association of donor T cells with target cell injury. Mod Pathol. 2014;27(6):788-99. Epub 2014/01/18.

94.	Bestard O, Nickel P, Cruzado JM, Schoenemann C, Boenisch O, Sefrin A, et al. Circulating alloreactive T cells correlate with graft function in longstanding renal transplant recipients. Journal of the American Society of Nephrology : JASN. 2008;19(7):1419-29. Epub 2008/04/18.

95.	Heeger PS, Greenspan NS, Kuhlenschmidt S, Dejelo C, Hricik DE, Schulak JA, et al. Pretransplant frequency of donor-specific, IFN-gamma-producing lymphocytes is a manifestation of immunologic memory and correlates with the risk of posttransplant rejection episodes. J Immunol. 1999;163(4):2267-75. Epub 1999/08/10.
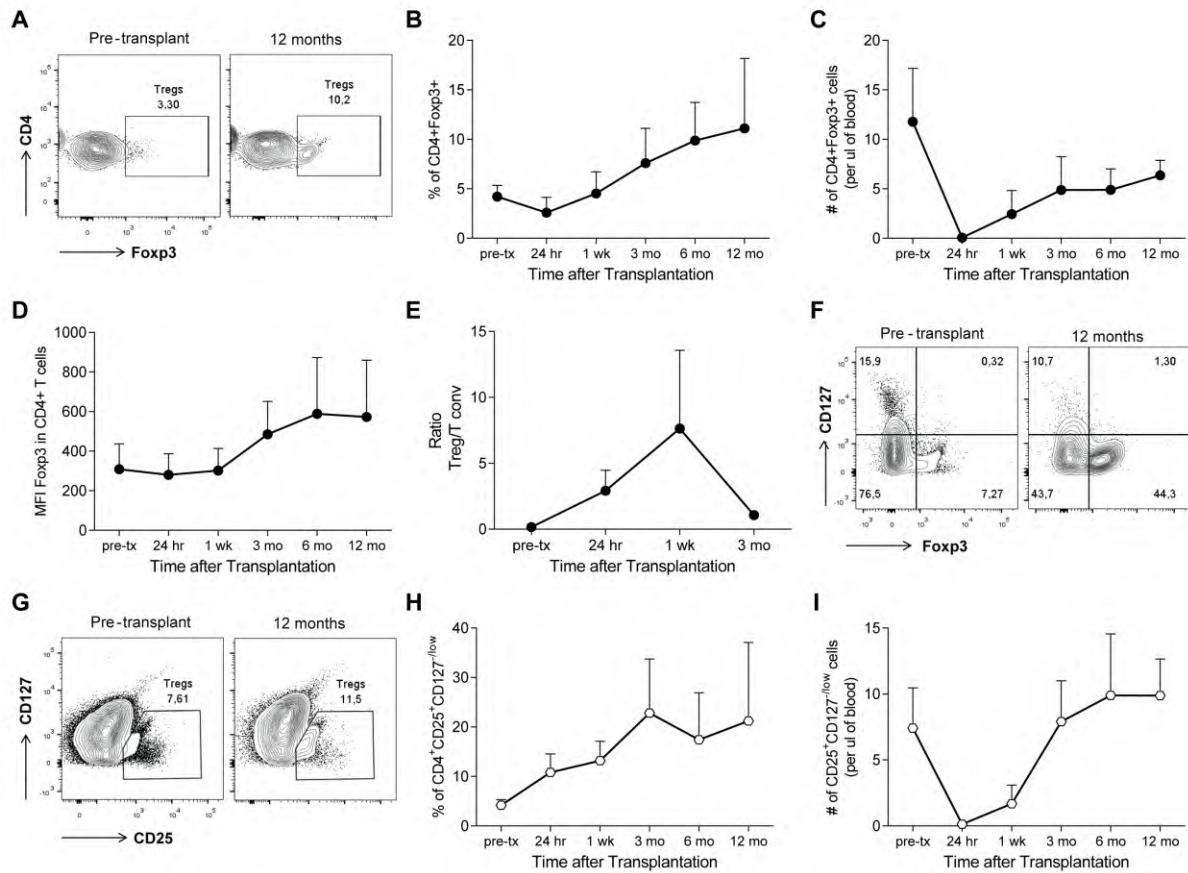
**Figure. 1**. **Clinical and histopathological findings in facial allograft rejection.** (**A**) Photographs and corresponding H&E graft stainings of representative patient (#5) during clinical cellular rejection episodes with graft erythema and edema (Grade II and III) compared to mild rejection on surveillance biopsy (Grade I) without significant erythema or edema. Grade I rejection shows normal epithelium, mild dermal edema, and a sparse perivascular lymphocytic infiltrate (arrow and higher magnification). Grade II rejection shows normal epithelium, development of superficial dermal edema, and associated lymphocytic vasculopathy (arrow and higher magnification) characterized by a brisk angiocentric lymphocytic infiltrate, endothelial prominence and sloughing. Grade III rejection retains lymphocytic vasculopathy (lower arrow) but also shows epithelial apoptosis associated with lymphoid exocytosis (higher arrow and magnification). (**B**) Timing of rejection in days and (**C**) grade of rejection according to time after transplant. Highly sensitized patient #4 who developed early acute humoral rejection characterized by neutrophil margination on H&E (arrow) (**D**) and positive C4d staining on endothelium by immunofluorescence, indicating local complement activation (**E**). Patient had provided written consent for publication of his photographs.
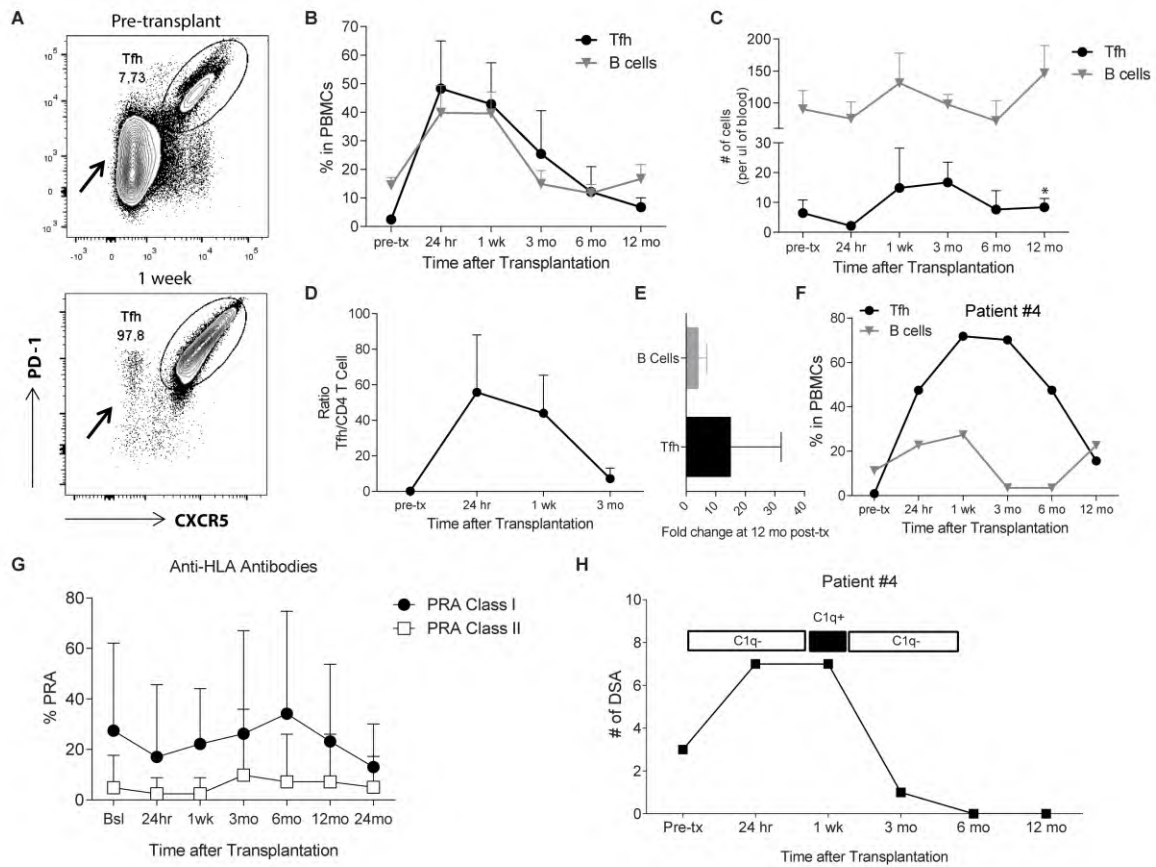
**Figure. 2**. **Analysis of CD4+ and CD8+ T cell phenotypes from face recipients overtime.** Percentages (**A**) and absolute numbers (**B**) of CD4+ and CD8+ T cells from face recipients at following time-points:
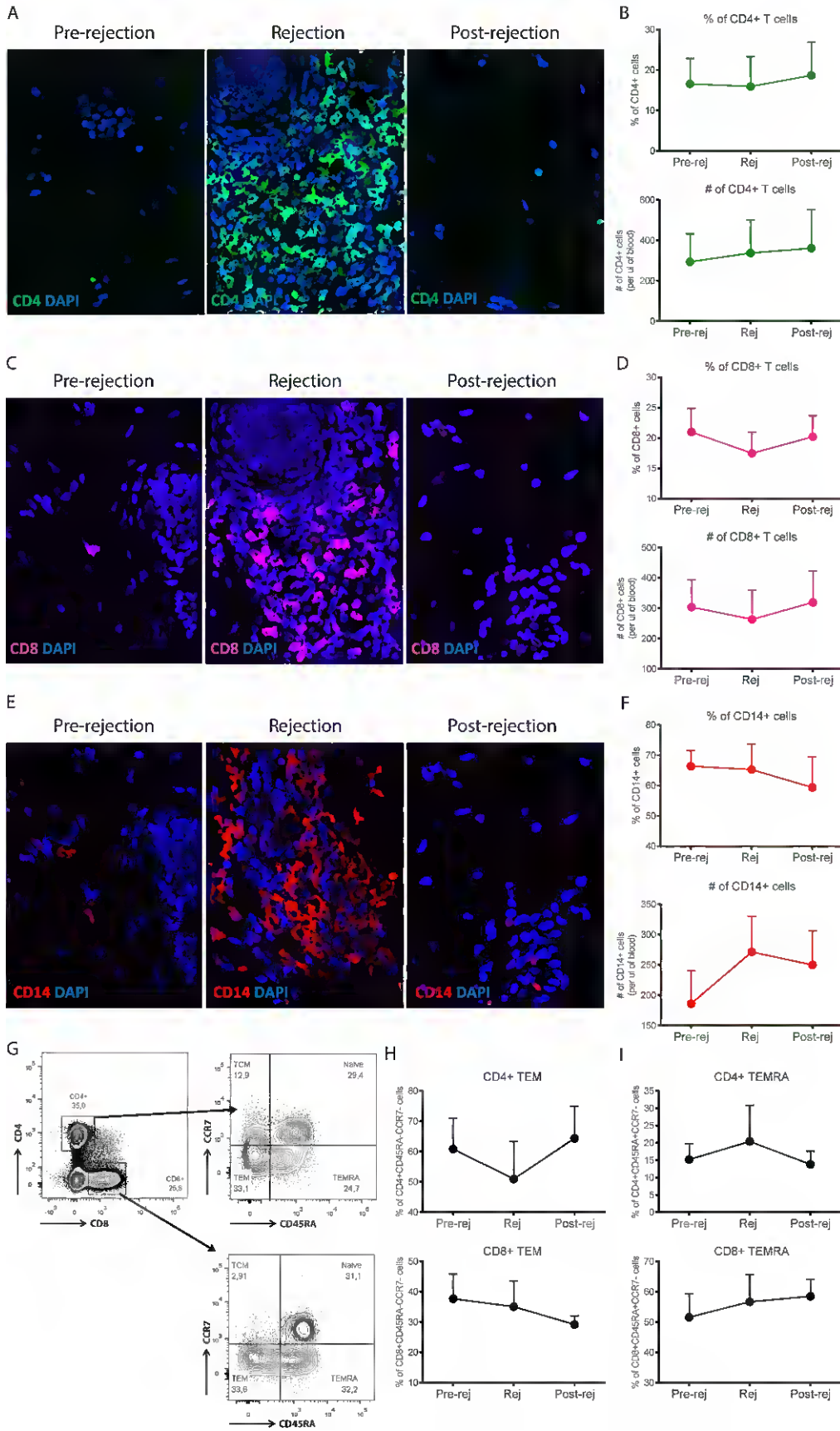
pre-transplant, 24h, 1 week, 3 months, 6 months and 12 months after transplant. Percentages of naïve (CCR7+CD45RA+), central memory (TCM: CCR7+CD45RA-), effector memory (TEM: CCR7-CD45RA-) and effector memory RA (TEMRA: CCR7-CD45RA+) CD4+ (**C**) and CD8+ T cells (**D)** over time. Pie charts of the mean CD4+ (**E**) and CD8+ (**F**) naïve, TCM, TEM and TEMRA at pre-transplant, 6 and 12 months post-transplant. (**G**) Representative contour plots of Th1 (CD4+CXCR3+CCR6-), Th2 (CD4+CXCR3-CCR6-) and Th17 (CD4+CXCR3-CCR6+) cells from patient #3. (**H**) Percentages of Th1, Th2 and Th17 cells from patients #1, # 2, #3, #5 and #6 overtime. (**I**) Representative contour plots of Th1, Th2 and Th17 cells from patient #4. (**J**) Percentages of Th1, Th2 and Th17 cells from patient #4 overtime. (**K**) IL-17A, IFN-$\gamma$ and IL-4 production by CD4+ T cells from patient #4 at 6 months post-transplant after stimulation *in vitro* with PMA+Ionomycin. Graphs displayed as mean ±SEM at each time point examined.
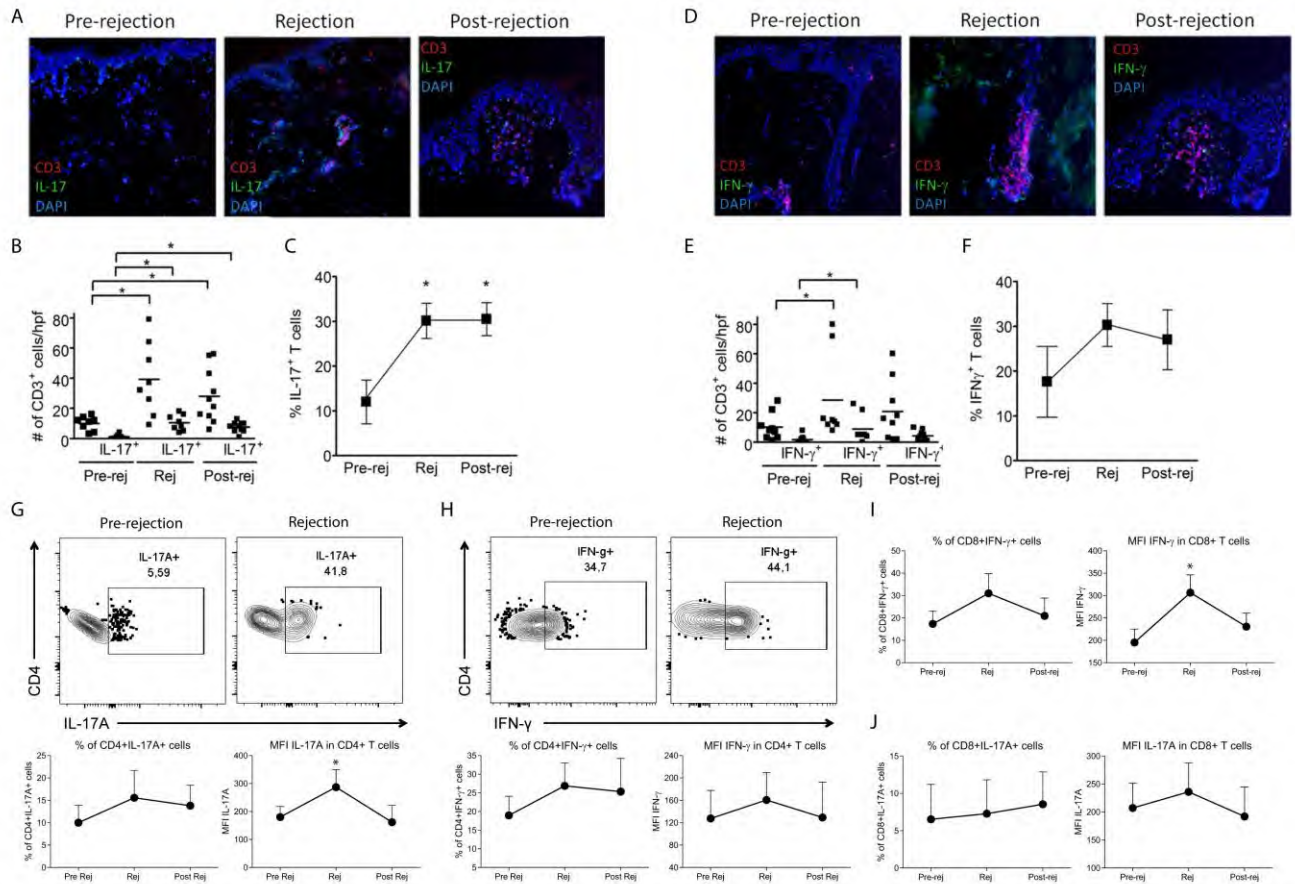
**Figure 3**. **Tregs expansion in face transplant patients.** (**A**) Representative contour plots of CD4+Foxp3+ T cells (Tregs) pre-transplant and 12 months post-transplant. Percentages (**B**) and absolute numbers (**C**) of CD4+Foxp3+ cells from face recipients at following time-points: pre-transplant, 24h, 1 week, 3 months, 6 months and 12 months after transplant. (**D**) Foxp3 MFI in CD4+ T cells overtime. (**E**) Ratio of Tregs to conventional T cells pre-transplant and at 24h, 1 week and 3 months post-transplant. (**F**) Representative contour plots on CD4+-gated T cells demonstrating that the Foxp3+ cells are not expressing CD127. (**G**) Representative contour plots of CD4+CD25+CD127^{-/low} cells (Tregs) pre-transplant and 12 months post-transplant. Percentages (**H**) and absolute numbers (**I**) of CD4+CD25+CD127^{-/low} cells from face transplant patients overtime. Graphs displayed as mean ±SEM at each time point examined.
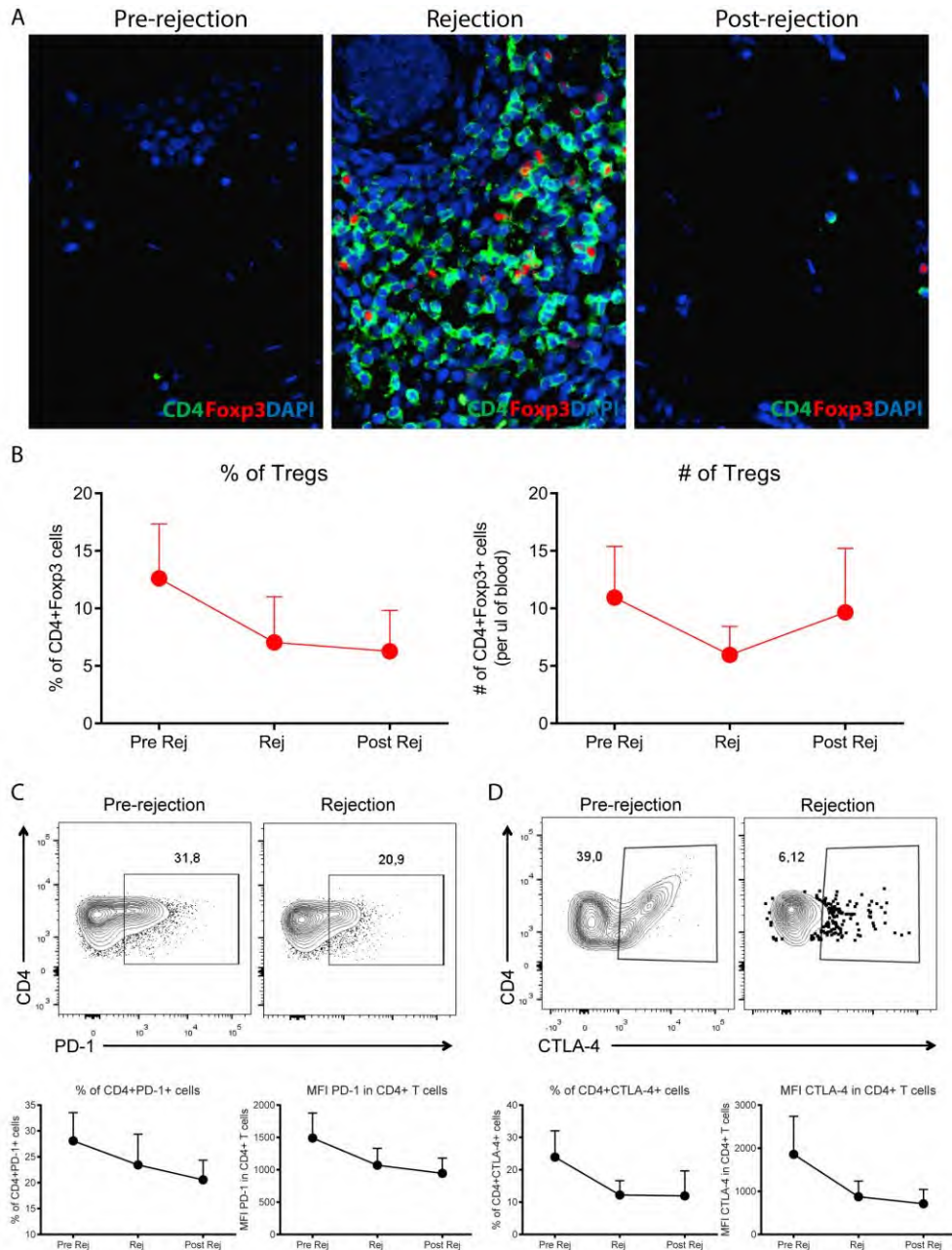
**Figure 4**. **Dynamics of B cells, Tfh cells and anti-HLA antibodies post-face transplant**. (**A**) Representative contour plots of CD4+PD-1+CXCR5+ cells (Tfh) pre-transplant (upper panel) and 1 week post-transplant (lower panel). Percentages (**B**) and absolute numbers (**C**) of B cells (CD19+) and Tfh cells from face recipients at following time-points: pre-transplant, 24h, 1 week, 3 months, 6 months and 12 months post-transplant  *=$p<0.05$ compared to pre-rejection (*Mann-Whitney* test). (**D**) Ratio of Tfh to CD4+ T cells pre-transplant and at 24h, 1 week and 3 months post-transplant. (**E**) Fold change of absolute numbers of B cells and Tfh at 12 months compared to pre-transplant. (**F**) Percentages of B cells and Tfh from highly sensitized patient 4. (**G**) Panel-reactive antibodies (PRA) for class I and class II anti-HLA antibodies overtime. (**H**) Number of circulating donor-specific antibodies and C1q-positivity of patient #4 at different time-points post-transplant. Graphs displayed as mean ±SEM at each time point examined.

**Figure 5**. **Predominance of CD4+, CD8+ and CD14+ cells in skin grafts during face transplant rejection**. (**A**) Representative immunofluorescence of CD4 staining (green) of skin biopsy specimens from pre-rejection, rejection and post-rejection time-points (DAPI in blue) (400x). (**B**) Percentages (upper graph) and absolute numbers (lower graph) of CD4+ cells from PBMCs at pre-rejection, rejection and post-rejection time-points. (**C**) Representative immunofluorescence of CD8 staining (pink) on skin grafts as in (A) (400x). (**D**) Percentages (upper graph) and absolute numbers (lower graph) of CD8+ cells from PBMC at pre-rejection, rejection and post-rejection time-points. (**E**) Representative immunofluorescence of CD14 staining (red) on skin grafts as in (A). (400x). (**F**) Percentages (upper graph) and absolute numbers (lower graph) of CD14+ cells from PBMC at pre-rejection, rejection and post-rejection time-points. (**G**) Representative contour plots of the gating strategy for effector memory (CCR7-CD45RA-) and effector memory RA (CCR7-CD45RA+) CD4+ or CD8+ T cells. (**H**) Percentages of effector memory CD4+ (upper graph) and CD8+ (lower graph) T cells at pre-rejection, rejection and post-rejection time-points. (**I**) Percentages of effector CD4+ (upper graph) and CD8+ (lower graph) T cells at pre-rejection, rejection and post-rejection time-points. Graphs displayed as mean ±SEM at each time point examined.

**Figure 6**. **Increased infiltration of IL-17 and IFN-γ- producing T cells in skin grafts during face transplant rejection.** (**A**) Representative triple color immunofluorescence images taken from skin biopsy specimens at pre-rejection, rejection and post-rejection time-points stained for CD3 (red), IL-17 (green) and nuclear stain DAPI (blue) (200x). (**B**) Total CD3+ and CD3+IL-17+ cells were counted using 8-10 high-powered fields (200x) from patient 3 and 4, and the absolute number of CD3+ and CD3+IL-17+ cells are shown with the mean (horizontal bar). *=p<0.05 (*Mann-Whitney* test). (**C**) Percentage of CD3+IL-17+ T cells was calculated from the total number of CD3+ T cells from each high power field. *=p<0.05 compared to the pre-rejection time point. (**D**) Representative triple color immunofluorescence of skin grafts stained for CD3 (red), IFN-γ (green) and nuclear stain DAPI (blue) (200x). (**E**) Total CD3+ and CD3+ IFN-γ+ cells were counted and displayed as described in (B). *=p<0.05 compared to the pre-rejection time point. (**F**) Percentage of CD3+IFN-γ+ T-cells were calculated and displayed as described in (C). (**G**) Representative contour plot of IL-17A production in blood CD4+ T cells at pre-rejection and rejection time-points (upper panels). Percentages of PBMC CD4+ IL-17A+ cells (bottom left graph) and IL-17 MFI in CD4+ T cells (bottom right graph) at pre-rejection, rejection and post-rejection time-points (**H**) Flow contour plots of IFN-γ producing CD4+ T cells as in (G). (**I**) Percentages of IFN-γ-producing CD8+ T cells (left graph) and IFN-γ MFI (right graph) at pre-rejection, rejection and post-rejection time-points. (**J**) Percentages of IL-17A-producing CD8+ T cells and IL-17A MFI as in (I). Graphs displayed as mean ±SEM at each time point examined. *=p<0.05 compared to pre-rejection (*Mann-Whitney* test).

**Figure 7. Characterization of circulating and graft infiltrating Tregs post-transplant.** (**A**) Representative immunofluorescence of CD4 (green) and Foxp3 (red) stainings of skin biopsy specimens from pre-rejection, rejection and post-rejection time-points (DAPI in blue) (400x). (**B**) Percentages (left graph) and absolute number (right graph) of CD4+Foxp3+ cells from patients' PBMCs at pre-rejection, rejection and post-rejection. (**C**) Representative contour plots, percentages (lower left) and absolute numbers (lower right) of CD4+PD-1+ cells from patients' PBMCs at pre-rejection, rejection and post-rejection. (**D**) Representative contour plots, percentages (lower left) and absolute numbers (lower right) of CD4+CTLA-4+ cells from patients' PBMCs at pre-rejection, rejection and post-rejection. Graphs displayed as mean ±SEM at each time point examined.

**Table 1.** Baseline characteristics of VCA transplant recipients and donors.

| | Patient 1 | Patient 2 | Patient 3 | Patient 4 | Patient 5 | Patient 6 |
|---|---|---|---|---|---|---|
| **Recipients' characteristics** | | | | | | |
| Age at transplant (yr) | 57 | 25 | 30 | 44 | 38 | 33 |
| Gender | F | M | M | F | M | M |
| Ethnicity | White | White | White | White | White | White |
| Cause of injury | Animal Attack | Electrical Burn | Electrical Burn | Chemical Burn | Gunshot | Gunshot |
| Surgery | Face, Bilateral Hands | Face | Face | Face | Face | Face |
| PRA (%) | 0 | 68 | 0 | 97 | 22 | 32 |
| Donor specific antibodies | Negative | Negative | Negative | Positive | Negative | Positive |
| HLA mismatch (A,B,C,DR,DQ,DP) | 8 | 8 | 5 | 11 | 8 | 7 |
| CMV status | Positive | Positive | Negative | Positive | Negative | Positive |
| EBV status | Positive | Positive | Positive | Positive | Positive | Positive |
| Induction type and dose | Antithymocyte globulin 1.5mg/kg/day x4; high dose steroids | Antithymocyte globulin 1.5mg/kg/day x4; high dose steroids | Antithymocyte globulin 1.5mg/kg/day x4; high dose steroids | Antithymocyte globulin 1.5mg/kg/day x4; high dose steroids | Antithymocyte globulin 1.5mg/kg/day x2/0.75mg/kg/day x2; high dose steroids | Antithymocyte globulin 1.5mg/kg/day x3; high dose steroids |
| Follow-up (yrs) | 4 | 4.2 | 4.1 | 2.3 | 1.1 | 0.6 |
| **Donors' characteristics** | | | | | | |
| Age | 42 | 48 | 31 | 56 | 51 | 23 |
| Gender | F | M | M | F | M | M |
| CMV status | Positive | Positive | Positive | Negative | Positive | Negative |
| EBV status | Positive | Positive | Positive | Positive | Positive | Positive |
| Ischemia time | 2hr | 4hr | 2hr | 3hr | 3hr | 1hr 30min |

# Supplementary Materials for

# Co-Dominant Role of IFN-γ- and IL-17-Producing T Cells During Rejection in Full Facial Transplant Recipients

**Authors:** Thiago J. Borges[1], Brian Smith[1], Luccie Wo[2], Jamil Azzi[1], Sudipta Tripathi[1], Jordan D. Lane[2], Ericka M. Bueno[2], John T. O'Malley[3], Rachael A. Clark[3], Stefan G. Tullius[4], Anil Chandraker[1], Christine G. Lian[5], George F. Murphy[5], Terry B. Strom[6], Bohdan Pomahac[2], Nader Najafian[1,7], Leonardo V. Riella[1,*]

*Corresponding author: lriella@rics.bwh.harvard.edu

## Supplementary Methods

*Histopathology and Immunofluorescence*

Histopathology of all specimens was evaluated by conventional hematoxylin and eosin (H&E) sections, and then further evaluated by immunofluorescence studies. Immunofluorescence was performed for single antibody labels, and in selected instances (CD4, FoxP3) by with two-channel identification of epitopes. Briefly, 5-mm-thick paraffin sections were incubated with primary antibodies against CD4 (Invitrogen), CD8 (Abcam), FoxP3 (BioLegend) or CD14 (Abcam) overnight and then incubated with Alexa Fluor 594-conjugated anti-mouse IgG and Alexa Fluor 488-conjugated anti-rabbit IgG (Invitrogen) at room temperature for 1 hour. The sections were cover slipped with ProLong Gold anti-fade with 4',6-diamidino-2-phenylindole (DAPI, Invitrogen). Sections were analyzed with a BX51/BX52

microscope (Olympus America, Melville, NY, USA), and images were captured using the CytoVision 3.6 software (Applied Imaging, San Jose, CA, USA). Single label immunofluorescence was also performed using isotype-specific irrelevant primary antibodies and with switching of the secondary antibodies to ensure specificity and exclude cross reactivity. For the cytokine staining on skin grafts, six μm cryosections were cut, air dried, fixed for 10 min in acetone and blocked with 20 μg/ml of human IgG (Jackson ImmunoResearch Laboratories). Sections were incubated with anti-IL-17 or anti-IFN-γ antibodies (Abcam), washed, and subsequently incubated with secondary goat anti-rabbit antibody conjugated with Alexa Fluor 488. Lastly, slides were incubated with anti-CD3 PE, washed, and mounted with DAPI-containing mounting media. Sections were photographed using a microscope (Eclipse 6600; Nikon) equipped with a 40x/0.75 objective lens (Plan Fluor; Nikon). Images were captured with a camera (SPOT RT model 2.3.1; Diagnostic Instruments) and were acquired with SPOT 4.0.9 software (Diagnostic Instruments). Multiple high-power fields (3-5 depending on the size of the skin biopsy section) were counted at each time point. Percentages and absolute numbers of cells at the different time points were compared using Mann-Whitney or one-way ANOVA statistical tests (refer to Supplementary Methods for details) and significance was defined as a p-value $<0.05$.

*Cytokine production in the skin:* 6 μm cryosections were cut, air dried, fixed for 10 min in acetone, rehydrated in TBS/0.1% saponin, and blocked with 20 μg/ml of human IgG (Jackson ImmunoResearch Laboratories) for 15 min at room temperature. Sections were incubated with anti-IL-17 or anti-IFN-γ antibodies (Abcam) for 2 hours, and then washed in TBS/0.1% Saponin for 10 min. Sections were then incubated with Goat Anti-rabbit secondary antibody conjugated to AlexaFluor 488 (AF488) (Life Technologies) for 1 hour at room temperatures. Sections were

washed for 10 min in TBS/0.1% saponin. Sections were then incubated with anti-CD3 directly conjugated to phycoerythrin (PE) for 1 hour at room temperature. Slides were washed again with TBS/0.1% saponin and then mounted using Prolong Gold Antifade with DAPI (Life Technologies) and examined immediately by immunofluorescence microscopy. Sections were photographed using a microscope (Eclipse 6600; Nikon) equipped with a 40x/0.75 objective lens (Plan Fluor; Nikon). Images were captured with a camera (SPOT RT model 2.3.1; Diagnostic Instruments) and were acquired with SPOT 4.0.9 software (Diagnostic Instruments).

Analyses of the photographs were performed in Photoshop Creative Suite 5 using the counting feature. Cells were only counted as positive if there were DAPI+ nuclei in association with either AlexaFluor488 or PE staining. Multiple high-power fields (3-5 depending on the size of the skin biopsy section) were counted at each time point.

Percentages and absolute numbers of cells at the different time points were compared using Mann-Whitney test and significance was defined as a p-value <0.05. Percentage of double positive cells compared to total T cells was compared using a one-way ANOVA analysis followed by a Bonferroni multiple comparison test and significance was defined as a p-value <0.05.

*Intracellular cytokine production*

Before stimulation, thawed PBMC from different time points were cultured overnight in RPMI 10% human AB serum for resting. After that, cells were stimulated with phorbol myristate acetate - PMA (50 ng/ml) and 500 ng/ml of Ionomycin (both from Sigma) for 5 h in the presence

of GolgiStop (BD Biosciences). Cells were stained and analyzed by flow cytometry analysis as described below.

*Flow cytometry analysis*

PBMCs from different time points from the same patient were thawed, stained and processed in the same day to avoid variability. Cells were stained on ice for CD4 (OKT4), CD127 (A019D5), CXCR5 (J252D4), PD-1 (EH12.2H7), CXCR3 (G025H7), CTLA-4 (L3D10), Notch1 (MHN1-519), CD123 (6H6), B220 (RA3-6B2), CD16 (3G8) from Biolegend; CD8 (SK1), CD25 (M-A251), CD197 (3D12), CD45RA (HI100), CCR6 (G034E3), CD11c (B-ly6), HLA-DR (L243) from BD Biosciences; CD14 (RMO52) from Beckman Coulter; CD56 (REA196) from Miltenyi; CD19 (SJ25-C1) from Invitrogen. For intracellular staining of Foxp3 (236A/E7), IFN-γ (4S.B3) and IL-17A (eBio64DEC17) from eBioscience; Ki67 (Ki-67) and IL-4 (8D4-8) from Biolegend, cells were fixed and permeabilized using Foxp3/Transcription Factor Staining Buffer Set (eBioscience), according to manufacturer`s instructions. Stained PBMCs were analyzed on a FACS Canto II flow cytometer (BD Biosciences) with FACSDiva software (BD Biosciences). Data were analyzed with FlowJo software (TreeStar). All the markers combination in order to identify the immune cell types can be found in Supplemental Table 1. Gating strategies can be found in Supplemental Figure 2.

*Peripheral donor-reactivity evaluation by ELISPOT*

Direct and indirect peripheral donor-reactivity was evaluated by ELISPOT as in (13). Briefly, for the evaluation of the direct pathway of allorecognition, we used $10^5$ irradiated cells

from donors as stimulators. For testing the indirect pathway of allorecognition, we used $2x10^6$ donor cell lysates. 96-well plates were coated with anti-IFN-γ antibodies (Thermo Scientific), overnight at 4°C. Then, recipient PBMCs ($3x10^5$) cells were used as responders and cultured for 24h (37°C, 5% $CO_2$) in the presence of stimulators cells/lysates and controls. Positivity was defined as >25 spots/$3x10^5$ responder PBMCs (94, 95). All tests were performed in triplicates with negative (medium) and positive (phytohemagglutinin - PHA) controls. Schematic view of the assay in Supplemental Figure 3A.

*Evaluation of donor-specific antibodies*

Serum samples from face transplant recipients obtained before the transplant were tested for presence of circulating donor-specific anti-HLA-A, -B, -Cw, -DR, -DQ, and -DP antibodies using of single antigen bead based assay (One Lambda) on a Luminex platform. The serum was also analyzed for the presence of C1q-binding donor-specific anti-HLA antibodies with the use of single-antigen flow bead assays according to the manufacturer's protocol (C1qScreenTM, One Lambda).

*Luminex assay*

Serum cytokine and chemokine levels from each transplant patient at different time points were measured using the bead-based Milliplex Human Cytokine/Chemokine Panel (Millipore), according to manufacturer's instructions and including: GM-CSF, GRO, IFN-γ, IL-1β, IL-1ra, IL-2, IL-4, IL-5, IL-6, IL-7, IL-8, IL-9, IL-10, IL-12 (p70), IL-13, IL-15, IL-17, IP-10, MCP-1, MCP-3, MCP-1a, MCP-1b, TNF-α and VEGF. Data were collected with a Luminex 200 system (Luminex Corporation).
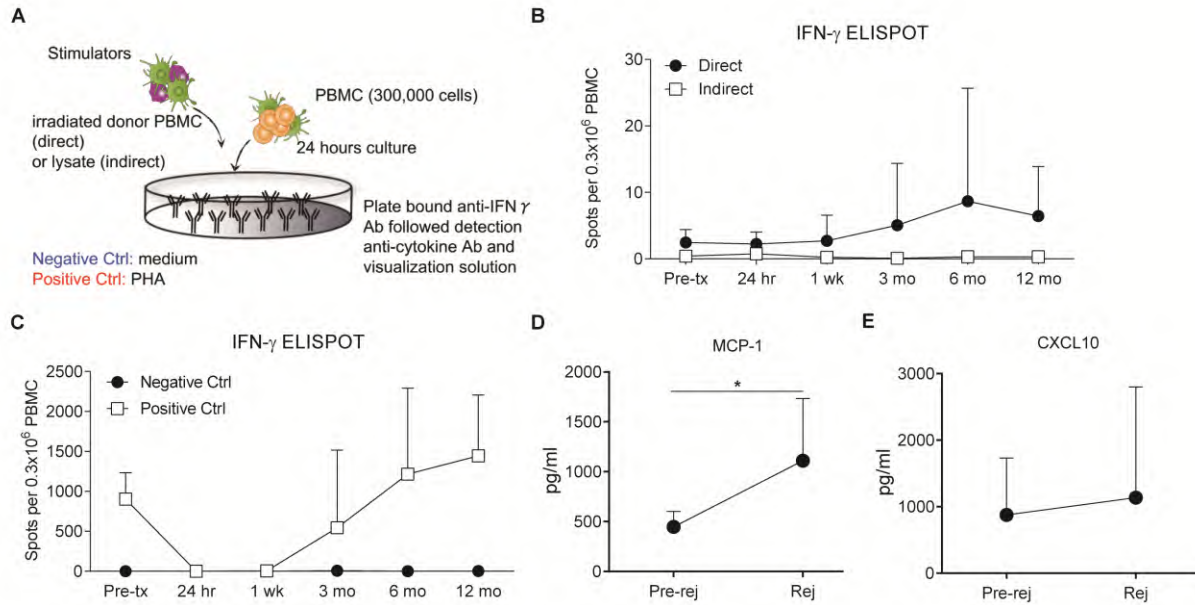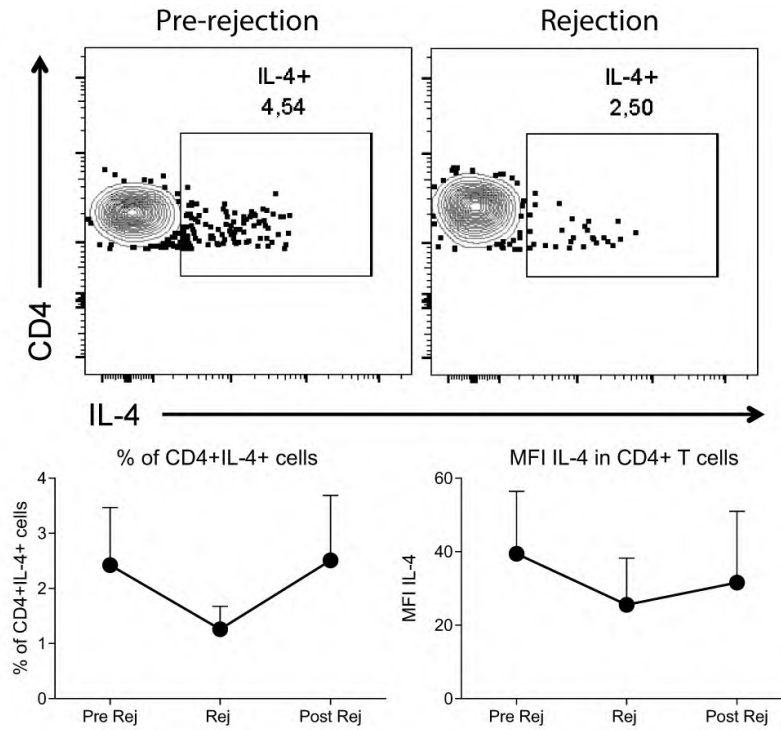
**Supplementary Figures**



**Supplemental Figure 1**. **Photographs of the six patients before transplantation and several months after surgery.** All patients provided written consent for publication of their photographs.
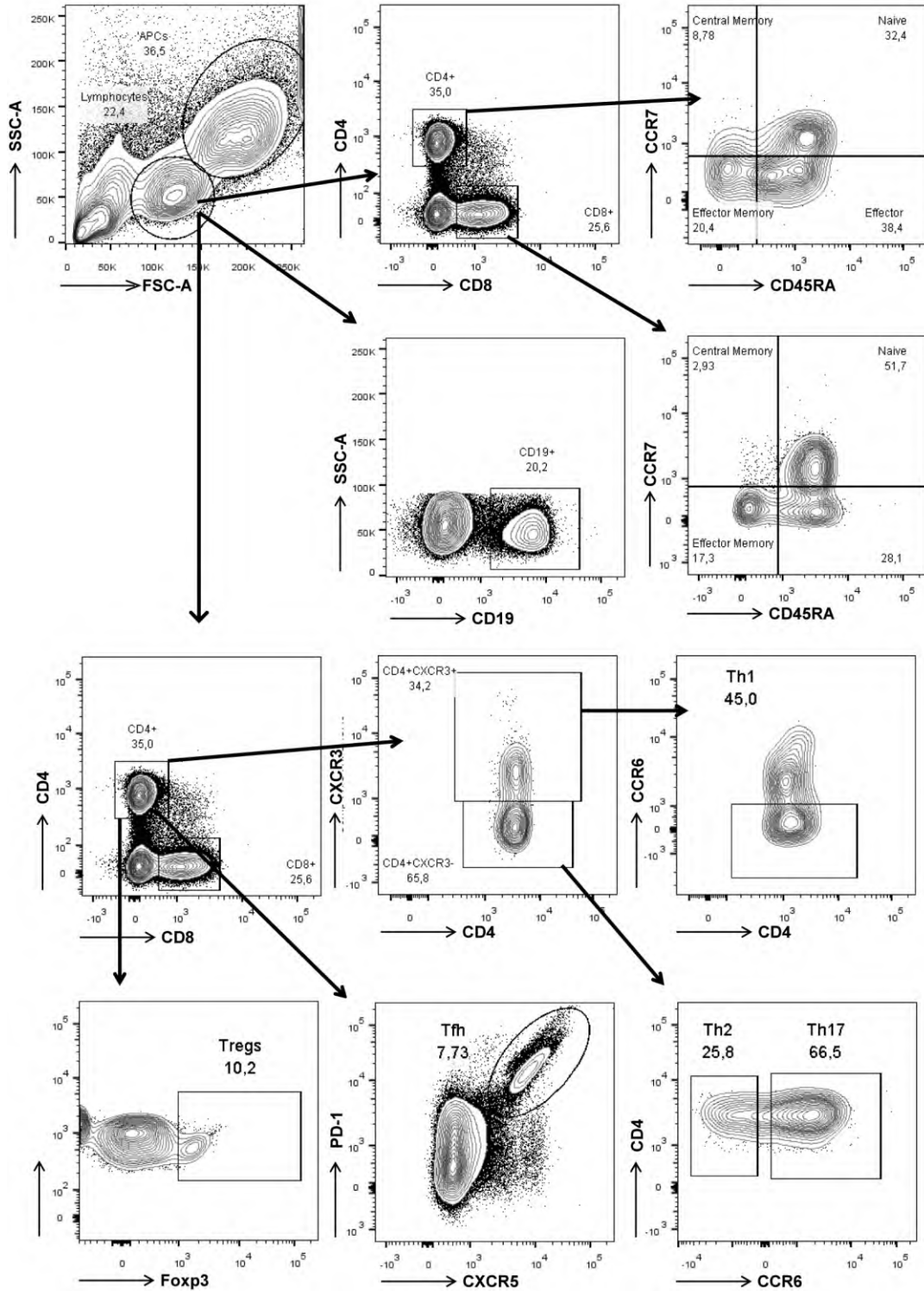
**Supplemental Figure 2. Gating strategy of the cell populations from peripheral blood analyzed in this study.** All samples were analyzed with FlowJo software.

**Supplemental Figure 3. Direct and indirect donor-specific T cell alloreactivity and serum cytokines post-transplant.** (**A**) Recipients' PBMCs were incubated for 24 hours in triplicates with irradiated donor cells or lysate of donor cells to assess direct and indirect alloreactivity, respectively. Negative controls (medium) and positive controls (PHA) were used. For cultures, ELISPOT plates coated with anti-human IFN-γ were employed. Further details on Material and Methods section. (**B**) Frequency of IFN-γ-producing alloreactive T cells after stimulation in vitro with irradiated donor cells or lysate of donor cells. (**C**) Frequency of IFN-γ-producing alloreactive T cells after stimulation in vitro with medium (negative) or PHA (positive control). (**D**) Serum MCP-1 and CXCL10 (**E**) mean concentrations with SD measured by Luminex pre-rejection and during rejection episode. *=$p < 0.05$ (*Mann-Whitney* test).

**Supplemental Figure 4. Cytokine characterization of CD4 and CD8 T cells at rejection episode.** Representative contour plot of IL-4 production in blood CD4+ T cells at pre-rejection and rejection time-points (upper panels). Percentages of circulating CD4+ IL-4+ cells (bottom left graph) and IL-4 MFI in CD4+ T cells (bottom right graph) at pre-rejection, rejection and post-rejection time-points.

## Supplementary Tables

**Supplemental Table 1**. T cell phenotypes analyzed in this study.

| T cells | |
|---|---|
| ***CD4+ T cells*** | $CD4^+CD8^-$ |
| TCM | $CD4^+CD8^-CCR7^+CD45RA^-$ |
| Naïve | $CD4^+CD8^-CCR7^+CD45RA^+$ |
| TEM | $CD4^+CD8^-CCR7^-CD45RA^-$ |
| TEMRA | $CD4^+CD8^-CCR7^-CD45RA^+$ |
| Th1 | $CD4^+CD8^-CXCR3^+CCR6^-$ |
| | $CD4^+CD8^-IFN\text{-}\gamma^+$ |
| | $CD4^+CD8^-IFN\text{-}\gamma^+IL\text{-}17^+$ |
| Th2 | $CD4^+CD8^-CXCR3^-CCR6^-$ |
| | $CD4^+CD8^-IL\text{-}4^+$ |
| Th17 | $CD4^+CD8^-CXCR3^-CCR6^+$ |
| | $CD4^+CD8^-IL\text{-}17^+$ |
| Tfh | $CD4^+CD8^-CXCR5^+PD\text{-}1^+$ |
| Tregs | $CD4^+CD8^-Foxp3^+$ |
| | $CD4^+CD8^-CD25^+CD127^{-/low}$ |
| | $CD4^+CD8^-CD127^-Foxp3^+$ |
| T conv | $CD4^+CD8^-Foxp3^-$ |
| | $CD4^+CD8^-CD25^-CD127^+$ |
| | $CD4^+CD8^-CD127^+Foxp3^-$ |
| | $CD4^+CD8^-CD127^+Foxp3^+$ |
| $PD\text{-}1^+$ | $CD4^+CD8^-PD\text{-}1^+$ |
| | $CD4^+CD8^-CD45RA^+PD\text{-}1^+$ |
| | $CD4^+CD8^-CD45RA^-PD\text{-}1^+$ |
| | $CD4^+CD8^-Foxp3^-PD\text{-}1^+$ |
| | $CD4^+CD8^-Foxp3^+PD\text{-}1^+$ |
| $CTLA\text{-}4^+$ | $CD4^+CD8^-CTLA\text{-}4^+$ |
| | $CD4^+CD8^-CD45RA^+CTLA\text{-}4^+$ |
| | $CD4^+CD8^-CD45RA^-CTLA\text{-}4^+$ |
| | $CD4^+CD8^-Foxp3^-CTLA\text{-}4^+$ |
| | $CD4^+CD8^-Foxp3^+CTLA\text{-}4^+$ |

| | |
|---|---|
| *CD8+ T cells* | CD4$^-$CD8$^+$ |
| TCM | CD4$^-$CD8$^+$CCR7$^+$CD45RA$^-$ |
| Naïve | CD4$^-$CD8$^+$CCR7$^+$CD45RA$^+$ |
| TEM | CD4$^-$CD8$^+$CCR7$^-$CD45RA$^-$ |
| TEMRA | CD4$^-$CD8$^+$CCR7$^-$CD45RA$^+$ |
| IFN-γ$^+$ | CD4$^-$CD8$^+$IFN-γ$^+$ |
| | CD4$^-$CD8$^+$IFN-γ$^+$IL-17$^+$ |
| IL-17$^+$ | CD4$^-$CD8$^+$IL-17$^+$ |
| IL-4$^+$ | CD4$^-$CD8$^+$IL-4$^+$ |
| PD-1$^+$ | CD4$^-$CD8$^+$PD-1$^+$ |
| | CD4$^-$CD8$^+$CD45RA$^+$PD-1$^+$ |
| | CD4$^-$CD8$^+$CD45RA$^-$PD-1$^+$ |
| CTLA-4$^+$ | CD4$^-$CD8$^+$CTLA-4$^+$ |
| | CD4$^-$CD8$^+$CD45RA$^+$CTLA-4$^+$ |
| | CD4$^-$CD8$^+$CD45RA$^-$CTLA-4$^+$ |

## Monocytes and B Cells

**Monocytes**

CD14$^+$

**B Cells**

CD19$^+$

**Supplemental Table 2.** Serum cytokine levels measured by Luminex assay according to rejection or pre-rejection time-points (n=8; *Mann–Whitney* nonparametric test).

| *Cytokine* | *Median Cytokine Levels (25th-75th Percentile) (pg/ml)* | | *P value* |
|---|---|---|---|
| | **Pre-rejection** | **Rejection** | |
| GM-CSF | 8.04 (7.12-9.43) | 0 (0-3.80) | 0.77 |
| GRO | 568 (336.5-688) | 583 (487.5-726.5) | 0.44 |
| IFN-γ | 0 (0-7.96) | 2.52 (0-4.15) | 0.39 |
| IL-1b | 0 (0-0) | 0 (0-1.16) | 0.37 |
| IL-1ra | 9.74 (0-9.74) | 9.6 (9.50-9.71) | 0.28 |
| IL-2 | 0 (0-0) | 0 (0-0) | 0.35 |
| IL-4 | 0 (0-0) | 0 (0-6.01) | 0.31 |
| IL-5 | 0 (0-0) | 0 (0-0) | |
| IL-6 | 0 (0-1.39) | 0 (0-3.45) | 0.89 |
| IL-7 | 0 (0-6.19) | 3.81 (0-8.57) | 0.42 |
| IL-8 | 12.41 (5.96-36.87) | 8.15 (6.2-24.10) | 0.47 |
| IL-9 | 0 (0-2.02) | 0 (0-0.62) | 0.39 |
| IL-10 | 2.61 (0-4.54) | 0 (0-12.43) | 0.85 |
| IL-12(p70) | 0 (0-0) | 0 (0-10.80) | 0.94 |
| IL-13 | 0 (0-0) | (0-5.02) | 0.29 |
| IL-15 | 0 (0-2.54) | 1.05 (0-3.01) | 0.62 |
| IL-17 | 1.8 (0-5.00) | 0 (0-2.53) | 0.23 |
| IP-10(CXCL10) | 582 (258-1532) | 607 (162.5-2376.5) | 0.76 |
| MCP-1 | 387 (329-472) | 951 (748-1381) | **0.01** |
| MCP-3 | 3.13 (1.57-14.82) | 0 (0-32.58) | 0.89 |
| MIP-1a | 7.74 (0-21.26) | 8.14 (1.75-22.09) | 0.88 |
| MIP-1b | 14.22 (10.18-29.85) | 34.21 (28.89-74.7) | 0.15 |
| TNF-α | 8.79 (2.95-11.46) | 5.53 (4.01-12.70) | 0.90 |
| VEGF | 83.03 (10.87-238.5) | 148 (73.70-224.5) | 0.65 |

## Anexo D - Emerging roles for scavenger receptor SREC-I in immunity

**Autores:** Ayesha Murshid, Thiago J. Borges, Stuart K. Calderwood

**Situação:** Publicado

**Revista:** *Cytokine*

**Referência:** Cytokine. 2015 Oct;75(2):256-60. doi: 10.1016/j.cyto.2015.02.009.

**Website:** http://www.sciencedirect.com/science/article/pii/S104346661500068X

**Motivação:** Esse trabalho foi realizado durante o período sanduíche realizado no Hospital Beth Israel Deaconess Medical Center, no laboratório do Prof. Stuart K. Calderwood.

# Emerging roles for scavenger receptor SREC-I in immunity

CrossMark
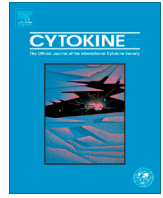
Ayesha Murshid [a], Thiago J. Borges [a,b], Stuart K. Calderwood [a,*]

[a] Department of Radiation Oncology, Beth Israel Deaconess Medical Center, Harvard Medical School, Boston, MA 02115, United States
[b] School of Biosciences and Biomedical Research Institute, Pontifícia Universidade Católica do Rio Grande do Sul (PUCRS), Porto Alegre, RS, Brazil

## ARTICLE INFO

## ABSTRACT

SREC-I is a class F scavenger receptor with key role in the immune response, particularly in antigen presenting cell (APC) such as macrophages and dendritic cells (DC). This receptor is able to mediate engulfment of dead cells as well as endocytosis of heat shock protein (HSP)–antigen complexes. SREC-I could thus potentially mediate the tolerizing influence of apoptotic cells or the immunostimulatory effects of HSP–peptide complexes, depending on context. This receptor was able to mediate presentation of external antigens, bound to HSPs through both the class II pathway as well as cross presentation via MHC class I complexes. In addition to its recently established role in adaptive immunity, emerging studies are indicating a broad role in innate immunity and regulation of cell signaling through Toll Like Receptors (TLR). SREC-I may thus play a key role in APC function by coordinating immune responses to internal and external antigens in APC.

## 1. Introduction

Scavenger receptors are a family of receptors that have in common the ability to bind to covalently modified proteins, most notably oxidized low density lipoprotein (oxidized LDL). The scavenging of oxidized LDL by endothelial cells plays a significant role in sparing organisms from pathologies such as atherosclerosis [1]. Interestingly the scavenger receptor family is grouped along functional lines and most such proteins have little sequence similarity [2,10]. One mystery associated with this protein family is that, although there is minimal homology in primary structures among scavenger receptor families, they can associate with a similar and equally diverse group of ligands [1,3]. SREC-I (Scavenger Receptor expressed by Endothelial cells), a member of the class F scavenger receptor family, 85.7 kD protein was first cloned from HUVEC (Human Umbilical Vein Endothelial Cells) cells and termed as scavenger receptor expressed by endothelial cells [2,26,31]. The primary structure of this scavenger receptor had minimal similarity with those of most other scavenger receptors previously characterized, although SREC-II which is a member of this same family was shown to have some common features in terms of the extracellular domains [12,26]. The extracellular domain of SREC is also similar to that of Feel-1 [22]. The extended extracellular domain (ED) of the class F receptors is comprised of epidermal growth factor like cysteine rich motifs (EGF repeats) while the unusually long intracellular domain contains a serine–proline rich region [25]. SREC-1, particularly in the ED, has significant homology with the *Caenorhabditis elegans* protein CED-1, a polypeptide involved in the uptake of apoptotic bodies [27]. Additional cell corpse engulfing proteins such as MEGF10, MEGF11 and MEGF12 are also CED-1 paralogs and, like SREC-I contain multiple EGF repeats within the ED [20,27]. Like other scavenger receptors the class F family are defined by their ability to bind, internalize and metabolize modified LDL species, such as acetylated (Ac) LDL, oxidized (Ox) LDL, a process involved in the pathogenesis of atherosclerosis [15,25,28]. It was also characterized as an endocytic receptor for calreticulin [4]. In addition to their roles in binding and internalizing these modified lipids, SREC-I was also shown to participate in other cellular functions such as cell–cell adhesion, antigen cross presentation, engulfment of apoptotic cells and innate immunity. The cell adhesion properties may involve SREC-I interaction with SREC-II counter-receptors on the partner cell [26]. SREC-I can also cooperate with pattern recognition receptor function in innate immunity (see below). This receptor has an additional role in mediating morphological changes when overexpressed in a fibroblasts suggesting its participation in morphogenesis of cells (A. Murshid, unpublished studies). The intracellular domain of SREC-1, which is extensive compared with that of other scavenger receptors, is largely uncharacterized. However, it has been shown that this cytosolic domain is capable of interacting with protein phosphatase 1α (PP1 α) in L cells and thus mediating morphological changes [13].

* Corresponding author at: Beth Israel Deaconess Cancer Center, 3 Blackfan Circle, Boston, MA 02115, USA. Tel.: +1 617 735 2947; fax: +1 617 735 2845.
E-mail address: scalderw@bidmc.harvard.edu (S.K. Calderwood).

## 2. SREC-I and antigen cross presentation

SREC-I has been shown to be a key receptor for heat shock proteins [8,29]. The physiological significance of extracellular HSPs is not entirely clear, although they are known to play key roles in the immune response [7]. HSPs can be immunostimulatory when associated with tumor antigens, transporting the chaperoned antigens into AP. In contrast, in different contexts, HSPs can play immunoregulatory roles and suppress T cell mediated immunity in inflammatory diseases [5,24]. We have attempted to discover physiologically relevant HSP receptors. We carried out forced expression of candidate receptors in a cell line, CHO that is null for HSP binding then assayed binding of fluorescently labeled Hsp70 or Hsp90 to those receptors expressing cell. Hsp70 was found to bind Class E receptor Lox-1, Class F receptor SREC-I and Class H receptor Feel-1/stabilin-1 [29]. In addition, Hsp70 was found to bind to some NK receptors found on the surface of natural killer cells [29]. As most of our studies have centered on SREC-I we will discuss this receptor in more detail in this review. SREC-I, in common with another scavenger receptor, LOX-I can bind with high avidity to HSPs, including Hsp70, Hsp90, Grp94, Hsp110 and Grp170 with or without associated antigens and appears to be an important common receptor for these proteins [3,19,21]. In addition, among all the scavenger receptors that have been characterized so far, we found that SREC-I and LOX-1 each appeared to mediate the majority of the cross presentation of the Ova SIINFEKL epitope chaperoned by Hsp90 or Hsp70 in BMDC [21].

Earlier it was demonstrated that HSP–antigen complexes could be bound to SREC-I and internalized in antigen presenting cells such as dendritic cells (DC) and macrophages (as well as a large variety of tissue culture cell lines [21]). An Hsp90–antigen–SREC-I internalization pathway was characterized in these cell types which was similar to a previously described mechanism involving *tubule like vesicles formation upon uptake of ligand–receptor complex* and known as CLIC (**C**lathrin **i**ndependent **c**arriers) or GEEC (**G**PI anchored protein-**e**nriched **e**ndocytic **c**ompartments) [9,10]. This pathway is distinct from endocytic mechanisms involving Clathrin and is heavily utilized by GPI-anchored proteins [32]. Although the significance of entry of HSP–SREC-I complexes through the CLIC/GEEC pathway is not entirely clear, this mechanism does appear to permit regulation of antigen cross presentation by signal transducing molecules as discussed below. Hsp90–polypeptide–SREC-I complexes were able to mediate cross presentation of external chaperoned antigens, mediating processing in both endosomal and proteasomal compartments.

It is not clear to what degree the antigen presentation pathways involved with HSP-chaperoned antigens are similar to those used by other forms of antigens. For free, unchaperoned antigens, dedicated receptors have been shown to direct antigens to either the MHC class II pathway or to cross-presentation via the MHC class I complexes [6,11]. We have demonstrated that antigens bound to Hsp90 could be internalized via SREC-I and later processed. Internalized antigens could be loaded onto either MHC class I (cross presentation) or MHC class II molecules (class II presentation). It is not known whether the scavenger receptor mediates triage between the two MHC pathways or whether the choice of pathways is stochastic. Antigen presentation then led to specific activation of both CD8+ and CD4+ T cells. In these parallel MHCI and MHCII antigen presentation pathways, SREC-I engagement by Hsp90-bound antigens increased Cdc42 GTPase activity, regulating actin assembly and polymerization and other signaling pathways such as Src kinase signaling [33,41].

Receptor mediated internalization of Hsp90 bound antigens rather than non-specific internalization of free antigens has two potential advantages. Such HSP chaperoned antigens can be protected from proteolysis during trafficking through the cell compartments and thus reduced amount of antigen would be required to initiate both CD4+ and CD8+ T cell priming [23]. It is however clear that we understand chaperone mediated antigen cross priming only in outline so far and that considerable further investigations are required in order to understand the basic mechanisms involved. SREC-I thus plays a key role in receptor-mediated uptake of chaperone-bound antigen presentation, protecting and transporting its charges to the key intracellular sites.

## 3. Role of SREC-I in apoptotic cells engulfment

The elimination of defective and unwanted cells by apoptosis is an essential process for maintenance of tissue homeostasis as well as contributing to tumor regression in cytotoxic therapies. A rapid and immunologically clean removal of these apoptotic cells is crucial for evading inflammation, immune tolerance and homeostasis [34]. Phagocytic cells recognize and engulf these dying cells through several surface receptors expressed by these cells or by the interaction of bridging soluble proteins that recognize "find-me" and "eat-me" signals presented in apoptotic cells, as lipid lysophosphatidylcholine (LPC) and phosphatidylserine (PS) [35].

The first suggestion that SREC-I could participate in the recognition and engulfment of apoptotic cells was when the transmembrane protein CED-1 from *C. elegans* was identified as an ortholog of human SREC-I. CED-1 was reported to be responsible for the recognition and internalization of apoptotic cells by *C. elegans*. This receptor has a sequence similarity and shares a similar overall structure with SREC-I [36]. Using GFP under control of *ced-1* promoter, it was demonstrated that CED-1 is expressed at high levels in cells that can act as endocytic cells along the surface of cell corpses but not in the dying cell. Mutations in the *ced-1* gene that cause loss of protein function resulted in a phenotype characterized by cell corpse retention, indicating that CED-1 is required for identification and engulfment of apoptotic cells in *C. elegans* [36].

More recently it was demonstrated that DC, macrophages and endothelial cells expressing SREC-I could bind phosphatidyl serine moieties exposed on the apoptotic cell surface [37]. Additionally, the same group demonstrated that CD8α+ DCs expressing higher levels of SREC-I were more capable of engulfing dying cells or apoptotic cells than those of SREC-I−/− mice. Forced expression of SREC-I in these SREC-I−/− DCs reversed the phenotypes and enhanced uptake of dying cells. These findings indicated a role of SREC-I in apoptotic cell engulfment and removing dying cells. Additionally these knock-out mice had a spontaneous lupus-like disease, with the presence of autoantibodies, indicating that impairment in the SREC-I-mediated clearance of apoptotic cells contributes to development of this autoimmune disorder [37].

## 4. Signaling through SREC-I

In addition to internalizing HSP-bound peptides, ligand-bound SRECI appears to play a significant role in cell signaling. These signaling properties appear to be related to the appearance of SREC-I in lipid rafts after binding ligands such as Hsp90 [21]. Lipid rafts are cholesterol and sphingolipid-rich membrane microdomains, floating in the bulk membrane, that can concentrate molecules involved in cell signaling [18]. Although lacking the glycerphophoinositide anchor domain motifs found in many raft-associated membrane proteins, SREC-I contains other motifs that would permit it to associate with lipid rafts [22]. The S-acylation of cysteine residues close to the transmembrane domain, with highly saturated palmitate residues, that can dissolve in the environment of the lipid raft has been associated with the ability of cells without
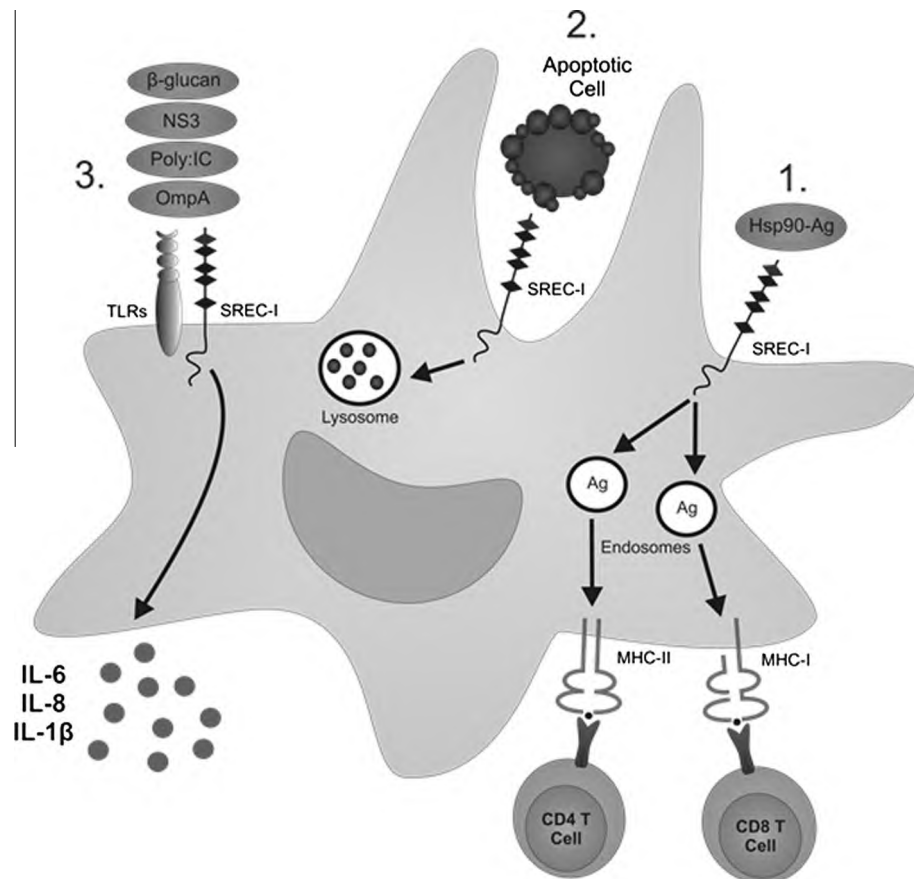
**Fig. 1.** Different roles of SREC-I in immunity and dead cell removal. 1. Antigen presentation: Hsp–Ag interacts with SREC-I on antigen presenting cells and thus becomes internalized by these cells. Cells then process the antigens and processed antigens can be loaded to either MHC-I or MHC-II molecules to activate adaptive immunity. 2. Apoptotic cell engulfment. SREC-I binds to apoptotic cells through phosphatidylserine moiety exposed on apoptotic cells and can thus engulf them. Apoptotic bodies are then internalized and processed in the lysosome. 3. Pathogens are recognized by both TLRs and SREC-I. This is accompanied by internalization of pathogens, activation of signaling and transcription and release of cytokines.

GPI anchor domains to enter lipid rafts [16–18]. SREC-I has five cysteine residues immediately adjacent to the transmembrane domain, making this a likely mechanism for the entry of SREC-I into lipid rafts. Although SREC-I activities, such as ability of ligand-binding and localization in the cell, has been shown to be regulated by glycosylation of specific sites of this receptor, it is not clear how ligand binding localizes SREC-I to lipid microdomains of plasma membrane. The N-glycan of Asparagine $N^{382}$ of SREC-I modulates the affinity to its ligand, whereas $N^{393}$ is responsible for its cellular localization [42].

We have demonstrated that Hsp90–SRECI complexes, but not unliganded SREC-I, could associate with the small GTPase Cdc42 and non-receptor tyrosine kinase Src, molecules tightly associated with lipid rafts [21]. Cdc42 and Src activity appeared to be important in regulating antigen cross presentation of Hsp90-associated antigens in DC.

Lipid micro domains such as rafts also concentrate intermediates in the TLR4 signaling pathway in response to innate immune stimuli [30]. We have found that SREC-I causes TLR4 to translocate to lipid microdomain in the presence of LPS (A. Murshid & SK Calderwood, in preparation). Our preliminary studies also showed significant co-localization of SREC-I ligand Hsp90 along with SREC-I and TLR4 in similar lipid raft domains (A. Murshid & SK Calderwood, in preparation). HSP-triggered signaling through SRECI may thus be involved both in amplifying antigen cross presentation and in stimulating innate immunity. It may be significant that the other major HSP-binding scavenger receptor associated with antigen cross presentation, LOX-1, although bearing no

sequence similarity compared with SRECI appeared to associate with TLRs on ligand binding and mediate immune responses in a similar way to SREC-I [14].

## 5. SREC-I, a potent receptor for inflammatory ligands

SREC-I can initiate immunological responses upon interacting with and binding to ligands such as peptide-bearing HSPs. This ligand–receptor interaction had distinct outcomes. In HSP–Ag uptake through SREC-I, binding could activate Src signaling which appeared to initiate internalization of the HSP–peptide–SREC-I complex to endocytic vesicles [21].

SREC-I has been shown to recognize modified self-ligands, such as acetylated LDL but also non-self molecules present in invading pathogens [25,27]. This feature indicated SREC-I as an important receptor for recognition of danger signals and the maintenance of tissue homeostasis as well as the control of infection. SREC-I was reported to trigger inflammatory signaling through the crosstalk with co-receptors, as TLR family members. The outer membrane protein A (OmpA) from *Klebsiella pneumoniae* was shown to be a ligand for SREC-I and LOX-1. In DCs and macrophages, exposure to OmpA induced the production of pro-inflammatory cytokines and chemokines, as IL-6 and IL-8 in a TLR2-dependent manner, suggesting a cooperative pathway between SREC-I/LOX-1 and TLR2 [38]. SREC-I also bound to the fungal pathogens *Cryptococcus neoformans* and *Candida albicans*, through the recognition of β-glucan residues exposed on the cell surface of these organisms. This scavenger

receptor in cooperation with TLR2 triggered the production of IL-1β, CXCL2 and CXCL1 upon exposure to *C. neoformans* [39]. SREC-I expressed by DCs was also demonstrated to bind to non-structural protein 3 (NS3) of the hepatitis C virus, leading to IL-6 production by these cells, in crosstalk with TLR2. Endocytosis of NS3 was required to NS3-induced IL-6 production, underlying the importance of SREC-I as a scavenger receptor in the control of infections [40].

Recently, TLR3 and TLR4 were also shown to cooperate with SREC-I in ligand mediated signaling and cytokine production [41]. SREC-I was demonstrated to enhance poly:IC-mediated TLR3 activation and downstream signaling (A. Murshid and SK Calderwood in preparation). TLR3 and SREC-I were shown to colocalize after poly:IC treatment and the formation of TLR3–SREC-I complexes increased IL-8 production by THP-1 macroophage/monocyte cells. Also, it was demonstrated that poly:IC-induced SREC-I–TLR3 interaction led to amplified NF-κB pathway activity and an increase in activated, phosphorylated forms of the MAP kinases p38 and c-jun kinase (JNK). MAPK activation was required for IL-8 and IL-6 production by THP-1 cells expressing both SREC-I and TLR3, upon poly:IC stimulation (A. Murshid and SK Calderwood in preparation). We also demonstrated that pathways downstream of LPS-TLR4 such as MAPK and NfkB were activated in cells expressing SREC-I (A. Murshid and SK Calderwood, in preparation).

## 6. Concluding remarks

Developing studies indicate a broad role for SREC-I in many areas of cell physiology with important functions in vascular endothelium, fibroblasts and immune cells. In immune cells, this receptor appears to play roles in both innate and adaptive immunity (Fig. 1). Its scavenger function also permits SREC-I to function in engulfment of dead cells as well as internalization of extracellular HSPs. It may thus be involved in immune tolerance when apoptotic cells are engulfed or by contrast in T cell stimulation when HSP–peptide complexes are internalized and chaperone antigens are presented by MHC classes I and II complexes. SREC-I is thus an important receptor in APC such as macrophages and DC (Fig. 1). SREC-I may also be a key component of innate immunity and may recognize molecules involved in sterile inflammation such as HSPs as well as PAMPS such as LPS and TLR3 ligands. The receptor may thus coordinate immune responses to internal and external antigens in DC.

## Acknowledgements

## References

[1] Goldstein JL, Ho YK, Basu SK, Brown MS. Binding site on macrophages that mediates uptake and degradation of acetylated low density lipoprotein, producing massive cholesterol deposition. Proc Natl Acad Sci USA 1979;76:333–7.

[2] Adachi H, Tsujimoto M. Structure and function of a novel scavenger receptor expressed in human endothelial cells. Tanpakushitsu Kakusan Koso Protein, Nucleic Acid, Enzyme 1999;44:1282–6.

[3] Greaves DR, Gough PJ, Gordon S. Recent progress in defining the role of scavenger receptors in lipid transport, atherosclerosis and host defence. Curr Opin Lipidol 1998;9:425–32.

[4] Berwin B, Delneste Y, Lovingood RV, Post SR, Pizzo SV. SREC-I, a type F scavenger receptor, is an endocytic receptor for calreticulin. J Biol Chem 2004;279:51250–7.

[5] Borges TJ, Lopes RL, Pinho NG, Machado FD, Souza AP, Bonorino C. Extracellular Hsp70 inhibits pro-inflammatory cytokine production by IL-10 driven down-

regulation of C/EBPbeta and C/EBPdelta. Int J Hypertherm: Official J Eur Soc Hypertherm Oncol, North Am Hypertherm Group 2013;29:455–63.

[6] Burgdorf S, Schuette V, Semmling V, Hochheiser K, Lukacs-Kornek V, Knolle PA, et al. Steady-state cross-presentation of OVA is mannose receptor-dependent but inhibitable by collagen fragments. Proc Natl Acad Sci USA 2010;107:E48–9 [author reply E50-41].

[7] Calderwood SK, Mambula SS, Gray Jr PJ, Theriault JR. Extracellular heat shock proteins in cell signaling. FEBS Lett 2007;581:3689–94.

[8] Calderwood SK, Theriault J, Gray PJ, Gong J. Cell surface receptors for molecular chaperones. Methods 2007;43:199–206.

[9] Doherty GJ, McMahon HT. Mechanisms of endocytosis. Annu Rev Biochem 2009;78:857–902.

[10] Gupta GD, Swetha MG, Kumari S, Lakshminarayan R, Dey G, Mayor S. Analysis of endocytic pathways in drosophila cells reveals a conserved role for GBF1 in internalization via GEECs. PLoS ONE 2009;4:e6768.

[11] Inaba K, Inaba M. Antigen recognition and presentation by dendritic cells. Int J Hematol 2005;81:181–7.

[12] Ishii J, Adachi H, Aoki J, Koizumi H, Tomita S, Suzuki T, et al. SREC-II, a new member of the scavenger receptor type F family, trans-interacts with SREC-I through its extracellular domain. J Biol Chem 2002;277:39696–702.

[13] Ishii J, Adachi H, Shibata N, Arai T, Tsujimoto M. Scavenger receptor expressed by endothelial cells (SREC)-I interacts with protein phosphatase 1alpha in L cells to induce neurite-like outgrowth. Biochem Biophys Res Commun 2007;360:269–74.

[14] Jeannin P, Bottazzi B, Sironi M, Doni A, Rusnati M, Presta M, et al. Complexity and complementarity of outer membrane protein A recognition by cellular and humoral innate immunity receptors. Immunity 2005;22:551–60.

[15] Krieger M. The other side of scavenger receptors: pattern recognition for host defense. Curr Opin Lipidol 1997;8:275–80.

[16] Levental I, Grzybek M, Simons K. Greasing their way: lipid modifications determine protein association with membrane rafts. Biochemistry 2010;49:6305–16.

[17] Levental I, Lingwood D, Grzybek M, Coskun U, Simons K. Palmitoylation regulates raft affinity for the majority of integral raft proteins. Proc Natl Acad Sci USA 2010;107:22050–4.

[18] Lingwood D, Kaiser HJ, Levental I, Simons K. Lipid rafts as functional heterogeneity in cell membranes. Biochem Soc Trans 2009;37:955–60.

[19] Manjili MH, Henderson R, Wang XY, Chen X, Li Y, Repasky E, et al. Development of a recombinant HSP110-HER-2/neu vaccine using the chaperoning properties of HSP110. Cancer Res 2002;62:1737–42.

[20] McPhee CK, Baehrecke EH. The engulfment receptor Draper is required for autophagy during cell death. Autophagy 2010;6:1192–3.

[21] Murshid A, Gong J, Calderwood SK. Heat shock protein 90 mediates efficient antigen cross presentation through the scavenger receptor expressed by endothelial cells-I. J Immunol 2010;2010(185):2903–17.

[22] Murshid A, Gong J, Calderwood SK. Molecular chaperone receptors: binding and trafficking of molecular chaperones by class F and class G scavenger receptors. In: Henderson B, Pockley AG (Eds.). Cellular trafficking of molecular chaperones in health and disease; 2011.

[23] Murshid A, Gong J, Calderwood SK. The role of heat shock proteins in antigen cross presentation. Front Immunol 2012;3:63.

[24] Oura J, Tamura Y, Kamiguchi K, Kutomi G, Sahara H, Torigoe T, et al. Extracellular heat shock protein 90 plays a role in translocating chaperoned antigen from endosome to proteasome for generating antigenic peptide to be cross-presented by dendritic cells. Int Immunol 2011;23:223–37.

[25] Pluddemann A, Neyen C, Gordon S. Macrophage scavenger receptors and host-derived ligands. Methods 2007;43:207–17.

[26] Zanin-Zhorov Alexandra, Cahalon Liora, Tal Guy, Margalit Raanan, Lider Ofer, Cohen Irun R. Heat shock protein 60 enhances CD4+ CD25+ regulatory T cell function via innate TLR2 signaling. J Clin Invest 2006;116(7):2022–32. http://dx.doi.org/10.1172/JCI28423.

[27] Suzuki E, Nakayama M. The mammalian Ced-1 ortholog MEGF10/KIAA1780 displays a novel adhesion pattern. Exp Cell Res 2007;313:2451–64.

[28] Tamura Y, Osuga J, Adachi H, Tozawa R, Takanezawa Y, Ohashi K, et al. Scavenger receptor expressed by endothelial cells I (SREC-I) mediates the uptake of acetylated low density lipoproteins by macrophages stimulated with lipopolysaccharide. J Biol Chem 2004;279:30938–44.

[29] Theriault JR, Adachi H, Calderwood SK. Role of scavenger receptors in the binding and internalization of heat shock protein 70. J Immunol 2006;177:8604–11.

[30] Triantafilou M, Miyake K, Golenbock DT, Triantafilou K. Mediators of innate immune recognition of bacteria concentrate in lipid rafts and facilitate lipopolysaccharide-induced cell activation. J Cell Sci 2002;115:2603–11.

[31] Adachi H, Tsujimoto M, Arai H, Inoue K. Expression cloning of a novel scavenger receptor from human endothelial cells. J Biol Chem 1997;272:30220–1217.

[32] Mayor S, Sabharanjak S, Maxfield FR. Cholesterol-dependent retention of GPI-anchored proteins in endosomes. EMBO J 1998;17:4626–38.

[33] Murshid A, Gong J, Calderwood SK. Hsp90–peptide complexes stimulate antigen presentation through the class II pathway after binding scavenger receptor SREC-I. Immunobiology 2014. http://dx.doi.org/10.1016/j.imbio.2014.08.001 [pii: S0171-2985(14)00135-1].

[34] Elliott MR, Ravichandran KS. Clearance of apoptotic cells: implications in health and disease. J Cell Biol 2010;189:1059–70. http://dx.doi.org/10.1083/jcb.201004096.

[35] Ravichandran KS, Lorenz U. Engulfment of apoptotic cells: signals for a good meal. Nat Rev Immunol 2007;7:964–74.

[36] Zhou Z, Hartwieg E, Horvitz HR. CED-1 is a transmembrane receptor that mediates cell corpse engulfment in C. elegans. Cell 2001;104:43–56.

[37] Ramirez-Ortiz ZG, Pendergraft 3rd WF, Prasad A, Byrne MH, Iram T, Blanchette CJ, et al. The scavenger receptor SCARF1 mediates the clearance of apoptotic cells and prevents autoimmunity. Nat Immunol 2013;14:917–26. http://dx.doi.org/10.1038/ni.2670.

[38] Jeannin P, Bottazzi B, Sironi M, Doni A, Rusnati M, Presta M, et al. Complexity and complementarity of outer membrane protein A recognition by cellular and humoral innate immunity receptors. Immunity 2005;22:551–60.

[39] Means TK, Mylonakis E, Tampakakis E, Colvin RA, Seung E, Puckett L, et al. Evolutionarily conserved recognition and innate immunity to fungal pathogens by the scavenger receptors SCARF1 and CD36. J Exp Med 2009;206:637–53. http://dx.doi.org/10.1084/jem.20082109.

[40] Beauvillain C, Meloni F, Sirard JC, Blanchard S, Jarry U, Scotet M, et al. The scavenger receptors SRA-1 and SREC-I cooperate with TLR2 in the recognition of the hepatitis C virus non-structural protein 3 by dendritic cells. J Hepatol 2010;52:644–51. http://dx.doi.org/10.1016/j.jhep.2009.11.031.

[41] Murshid A, Gong J, Calderwood SK. Hsp90–peptide complexes stimulate antigen presentation through the class II pathway after binding scavenger receptor SREC-I. Immunobiology 2014. http://dx.doi.org/10.1016/j.imbio.2014.08.001 [pii: S0171-2985(14)00135-1. Epub ahead of print].

[42] Sano M, Korekane H, Ohtsubo K, Yamaguchi Y, Kato M, Shibukawa Y, et al. N-glycans of SREC-I (scavenger receptor expressed by endothelial cells): essential role for ligand binding, trafficking and stability. Glycobiology 2012;22(5):714–24. http://dx.doi.org/10.1093/glycob/cws010 [Epub 2012 Jan 25].

**Autores:** Kassem Safa, Shunsuke Ohori, Thiago J. Borges, Mayuko Uehara, Ibrahim Batal, Tetsunosuke Shimizu, Ciara N. Magee, Roger Belizaire, Reza Abdi, Chuan Wu, Anil Chandraker, Leonardo V. Riella

**Situação:** Publicado

**Revista:** *Journal of the American Society of Nephrology (JASN)*

**Referência:** J Am Soc Nephrol. 2015 Oct;26(10):2341-7. doi: 10.1681/ASN.2014090914.

**Website:** http://jasn.asnjournals.org/content/26/10/2341.long

**Motivação:** Esse trabalho foi realizado durante o período sanduiche realizado no Hospital Brigham and Women's, no laboratório do Prof. Leonardo Riella.

# Salt Accelerates Allograft Rejection through Serum- and Glucocorticoid-Regulated Kinase-1–Dependent Inhibition of Regulatory T Cells

Kassem Safa,*[†] Shunsuke Ohori,* Thiago J. Borges,*[‡] Mayuko Uehara,* Ibrahim Batal,[§] Tetsunosuke Shimizu,* Ciara N. Magee,*[‖] Roger Belizaire,[§] Reza Abdi,* Chuan Wu,[¶] Anil Chandraker,* and Leonardo V. Riella*

*Schuster Family Transplantation Research Center, Renal Division, Brigham and Women's Hospital, Harvard Medical School, Boston, Massachusetts; [†]Transplant Center and Division of Nephrology, Massachusetts General Hospital, Harvard Medical School, Boston, Massachusetts; [‡]School of Biosciences and Biomedical Research Institute, Pontifical Catholic University of Rio Grande do Sul, Porto Alegre, Rio Grande do Sul, Brazil; [§]Department of Pathology, Brigham and Women's Hospital, Boston, Massachusetts; [‖]Department of Renal Medicine and Transplantation, Royal Free London, National Health Service Foundation Trust, London, United Kingdom; and [¶]Center for Neurologic Diseases, Brigham and Women's Hospital, Harvard Medical School, Boston, Massachusetts

## ABSTRACT

A high-salt diet (HSD) in humans is linked to a number of complications, including hypertension and cardiovascular events. Whether a HSD affects the immune response in transplantation is unknown. Using a murine transplantation model, we investigated the effect of NaCl on the alloimmune response *in vitro* and *in vivo*. Incremental NaCl concentrations *in vitro* augmented T cell proliferation in the settings of both polyclonal and allospecific stimulation. Feeding a HSD to C57BL/6 wild-type recipients of bm12 allografts led to accelerated cardiac allograft rejection, despite similar mean BP and serum sodium levels in HSD and normal salt diet (NSD) groups. The accelerated rejection was associated with a reduction in the proportion of CD4$^+$Foxp3$^+$ regulatory T cells (Tregs) and a significant decrease in Treg proliferation, leading to an increased ratio of antigen-experienced CD4$^+$ T cells to Tregs in mice recipients of a HSD compared with mice recipients of a NSD. Because serum- and glucocorticoid-regulated kinase-1 (SGK1) has been proposed as a potential target of salt in immune cells, we fed a HSD to CD4$^{Cre}$SGK1$^{fl/fl}$ B6-transplanted recipients and observed abrogation of the deleterious effect of a HSD in the absence of SGK1 on CD4$^+$ cells. In summary, we show that NaCl negatively affects the regulatory balance of T cells in transplantation and precipitates rejection in an SGK1-dependent manner.

The discovery of salt is considered a fundamental milestone for humanity; throughout history, salt extraction, possession, and intake were a reflection of the prosperity and wealth of a nation. Virtual absence of dietary salt, as seen in the Yanomami tribes living in the Amazon rainforests, is associated with zero incidence of hypertension,[1] whereas a typical Western salt-rich diet has long been associated with hypertension and consequent cardiovascular morbidities.[2] Surprisingly, however, it has recently been shown that salt intake also affects the immune system: using a murine experimental autoimmune encephalomyelitis (EAE) model, mice fed a high-salt diet (HSD) had exacerbated disease mediated by the induction of pathogenic T$_H$17 T cells.[3–5] Furthermore, HSD has also been shown to promote lymph capillary network hyperplasia and increased skin infiltration by mononuclear phagocytic cells in mice and rats.[6,7]

In transplantation, advances in immunologic screening combined with developments in immunosuppression achieved in the last several decades have resulted in significant improvements in early graft survival; the rates of late allograft loss, however, remain unacceptably high.[8] There have been only isolated reports examining the correlation of salt intake with hypertension after transplantation,[9,10] whereas there are no reports of the potential contribution of salt intake to the incidence of rejection and allograft survival. It is, therefore, unknown whether dietary salt consumption could affect the

alloimmune response and long-term allo-graft survival. In this report, we sought to examine the effect of salt on alloimmunity. We report, for the first time, that salt augments *in vitro* allospecific T cell proliferation, whereas in a mouse model of solid organ transplantation, feeding mice an HSD results in accelerated allograft rejection caused by disturbance of the regulatory balance of T cells *in vivo*.

We first examined the effect of higher salt concentration ([NaCl]) on T cell proliferation *in vitro* using cultures of naive murine splenocytes incubated in medium enriched with incremental concentrations of NaCl (ranging from 0 to 40 mM) in the presence of aCD3 and aCD28 (2 $\mu$g/ml) (Figure 1A). We observed that increasing [NaCl] from 0 to 40 mM resulted in a significant increase in proliferation, which was measured by thymidine incorporation, from 23,674$\pm$2063 to 49,801$\pm$2423 counts per minute ($P<0.001$). To further investigate this observation in an alloimmune milieu (Figure 1B), we primed reporter C57Bl/6 Foxp3.GFP mice (B6 wild type [WT]) *a priori* with intraperitoneal injections of BALB/c splenocytes; 2 weeks later, we isolated sensitized CD4$^+$Foxp3$^-$ cells from these mice and cultured them with irradiated BALB/c CD3$^-$ splenocytes in the presence of incremental [NaCl]. Indeed, increasing [NaCl] from 0 to 40 mM again resulted in a significant increase in T cell proliferation from 7355$\pm$565.5 to 18,588$\pm$1635 counts per minute ($P=0.004$). This increase in proliferation was specific to NaCl. Adding urea to culture medium at 80 mM concentration resulted in decreased cell proliferation compared with standard medium as measured by CFSE-negative populations (77.1%$\pm$0.3% versus 79.2% $\pm$0.3%, respectively; $P=0.01$), whereas the addition of equiosmolar NaCl concentration (40 mM) resulted in increased cell proliferation compared with standard medium (85.2%$\pm$0.6% versus 79.2%$\pm$0.3%, respectively; $P<0.001$).

In light of these encouraging *in vitro* findings, we then investigated the *in vivo* response using a mouse model of chronic rejection, in which bm12 hearts are transplanted into B6 recipients. In
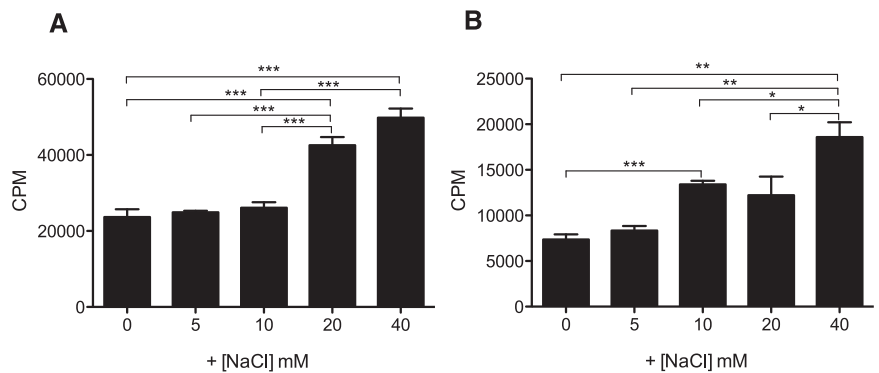


**Figure 1.** Increasing NaCl concentration *in vitro* augments polyclonal and allospecific T cell proliferation. (A) Proliferation of splenocytes after stimulation with aCD3 and aCD28 (2 $\mu$g/ml) in the presence of incremental concentrations of NaCl. (B) Proliferation of splenocytes after allospecific stimulation in the presence of incremental concentrations of NaCl. B6 Foxp3.GFP mice were sensitized with intraperitoneal BALB/c splenocytes injection; 2 weeks later, CD4$^+$Foxp3$^-$ cells were isolated by FACS sorting and cultured with magnetically isolated, irradiated BALB/c CD3$^-$ splenocytes. Thymidine was added at 72 hours of culture, and incorporation was quantified 12 hours later. $P$ values >0.05 are omitted. CPM, counts per minute. *$P<0.05$; **$P<0.01$; ***$P<0.001$;
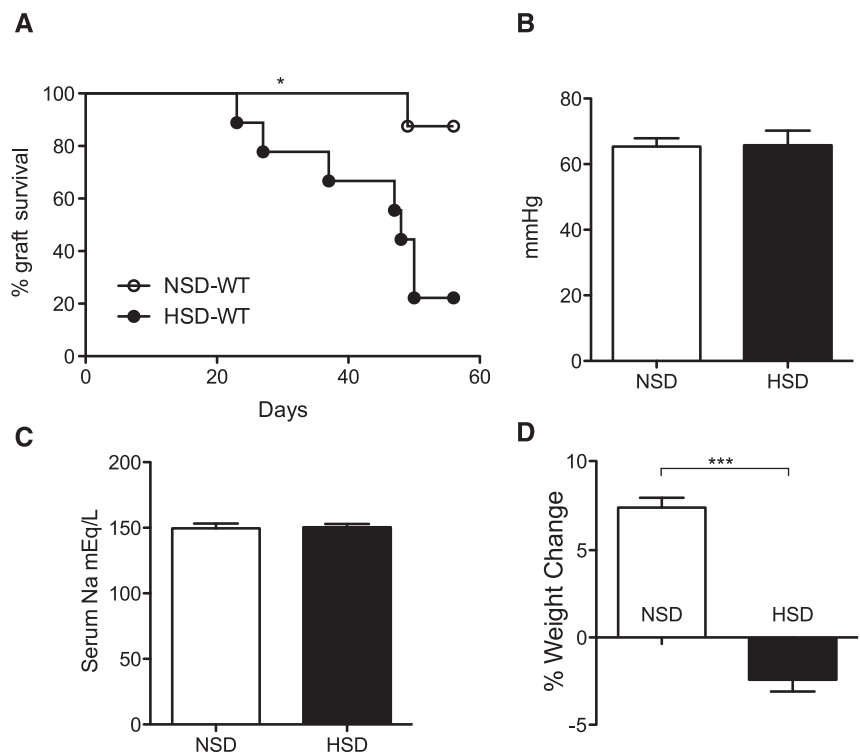


**Figure 2.** HSD accelerates cardiac allograft rejection independently of serum sodium or BP. (A) Kaplan–Meier curves of allograft survival ($n=8$–9 per group) of bm12 hearts transplanted into B6 recipients fed either a NSD or a HSD. (B) Tail cuff MAP measured at 25 days post-transplantation ($n=8$ per group; $P=0.93$). (C) Serum sodium of transplanted mice measured at 3 weeks post-transplantation ($n=6$ per group; $P=0.80$). (D) Percentage weight change at 3 weeks post-transplantation in relation to baseline weight ($n=4$ per group). Dietary modification was started 2 weeks before transplantation. *$P<0.05$; ***$P<0.001$.

this MHC class II–mismatched cardiac transplant model, allografts typically survive >56 days, although they develop progressive vasculopathy.[11–14] The survival of allografts in this model is dependent on the presence of regulatory T cells (Tregs) that inhibit the expansion of the small clone size of allospecific effector T cells, which recognize the single mismatched MHC II molecule on donor grafts.[12,15,16] B6 recipients were fed either normal-salt diet (NSD) or HSD and allowed unrestricted access to free water. We found that feeding mice a HSD resulted in decreased allograft

survival compared with NSD, with a median survival time (MST) of 48 days compared with >56 days, respectively ($n=8$–9 per group; $P=0.01$) (Figure 2A). Given the nature of the transplant (vascularized) and the intervention (HSD), we investigated the potential influence of hypertension: measurement of BP (Figure 2B) 25 days posttransplantation showed that mice fed a NSD or a HSD had similar mean arterial pressures (MAPs) of $65.35\pm2.5$ and $65.76\pm4.4$ mmHg, respectively ($n=8$ per group; $P=0.93$). We also evaluated the effect of diet on serum sodium and weight

change (Figure 2, C and D): mice fed a NSD or a HSD had serum sodium of $149.5\pm3.7$ and $150.4\pm2.4$ mEq/L ($n=6$–7 per group; $P=0.83$) and percentage weight change of $7.449\%\pm0.5\%$ and $-2.421\%\pm0.6\%$ ($n=4$ per group; $P<0.001$), respectively. To reconcile the *in vitro* effects of higher sodium concentration with the *in vivo* findings associated with HSD despite unchanged serum sodium, it is worth mentioning that previous work had shown that HSD results in increased interstitial fluid and lymphatic sodium concentration without effect on serum sodium concentration.[7]
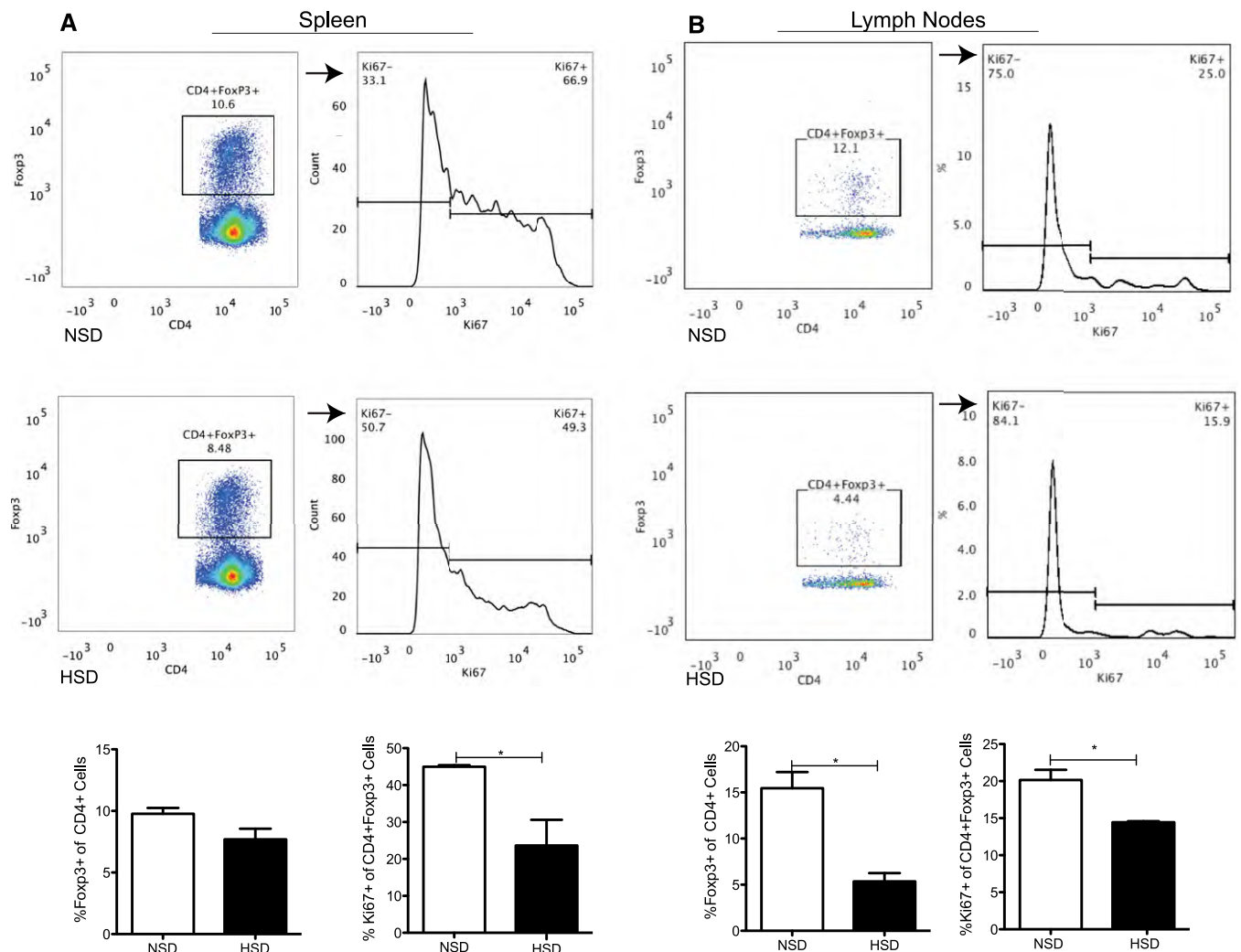


**Figure 3.** Transplant recipients fed with an HSD displayed both decreased proportion and proliferation of Tregs; bm12 hearts were transplanted into B6 mice fed with either an NSD or an HSD. Recipients were then euthanized at 25 days after transplantation; spleens and allograft-draining LNs were harvested and analyzed by flow cytometry. Representative dot plots and histograms of flow cytometry gating strategy on CD4^{+}, Foxp3^{+}, and Ki67^{+} subsets in (A) spleens and (B) LNs. Respective bar plots of percentages of Tregs (CD4^{+}Foxp3^{+}) and their proliferation (CD4^{+}Foxp3^{+}Ki67^{+}) are included. $n=3$ per group. Data are representative of three independent experiments. *$P<0.05$.

To elucidate the mechanisms underlying the accelerated rejection observed with HSD, we immunophenotyped lymphocytes isolated from the allograft-draining lymph nodes (LNs) and spleens 25 days post-transplantation using flow cytometry (Figure 3). Analysis of the LNs of recipients fed a HSD revealed a significant reduction in the proportion of Tregs (Foxp3$^+$ of CD4$^+$ T cells) compared with those fed a NSD (5.36%±0.9% versus 15.47%±1.7%, respectively; $P$=0.02); furthermore, these Tregs proliferated significantly less than those isolated from NSD-fed mice, which was determined by expression of the intracellular marker Ki67 (14.45%±0.15% versus 20.17%± 1.37%, respectively; $P$=0.05). There was a slight reduction in the proportion of splenic Tregs, albeit not statistically significant (7.69%±0.87% versus 9.77%±0.46% with NSD, respectively; $P$=0.10), whereas the proliferation of splenic Tregs (Ki67$^+$ of CD4$^+$Foxp3$^+$ cells) was also reduced in mice fed a HSD compared with a NSD (23.65% ±6.9% versus 44.97%±0.42%; $P$=0.03). The ratio of splenic CD4$^+$CD44$^+$/CD4$^+$ Foxp3$^+$ cells (Teffmem/Treg) was increased in the HSD group compared with the NSD group (2.570±0.12 versus 1.547±0.15, respectively; $P$=0.02). Although salt has been shown to induce Th17 cells (CD4$^+$IL-17$^+$) expansion in an EAE model,[4] spleen Th17 cells were extremely rare in our model and not significantly different between groups (0.22%±0.1% versus 0.08%±0.04%, respectively; $P$=0.28). In sum, the accelerated rejection seen in HSD-fed recipients was associated with a reduction in the proportion of Tregs, primarily in the draining LNs, along with a significant decrease in their proliferation, leading to an increase in the CD4$^+$ Teffmem/Treg ratio compared with NSD-fed recipients. Given these findings, we investigated the extent of acute rejection and allograft Treg infiltration. Histologic examination of the grafts 25 days post-transplant revealed a similar degree of rejection in both groups as measured by the International Society of Heart and Lung Transplantation classification[27] (ISHLT-R) score (2.3±0.3 versus 2.4±0.2, respectively;
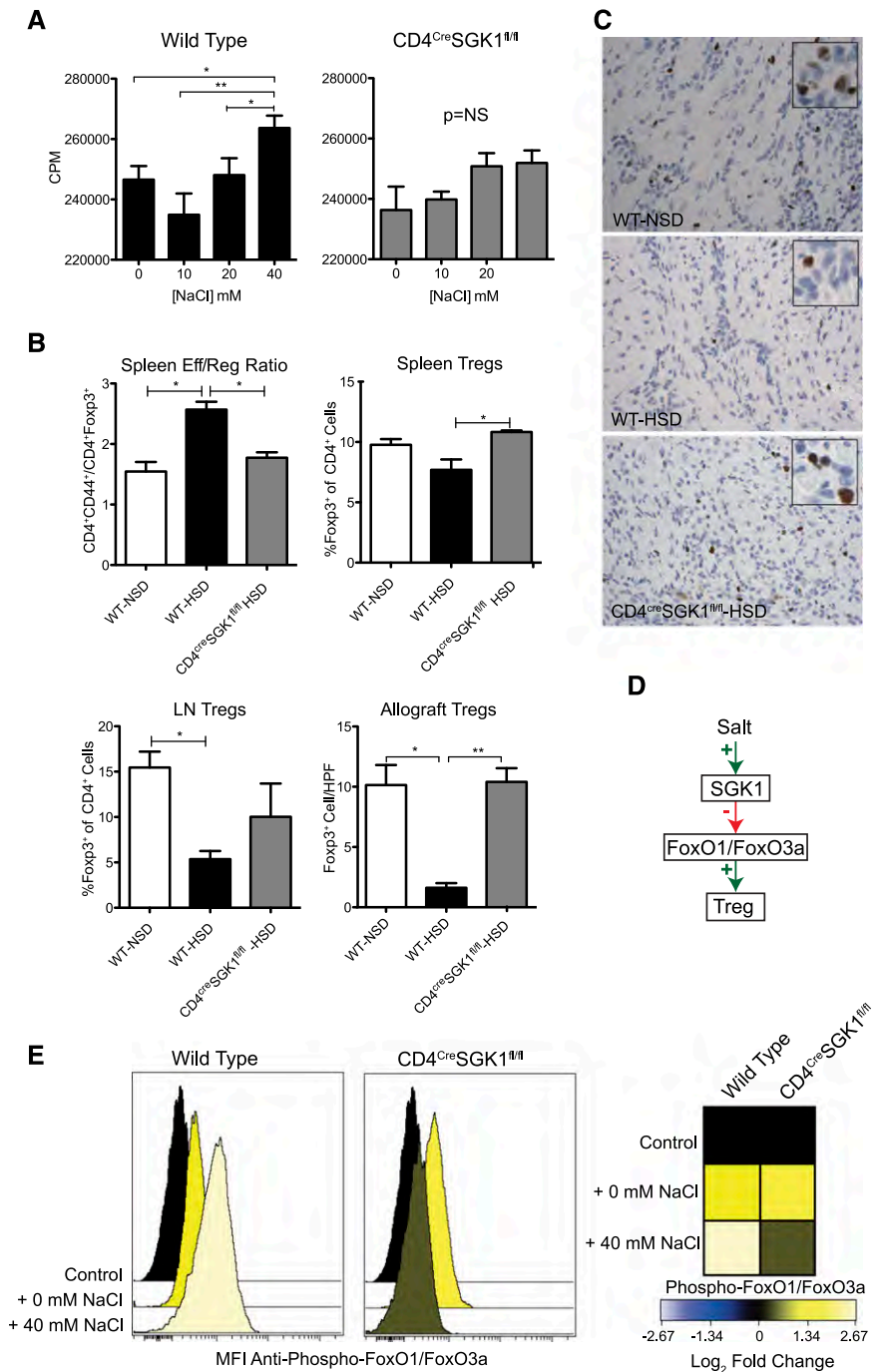


**Figure 4.** Mice lacking SGK1 in CD4$^+$ T cells seem to be protected against both the *in vitro* NaCl-induced increased proliferation and the *in vivo* effects of HSD in transplantation. (A) WT or CD4$^{Cre}$SGK1$^{fl/fl}$ B6 mice were sensitized with intraperitoneal BALB/c splenocytes injections; 2 weeks later, CD4$^+$ T cells were magnetically isolated and cultured for 72 hours with irradiated BALB/c CD3$^-$ cells in the presence of incremental concentrations of NaCl. Proliferation was measured by thymidine incorporation (*n*=6 per group). (B) Spleen Teffmem/Treg ratios (CD4$^+$CD44$^+$/CD4$^+$Foxp3$^+$) and Tregs in spleens, draining LNs, and allografts at 25 days after transplantation from WT B6 mice placed on NSD, WT mice on HSD, and CD4$^{Cre}$SGK1$^{fl/fl}$ B6 mice on HSD (*n*=3 per group). Data are representative of three independent experiments. (C) Photomicrographs of high-power fields (×400) of immunohistochemistry staining of Foxp3$^+$ cells in bm12 cardiac allografts 25 days after transplantation in WT B6 mice placed on NSD, WT B6 mice placed on HSD, and CD4$^{Cre}$SGK1$^{fl/fl}$

$n$=5–6 per group; $P$=0.88); however, there was significantly decreased Foxp3$^+$ cell infiltration in mice fed HSD compared with NSD (1.6±0.3 versus 10.1±1.6 cells per HPF, respectively; $n$=3 per group; $P$=0.02) as measured by immunohistochemistry.

Serum- and glucocorticoid-regulated kinase-1 (SGK1) is a signaling kinase that is induced by a variety of stimuli, including glucocorticoids, aldosterone, and hypertonicity.[17–19] SGK1 has been shown to play a major role in sodium homeostasis and is expressed in a wide array of cells, including those of the immune system. As an example, SGK1 activation was shown to promote Th17 cell polarization in an EAE model.[4,5] Furthermore, in an experimentally induced asthma model in mice, SGK1 activation favored $T_H2$ phenotype polarization, and SGK1 deletion in T cells was protective against asthma.[20] We hypothesized that the deleterious effects consequent to HSD consumption observed in our model were mediated by SGK1, and therefore, we sought to examine its potential role. Using mice with selective deletion of SGK1 in CD4$^+$ cells (CD4$^{Cre}$SGK1$^{fl/fl}$), we again examined the effect of incremental concentrations of salt on proliferation *in vitro* followed by investigation of the alloimmune response *in vivo* using our cardiac transplantation model.

*In vitro*, the salt-induced increased proliferation of BALB/c–primed WT B6 CD4$^+$ T cells was abrogated when primed B6 CD4$^{Cre}$SGK1$^{fl/fl}$ CD4$^+$ T cells were used instead (ANOVA $P$ values of 0.01 versus 0.11, respectively) (Figure 4A). *In vivo*, the observed accelerated rejection of bm12 hearts transplanted into WT B6 mice fed an HSD was abrogated in HSD-fed B6 CD4$^{Cre}$SGK1$^{fl/fl}$ mice (MST>56 days). Furthermore, the proportion of splenic Tregs was also similar between HSD-fed CD4$^{Cre}$SGK1$^{fl/fl}$ mice

and NSD-fed controls (10.83%±0.12% versus 9.770%±0.4676%; $n$=3 per group; $P$=0.09) (Figure 4B), resulting in a similar splenic Teffmem/Treg ratio between groups (1.773±0.08 versus 1.547±0.15; $n$=3 per group; $P$=0.28). The proportion of Tregs in allograft-draining LN did not significantly differ between HSD-fed B6 CD4$^{Cre}$SGK1$^{fl/fl}$ mice and NSD-fed controls (10.03%± 3.6% versus 15.47%±1.7%, respectively; $n$=3 per group; $P$=0.22). On allograft histology, we observed a similar degree of acute rejection between WT mice fed NSD, WT mice fed HSD, and CD4$^{Cre}$SGK1$^{fl/fl}$ mice fed HSD (2.3±0.3 versus 2.4±0.2 versus 2.67±0.3, respectively; $n$=3–6 per group; ANOVA $P$=0.78); however, the HSD-induced reduction in allograft Tregs observed in WT mice was again abrogated in HSD-fed CD4$^{Cre}$SGK1$^{fl/fl}$ mice (1.61±0.3 versus 10.4±1.3 cells per HPF, respectively; $n$=3 per group; $P$<0.01) (Figure 4C), indicating a critical role of SGK1 in the acceleration of rejection by reducing Tregs in mice fed a HSD.

Two transcription factors, FoxO1 and FoxO3a, play an important role in regulating Foxp3 expression in Tregs,[21,22] and their deletion in mice results in a fatal multifocal inflammatory disorder caused by a defect in Tregs.[23] Interestingly, SGK1 is known to inactivate both FoxO1 and FoxO3a by phosphorylating them and promoting their sequestration in the cytoplasm.[4,24,25] Therefore, we hypothesized that salt may inhibit FoxO1/3a by activation of SGK1, leading ultimately to the reduction in Tregs that we observed thus far (Figure 4D). To test this hypothesis, we measured phosphorylated FoxO1 and FoxO3a by flow cytometry in WT and CD4$^{Cre}$SGK1$^{fl/fl}$ Tregs cultured with and without additional NaCl. Indeed, increasing [NaCl] in culture medium resulted in increased FoxO1/FoxO3a phosphorylation in an

SGK1-dependent fashion (Figure 4E), indicating a direct correlation between salt, SGK1 activation, FoxO1/FoxO3a phosphorylation, and ultimately, Treg inhibition.

In summary, we report, for the first time, immunologic effects of salt consumption in a mouse model of solid organ transplantation. First, we showed increased proliferation of primed T cells after exposure to higher [NaCl]. Second, we observed that HSD-fed mice displayed accelerated allograft rejection in the absence of elevated BP or alteration of serum sodium concentration. Third, we found that, in transplanted mice fed HSD, there was a shift in the Teffmem/Treg balance and that HSD was associated with both decreased proliferation of splenic and graft-draining LN Tregs and significantly fewer Tregs infiltrating the allograft. Fourth, we examined SGK1 as a potential mediator of our observations: using a conditional knockout model in which CD4$^+$ T cells lack SGK1, we found that the increased proliferation, accelerated rejection, skewing of Teffmem/Treg balance, and decreased allograft Tregs observed in HSD-fed WT recipients were abrogated by the lack of SGK1. Our findings constitute a proof of concept of a deleterious, immune-modifying role of salt in accelerating rejection in transplantation, complementing previous evidence of salt-induced autoimmunity. Given the endemic nature of salt consumption, additional investigation of its effect in human transplantation is warranted.

## CONCISE METHODS

### Mice

WT C57BL/6 (B6), bm12, and BALB/c mice were purchased from The Jackson Laboratory. B6 CD4$^{Cre}$SGK1$^{fl/fl}$ mice were a gift from the Kuchroo Laboratory. All mice were 8–12 weeks of age, and they were harbored and used in accordance with Harvard Medical School and National Institutes of Health guidelines.

### Transplantation

Vascularized heart grafts were placed in an intra-abdominal location using microsurgical techniques as described by Corry *et al.*[26]

B6 mice placed on HSD. (D) Effect of salt on Tregs. Green arrows represent activation, whereas the red arrow represents inhibitory signals. (E) Phosphorylated (inactivated) FoxO1 and FoxO3a transcription factors measured in control and CD4$^{Cre}$SGK1$^{fl/fl}$ Tregs cultured with and without additional NaCl (+0 and +40 mM, respectively); BioHeat map generated by flow cytometry illustrates fold change in the mean fluorescent intensity (MFI) of anti-phosphorylated FoxO1/FoxO3a. CPM, counts per minute. *$P$<0.05; **$P$<0.01.

Graft function was assessed by palpation of the heartbeat; rejection was determined by complete cessation of palpable heartbeat and confirmed by direct visualization after laparotomy. Graft survival is shown as the MST in days. Mechanistic experiments with transplanted mice were performed at the time point in which rejection started to occur in the HSD-treated group (approximately day 25 post-transplant).

### Diet Modification

Mice were fed either standard chow containing 0.28% Na (NSD) or chow containing 3.15% Na (HSD; 1810179; Pharmaserv Inc.) beginning 2 weeks before transplantation and continued thereafter. Mice were allowed continuous access to free water.

### Serum Sodium and BP Measurements

Sodium was measured by the Roche Cobas c501 Module sodium ion–specific electrode on mice sera after at least 3 weeks on HSD or NSD. BP was measured by tail transmission photoplethysmography by the Visitech System BP-2000 Series II, and MAP was calculated as follows: $MAP=[(2\times diastolic)+systolic]/3$.

### *In Vitro* Culture Media

Standard culture medium was enriched to attain additional NaCl concentrations between 0 and 40 mM by adding NaCl (Sigma Life Science). Osmotic control was done with urea-enriched culture media (0–80 mM; Sigma Life Science).

### *In Vitro* Cell Cultures and Proliferation Assay

For polyclonal proliferation, naïve B6 splenocytes were cultured with aCD3 and aCD28 (final well concentration of 2 $\mu$g/ml) and increments of NaCl-enriched culture media for 72 hours. For allospecific proliferation, WT B6, B6 FoxP3.GFP, or B6 CD4$^{Cre}$SGK1$^{fl/fl}$ mice were sensitized with an intraperitoneal injection of 15 million BALB/c splenocytes and euthanized at least 2 weeks thereafter. CD4$^+$FoxP3.GFP$^-$ T cells were isolated by FACS sorting and cocultured in culture media enriched by incremental concentrations of NaCl with irradiated CD3$^-$–depleted BALB/c splenocytes. Proliferation was measured 72 hours later by quantification of thymidine incorporation. For osmotic control,

cells were stained with 10 $\mu$M CFSE in the presence of additional salt (0–40 mM) or urea (0–80 mM), and proliferation was measured by CFSE dilution by flow cytometry 72 hours later.

### Flow Cytometry

Transplanted mice spleens and draining LNs were harvested, and single-cell suspensions were prepared. Cells were stained with fluorochrome-labeled mAbs against CD4, CD8, B220, CD62 ligand (CD62L), CD44, CD25, Ki67, and Foxp3. Intracellular staining for Foxp3 and Ki67 was performed after permeabilization of the cells using the eBioscience Foxp3 Fixation/Permeabilization Solution. Flow cytometry was performed using a BD FACSCanto II Cytometer and analyzed using FlowJo software.

### Phosphorylated FoxO1 and FoxO3a Measurement

Tregs were isolated using the EasySep Mouse CD4$^+$CD25$^+$ Regulatory T Cell Isolation Kit (Stem Cell). Cells were cultured with aCD3 and aCD28 (final well concentration of 2 $\mu$g/ml) for 10 or 60 min with and without additional NaCl. Cells were then fixed with BD Cytofix (BD Biosciences) and permeabilized with Perm Buffer III (BD Biosciences); then, they were stained with a primary anti-phospho–FoxO1/3a$^{T24/T32}$ antibody (Cell Signaling Technology) and a secondary anti-rabbit IgG Alexa 488 antibody (Molecular Probes). Flow cytometry was performed using a BD FACSCanto II Cytometer and analyzed using FlowJo software. BioHeat maps were generated with the web-based software Cytobank (www.cytobank.org).

### Histopathology

Cardiac graft samples from transplanted mice were harvested from both NSD- and HSD-fed groups at 25 days post-transplantation. Grafts were then fixed in 10% formalin, embedded in paraffin, transversely sectioned, and stained with H&E stain. Using the revised ISHLT-R,[27] a blinded transplant pathologist graded the degree of rejection (0–3). Immunohistochemistry for Foxp3$^+$ cells was performed on formalin-fixed, paraffin-embedded allografts sections; cells were counted in at least 10 high-power fields per sample, and individual sample counts were averaged thereafter.

### Statistical Analyses

Statistical analyses were performed using Prism 5.0b of Graphpad software. Kaplan–Meier curves were used to generate allograft survival curves, and log-rank test was used to compare median survival. Two-way unpaired $t$ test and ANOVA were used to compare datasets. $P$ values $<0.05$ were considered statistically significant.

## DISCLOSURES
None.

## REFERENCES

1. Mancilha-Carvalho JJ, Souza e Silva NA: The Yanomami Indians in the INTERSALT Study. *Arq Bras Cardiol* 80: 289–300, 2003
2. He FJ, MacGregor GA: A comprehensive review on salt and health and current experience of worldwide salt reduction programmes. *J Hum Hypertens* 23: 363–384, 2009
3. O'Shea JJ, Jones RG: Autoimmunity: Rubbing salt in the wound. *Nature* 496: 437–439, 2013
4. Wu C, Yosef N, Thalhamer T, Zhu C, Xiao S, Kishi Y, Regev A, Kuchroo VK: Induction of pathogenic TH17 cells by inducible salt-sensing kinase SGK1. *Nature* 496: 513–517, 2013
5. Kleinewietfeld M, Manzel A, Titze J, Kvakan H, Yosef N, Linker RA, Muller DN, Hafler DA: Sodium chloride drives autoimmune disease by the induction of pathogenic TH17 cells. *Nature* 496: 518–522, 2013
6. Machnik A, Neuhofer W, Jantsch J, Dahlmann A, Tammela T, Machura K, Park JK, Beck FX, Müller DN, Derer W, Goss J, Ziomber A, Dietsch P, Wagner H, van Rooijen N, Kurtz A, Hilgers KF, Alitalo K, Eckardt KU, Luft FC, Kerjaschki D, Titze J: Macrophages regulate salt-dependent volume and blood pressure by a vascular endothelial growth factor-C-dependent buffering mechanism. *Nat Med* 15: 545–552, 2009
7. Wiig H, Schröder A, Neuhofer W, Jantsch J, Kopp C, Karlsen TV, Boschmann M, Goss J,

Bry M, Rakova N, Dahlmann A, Brenner S, Tenstad O, Nurmi H, Mervaala E, Wagner H, Beck FX, Müller DN, Kerjaschki D, Luft FC, Harrison DG, Alitalo K, Titze J: Immune cells control skin lymphatic electrolyte homeostasis and blood pressure. *J Clin Invest* 123: 2803–2815, 2013

8. Vincenti F: Are calcineurin inhibitors-free regimens ready for prime time? *Kidney Int* 82: 1054–1060, 2012

9. Ramesh Prasad GV, Huang M, Nash MM, Zaltzman JS: The role of dietary cations in the blood pressure of renal transplant recipients. *Clin Transplant* 20: 37–42, 2006

10. van den Berg E, Geleijnse JM, Brink EJ, van Baak MA, Homan van der Heide JJ, Gans RO, Navis G, Bakker SJ: Sodium intake and blood pressure in renal transplant recipients. *Nephrol Dial Transplant* 27: 3352–3359, 2012

11. Sayegh MH, Wu Z, Hancock WW, Langmuir PB, Mata M, Sandner S, Kishimoto K, Sho M, Palmer E, Mitchell RN, Turka LA: Allograft rejection in a new allospecific CD4+ TCR transgenic mouse. *Am J Transplant* 3: 381–389, 2003

12. Yang J, Riella LV, Boenisch O, Popoola J, Robles S, Watanabe T, Vanguri V, Yuan X, Guleria I, Turka LA, Sayegh MH, Chandraker A: Paradoxical functions of B7: CD28 costimulation in a MHC class II-mismatched cardiac transplant model. *Am J Transplant* 9: 2837–2844, 2009

13. Riella LV, Liu T, Yang J, Chock S, Shimizu T, Mfarrej B, Batal I, Xiao X, Sayegh MH, Chandraker A: Deleterious effect of CTLA4-Ig on a Treg-dependent transplant model. *Am J Transplant* 12: 846–855, 2012

14. Riella LV, Yang J, Chock S, Safa K, Magee CN, Vanguri V, Elyaman W, Lahoud Y, Yagita H, Abdi R, Najafian N, Medina-Pestana JO, Chandraker A: Jagged2-signaling promotes IL-6-dependent transplant rejection. *Eur J Immunol* 43: 1449–1458, 2013

15. Schenk S, Kish DD, He C, El-Sawy T, Chiffoleau E, Chen C, Wu Z, Sandner S, Gorbachev AV, Fukamachi K, Heeger PS, Sayegh MH, Turka LA, Fairchild RL: Alloreactive T cell responses and acute rejection of single class II MHC-disparate heart allografts are under strict regulation by CD4+ CD25+ T cells. *J Immunol* 174: 3741–3748, 2005

16. Lee MK 4th, Moore DJ, Jarrett BP, Lian MM, Deng S, Huang X, Markmann JW, Chiaccio M, Barker CF, Caton AJ, Markmann JF: Promotion of allograft survival by CD4+CD25+ regulatory T cells: Evidence for in vivo inhibition of effector cell proliferation. *J Immunol* 172: 6539–6544, 2004

17. Chen SY, Bhargava A, Mastroberardino L, Meijer OC, Wang J, Buse P, Firestone GL, Verrey F, Pearce D: Epithelial sodium channel regulated by aldosterone-induced protein sgk. *Proc Natl Acad Sci U S A* 96: 2514–2519, 1999

18. Leong ML, Maiyar AC, Kim B, O'Keeffe BA, Firestone GL: Expression of the serum- and glucocorticoid-inducible protein kinase, Sgk, is a cell survival response to multiple types of environmental stress stimuli in mammary epithelial cells. *J Biol Chem* 278: 5871–5882, 2003

19. Webster MK, Goya L, Ge Y, Maiyar AC, Firestone GL: Characterization of sgk, a novel member of the serine/threonine protein kinase gene family which is transcriptionally induced by glucocorticoids and serum. *Mol Cell Biol* 13: 2031–2040, 1993

20. Heikamp EB, Patel CH, Collins S, Waickman A, Oh MH, Sun IH, Illei P, Sharma A, Naray-Fejes-Toth A, Fejes-Toth G, Misra-Sen J, Horton MR, Powell JD: The AGC kinase SGK1 regulates TH1 and TH2 differentiation downstream of the mTORC2 complex. *Nat Immunol* 15: 457–464, 2014

21. Harada Y, Harada Y, Elly C, Ying G, Paik JH, DePinho RA, Liu YC: Transcription factors Foxo3a and Foxo1 couple the E3 ligase Cbl-b to the induction of Foxp3 expression in induced regulatory T cells. *J Exp Med* 207: 1381–1391, 2010

22. Merkenschlager M, von Boehmer H: PI3 kinase signalling blocks Foxp3 expression by sequestering Foxo factors. *J Exp Med* 207: 1347–1350, 2010

23. Ouyang W, Beckett O, Ma Q, Paik JH, DePinho RA, Li MO: Foxo proteins cooperatively control the differentiation of Foxp3+ regulatory T cells. *Nat Immunol* 11: 618–627, 2010

24. Di Pietro N, Panel V, Hayes S, Bagattin A, Meruvu S, Pandolfi A, Hugendubler L, Fejes-Tóth G, Naray-Fejes-Tóth A, Mueller E: Serum- and glucocorticoid-inducible kinase 1 (SGK1) regulates adipocyte differentiation via forkhead box O1. *Mol Endocrinol* 24: 370–380, 2010

25. Brunet A, Park J, Tran H, Hu LS, Hemmings BA, Greenberg ME: Protein kinase SGK mediates survival signals by phosphorylating the forkhead transcription factor FKHRL1 (FOXO3a). *Mol Cell Biol* 21: 952–965, 2001

26. Corry RJ, Winn HJ, Russell PS: Primarily vascularized allografts of hearts in mice. The role of H-2D, H-2K, and non-H-2 antigens in rejection. *Transplantation* 16(4): 343–350, 1973

27. Stewart S, Winters GL, Fishbein MC, Tazelaar HD, Kobashigawa J, Abrams J, Andersen CB, Angelini A, Berry GJ, Burke MM, Demetris AJ, Hammond E, Itescu S, Marboe CC, McManus B, Reed EF, Reinsmoen NL, Rodriguez ER, Rose AG, Rose M, Suciu-Focia N, Zeevi A, Billingham ME: Revision of the 1990 working formulation for the standardization of nomenclature in the diagnosis of heart rejection. *J Heart Lung Transplant* 24: 1710–1720, 2005

**Autores:** Ayesha Murshid, Jianlin Gong, Ridwan Ahmad, Thiago J. Borges, Stuart K. Calderwood

**Situação:** Publicado

**Revista:** *Immunobiology*

**Referência:** Immunobiology. 2015 Jun;220(6):823-32. doi: 10.1016/j.imbio.2014.12.011.

**Website:** http://www.sciencedirect.com/science/article/pii/S0171298514002800

**Motivação:** Esse trabalho foi realizado durante o período sanduíche realizado no Hospital Beth Israel Deaconess Medical Center, no laboratório do Prof. Stuart K. Calderwood.

# Scavenger receptor SREC-I promotes double stranded RNA-mediated TLR3 activation in human monocytes

Ayesha Murshid [a], Jianlin Gong [b], Ridwan Ahmad [a], Thiago J. Borges [a,c], Stuart K. Calderwood [a,*]

[a] Department of Radiation Oncology, Beth Israel Deaconess Medical Center, Harvard Medical School, Boston, MA 02215, United States
[b] Boston University Medical Center, United States
[c] School of Biosciences and Biomedical Research Institute, Pontifícia Universidade Católica do Rio Grande do Sul (PUCRS), Porto Alegre, RS, Brazil

## ARTICLE INFO

## ABSTRACT

Scavenger receptor associated with endothelial cells (SREC-I) was previously shown to be expressed by immune cells and to play a role in CD8^{+}-mediated T cell immunity. SREC-I was also shown to modulate the function of Toll like receptors with essential roles in innate immunity. Here we have shown that SREC-I enhanced double stranded RNA (dsRNA)-mediated Toll like receptor-3 (TLR3) activation. Viral double stranded RNA (dsRNA) was demonstrated to be a pathogen associated molecular pattern (PAMP) signaling viral infection. We found that in human monocyte/macrophage THP1 cells as well as murine bone marrow derived macrophages SREC-I led to elevated responses to the dsRNA-like molecule polyinosine–polycytidylic acid (Poly I:C) and enhanced production of inflammatory cytokines. Our data also showed that intracellular/endocytic TLR3 could directly interact with SREC-I in the presence of Poly I:C. The internalized ligand, along with TLR3 and SREC-I localized in endosomes within macrophages and in HEK293 cells engineered to express TLR3 and SREC-I. SREC-I also stimulated dsRNA-mediated TLR3 activation of signaling through the NFκβ, MAP kinase and interferon regulatory factor 3 (IRF3) pathways leading to expression of cytokines, most notably interleukin-8 and interferon-β. We therefore hypothesized that SREC-I could be a receptor capable of internalizing Poly I:C, boosting TLR3 mediated inflammatory signaling and stimulating cytokine production in macrophages.

© 2015 Elsevier GmbH. All rights reserved.

## Introduction

Toll like receptors (TLRs) and pattern recognition receptors have been shown to be responsible for activating immune responses in the presence of pathogens or pathogen-associated molecules (Akira and Takeda, 2004). These receptors were also shown to transduce signals for innate immunity in the presence of pathogen associated molecular pattern (PAMP) molecules (Akira and Takeda, 2004; Beutler 2004). The TLRs are members of a protein family the individual members of which differ in terms of their ligand specificity, cellular localization and signaling pathways. TLRs 1, 2, 4, 5 and 6 were detected on the plasma membrane while others such as TLR 3, 7 and 9 were characterized as "endosomal TLRs" (Akira and Takeda, 2004; McGettrick and O'Neill, 2010). Among endosomal TLRs, TLR3 was unique in being activated by binding viral double stranded

RNA (dsRNA) (Kumar et al., 2006; Takahashi et al., 2006). Viral double stranded RNA, produced during the replication of many viruses has been shown to be a PAMP, indicating viral infection (Pirher et al., 2008; Alexopoulou et al., 2001). The other commonly known nucleic acid PAMP, CpG DNA (unmethylated bacterial DNA) was found to be recognized by another member of the endosomal TLR family, TLR9 (Chuang et al., 2002). These endosomal receptors were shown to translocate from their storage site in the endoplasmic reticulum (ER) to endosomal sites upon arrival of internalized PAMP ligands at the endosomes. It has been shown that immune cells possess several systems for response to dsRNA including TLR3 present in endosomes, as well as number of cytoplasmic sensors including protein kinase R, RIG-1 (retinoic acid-inducible gene I) and the recently discovered surface relocated TLR3 (Pohar et al., 2013). These molecules were established as sensors of dsRNA in several cellular compartments and were shown to activate the innate immune response by triggering a number of signaling cascades, including the NFκB, IRF3 and MAP kinase pathways (Liu et al., 2008). Such dsRNA sensors were thus implicated in transcription of cytokine genes. Recently it was shown that TLR3 could localize to

the cell surface in the presence of dsRNA and UNC93B1 (an accessory protein shown to interact with TLRs 3, 7, 9, 11 and 14) in some endothelial, epithelial and fibroblastic cells (such as human lung fibroblast cells) (Andrade et al., 2013; Brinkmann et al., 2007; Pifer et al., 2011). Recently there was a report on the role of the ectodomain of TLR3 in trafficking to the plasma membrane (Pohar et al., 2014).

We have examined another class of potential sensors for dsRNA – scavenger receptors which have been shown to bind polyanionic ligands. We detected SREC-I both on the cell surface and in endosomes along with TLR3, on stimulation with Poly I:C. SREC-I could play roles in detecting dsRNA in alternative cellular compartments and could potentially trigger the trafficking of TLR3 from the surface to endosomes where actual signaling could likely occur. We have therefore examined the ability of SREC-I to modulate the response of immune cells to the model dsRNA-Poly I:C.

## Materials and methods

### Reagents and Abs

Rabbit polyclonal human anti SREC-I Ab was rabbit monoclonal was custom synthesized by GenScript (Piscataway, NJ) against the specific peptide sequence (TQGTQGSTLDPAGQC). Commercially available anti SREC-I abs was also purchased from Atlas Antibodies. Anti TLR3 Ab was from Abcam. All secondary fluorescent Abs were from Jackson Immunoresearch Laboratories. Rhodamine-labeled TLR3 was purchased from Invivogen. Poly I:C HMW was purchased from Invivogen. TLR3-CFP plasmid was from Addgene. Anti Phospho-p38, anti p38, anti phospho-JNK, anti JNK, anti phospho-p65, anti p65, anti Src anti-phosphor-Src (416), IRF3 antibodies were purchased from Cell Signaling Technology. Anti LAMP1 and anti GFP antibodies were from Abcam. Anti phospho-IRF3 antibodies were from Abcam. PP2 and Bafilomycin were purchased from Sigma–Aldrich. Normocin was from Invivogen.

### Cells and culture conditions

THP1 and HEK293 cells were transfected with human full length SREC-I in pcDNA3 for stable expression of SREC-I. HEK293 cells stable TLR3 was purchased from Invivogen and cultured according to manufacturer's instruction. THP1 and HEK293 cells were maintained in RPMI 1640 and DMEM respectively with 10% heat inactivated FBS and penicillin–streptomycin. For generation of stable SREC-I-expressing cell lines, cells were selected and maintained in the same medium plus 400 mg/ml G418. HEK293-TLR3 stable cell line was also maintained with 100 μg/ml Normocin. Differentiation of THP1 macrophages from undifferentiated ones was performed by treating the cells with 5–10 ng/ml of phorbol 12-myristate 13-acetate (PMA) for 72 h or 50 ng/ml for overnight. SREC-I expression in differentiated THP1 macrophages was induced by incubating cells with 1–5 ng/ml of LPS for 12 h. Bone marrow derived cells were isolated from C57/BL6J mice. The cells were then grown in RPMI supplemented with 10% heat inactivated serum and penicillin and streptomycin, along with L929 supernatant (media) to differentiate into macrophages. For inducing SREC-I expression in these macrophages, cells were incubated with 1–5 ng/ml of LPS for 12 h.

### Plasmids

The pcDNA3.1-SREC-I (human) was a generous gift from Dr. H. Adachi. FLAG–SREC-I construct was made in 3xFLAG-CMV vector as described in Murshid et al. (2010). TLR3-CFP was from Addgene. Human SREC-I-GFP was constructed in EGFP-N1 vector (Clontech).

Both human and mice SREC-I (siRNA) and TLR3 (siRNA) constructs were purchased from Santa Cruz Biotech.

### Immunofluorescence and microscopic analysis of Poly I:C internalization

HEK293 and bone marrow derived macrophages cells were incubated with Poly I:C for 20–30 min on ice. The ice-cold medium was then replaced by warm medium and incubated at 37 °C for different periods. Cells were later washed with ice-cold stripping buffer (50 mM sodium citrate and 280 mM sucrose [pH 4.6]) to remove unbound ligand. Later, the cells were fixed with 4% paraformaldehyde and permeabilized with 0.1% Triton X-100. Cells were stained with different primary (anti FLAG m2, anti LAMP1, and anti TLR3 antibodies) and secondary antibodies (Goat anti mouse Alexa 488, Goat anti rabbit/mouse Cy3, Goat anti mouse/rabbit Cy5) and later analyzed using a Zeiss 510 confocal microscope (Carl Zeiss, Jena, Germany). Fluorophores were visualized using the following filter sets: 488 nm excitation and band pass 505–530 emission filter for Alexa 488; 543 nm excitation and band pass 560–615 for Cy3; and 633 excitation and long pass 650 for Cy5. Images were taken using a 633 numerical aperture 1.4 oil immersion objective lens (Carl Zeiss, Jena, Germany). Figures were made using Adobe Photoshop 7.0 (Adobe Systems, San Jose, CA) with little or no contrast adjustments without altering original images.

### SEAP reporter assay

The secreted form of embryonic alkaline phosphatase (SEAP)-NFκβ promoter-reporter assay kit was utilized as a convenient and sensitive method to determine promoter activity in cells transfected with the SEAP expression plasmid. HEK293 cells were transfected with plasmids encoding FLAG-SREC-I, TLR3 and the reporter constructs NFκβ-SEAP and CMV-SEAP (control expression vector). NFκβ activity was measured indirectly by catalytic hydrolysis reaction of $p$-nitrophenyl phosphate producing a yellow end product that was read spectrophotometrically at 405 nm.

### Western blotting and immunoprecipitation

HEK293 cells stably expressing TLR3 were transfected with SREC-I-GFP and then incubated with or without Poly I:C (10 μg/ml) for 30 min. Cells were then washed with ice-cold Dulbecco's phosphate-buffered saline (PBS) and lysed in NP-40 lysis buffer (containing 1% Nonidet P-40, 150 mM NaCl, 1 mM EDTA, 1 mM PMSF, 1× HALT protease and phosphatase inhibitor cocktail (Thermo Scientific). For Western blotting, 15–30 μg of protein were resolved by 4–15% gradient SDS–PAGE and transferred to PVDF (polyvinylidene fluoride) membranes. Membranes were immunoblotted with primary antibodies and later secondary antibodies that are HRP-conjugated. The membrane reactions were visualized by Perkin Elmer enhanced chemiluminescence reagents. For immunoprecipitation, 1 mg of cell extract was incubated with 5 μg of anti rabbit-GFP antibody or IgG (control) for 2 h at 4 °C followed by incubation with 20 μl of protein G (50% slurry, GE healthcare) plus-sepharose beads for either 2 h at room temperature or overnight at 4 °C. The beads were then washed with NP40-lysis buffer and complexes were eluted by boiling in Laemmli sample buffer.

### ELISA

A human microanylate ELISA array was used to measure cytokine production by human THP1 cells treated with TLR3 ligand Poly I:C. Values represent the optical density. The kit was purchased
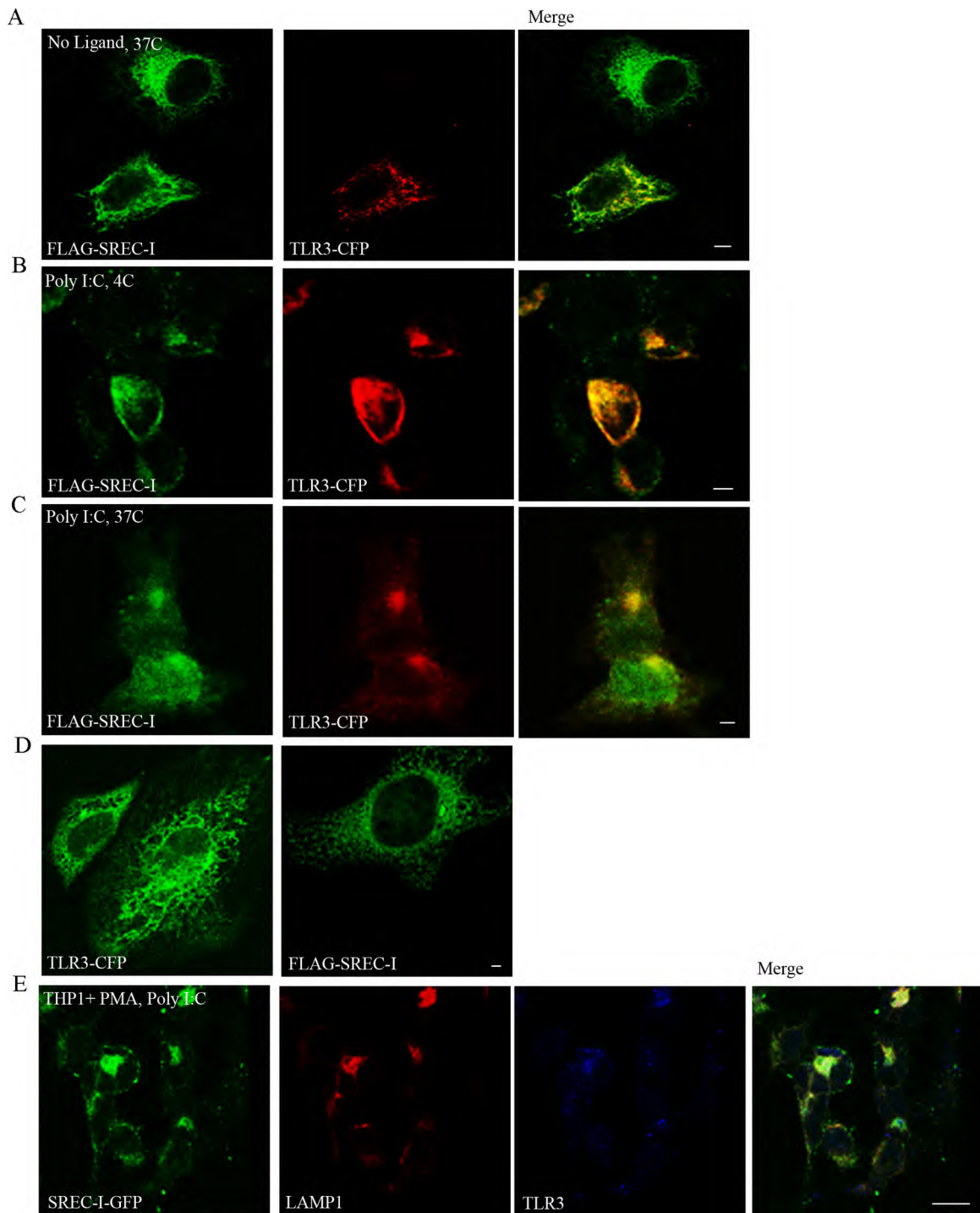
**Fig. 1.** TLR3 was colocalized with SREC-I at the cell surface and in intracellular compartments in the presence of Poly I:C. (A and B) TLR3 colocalized with SREC-I in HEK 293–TLR3–SREC-I overexpressing cells. HEK293 cells were transfected with FLAG-SREC-I and TLR3-CFP for 22 h. Cells were then incubated without (A) or with (B) Poly I:C (10 μg/ml) on ice for 30 min. Cells (A) and (B) were then fixed with 4% para formaldehyde and permeabilized with 0.1% Triton X-100 (A) or not (B). Cells were then stained for FLAG with anti-FLAG M2 antibody (green). (C) HEK293 cells were transfected with FLAG-SREC-I and TLR3-CFP for 22 h. Cells were then incubated Poly I:C (10 μg/ml) on ice for 30 min followed by incubation with warm media at 37 °C for 20 min. Cells were then fixed with 4% PFA and permeabilized with 0.1% Triton X-100. Cells were stained with anti-FLAG antibody (green). (D) HEK293 cells were transfected with FLAG-SREC-1 or TLR3-CFP for 18 h. Cells were incubated with Poly I:C (10 μg/ml) for 1 h and then fixed and stained with anti-FLAG M2 ab (green). (E) Differentiated THP1 cells were transfected with FLAG-SREC-I and TLR3-CFP for 22 h. Cells were then incubated with Poly I:C (10 μg/ml) for 1 h and then fixed and permeabilized as in (D). Cells were stained for SREC-I (green), with anti-FLAG Ab, LAMP1 with anti-LAMP1 (red). TLR3-CFP is in blue. Experiments were repeated twice with reproducible findings. Scale bar 2 μm. (For interpretation of the references to color in this figure legend, the reader is referred to the web version of the article.)

from Qiagen (SA Biosciences) according to manufacturer's protocol. THP1 cells and BMDM (bone marrow derived macrophages) were treated transfected with siRNA of SREC-I for 72 h and cells were then incubated with Poly I:C (10 μg/ml) or not. The secreted cytokines were measured using ELISA microanylate array kit or other kits from BD Biosciences (IL-6, IL-8, and IFNβ). The optical density was measured either using BioRad plate or BioTec reader using appropriate software and wavelength.

## Results

We first investigated the relative cellular locations of SREC-I and TLR3 without and with exposure to ligand. Experiments were carried out in HEK 293 initially for ease in gene transfection. Prior to addition of Poly I:C, FLAG-SREC-I was found largely in intracellular organelles resembling endosomes or endoplasmic reticulum (ER), while TLR3 (TLR3-CFP) appeared to reside largely in cytoplasmic membrane structures (Fig. 1A). Upon Poly I:C exposure in HEK293 cells expressing FLAG-SREC-I, the TLR3-CFP appeared to become co-localized along with the SREC-I at plasma membrane-endosomal sites (Fig. 1B). Incubation of the cells expressing FLAG-SREC-I and TLR3-CFP with Poly I:C at 37 °C, resulted in relocalization of the receptors to an intracellular compartment (Fig. 1C). On the other hand, in control experiments, we did not observe Poly I:C induced translocation of FLAG-SREC-I to the plasma membrane from cytosolic compartments in HEK293 cells lacking TLR3 (Fig. 1D). In addition, TLR3-CFP was not re-localized to the plasma membrane in the presence of Poly I:C in HEK293 cells that did not express SREC-I (Fig. 1D) suggesting a role for SREC-I for relocation of TLR3.

We also carried out experiments in cells of myeloid lineage (Fig. 1E). These were THP1 human monocytes differentiated to macrophages by exposure to PMA. In common with the HEK293 experiments (Fig. 1C), treatment with Poly I:C led to localization of both SREC-I and TLR3 in intracellular vesicles (Fig. 1E). Interestingly, many of these structures were stained with antibodies to the lysosomal protein LAMP1 suggesting co-localization of SREC-I and TLR3 to a lysosomal/endolysosomal compartment after Poly I:C treatment.

It was suggested in earlier reports that TLR3 trafficking to the endosomes and plasma membrane required UNC93B1 activity (Pohar et al., 2013). However we observed trafficking of TLR3 to the plasma membrane in HEK293 cells that do not express UNC93B1cells but engineered to express SREC-I. It was shown recently by Poher et al. that even though UNC93B1 could activate TLR3 and be responsible for TLR3 trafficking from ER to endo/lysosomal sites, this adaptor itself did not traffic to the plasma membrane along with TLR3 (Kim et al., 2008). This group later reported that the ectodomain was responsible for plasma membrane translocation of TLR3 in the presence of UNC93B1 (Pohar et al., 2013, 2014). Here we observed that TLR3 could traffic to the plasma membrane in the absence of UNC93B1 expression. We also observed colocalization of TLR3 and SREC-I in the endo/lysosomal compartment in the presence of Poly I:C in bone marrow derived macrophages (data not shown). As these two receptors are localized in ER or endosomal membrane compartments without or with Poly I:C respectively, it could be predicted that activated SREC-I might be an ER to cell surface trafficking/translocating receptor for TLR3. Thus SREC-I could potentially substitute for UNC93B1 in cells lacking or deficient in UNC93B1 expression.

We next asked whether SREC-I could interact physically with TLR3 using co-immunoprecipitation analysis. Indeed, SREC-I was minimally co-immunoprecipitated with TLR3 by exposure of HEK293-TLR3 stable cells overexpressing SREC-I-GFP to Poly I:C (Fig. 2). We did not see any sort of interaction between these two receptors in the absence of TLR3 ligand. Thus these two receptors might interact directly in response to Poly I:C.

We next examined signaling pathways that could potentially transmit the effects of poly I:C-induced SREC-I–TLR3 interactions into the cytoplasm. We investigated activity of the NFκβ pathway and of the MAP kinases, p38 and c-jun kinase (JNK) using phospho-specific antibodies that detect the phosphorylated, active forms of p65, p38 and JNK (Fig. 3A–C) and NFκβ activity was also monitored by the SEAP promoter-reporter assay (Fig. 3F). Experiments were initially carried out in HEK293 cells with forced expression of: (a) neither receptor, (b) TLR3 alone or (c) TLR3 plus SREC-I. We found



Hek 293-TLR3
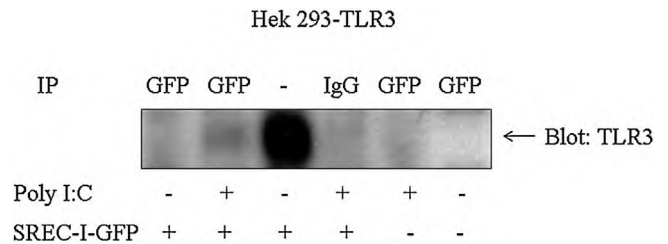
**Fig. 2.** TLR3 was associated with SREC-I in the presence of Poly I:C in HEK293 cells. HEK293 cells stably expressing TLR3 was transfected with SREC-I-GFP for 22 h. Cells were then treated with or without 10 μg/ml Poly I:C for 30 min. Cell lysates were collected and SREC-I-GFP was immunoprecipitated using anti-GFP antibody and anti-GFP Ab and then the precipitated complexes were subjected to SDS–PAGE analysis followed by blotting for TLR3 using anti-TLR3 antibody. Experiments were carried out twice, reproducibly.

that maximal activation of p38, JNK and NFκB required both TLR3 and SREC-I (Fig. 3A–C). Likewise with NFκB reporter assays, maximal NFκB activation required expression of both TLR3 and SREC-I (Fig. 3E).

We also carried out parallel experiments on NFκB activity in BMDM and observed an elevated level of phospho-p65 in BMDM expressing both TLR3 and SREC-I (Fig. 3D). As BMDM express both receptors constitutively, levels of SREC-I were modulated by RNA interference using siRNA. Indeed, BMDM cells knocked down for SREC-I showed decreased levels of phosphorylated p65 comparing to the level seen in cells expressing both receptors (Fig. 3D).

We next measured activity of IFR3 (Interferon Regulatory factor 3) in BMDM cells expressing both TLR3 and SREC-I or cells expressing TLR3 alone (SREC-I was knocked down using siRNA). IRF3 plays a critical role in immunity to DNA and RNA viruses and becomes phosphorylated in the presence of dsRNA (Gu et al., 2014). We observed the level of phosphorylated IFR3 in BMDM to be increased in cells expressing both SREC-I and TLR3, in the presence of Poly I:C, compared to TLR3 only where activation was minimal (Fig. 3F).

We next studied the role of SREC-I in Poly I:C-mediated cytokine release. We used an array approach to examine a range of cytokines. Assays were carried out on wild type, undifferentiated THP1 monocytic cells overexpressing TLR3 with or without SREC-I (Fig. 4). Secretion of IL-8 (Interleukin-8) from THP1 cells was minimal in the absence of ligand when either receptor was absent (Fig. 4). However, ligand-dependent secretion of IL-8 was strongly enhanced when SREC-I was overexpressed along with TLR3 (compared to TLR3 alone). There were minimal SREC-I mediated changes in secretion of other cytokines including IFNγ and TNFα. As IL-8 seemed a major target for Poly I:C–SREC-I–TLR3, we then examined a range of other chemokines (Fig. 4B). As in Fig. 4A, IL-8 was released at maximum levels by THP1 cells expressing both receptors in the presence of Poly I:C compared to control cells, while the release of MCP-1, RANTES, IP-10 and MIG was strongly induced in the presence of TLR3 with or without SREC-I overexpression (Fig. 4B). We observed an approximate 2.5-fold increase in IL-8 release in cells expressing both SREC-I and TLR3 compared with those expressing TLR3 alone (Fig. 4B). Again these effects were specific for IL-8 and were not duplicated for the other chemokines.

We then investigated the role of MAPK phosphorylation in IL-8 and IL-6 secretion by THP1 cells. THP1 cells engineered to overexpress both SREC-I and TLR3 released significantly more IL-8 in the presence of 10 μg of Poly I:C in comparison to the cells expressing SREC-I or TLR3 only (Fig. 5A). SREC-I alone did not mediate a detectable response to Poly I:C. Release of IL-6 after Poly I:C exposure was similarly regulated by SREC-I and TLR3 (Fig. 5C). Earlier we had observed an increase in phosphorylation of MAP kinases in cells expressing both TLR3 and SREC-I in the presence of Poly I:C (Fig. 2A and B). We now examined whether activation of these
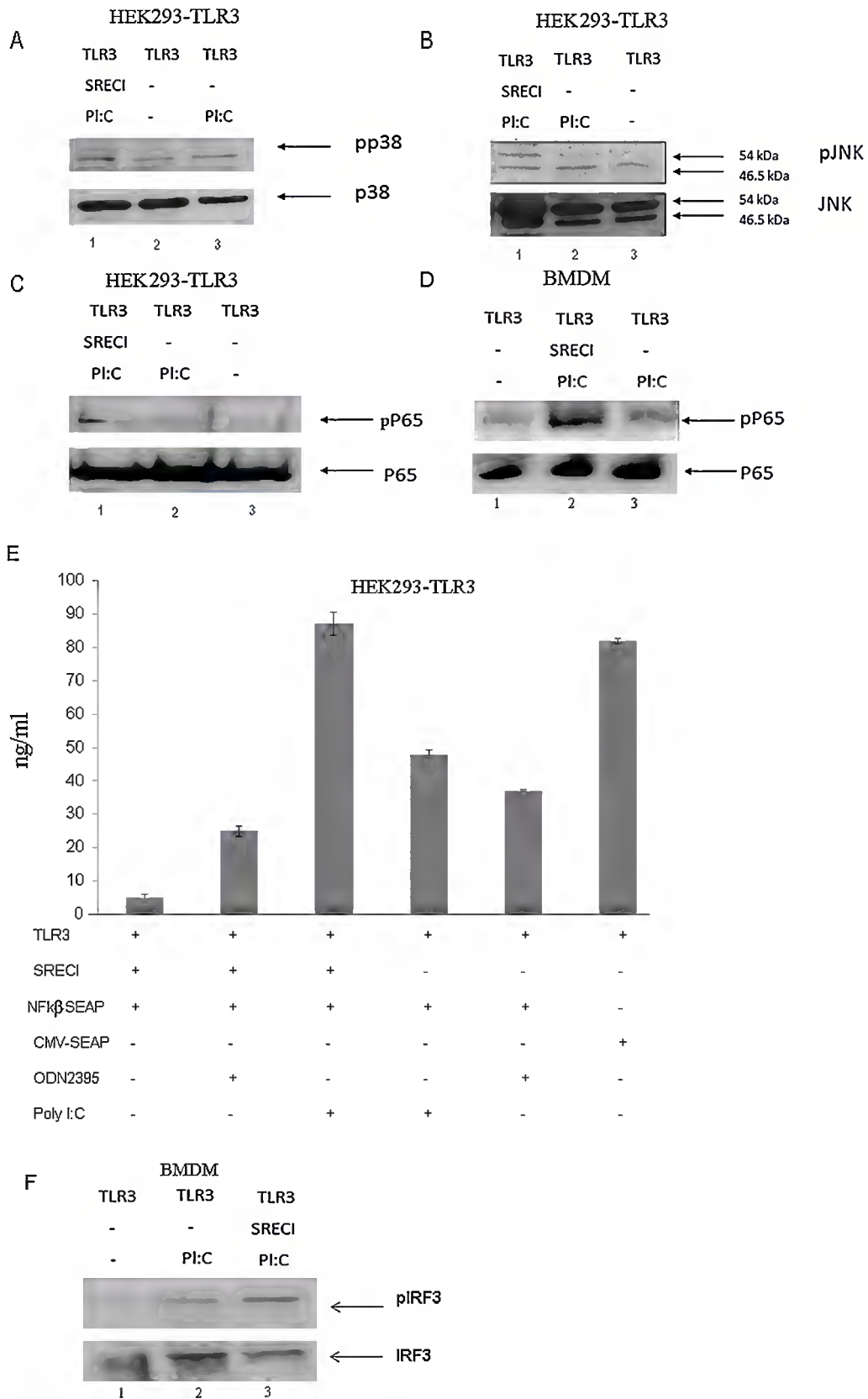
**Fig. 3.** Poly I:C enhanced MAP Kinase and NFκβ activity in the presence of both TLR3 and SREC-I. (A–C) HEK293–TLR3 cells were transfected with SREC-I or untransfected HEK293–TLR3 cells were then incubated with or without Poly I:C (10 μg/ml) for 2 h. Cell lysates were collected and then subjected to SDS–PAGE and western blotting with appropriate antibodies. (D) Bone marrow derived macrophages (BMDM) were transfected with siRNA of SREC-I for 72 h. Cells were then incubated with Poly I:C (or not) as in (A). Cell were lysed and equal amount of protein were subjected to SDS–PAGE and western blotting using anti-phospho-p65 antibody and anti-p65 antibody. (E) BMDM cells were treated as in (D) and then cell lysates were subjected to SDS–PAGE and western blotting using antibodies shown in (E). (F) HEK293–TLR3 cells were transfected with SREC-I or not and also NFκβ-SEAP/CMV-SEAP constructs. Cells were incubated with Poly I:C (10 μg/ml)/ODN2395 (10 μg/ml), a non TLR3 ligand. NFκβ activity was measured as instructed by NFκβ-SEAporter assay kit. Similar results were observed in two separate experiments.
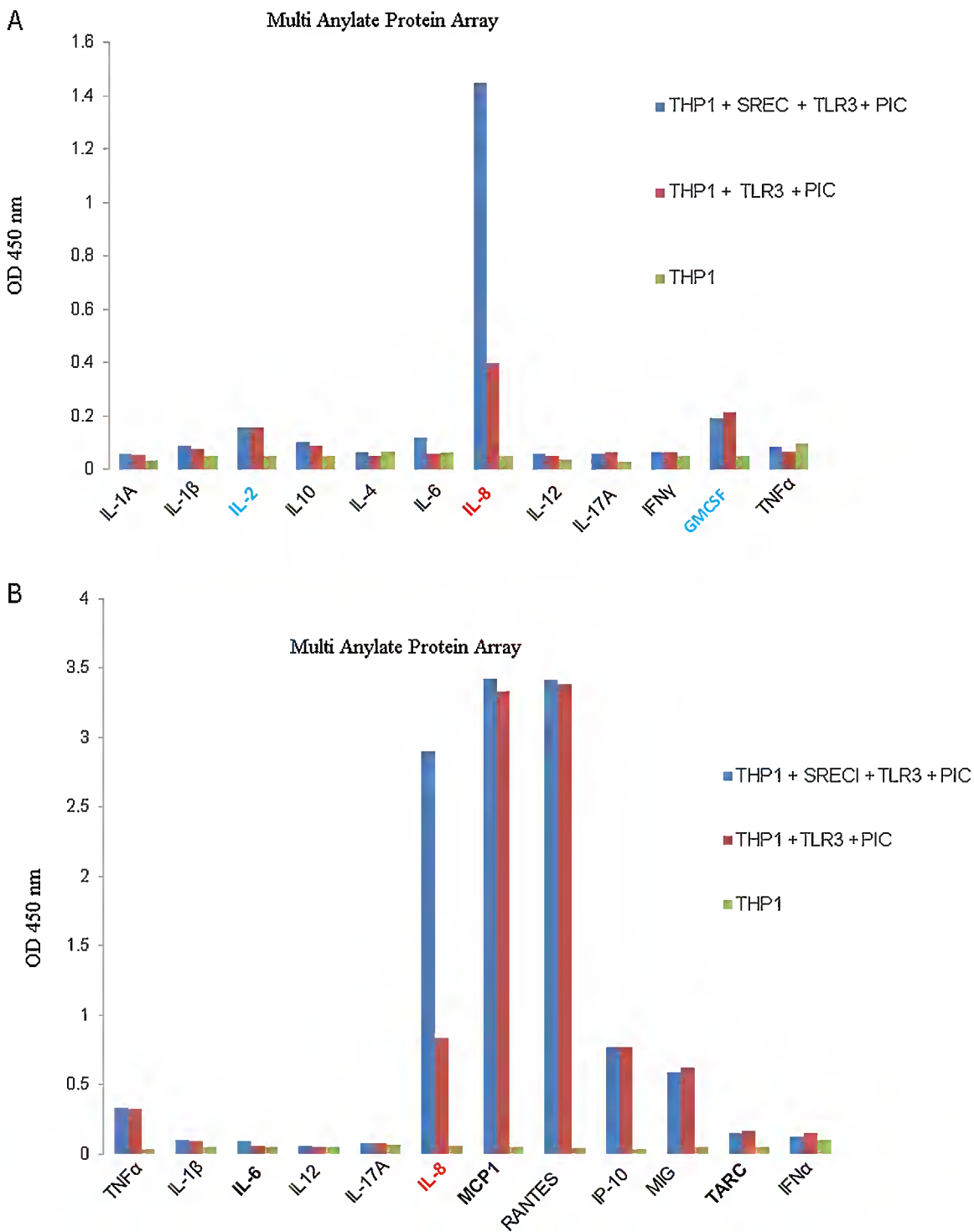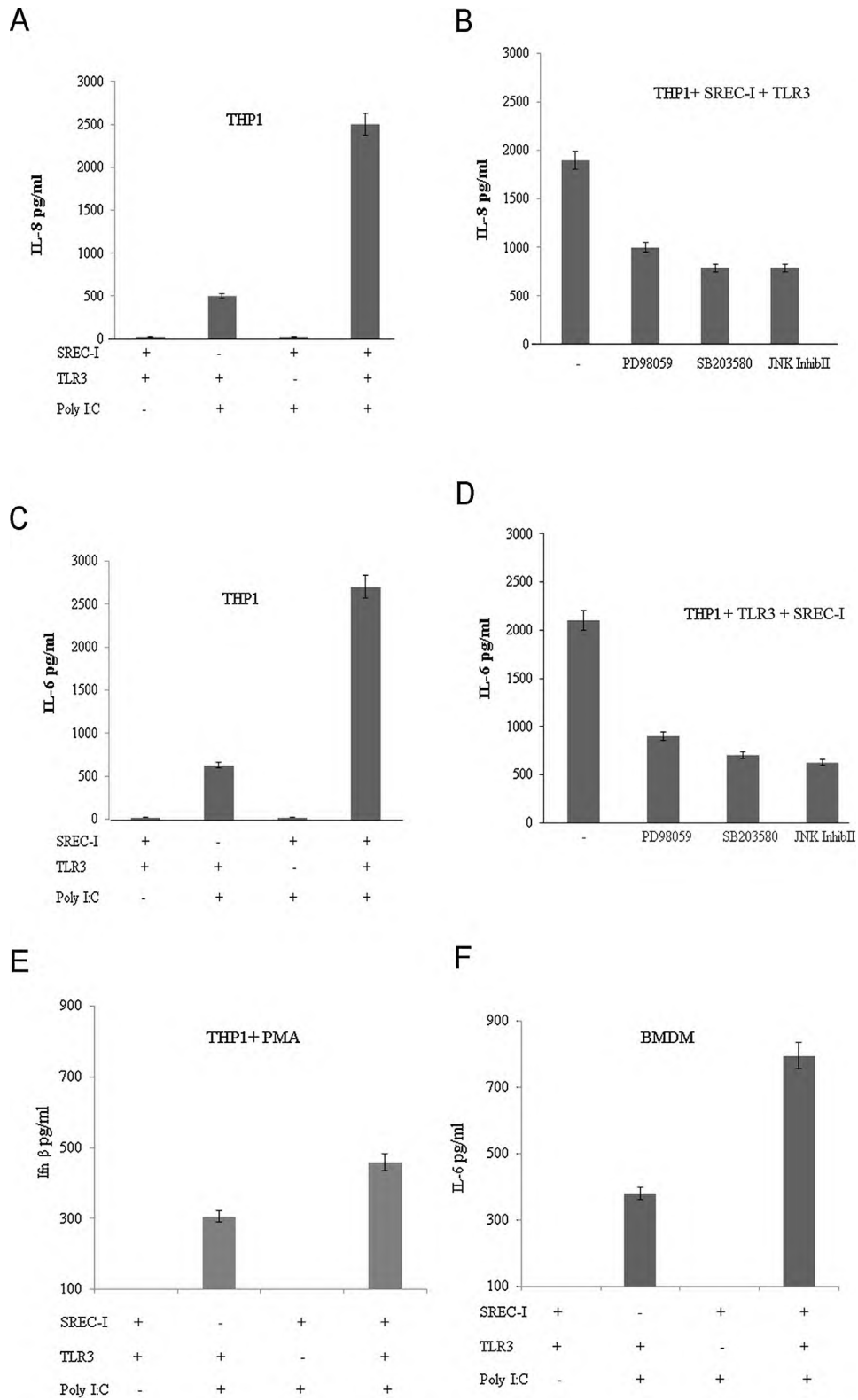
**Fig. 4.** SREC-I enhanced IL-8 release from THP1 cells in the presence of TLR3 ligand. (A) THP1 cells were transfected with TLR3 or TLR3 and SREC-I expression plasmids for 22 h. Cells were incubated with 10 μg Poly I:C for 12 h and then assayed for cytokine production using a human cytokine multianylate ELISA array kit according to manufacturer's protocol. (B) THP1 cells treated as in (A) and then assayed for chemokines using multianylate ELISA array kit according to Manufacturer's protocol. Data represent the mean of two independent experiments.

upstream MAP kinase pathways was necessary for IL-8 and IL-6 release by these cells. THP1 cells were incubated with PD98059 a specific ERK inhibitor, SB203580 a p38 inhibitor or the JNK inhibitor II for 1 h before incubation with Poly I:C (Fig. 5B and D). We observed sharp decreases in both Poly I:C-induced IL-8 and IL-6 release when the cells were exposed to each of these inhibitors prior to incubation with Poly I:C. It therefore seemed that, cytokine release involved activation of each of the three MAP kinase pathways. We

also observed increased secretion of IL-6 in an alternative cell type, BMDM expressing both TLR3 and SREC-I (Fig. 5F). Knocking down either of these receptors by siRNA decreased secretion of this proinflammatory cytokine, Il-6 by these cells (Fig. 5F).

We next examined the release of the IRF3 target cytokine IFNβ in THP1 after differentiation of these cells to macrophages with PMA for a prolonged period, 72 h (Fig. 5E). (Differentiation upregulates TLR3 to detectable levels – data not shown.) Wild

**Fig. 5.** Poly I:C–SREC-I–TLR3-induced IL-8 release required MAP Kinase activity. (A) THP1 cells were transfected with TLR3/SREC-I or TLR3 and SREC-I expression plasmids for 22 h. Cells were incubated with Poly I:C (10 μg/ml) for 12 h and then assayed for IL-8 release. (B) THP1 cells were transfected with SREC-I and TLR3 for 22 h and then incubated with the ERK inhibitor (PD98059), p38 inhibitor (SB203580) or the JNK inhibitor (JNK inhibitor II) (10 μM) for 1 h right before incubation with incubation with Poly I:C for 12 h. IL-8 secretion was assayed according to manufacturer's instructions. (C) THP1 cells were treated as in (A) and then IL-6 release was assayed according to manufacturer's instruction. (D) THP1 cells were treated as in (B) and IL-6 release was assayed. (E) THP1 cells were treated with PMA (5–10 ng/ml) for 72 h. Cells were then transfected with siRNA SREC-I or siRNA TLR3. Cells were incubated with Poly I:C for 12 h and then IFNβ release was measured according to manufacturer's protocol. (F) BMDM cells were transfected with siRNA SREC-I/TLR3 or not. Wild type or TLR3 knocked down (siRNA) cells were also treated with 1–5 ng/ml of LPS for 12 h. Cells were then incubated with Poly I:C for 12 h. Secreted IL-6 in media was measured according to manufacturer's protocol. Experiment was repeated twice. Data shown are the mean ± SD of results from those two experiments.
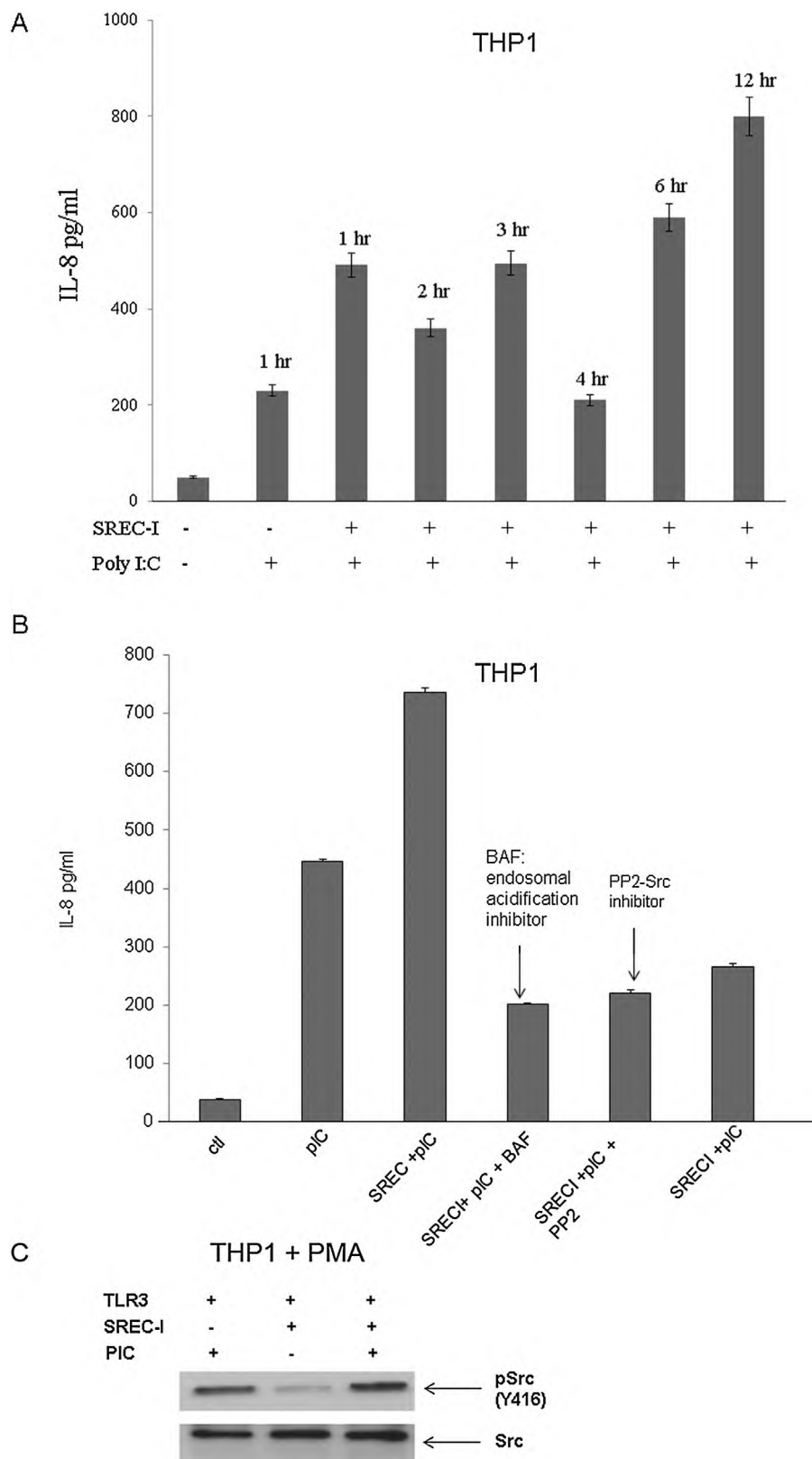
**Fig. 6.** Poly I:C-TLR3-mediated IL-8 release required SREC-I mediated internalization and acidification of endosomes. (A) THP1–TLR3 cells were transfected with or without SREC-I for 22 h and then incubated with 10 μg Poly I:C for indicated time. IL-8 release from cells was then assayed. (B) THP1-TLR3 cells were transfected as in (A) and then incubated with or without Bafilomycin A (0.2 μM for 20 min) or PP2 (10 μM for 12 h). Cells were incubated with Poly I:C for 12 h and then IL-8 release from THP1 cells were assayed. (C) Differentiated THP1 cells were transfected with siRNA SREC-I for 72 h and then cells were treated with Poly I:C (10 μg/ml) for 2 h. Cells were then lysed and equal amount of protein in lysate were subjected to SDS–PAGE and western blotting using appropriate antibodies. Experiments were carried out twice reproducibly.

type differentiated THP1 macrophages were also treated with LPS (1–5 ng/ml) for 12 h for inducing SREC-I expression prior to incubation with Poly I:C (Fig. 5E). It has been shown earlier that LPS incubation can induce expression of SREC-I in macrophages (Tamura et al., 2004). These cells were then transfected with either siRNA species targeting SREC-I or TLR3. Cells expressing TLR3 only (SREC-I knockdown) responded to Poly I:C to release IFNβ while secretion was increased when cells expressed both the receptors (Fig. 5E). A limited number of parallel experiments were carried out on BMDM. We observed sharp increases in IL-6 release by BMDM expressing IRF3 treated with Poly I:C and these were amplified by SREC-I expression.

Since IL-8 release in the presence of Poly I:C and SREC-I was significant in the experiments shown earlier, we next focused on this cytokine. In kinetic studies, we found IL-8 secretion to be significantly increased after 1 h incubation with Poly I:C when THP1 cells overexpressed both receptors (Fig. 6A). We also noticed that the amount of IL-8 release was decreased with 4 h incubation with Poly I:C (Fig. 6A). Later we also observed a second wave of IL-8 release after 6 h and 12 h incubation with Poly I:C in the same THP1 cells overexpressing both SREC-I and TLR3. Although we saw earlier that both TLR3 and SREC-I could be colocalized on the surface in the presence of Poly I:C, it was not clear whether signaling was initialized at the cell surface or at the endosomal site.

In previous studies we had observed that, in case of LPS–TLR4–SREC-I signaling, the kinase c-Src was necessary for cytokine release and internalization of ligand–receptor complexes. In addition, it was not clear whether MAP kinase signaling was initiated at the cell surface upon Poly I:C–TLR3 interaction or in the endosomes after internalization of Poly I:C–TLR3–SREC-I complexes. TLR3 activation and ligand binding affinity have been shown to be dependent on both dsRNA length and pH (Cain et al., 1989; de Bouteiller et al., 2005). It was additionally shown that slightly acidic pH (pH 4.5–6.7) was optimum for dsRNA–TLR3 response (de Bouteiller et al., 2005). Even though plasma membrane association of both the receptors SREC-I and TLR3 with Poly I:C was detected above, it was not clear whether this ligand–receptor interaction could initiate signaling from the plasma membrane. We therefore examined the effects of c-Src inhibition as well as blockade of endosomal acidification on IL-8 release. We observed inhibition of Poly I:C-induced cytokine release after incubation with Bafilomycin A (inhibitor of endosomal acidification) treatment as well as PP2 (the Src kinase inhibitor) (Fig. 6B) in THP1 expressing both TLR3 and SREC-I. We knocked down SREC-I and found a sharp decrease in IL-8 release compared to that of cells expressing both receptors (Fig. 6B, lanes 3 and 6). Our findings suggested that both c-Src activity and endosomal acidification were required for IL-8 secretion induced by formation of an activated Poly I:C–TLR3–SREC-I complex. In control experiments, we also observed increased phosphorylated cSrc (Y416) in differentiated THP1 macrophage cells expressing TLR3 and SREC-I compared to cells not treated with Poly I:C (Fig. 6C).

## Discussion

Our experiments demonstrated that SREC-I could influence the intracellular location of TLR3, the rate of MAPK and NFκβ signaling and the degree of cytokine expression in monocytes and macrophages exposed to Poly I:C (Fig. 7). SREC-I thus could be important in antiviral responses in monocytes and macrophages. Our data suggested that SREC-I could mediate Poly I:C induced trafficking of TLR3 from the ER to the plasma membrane and to endosomes at which site activated TLR3 likely mediated signaling to NFκβ, IRF3 and the MAPK family (Liu et al., 2008). Localization of SREC-I to endosome/lysosome organelles may be key, as signaling through TLR3 was shown previously to require the low pH
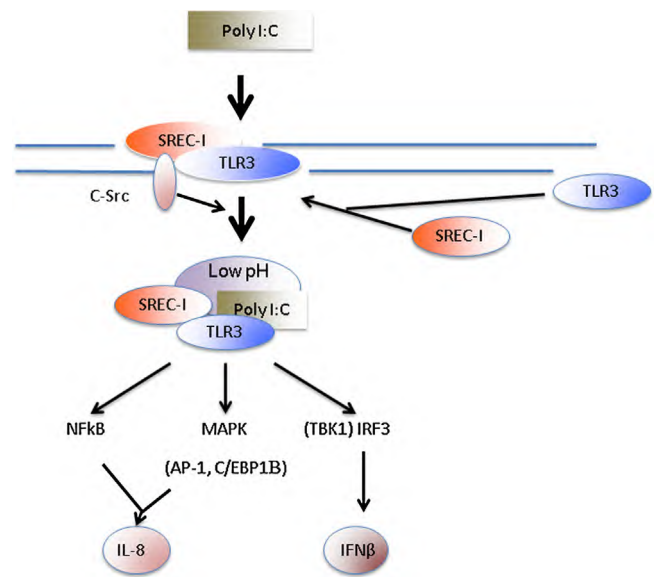


**Fig. 7.** Role of SREC-I in response to double stranded RNA. Double stranded RNA species Poly I:C interacts with macrophages leading to recruitment of SREC-I and TLR3 to the cell surface where they form a membrane complex that interacts with c-Src. The latter kinase then regulates endocytosis of the SREC-I/TLR3/Poly I:C complexes in endosomes. The complex finally resides in endosomes with low intravesicular pH, marked with lysosomal protein LAMP1. TLR3 is able to signal from such complexes and launches NFκB, MAPK and IRF3 signaling. (IRF3 is activated by the kinase TBK1.) Activated NFκB, AP-1 and C/EBPβ are known to interact with the IL-8 gene while activated IRF3 leads to synthesis of IFN-β.

environment offered by these compartments (de Bouteiller et al., 2005; Cain et al., 1989). Interestingly SREC-I appeared to have a similar effect on MHC class II signaling in DC in which, in previous studies, we saw trafficking of MHC class II molecules through an ER > plasma membrane > endosome/lysosome pathway in a SREC-I dependent manner. In this case the end result was increased antigen presentation by the MHC class II molecules and triggering of adaptive immunity rather than the effects on innate immunity envisaged here. Among pro-inflammatory cytokines, SREC-I appeared to strongly bias expression towards IL-8 (Fig. 4). The IL-8 promoter has been shown to interact with the factors NFκB, AP-1 and C/EBP β. This is consistent with the cell signaling experiments carried out here as AP-1 and C/EBP β activated downstream of MAPK signaling (Fig. 3). However, these factors are also involved in activation of many other cytokines, suggesting a novel input from SREC-I signaling that is selective for IL-8. The large intracellular domain of SREC-I is largely uncharacterized and future studies of this structure may clarify such regulation (A. Murshid & SK Calderwood, unpublished).

TLR3 has been shown to participate in adaptive immunity by triggering maturation of CD8α+ DC and T cell activation in response to virally infected cells. SREC-I, which was shown previously to be present in DC, could play a significant role in this regard as it appeared to be involved in engulfment of cell corpses (Ramirez-Ortiz et al., 2013). SREC-I was identified as a paralog of the *Caenorhabditis elegans* engulfment factor CED-1 (Zhou et al., 2001). SREC-I could thus contribute to cell corpse engulfment as well as assisting in the TLR3 response to viral PAMPs such as ds RNA in the dead cells, leading to inflammatory signaling cascades including the NFκβ pathway upstream of DC maturation (Ramirez-Ortiz et al., 2013). Our current studies showed sturdy activation of NFκB by Poly I:C downstream of SREC-I–TLR3 interactions (Fig. 3). Mature CD8α+ DC could then signal to CD4+ and CD8+ T cells and trigger an antigen-specific immune response to virus. The role of IL-8 in the antiviral response is less clear. However IL-8 was shown to induce

chemotaxis of target cells as well as endocytic activity in respiratory tract infection with Respiratory Syncytial Virus and was thus associated with extravasation and trafficking of leukocytes to infected regions (Fiedler et al., 1995; Hacking et al., 2004). Recent studies have shown that Poly I:C induced proinflammatory cytokine release required activation of MAP kinase, ERK, p38 and JNK and phosphorylation of p65 subunit of NFκβ (Liu et al., 2008). We found that the activation of MAP kinase and NFκβ in the presence of Poly I:C and TLR3 only was relatively minor compared to cells expressing both TLR3 and SREC-I, suggesting that this scavenger receptor participated in Poly I:C recognition and internalization as well as immune signaling.

## Conflict of interest

There are no conflicts of interest for any of the authors regarding this manuscript.

## Acknowledgements

## References

Akira, S., Takeda, K., 2004. Toll-like receptor signalling. Nat. Rev. Immunol. 4, 499–511.

Alexopoulou, L., Holt, A.C., Medzhitov, R., Flavell, R.A., 2001. Recognition of double-stranded RNA and activation of NF-kappaB by Toll-like receptor 3. Nature 413, 732–738.

Andrade, W.A., Souza, Mdo.C., Ramos-Martinez, E., Nagpal, K., Dutra, M.S., Melo, M.B., Bartholomeu, D.C., Ghosh, S., Golenbock, D.T., Gazzinelli, R.T., 2013. Combined action of nucleic acid-sensing Toll-like receptors and TLR11/TLR12 heterodimers imparts resistance to *Toxoplasma gondii* in mice. Cell Host Microbe 13, 42–53, http://dx.doi.org/10.1016/j.chom.2012.12.003.

Beutler, B., 2004. Innate immunity: an overview. Mol. Immunol. 40, 845–859.

Brinkmann, M.M., Spooner, E., Hoebe, K., Beutler, B., Ploegh, H.L., Kim, Y.M., 2007. The interaction between the ER membrane protein UNC93B and TLR3, 7, and 9 is crucial for TLR signaling. J. Cell Biol. 177, 265–275.

Cain, C.C., Sipe, D.M., Murphy, R.F., 1989. Regulation of endocytic pH by the Na+K+-ATPase in living cells. Proc. Natl. Acad. Sci. USA 86, 544–548.

Chuang, T.H., Lee, J., Kline, L., Mathison, J.C., Ulevitch, R.J., 2002. Toll-like receptor 9 mediates CpG-DNA signaling. J. Leukoc. Biol. 71, 538–544.

de Bouteiller, O., Merck, E., Hasan, U.A., Hubac, S., Benguigui, B., Trinchieri, G., Bates, E.E., Caux, C., 2005. Recognition of double-stranded RNA by human toll-like receptor 3 and downstream receptor signaling requires multimerization and an acidic pH. J. Biol. Chem. 280, 38133–38145.

Fiedler, M.A., Wernke-Dollries, K., Stark, J.M., 1995. Respiratory syncytial virus increases IL-8 gene expression and protein release in A549 cells. Am. J. Physiol. 269, L865–L872.

Gu, M., Zhang, T., Lin, W., Liu, Z., Lai, R., Xia, D., Huang, H., Wang, X., 2014. Protein phosphatase PP1 negatively regulates the Toll-like receptor- and RIG-I-like receptor-triggered production of type I interferon by inhibiting IRF3 phosphorylation at serines 396 and 385 in macrophage. Cell Signal. 26 (12), 2930–2939.

Hacking, D., Knight, J.C., Rockett, K., Brown, H., Frampton, J., Kwiatkowski, D.P., Hull, J., Udalova, I.A., 2004. Increased in vivo transcription of an IL-8 haplotype associated with respiratory syncytial virus disease-susceptibility. Genes Immun. 5, 274–282.

Kim, Y.M., Brinkmann, M.M., Paquet, M., Ploegh, H.L., 2008. UNC93B1 delivers nucleotide-sensing toll-like receptors to endolysosomes. Nature 452, 234–238, http://dx.doi.org/10.1038/nature06726.

Kumar, A., Zhang, J., Yu, F.S., 2006. Toll-like receptor 3 agonist poly(I:C)-induced antiviral response in human corneal epithelial cells. Immunology 117, 11–21.

Liu, Y., Kimura, K., Yanai, R., Chikama, T., Nishida, T., 2008. Cytokine, chemokine, and adhesion molecule expression mediated by MAPKs in human corneal fibroblasts exposed to poly(I:C). Invest. Ophthalmol. Vis. Sci. 49, 3336–3344, http://dx.doi.org/10.1167/iovs.07-0972.

McGettrick, A.F., O'Neill, L.A., 2010. Curr. Opin. Immunol. 22, 20–27, http://dx.doi.org/10.1016/j.coi.2009.12.002.

Murshid, A., Gong, J., Calderwood, S.K., 2010. Heat shock protein 90 mediates efficient antigen cross presentation through the scavenger receptor expressed by endothelial cells-I. J. Immunol. 185, 2903–2917, http://dx.doi.org/10.4049/jimmunol.0903635.

Pifer, R., Benson, A., Sturge, C.R., Yarovinsky, F., 2011. UNC93B1 is essential for TLR11 activation and IL-12-dependent host resistance to *Toxoplasma gondii*. J. Biol. Chem. 286, 3307–3314, http://dx.doi.org/10.1074/jbc.M110.171025.

Pirher, N., Ivicak, K., Pohar, J., Bencina, M., Jerala, R., 2008. A second binding site for double-stranded RNA in TLR3 and consequences for interferon activation. Nat. Struct. Mol. Biol. 15, 761–763, http://dx.doi.org/10.1038/nsmb.1453.

Pohar, J., Pirher, N., Benčina, M., Manček-Keber, M., Jerala, R., 2013. The role of UNC93B1 protein in surface localization of TLR3 receptor and in cell priming to nucleic acid agonists. J. Biol. Chem. 288, 442–454, http://dx.doi.org/10.1074/jbc.M112.413922.

Pohar, J., Pirher, N., Benčina, M., Manček-Keber, M., Jerala, R., 2014. The ectodomain of TLR3 receptor is required for its plasma membrane translocation. PLoS One 9, e92391, http://dx.doi.org/10.1371/journal.pone.0092391.

Ramirez-Ortiz, Z.G., Pendergraft 3rd, W.F., Prasad, A., Byrne, M.H., Iram, T., Blanchette, C.J., Luster, A.D., Hacohen, N., El Khoury, J., Means, T.K., 2013. The scavenger receptor SCARF1 mediates the clearance of apoptotic cells and prevents autoimmunity. Nat. Immunol. 14, 917–926, http://dx.doi.org/10.1038/ni.2670.

Takahashi, N., Yamada, T., Narita, N., Fujieda, S., 2006. Double-stranded RNA induces production of RANTES and IL-8 by human nasal fibroblasts. Clin. Immunol. 118, 51–58.

Tamura, Y., Osuga, J., Adachi, H., Tozawa, R., Takanezawa, Y., et al., 2004. Scavenger receptor expressed by endothelial cells I (SREC-I) mediates the uptake of acetylated low density lipoproteins by macrophages stimulated with lipopolysaccharide. J. Biol. Chem. 279 (30), 30938–30944.

Zhou, Z., Hartwieg, E., Horvitz, H.R., 2001. CED-1 is a transmembrane receptor that mediates cell corpse engulfment in *C. elegans*. Cell 104, 43–56.

**Autores:** Ayesha Murshid, Jianlin Gong, Thomas Prince, Thiago J. Borges, Stuart K. Calderwood

**Situação:** Publicado

**Revista:** *PLoS ONE*

**Referência:** PLoS One. 2015 Apr 2;10(4):e0122529. doi: 10.1371/journal.pone.0122529.

**Website:** http://journals.plos.org/plosone/article?id=10.1371/journal.pone.0122529

**Motivação:** Esse trabalho foi realizado durante o período sanduíche realizado no Hospital Beth Israel Deaconess Medical Center, no laboratório do Prof. Stuart K. Calderwood.

# Scavenger Receptor SREC-I Mediated Entry of TLR4 into Lipid Microdomains and Triggered Inflammatory Cytokine Release in RAW 264.7 Cells upon LPS Activation

Ayesha Murshid[1], Jianlin Gong[2], Thomas Prince[1], Thiago J. Borges[1,3], Stuart K. Calderwood[1]*

1 Molecular and Cellular Radiation Oncology, Beth Israel Deaconess Medical Center, Harvard Medical School, Center for Life Sciences, 3 Blackfan Circle, Boston, Massachusetts, United States of America, 2 Stress Response Center, Boston University Medical Center, Boston, Massachusetts, United States of America, 3 School of Biosciences and Biomedical Research Institute, Pontifícia Universidade Católica do Rio Grande do Sul (PUCRS), Porto Alegre, RS, Brazil

* scalderw@bidmc.harvard.edu

## Abstract

Scavenger receptor associated with endothelial cells I (SREC-I) was shown to be expressed in immune cells and to play a role in the endocytosis of peptides and antigen presentation. As our previous studies indicated that SREC-I required intact Toll-like receptor 4 (TLR4) expression for its functions in tumor immunity, we examined potential interactions between these two receptors. We have shown here that SREC-I became associated with TLR4 on binding bacterial lipopolysaccharides (LPS) in RAW 264.7 and HEK 293 cells overexpressing these two receptors. The receptors then became internalized together in intracellular endosomes. SREC-I promoted TLR4-induced signal transduction through the NF-kB and MAP kinase pathways, leading to enhanced inflammatory cytokine release. Activation of inflammatory signaling through SREC-I/TLR4 complexes appeared to involve recruitment of the receptors into detergent-insoluble, cholesterol-rich lipid microdomains that contained the small GTPase Cdc42 and the non-receptor tyrosine kinase c-src. Under conditions of SREC-I activation by LPS, TLR4 activity required Cdc42 as well as cholesterol and actin polymerization for signaling through NF-kB and MAP kinase pathways in RAW 264.7 cells. SREC-I appeared to respond differently to another ligand, the molecular chaperone Hsp90 that, while triggering SREC-I-TLR4 binding caused only faint activation of the NF-kB pathway. Our experiments therefore indicated that SREC-I could bind LPS and might be involved in innate inflammatory immune responses to extracellular danger signals in RAW 264.7 cells or bone marrow-derived macrophages.

## Introduction

SREC-I (scavenger receptor associated with endothelial cells) is the product of the *SCARF1* gene and is a member of the class F family of scavenger receptors (SR), transmembrane proteins with roles in endothelial cell biology and the immune response [1–4]. Like other SR, SREC-I was shown to bind a spectrum of ligands, including the modified proteins acetylated low density lipoprotein and products such as fungal pathogens [5, 6]. SREC-I also bound heat shock protein 90 (Hsp90)-antigen/peptide complexes and thus transmitted the immunostimulatory effects of these chaperone-antigen complexes into antigen presenting cells [2]. Our previous studies also indicated roles for Toll Like Receptors (TLRs) and an associated adaptor molecule MyD88 (myeloid differentiation primary response 88 protein) in the immune effects of HSP vaccines [3].

TLR4 was shown previously to induce inflammatory signaling when bound to LPS derived from Gram negative bacteria [7]. Sequence analysis showed that TLR4 contains an intracellular TIR domain (Toll/IL-1 receptor (TIR) homology domain) shared with the IL-1R, a motif involved in signal transduction [7]. All TLRs were shown to belong to the PRR (pattern recognition receptor) class, shown to recognize pathogen-associated molecular patterns (PAMPs) and thus contribute to innate immunity [8, 9]. Each member of the TLR family has been shown to be distinct in recognizing unique PAMPs derived from different organisms and selectively launching inflammatory signals [7, 8]. After exposure to LPS, TLR4 was shown to stimulate inflammatory gene expression by activating transcription factors including NF-kB, IRF3, NF-IL6 and AP-1 [10, 11]. Such transcriptional activation led to, in turn, the expression and secretion of cytokines, chemokines, type I interferons (IFN-1) and other proinflammatory mediators. However, TLR4 did not bind directly to LPS and was instead shown to rely on primary cell surface receptors, most notably CD14 to associate with the ligand [12, 13]. In addition, the protein MD2 was associated with TLR4 on the cell surface and conferred responsiveness to LPS [14]. However, CD14 did not appear to play an exclusive role in LPS responses and a fraction of the TLR4 activity was observed even under CD14 knockout conditions [15]. Recent studies suggested that SR could interact with TLR4 and mediate inflammatory signaling under some conditions [16]. We have focused on SREC-I in this regard, as our studies have shown this receptor to be involved in antitumor immunity in functional association with TLR2 and TLR4 [3, 17].

In the present study, we asked if SREC-I could interact directly with TLR4 to modify inflammatory signaling and cytokine expression. We showed that exposure to either LPS or the SREC-I ligand Hsp90 initiated profound levels of association of SREC-I with TLR4. In addition, SREC-I was able to mediate LPS-induced TLR4 signaling even in the absence of CD14, suggesting that this SR could act as a receptor for LPS. Although LPS and Hsp90 both triggered SREC-I-TLR4 interactions, LPS was more efficient in stimulating inflammatory signaling. Interestingly, ligand bound SREC-I appeared to play a dominant role in the intracellular localization of TLR4. Activation of SREC-I led to the sequestration of TLR4 in lipid microdomains enriched in cholesterol and signaling molecules such as c-src and Cdc42. Through this pathway, SREC-I appeared to mediate a component of LPS-induced cytokine release in macrophages.

## Methods and Materials

Experiments, where possible employed cells maintained in tissue culture. Some experiments however required fresh primary macrophages for physiological relevance. There were no similar methods or models available for these experiments and the methods and models used are the ones that are more effective for this immunological based treatment strategy. Approaches

to animal experimentation were based on guidelines taken from the Weatherall Report- "The use of non-human primates in research." Experiments are also conducted during the week so that lab personnel and ARF staff could adequately monitor mice. The animals were sacrificed humanely and then bones were taken to prepare bone marrow derived macrophages. We did not see any signs of pain and distress in this procedure. The databases of Pubmed, Medline and OVID were searched to determine if there were alternative methodsormodelsfor bone marrow studies for cytokine assayand we were able to find no alternatives. Experiments were approved by the BIDMC Animal Care Use Committee under IACUCC0792012, approved in 2012 and renewed on Nov 6, 2014 as: "The role of HSF1 and Hsp70 on innate immunity."

## Mice

C57BL/6, wild type (WT) mice were from the Jackson Laboratories, Maine. C57BL/6 TLR4 KO ($tlr4^{-/-}$) mice were obtained from S. Levitz (Boston Medical School). Mice were maintained in micro-isolator cages under specific pathogen free condition. C57BL/6 SCARF KO ($scarf^{-/-}$) tibia and fibula were a generous gift from Dr. Terry Means (Massachusetts General Hospital).

## Antibodies and Reagents

LPS (*E. coli* 0127:B8) was purchased from Sigma-Aldrich (St. Louis, MO). Ultrapure *E. coli* K12 (LPS-EK-ultrapure) was purchased from Invivogen, San Diego, CA. Mouse anti-human SREC-I monoclonal antibody was a gift from Dr. H. Adachi (Laboratory of Cellular Biochemistry, Riken, Saitama, Japan) and rabbit monoclonal mouse anti-SREC-I ab was custom synthesized by GenScript (Piscataway, NJ) against specific peptide sequence (TQGTQGSTLDPAGQC). Rabbit polyclonal anti p38, phospho p38, phospho-NF-kB, NF-kB, phospho ERK2/1, ERK2/1, phospho JNK, JNK antibodies were purchased from Cell Signaling Inc. The inhibitors and chemicals Cytochalasin D, methyl beta cyclo dextrin (MβCD), 4-amino-5-(4-methylphenyl) -7-(t-butyl) were from Sigma-Aldrich and pyrazolo [3,4-d]-pyrimidine (PP1) was from EMD Millipore Corp., Billerica, MA. *Clostridium difficile* toxin B (CTX-B) was purchased from Calbiochem Billerica, MA. Mouse monoclonal anti-FLAG antibody (M2) was purchased from Sigma-Aldrich, St. Louis, MO. FITC labeled anti-CD56 antibody was purchased from BioLegend, San Diego, CA.The ELISA kits were from R&D Systems, Minneapolis, MN and BD Biosciences, San Jose, CA. Alexa labeled LPS was from Life Technologies, Grand Island, NY. Mouse monoclonal anti HA antibody was from Covance, Dedham, MA. Mouse monoclonal anti-TLR4 antibody was from Abcam, Cambridge, MA. Antibodies for macrophage, anti-MAC1 and anti-F4/80 were from eBioscience, San Diego, CA. Hsp90 was purified by us from Sf9 cells as described and carefully tested for endotoxin contamination as also described previously [2, 18]. Endotoxin contaminated preparations were discarded. MyD88 and TRIF blocking peptides were purchased from Imgenex Corp., San Diego, CA and InvivoGen, San Diego, CA, respectively. Alexa labeled LPS (*E. coli* 0127:B8) was from Sigma-Aldrich, St. Louis, MO. OxLDL was from Biomedical Technologies Inc., Ward Hill, MA. The mouse anti SR-A antibody (2F8) was from Hycult Biotech., Plymouth Meeting, PA. Anti CD14 ab was from Abcam, Cambridge, MA and CD14 neutralizing ab was purchased from R&D Systems, Minneapolis, MN. Anti IRF3 and phospho-IRF3 were purchased from Cell Signaling, Danvers, MA.

## Cells and culture conditions

Wild type HeLa and HEK 293, Raw 264.7 cells were maintained in DMEM (with 4.5 g/L glucose) supplemented with 10% heat inactivated FBS, streptomycin and penicillin. HEK 293 expressing TLR4-CD14-MD2 cells were maintained in the medium described for HEK 293 and

HeLa cells with 100 µg/ml Normocin. CHO-SREC-I cells were maintained in F12K media supplemented with 10% heat inactivated FBS, streptomycin and penicillin and 400 µg/ml G418. All cells were maintained in a 5% $CO_2$ humidified incubator.

## Bone marrow-derived macrophage preparation

Macrophages were obtained from mouse bone marrow culture using the method described by Weischenfeldt and Porse (2008). Briefly, bone marrow macrophages were enriched by lysis of red cells. Cells were then passed through a cell strainer then grown in L929 conditioned medium for proliferation and differentiation into a homogenous population of mature bone marrow-derived macrophages.

## Plasmids and Transfection

The pcDNA3.1-SREC-I (human) was a generous gift from Dr. H. Adachi. The FLAG-SREC-I construct was constructed from the 3xFLAG-CMV vector. Human and mouse siRNA SREC-I and TLR4 was purchased from Santa Cruz Biotechnology Inc., Dallas, TX.

## SEAP reporter assay

The secreted form of embryonic alkaline phosphatase (SEAP)–NF-kB promoter-reporter assay kit was utilized as a convenient and sensitive method to determine promoter activity in cells transfected with the SEAP expression plasmid. HeLa cells were transfected with plasmids encoding FLAG-SREC-I, TLR4 and the reporter constructs NF-kB-SEAP and CMV- (control expression vector). NF-kB activity was measured indirectly by catalytic hydrolysis reaction of $p$-nitrophenyl phosphate producing a yellow end product that was read spectrophotometrically at 405 nm.

## Western Blotting and Immunoprecipitation

HEK 293 cells expressing TLR4 and SREC-I were treated with or without LPS and Hsp90. Cells were then washed with ice-cold Dulbecco's phosphate-buffered saline (PBS) and lysed in NP-40 lysis buffer (containing 1% Nonidet P-40, 150 mM NaCl, 1mM EDTA, 1 mM PMSF, 1x HALT protease and phosphatase inhibitor cocktail (Thermo Scientific). For Western blotting, 15–30 µg of protein were resolved by 4–15% gradient SDS-PAGE and transferred to PVDF (polyvinylidenefluoride) membranes. Membranes were immunoblotted with primary antibodies and later secondary antibodies that are HRP-conjugated. The membrane reactions were visualized by Perkin Elmer enhanced chemiluminescence reagents. For immunoprecipitation, 1 mg of cell extract was incubated with 5 µg of the selected antibody for 2 hours at 4°C followed by incubation with 20 ul of protein A (50% slurry, GE healthcare) plus-sepharose beads for either 2 hours at room temperature or overnight at 4°C. The beads were then washed with NP-40 lysis buffer and complexes were eluted by boiling in Laemmle sample buffer.

## Isolation of Lipid microdomain

Raw 264.7 cells (80–90% confluent) were incubated with or without ice cold LPS (1 µg/ml) for 3–5 minutes and then lysed with lysis buffer (Sigma) containing, 1% Triton X-100 and protease inhibitor cocktail (Sigma). Immediately before the assay, 1 ml of lysis buffer containing 1% Triton X-100 for each gradient was prepared on ice. The density gradient was made of 4 layers of OptiPrep with different concentrations: 35%, 25%, 20% and 0%. Lower layer (35% OptiPrep) contains the cell lysate. The 35% Gradient layer mixed with cell lysate was placed at the bottom of pre-cooled ultracentrifuge tube and then the centrifugation performed at ~200,000xg using

TFT 65.13 rotor for 4 hours at 4°C. Fractions including the fraction containing lipid microdomain were gently removed.

*ELISA*: IL-6, TNF-α were purchased from R&D Biosystem, Minneapolis, MN, BD Biosciences, San Jose, CA, PBL interferon sources, IFN-β was from West Logan, Utah. ELISA of cell media for cytokine release was performed for each cytokine according to manufacturer's protocol using appropriate antibody.

## LPS binding experiments by flow cytometry

Cells were preincubated without or with mBSA (50 mg/ml) or Alexa labeled LPS (1 μg/ml) at 4°C in FACS buffer (PBS containing 0.1% BSA and 0.05% NaN3). The cells were then washed with FACS buffer twice, fixed with 4% paraformaldehydefor 10 min, and analyzed for binding of Alexa-LPS with FACSCanto II and FACSDiva (BD Biosciences, San Jose, CA).

## Immunofluorescence and Microscopy

Cells were labeled or incubated with Alexa-LPS or FITC-anti-CD59 antibody on ice or at 37°C for 20–30 minutes then fixed with 4% para-formaldehyde and either permeabilized using 0.1% Triton X 100 (for visualizing intracellular proteins) or not (for surface expression or binding) using 0.1% Triton X 100. Cells were stained with primary antibodies and then washed three times with 1x PBS and stained again with fluorophore-conjugated secondary antibodies. Fluorophores were visualized using the following filter sets: 488 nm excitation and band pass 505–530 emission filter for Alexa 488; 543 nm excitation and band pass 560–615 for Cy3/Alexa 564; and 633 excitation and long pass 650 for Cy5.

## Results

### SREC-I was associated with TLR4 in the presence of LPS and was present in LPS-TLR4 complexes

We first investigated the effects of LPS on SREC-I the intracellular localization of SREC-I (Fig 1). As SREC-I was shown to be expressed at low levels in resting macrophages (B. Zhou & SK Calderwood, unpublished data), we carried out overexpression of the receptor in the mouse macrophage cell line Raw 264.7 to permit effective visualization by immunofluorescence. We then incubated these cells with *Escherichia coli* derived LPS (1 μg/ml) at 4°C, fixed the cells and analyzed SREC-I and TLR4 localization by confocal microscopy. Prior to LPS exposure, SREC-I was detected largely in the cytosol whereas TLR4 was mostly membrane-associated; minimal overlap between these fluorescence signals was observed (Fig 1A). However, TLR4 and SREC-I became partially coincident on the cell surface in the presence of LPS as indicated by the strong overlap in fluorescence patterns in cells at 4°C (Fig 1A and 1B). We then investigated internalization of TLR4 and SREC-I in LPS treated cells after warming the medium to 37°C (Fig 1C). LPS exposure prompted internalization of both receptors at 37°C and their relocation to intracellular vesicles, with some of these structures marked both by anti TLR4 and anti-FLAG antibodies (for SREC-I) (Fig 1D). We also showed fluorescent, Alexa-labeled LPS to be localized in intracellular vesicles containing TLR4 and SREC-I at 37°C, suggesting partial co-internalization of SREC-I, LPS and TLR4 (Fig 1C and 1D). As TLR4 was not shown previously to bind directly to LPS, these results suggested SREC-I to be a recognizing receptor for LPS and that could induce the recruitment of TLR4 to SREC-I marked regions on the cell surface. Although CD14 is a well-established LPS recognizing molecule cooperating with TLR4, our experiments suggested that SREC-I was also capable of recognizing the endotoxin and interacting with TLR4.
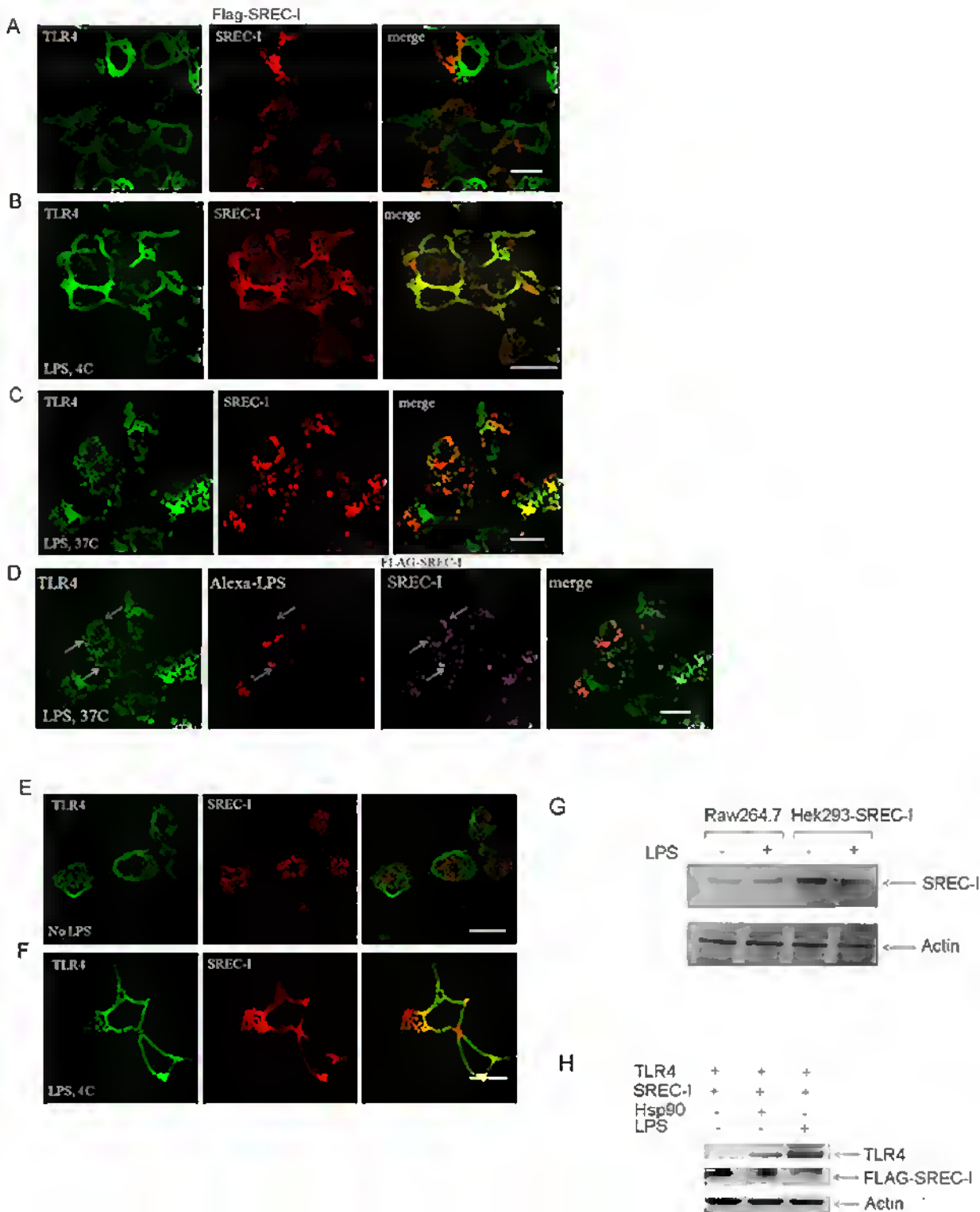
Fig 1. Ligand-bound SREC-I colocalized with TLR4 after LPS treatment. A, SREC-I and TLR4 did not interact in the absence of LPS. Raw 264.7 cells were transfected with FLAG-SREC-I for 22 hours. Cells were then fixed and stained with anti TLR4 ab (green) and anti-FLAG ab (red). B, TLR4 colocalized with SREC-I in the presence of LPS. Raw 264.7 cells overexpressing FLAG-SREC-I were exposed to LPS (1 µg/ml) for 20–30 min at 4°C. Cells were then fixed and stained for TLR4 (green) and FLAG (red). Percent colocalization with or without LPS is shown in the adjacent histogram. C, D, LPS, TLR4 and SREC-I were internalized at 37°C. Raw 264.7 cells overexpressing FLAG-SREC-I were incubated with Alexa LPS (1 µg/ml) at 4°C for 20 mins and then

medium was replaced with warm medium. Cells were then incubated at 37°C for 10–15 mins. Cells were fixed and stained for TLR4 (green, C, D) and FLAG-SREC-I (red in C, purple in D). Alexa LPS was shown in red (D). **E, F,** Endogenous TLR4 and SREC-I did not colocalize in the absence of LPS. Raw 264.7 cells were treated for 30 mins with LPS (1 μg/ml) and then fixed and stained for TLR4 (green) and SREC-I (red). **E,** TLR4 and SREC-I colocalize in the presence of LPS. Cells were labeled with LPS (1μg/ml) for 20–30 minutes at 4°C then fixed and stained for TLR4 (green) and SREC-I (red) (F). **G,** SREC-I expression level in Raw 264.7 cells and in cells overexpressing FLAG-SREC-I. **H,** SREC-I interacted with TLR4 physically in the presence of LPS (1 μg/ml). HEK 293 cells expressing FLAG-SREC-I and TLR4s were treated with or without Hsp90 or LPS. FLAG-SREC-I was then immunoprecipitated (IP) with FLAG ab. The IP complex was separated with SDS-PAGE and blotted for TLR4. The amount of FLAG-SREC-I immunoprecipitated was determined and β-actin was used as a loading control. All images were representative of 3 different planes from each sample. Each experiment was performed 3 times reproducibly. Scale bar, 5 μm.

To further confirm receptor co-association in the presence of LPS (1 μg/ml) under conditions of native expression, we next activated Raw 264.7 cells by pre-exposure to LPS (1–5 ng/ml) to increase expression of SREC-I to levels detectable by immunofluorescence (3) before experiment. After recovery from the activating LPS exposure for 24hr, cells were then transiently re-exposed to LPS (1 μg/ml) for 20–30 minutes on ice, then fixed and stained for SREC-I and TLR4 (Fig 1E and 1F). As with the overexpression studies, TLR4 and SREC-I appeared to become co-localized on the plasma membrane in the presence of LPS. We saw minimal evidence of co-localization of the receptors in controls in the absence of the endotoxin. Levels of SREC-I in Raw 264.7 cells used in (Fig 1E and 1F) and in FLAG-SREC-I overexpressed HEK 293 cells used in the experiment were shown in Fig 1G.

To investigate biochemically a physical interaction between TLR4 and SREC-I we next used HEK 293 cells (low in *Scavenger Receptors, SR* expression) for co-immunoprecipitation studies. These cells were used rather than Raw 264.7 to avoid the potentially complicating presence of other SR family members on SREC-I interaction with TLR4 (Fig 1H). While we found minimal evidence of co-precipitation of FLAG-SREC-I and TLR4 in control, unstimulated cells (lane 1) these proteins interacted substantially in the presence of either LPS or another SREC-I ligand, Hsp90 (Fig 1H, lanes 2, 3). These experiments indicated binding of SREC-I and TLR4 only in the presence of either TLR4 or SREC-I ligands such as Hsp90.

For these studies, we used LPS at a concentration of 1 μg/ml for the ligand-receptor localizationas this amount of LPS could bring its receptors CD14/SREC-I to the plasma membrane and bind efficiently and could easily be detected when dye-tagged.

## SREC-I enhanced LPS-TLR4 mediated NF-kB activity

As NF-kB is the most potent proinflammatory transcription factor, we examined the potential role of SREC-I in its activation by LPS. TLR4 activation has been shown to trigger activation of NF-kB. We next examined therefore the potential activity of SREC-I in LPS triggered NF-kB signaling in HEK 293 cells. As mentioned above, in contrast to Raw 264.7, HEK 293 cells were shown to be deficient in most SR family members (including SREC-I), thus SREC-I-specific effects could be examined in isolation in transfectants. This HEK 293 cell line stably expressed CD14, TLR4 and MD2; CD14 independent signaling was determined using CD14 blocking peptides (CD14-inh, 10 μg/ml), while the role of TLR4 was probed using RNA interference. The CD14 blocking peptide ab was first tested in THP1 cells by its ability to neutralize LPS-induced TNF-α secretion. The ab neutralized >60% of LPS induced cytokine release in this cell line. NF-kB activation was assayed by determining phosphorylation of its *trans*-activating subunit p65/Rel on serine 536 [19]. We then compared LPS-induced NF-kB signaling in cells expressing TLR4 and the LPS recognizing and signaling adaptor proteins CD14 and MD2 (Fig 2A, lane 1) without (lane 1) or with SREC-I (lane 2). LPS activated NF-kB in the absence of CD14 but with SREC-I expression (lane 2). Minimal signaling was observed in the absence of TLR4 with or without SREC-I (lanes 3, 4). This experiment showed therefore a role for SREC-I
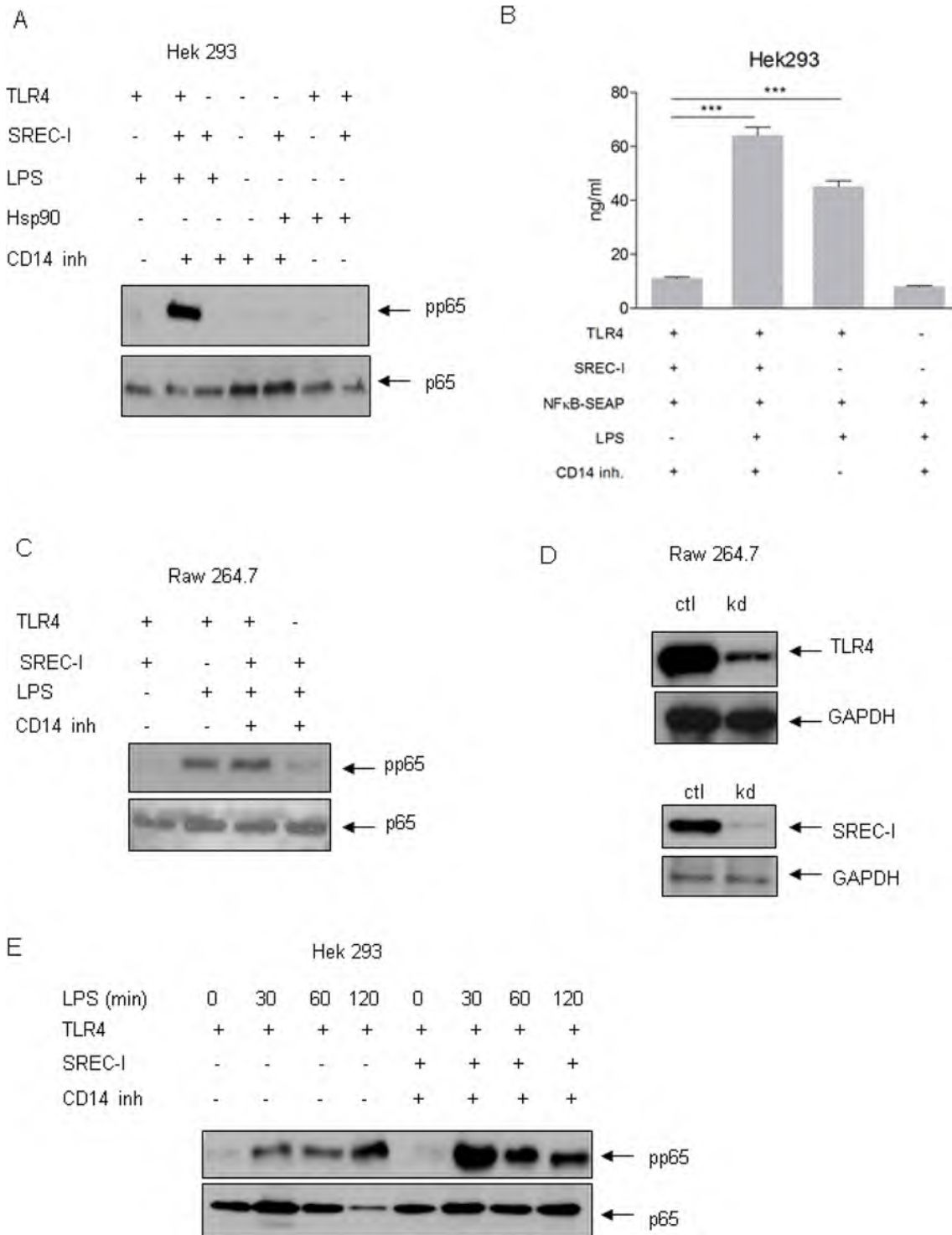
Fig 2. SREC-I supported LPS-TLR4 mediated NF-kB (phospho-p65). **A,** Phospho-p65, (S536/Rel) level was increased in cells expressing SREC-I with TLR4 in the presence of LPS. HEK 293 cells expressing TLR4-MD2-CD14 and/or SREC-I, SREC-I only were treated with or without LPS (1 μg/ml) or Hsp90 for 5–7 hours. Cell lysates were then collected and SDS-PAGE was performed. Phospho-p65 levels were measured. Total level of p65 was measured in the same lysate. Total p65 level was determined. **B,** HEK 293 cells expressing SREC-I and TLR4 or TLR4 only were transfected with NF-kB-SEAP and incubated with LPS (1 μg/ml) for 5 hours. NF-kB activity was measured as instructed by NF-kB-SEAporter assay kit. **C,** Raw 264.7 cells were transfected with siRNA for SREC-I/TLR4 for 72 hours and incubated with LPS (1 μg/ml) with or without CD14 neutralizing peptide (inhibitor). Phospho-p65 level is increased with LPS incubation in cells expressing both TLR4 and SREC-I. **D,** Raw 264.7 cells were transfected with ctl (scr) siRNA or TLR4 siRNA/SREC-I siRNA for 72 hours. Cell lysates were isolated and later SDS-PAGE was performed. **E,** HEK 293 cells expressing TLR4, MD-2, CD14 or TLR4, MD-2, CD14 and

SREC-I were incubated with LPS (1 µg/ml) for indicated time. Cells lysates were collected and equal amount of protein was loaded for SDS-PAGE experiment. For blocking CD14 activity, cells were treated with 10 µg/ml of anti CD14 neutralizing antibody. Error bars in graph show S.D. between three replicate experiments. *P* <0.0001 values were generated by ANOVA using the Bonferroni post-test.

doi:10.1371/journal.pone.0122529.g002

as recognizing receptor for LPS that could interact with TLR4. We also asked if exposure to an alternative SREC-I ligand, Hsp90 could trigger p65 phosphorylation (Fig 2A, lanes 5–7). However, minimal increases in phospho-536-p65/Rel levels were induced by Hsp90 even in cells expressing SREC-I plus TLR4 (Fig 2A).

Next, we further examined the role of SREC-I as a recognizing receptor for LPS and a partner for TLR4 using an NF-kB reporter assay. We assayed NF-kB activity in the CD14, TLR4 and MD2 producing HEK 293 cells with or without SREC-I expression (Fig 2B). We again found that exposure to LPS could activate NF-kB additively with SREC-I and TLR4 co-expression (Fig 2B). In the absence of LPS, reporter activity was minimal but was activated by the endotoxin in cells expressing either SREC-I+TLR4 (lane 2) or CD14 +TLR4 (lane 3). Activity was minimal in the absence of TLR4 (Fig 2B, lane 4). LPS could also activate NF-kB signaling in the CD14 expressing Raw 264.7 cell line (lane 2) (Fig 2C). In addition, in the presence of CD14 neutralizing antibodies, LPS activated NF-kB when SREC-I was expressed in these cells (Fig 2C, lane 3). However depletion of TLR4 by siRNA inhibited LPS-mediated p65/Rel-serine 536 phosphorylation (lane 4). The expression levels of TLR4 and SREC-I in cells transfected with control (ctl) and sequence specific siRNA (kd) is shown in Fig 2D. We also measured the kinetics of LPS-induced NF-kB activation by probing levels of phospho-536-p65/Rel (pp65) as in A (Fig 2E). In cells expressing TLR4 and CD14, we observed the prolonged activation of p65/Rel-S536 phosphorylation that was exceeded in cells expressing both TLR4 and SREC-I. This increase in p65 phosphorylation in SREC-I expressing cells did not require the CD14 recognition of LPS.

## LPS in SREC-I and TLR4 expressing cells increased MAPK activity

In the next series of experiments, we asked whether SREC-I could also mediate signaling through the mitogen activated protein kinase (MAP kinase) pathways. The MAPK family members are important in activation of alternative factors in inflammatory cytokine transcription such as AP-1 and NF-IL6 [20]. We therefore examined levels of activated phosphorylated c-jun kinase (JNK), p38 MAPK (pp38) and ERK-MAPK (pp42 MAPK and pp44 MAPK) after LPS stimulation (Fig 3, S1 Fig). Indeed, SREC-I expression was permissive for LPS-induced JNK, p38 and ERK pathways in TLR4 expressing HEK 293 cells even when CD14 activity was deterred by CD14 neutralizing ab (CD14 inhibitor) (Fig 3A, 3B and 3C). We also found that SREC-I could mediate LPS-induced MAPK activity in Raw 264.7 cells (Fig 3D). MAPK activation was sustained by either CD14 (lane 2) or SREC-I (Fig 3D, lane 3). These experiments suggested that SREC-I could maintain TLR4 mediated LPS signaling even in the presence of the CD14 neutralizing peptide as with the earlier experiments on NF-kB signaling (Figs 2 and 3).

In further experiments we examined LPS-TLR4 induced IRF3 activity, which occurs only after TLR4 endocytosis (Fig 3E). This signaling pathway is initiated after LPS-TLR4 undergoes endocytosis through adaptors other than MyD88 and leads to signaling through the transcription factor IFN, a molecule that regulates transcription of Interferon-β (IFN-β) [21]. IFN-β plays a key role in antigen presentation and adaptive immunity [22]. We thus aimed to determine if SREC-I was involved in internalization of TLR4 induced signaling activity initiated from the endosomes. Indeed we found LPS-TLR4 to be endocytosed and to activate IRF3 in both CD14 active cells (Fig 3E, lane 2), as well as CD14 inhibited cells expressing SREC-I (Fig 3E, lane 3). These experiments suggested a potential role for SREC-I in internalizing LPS-TLR4
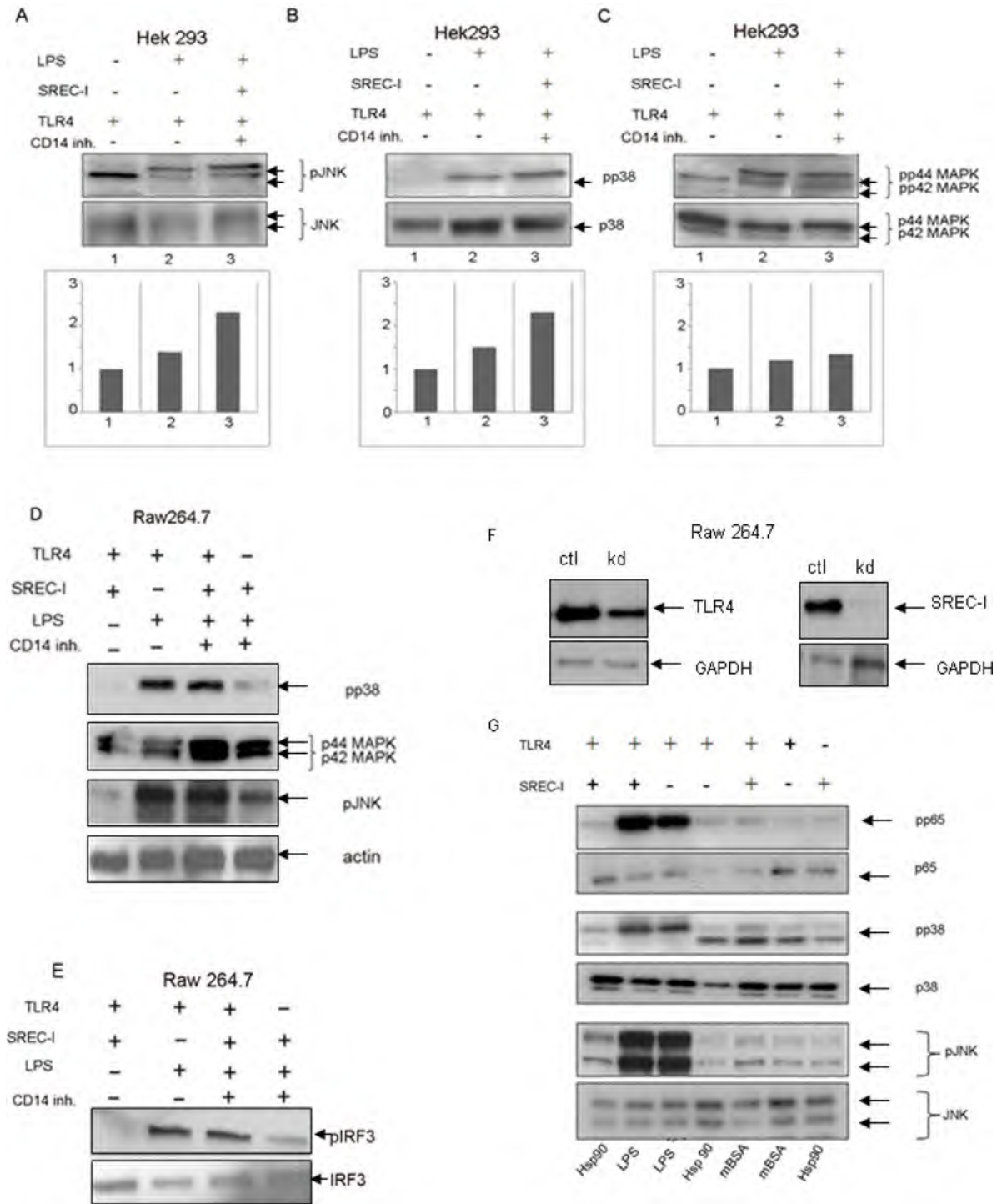
**Fig 3. SREC-I expression led to enhanced NF-kB and MAPK activities in cells expressing TLR4 in the presence of LPS. A, B, C,** SREC-I could increase LPS-TLR4 activation of MAPK. HEK 293 cells expressing TLR4-MD2-CD14, TLR4-MD2-CD14-SREC-I were incubated with LPS (1 µg/ml) for 5 hours (CD14 neutralizing peptide added to SREC-I incubation). Cell lysates were collected and levels of phosphorylated JNK (A), p38 (B), ERK1/2 MAPK assayed (C). **D,** SREC-I was shown to activate LPS-TLR4 induced MAPK signaling. Raw 264.7 cells were transfected with siRNA SREC-I/TLR4 and then incubated with or without LPS in the presence of CD14 neutralizing ab (inhibitor) or not. Cell lysates were collected and subjected to SDS-PAGE and Western Blotting. **E,** SREC-I was involved and IRF3 activity in the absence of CD14. Raw 264.7 cells were treated as in D and then cell lysates were collected and subjected to SDS-PAGE and Western blotting with appropriate antibodies. **F,** Raw 264.7 cells were transfected with ctl siRNA (scr) or TLR4/SREC-I for 72 hours. Cell lysates were collected and equal protein was subjected to SDS-PAGE and Western Blotting. **G,** Phospho-p65 levelswere high in cells expressing TLR4-SREC-I. HEK 293 cells expressing TLR4-MD2, SREC-I-MD2, TLR4-MD2-SREC-I were incubated with mBSA (10 µg/ml), LPS (1 µg/

ml), Hsp90 (10 µg/ml), Hsp90 (10 µg/ml) for 3–5 hours. Cell lysates were collected and levels of phospho-p65, p65, phospho-p38, p38, phospho-JNK and JNK measured. Densitometric analysis of gel intensity was performed using Image J software. Experiments were repeated reproducibly three times.

complexes and activating IFN-β production through phosphorylation and activation of IRF3. The downregulated expression of SREC-I and TLR4 in Raw 264.7 cells with siRNA specific for these two receptors is shown in Fig 3F.

Next, the ability of other ligands for SREC-I, including Hsp90 and maleylated BSA (mBSA) to activate NF-kB, p38-MAPK and c-Jun kinase (JNK) was queried (Fig 3G). However, neither mBSA nor Hsp90 significantly activated the NF-kB or the MAPK pathways in cells expressing SREC-I only, TLR4+CD14 or TLR4+SREC-I (plus CD14 neutralizing ab), suggesting LPS-specific signaling events not duplicated by other SREC-I ligands (Fig 3G). By contrast LPS strongly activated each pathway in positive controls (Fig 3G, second and third lane).

## Downstream factors in TLR4-NF-kB Signaling

MyD88 was first characterized as an essential adaptor for all TLRs [23]. This protein was shown to possess a C-terminal TIR domain through which it interacted with TLR family members [24]. In addition, it was shown that macrophages from MyD88 knock-out mice exhibited minimal responses to LPS, indicating an essential role for this molecule in LPS-mediated signaling [25]. MyD88 was required for robust, SREC-I mediated immune responses to tumor antigens [3]. In addition to MyD88, TLR4 has also been shown to activate NF-kB signaling in association with the adaptor molecule, TRIF (TIR-domain-containing adapter-inducing interferon-β) [26–28]. TLR4 is the only member of the TLR family shown to interact with both MyD88 and TRIF [28]. Thus LPS-TLR4 could mediate downstream signaling in both MyD88-dependent and MyD88-independent (TRIF dependent) manners. Therefore, we next asked whether SREC-I could also interact with TRIF in an LPS-dependent manner.

We investigated whether the SREC-I-TLR4 interaction led to LPS-mediated NF-kB signaling through either (1) MyD88 or (2) TRIF (Fig 4). We used MyD88 and TRIF blocking peptides to probe the roles of these adaptors. The MyD88 inhibitory peptide used here was shown to block MyD88 signaling by inhibiting its homodimerization whereas the TRIF inhibitory peptide interfered with TLR4-TRIF binding [29, 30]. We compared HEK 293 cells (that normally express MyD88) which were manipulated by transfection or CD14 blocking to produce either: (A) a TLR4 plus SREC-I phenotype, (B) SREC-I alone or (C) a TLR4 plus CD14 phenotype. The densitometric analysis of band intensity from one experiment is shown beneath the immunoblots in Fig 4. In the TLR4 plus SREC-I conditions, LPS activated NF-kB activity (Fig 4A, lane 3) and these effects were inhibited by the MyD88 blocking peptide (Fig 4A, lane 2). Likewise in the presence of CD14 and TLR4, LPS activated NF-kB (Fig 4C, lane 3) and these effects were inhibited by the MyD88 blocking peptide (Fig 4C, lane 2). In cells expressing SREC-I alone, without TLR4 there was less pronounced NF-kB activation that was however also inhibited by the MyD88 blocking peptide (Fig 4B). The control peptide that did not block MyD88 had minimal effects on NF-kB activation (Fig 4A–4C, third lanes). TRIF blocking peptides also inhibited LPS induced activation of NF-kB in a similar way to the MyD88 inhibitory peptide under each condition, except for the cells expressing SREC-I only (Fig 4D, 4E and 4F). These findings suggested that this peptide could inhibit interactions between TLR4 and TRIF (Fig 4D, 4E and 4F). In the experiment under SREC-I alone conditions, activation of NF-kB by LPS was too faint to draw conclusions (Fig 4E).

These results suggested that SREC-I, in addition to CD14 could recognize extracellular LPS and, when bound to this ligand, could further interact with TLR4, and either MyD88 or TRIF to activate NF-kB signaling (Fig 4A–4F). SREC-I alone signaled to NF-kB only very faintly and
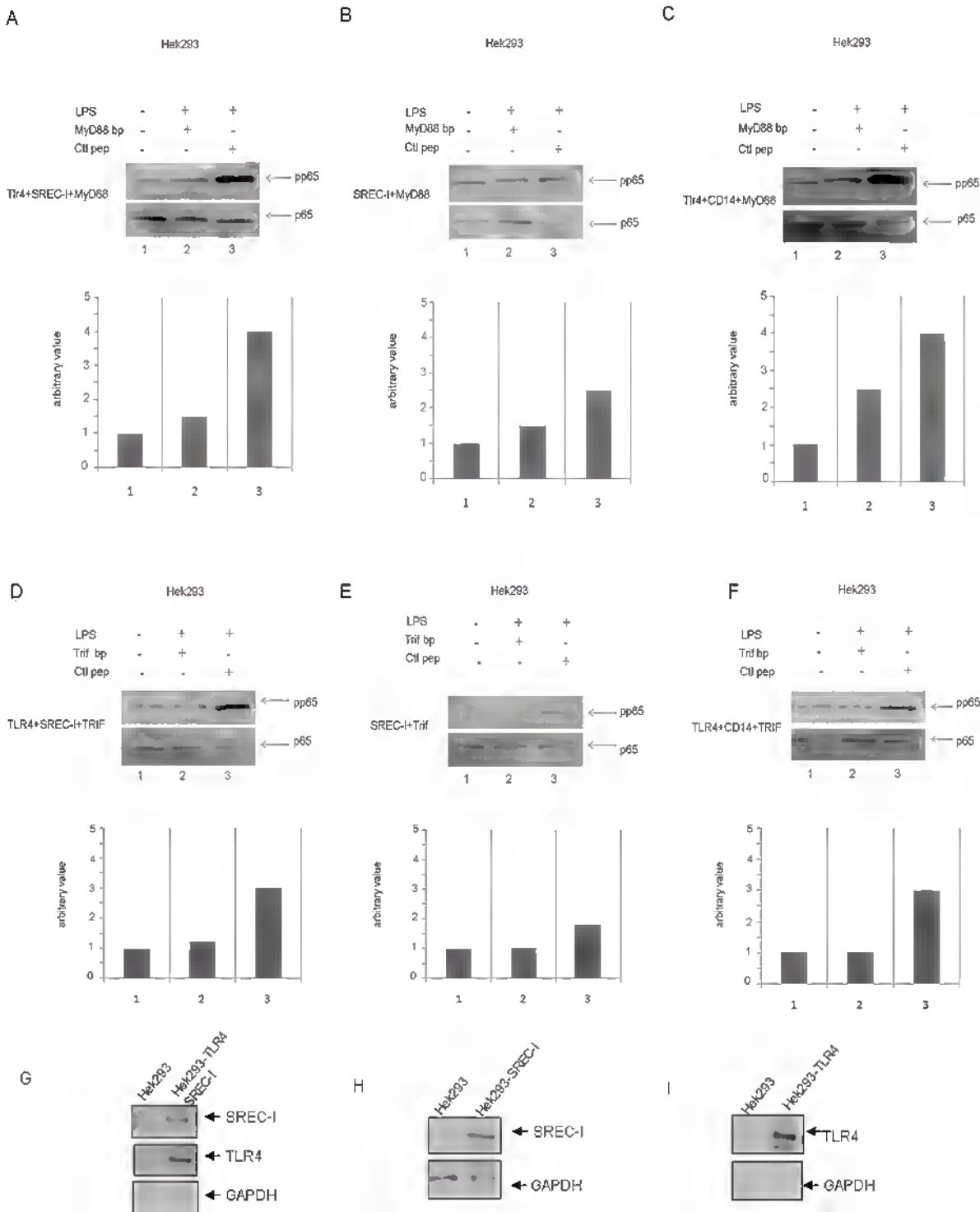
**Fig 4. SREC-I required adaptor proteins MyD88 and TRIF for downstream NF-kB activation. A, B, C,** MyD88 was involved in LPS-TLR4-SREC-I (A), LPS-SREC-I (B) or LPS-TLR4 (C) activation of NF-kB. HEK 293 cells expressing TLR4-MD2-SREC-I-MyD88, SREC-I-MD2-MyD88 and TLR4-MD2-MyD88-CD14 were treated with MyD88 blocking peptide (100 μM for 24 hours), or control peptide (100 μM for 24 hrs) as indicated. Cells were then treated with LPS (1 μg/ml) for 5 hours in the presence of blocking peptides. Densitometric analysis of bands in gels is shown. **D, E, F,** TRIF was involved in LPS-TLR4-SREC-I, LPS-TLR4 or LPS-SREC-I activation of NF-kB. HEK 293 cells (+MD2) expressing receptors and adaptor TRIF and CD14 as indicated were incubated with TRIF blocking peptide or control peptide (50 μM for 6 hours) and incubated with LPS for 5 hours. Phospho-p65 levels in cell lysates were then analyzed by SDS-PAGE and Western blotting. TLR4 only cells also express CD14 as shown. Densitometric analysis of band intensity is shown below. Each experiment was repeated 3 times. **G, H, I,** Protein lysates from HEK 293 cells stably expressing TLR4 and SREC-I, TLR4 only and SREC-I only were analyzed by SDS-PAGE and Western blotting. Relative protein expression levels are thus shown in the blot.

doi:10.1371/journal.pone.0122529.g004

would likely require TLR4 for significant LPS activation (Fig 4B and 4E). Expression of SREC-I, TLR4 in HEK 293 cells overexpressing TLR4/SREC-I or TLR4 + SREC-I is shown in Fig 4G, 4H and 4I).
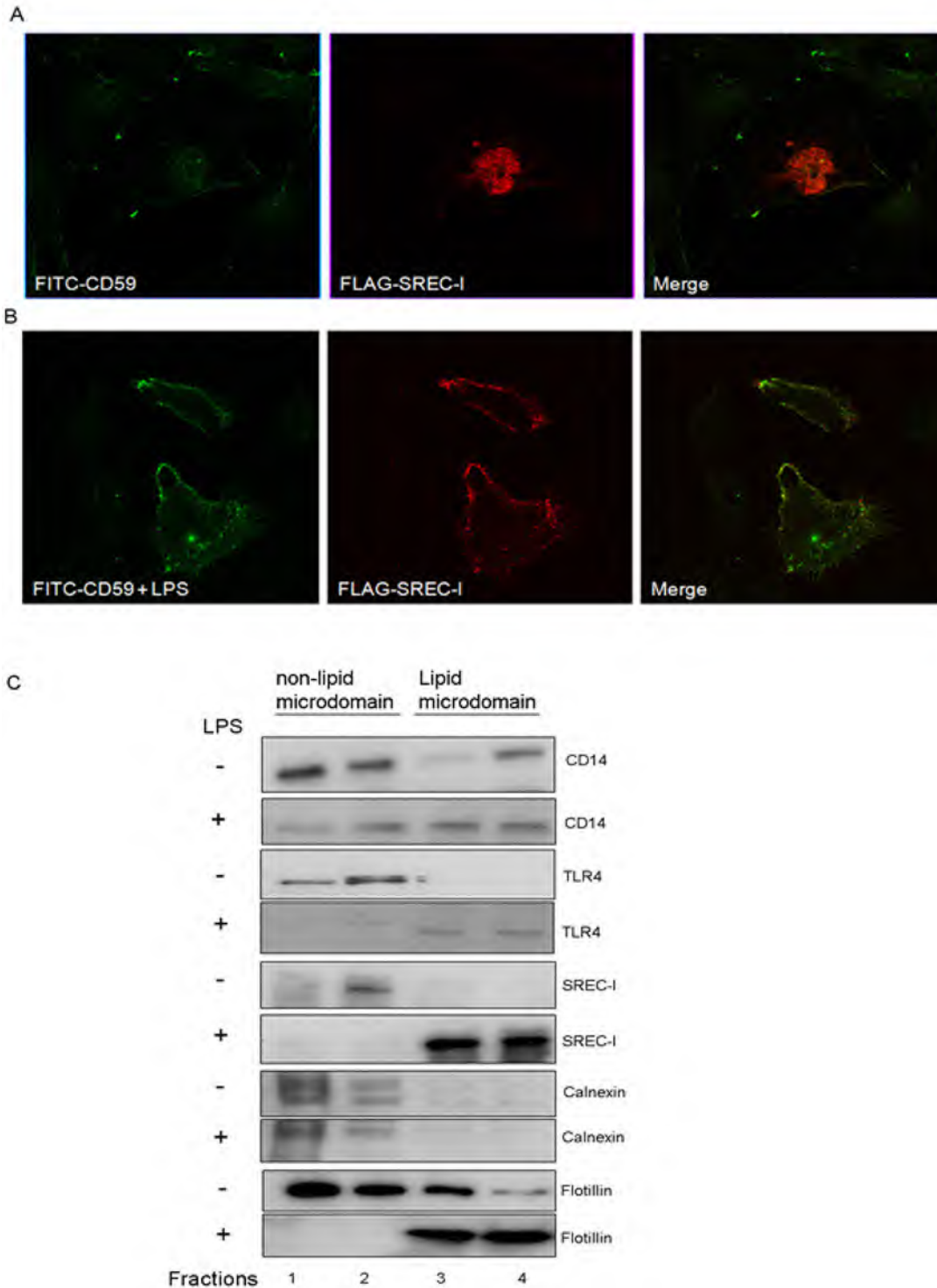
## SREC-I was localized to detergent-insoluble lipid microdomains in the presence of LPS

In previous studies of SREC-I, we showed this receptor to be internalized by a pathway involving segregation of ligand-SREC-I complexes into detergent insoluble lipid microdomains and subsequent endocytosis through the *GPI-anchored protein (GP-AP) enriched early endosomal compartment* (GEEC) pathway [2, 31, 32]. The ligand (Hsp90-peptide complex) uptake and antigen cross presentation were inhibited by antagonists of cholesterol localization, actin polymerization and the small GTPase Cdc42, characteristic of endocytosis through the pathway taken by GPI-AP [2]. In addition, the activity of c-Src, a protein whose levels are enriched in lipid microdomains was required for ligand internalization by SREC-I [2, 33]. We therefore examined whether LPS could trigger transmembrane signaling through SREC-I/TLR4 by similar mechanisms. We first compared the intracellular localization of transfected SREC-I with that of a lipid microdomain marker, the GPI-anchored protein CD59; this protein is expressed in HeLa cells and internalized in a Cdc42 dependent manner into GEEC. For these experiments, FLAG-SREC-I was expressed in HeLa cells that were then incubated with LPS at 4°C for 30 minutes. LPS exposure led to SREC-I localization to a CD59-marked compartment on the plasma membrane (Fig 5A and 5B).

Next, we isolated detergent insoluble lipid microdomains/lipid raft fractions from LPS-treated or untreated Raw 264.7 cells. The lipid microdomainfractionsfrom cell lysates were prepared using *OptiPrep* layers and ultracentrifugation at ~200,000xg for 4 hours. Proteins isolated from such lipid microdomain fractions were then characterized by immunoblot assay (Fig 5C). SREC-I appeared to be absent from the detergent insoluble lipid microdomain fractions in controls, but in the presence of LPS was localized quantitatively to these fractions along with raft marker Flotillin, as well as, significantly, TLR4 (Fig 5C). However, there appeared to be little migration of CD14 (which is a GPI-anchored protein) into the microdomain fractionswith or without LPS (Fig 5C). As a further control we examined the behavior of endoplasmic reticulum-localized protein calnexin, which was observed to be absent from the lipid microdomain fractions with or without LPS (Fig 5C). These findings further suggested a role for sequestration in the lipid microdomains in LPS mediated SREC-I–TLR4 interactions.

## Role for entry into detergent insoluble plasma membrane lipid microdomainsin LPS-SREC-I-MAPK signaling

Next we examined the potential role of SREC-I localization to CD59-marked/lipid microdomainin TLR4 signaling through the JNK, p38 MAPK and NF-kB pathways using the HEK 293 system described above (Fig 6). We incubated cells with a number of agents known to disrupt lipid microdomains and formation of the GEEC compartment. These included cholesterol sequestering agent methyl β cyclodextrin (MβCD) and other inhibitors such as PP2 (Src kinase inhibitor), cytochalasin D (actin depolymerizing agent) and *Clostridium. Difficile* Toxin B (Rho GTPase inhibitor). These inhibitors each blocked internalization of antigen-bound SREC-I and subsequent antigen cross presentation in our prior studies [2]. In cells transfected with CD14 and TLR4, LPS induced efficient signaling through each pathway and these events were not markedly reduced by any of the inhibitors (Fig 6, 11th-14th lanes). However LPS-induced activation of JNK and p38as well as NF-kB in cells with combined SREC-I/TLR4 expression (Fig 6, lanes 3–6) was blocked by many of the inhibitors (Fig 6). MβCD and Toxin B were

**Fig 5. SREC-I became localized in detergent insoluble lipid microdomainsafter LPS exposure. A,B,** FLAG-SREC-I were localized to lipid microdomains marked by the GPI anchored protein CD59 on the plasma membrane in the presence of LPS (B). HeLa cells expressing FLAG-SREC-I were incubated with LPS (1 µg/ml) and FITC labeled (red, in figure) anti CD59 ab (10 µg/ml for 30 minutes on ice at 4°C). Cells were then fixed on ice and stained for FLAG (green) using anti FLAG M2 ab. FLAG-SREC-I expressing cells were also incubated with FITC-anti-CD59 ab at 4°C for 30 mins. Cells were stained with anti-FLAG ab (secondary antibody, red). Confocal Microscopy was then used to analyze the localization of the proteins. **C,** SREC-I was localized to lipid microdomains after LPS exposure. Raw 264.7 cells were stimulated with LPS (1 µg/ml) or incubated without LPS and lipid microdomains were isolated using *Optiprep* density gradient centrifugation. 1 ml fractions (total 4) were collected from the top of the centrifuge tubes. Fractions containing detergent soluble membrane proteins were also indicated. All fractions were later separated on polyacrylamide gels, electrophoretically blotted and probed with antibodies as indicated. Flotillin was used as marker for lipid microdomain rich fractions (shown in lane 3 and 4).
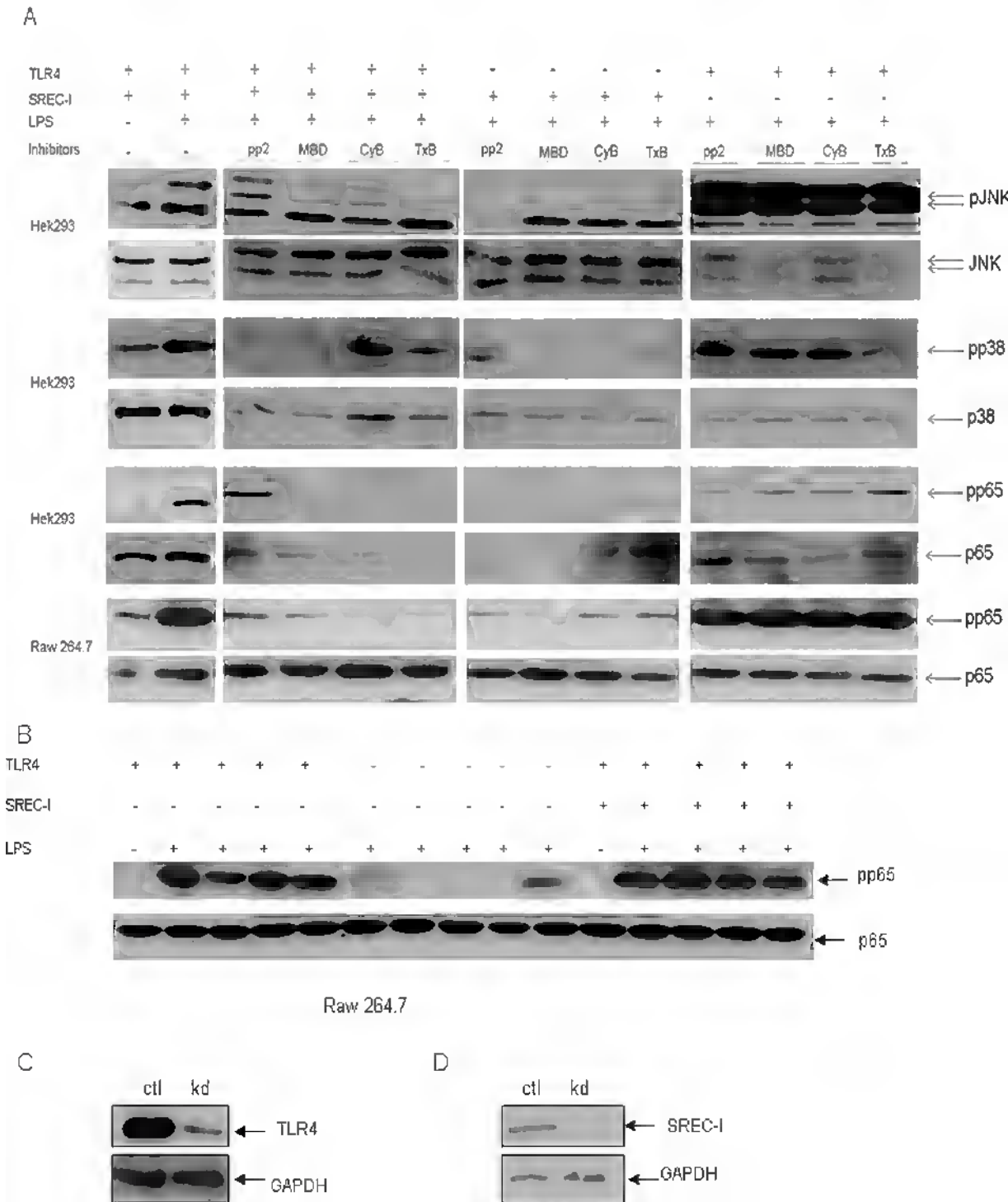
**Fig 6. Intact lipid microdomains were essential for LPS-SREC-I-TLR4-induced MAPK signaling. A,** HEK 293 cells expressing TLR4-MD2-CD14, SREC-I-TLR4-MD2-CD14 were treated with or without CD14 neutralizing peptide (inhibitor). Cells were then incubated with LPS (1 μg/ml) for 3 hrs. Cell lysates were run on SDS-PAGE and then immunoblotted with phospho-specific antibodies for JNK, p38, p65 and anti-JNK ab, p38 ab and anti-p65 ab. Drugs including PP2 (10 μM Srcinhibitor), MβCD (MBD, 10 mM, cholesterol sequestering agent), TxB (2 ng/ml, Clostridium Toxin B) were added to inhibit the functions of Src kinase, lipid microdomain formation and Rho GTPase activities as indicated. Raw 264.7 cells were transfected with siRNA for TLR4/SREC-I and then treated as described above. These experiments were repeated reproducibly 2 times. **B,** Raw 264.7 cells expressing TLR4, SREC-I or TLR4 only was incubated with LPS (1 μg/ml) for 3 hrs. Cell lysates were collected and then subjected to SDS-PAGE and Western Blotting. **C, D,** Raw 264.7 cells were transfected with indicated siRNA for 72 hours. Cell lysates were collected and equal amount of protein was subjected to SDS-PAGE and Western Blotting. Expression of SREC-I and TLR4 is shown in Raw 264.7 cells.

doi:10.1371/journal.pone.0122529.g006

particularly effective in this regard and blocked signaling through each pathway. Minimal signaling through the JNK, p38 or NF-kB pathways was observed in cells expressing SREC-I alone (Fig 6, lanes 7–10). This finding was predictable from the earlier experiments indicating a need for association with TLR4 in order for SREC-I to activate these pathways. This experiment suggested that TLR4 became co-localized with SREC-I after LPS exposure in new microdomains within the membrane and required enriched cholesterol, actin cytoskeleton function and small Rho GTPase activity for signaling pathways (Fig 6). When the experiments were repeated in Raw 264.7 cells, we again saw that inhibitors of lipid microdomain formation blocked NF-kB signaling in cells coordinately expressing TLR4 and SREC-I (Fig 6). As before, the inhibitors failed to disrupt NF-kB signaling in cells expressing TLR4 without SREC-I (Fig 6). These experiments, carried out in both HEK 293 and Raw 264.7 cells, indicated TLR4 signaling from either a lipid microdomain fraction or an internal endosomal compartment after SREC-I/TLR endocytosis via the GEEC pathway (Fig 6). We again confirmed the activation of NF-kB through phosphorylated p65 level in the presence of LPS in Raw 264.7 cells expressing TLR4 and SREC-I in the absence of inhibitors suggesting the role of lipid microdomain in activating LPS-SREC-I-TLR4 signaling (Fig 6B).

## Role of SREC-I in LPS-mediated inflammatory cytokine release

As the above experiments indicated SREC-I mediated, TLR4 dependent signaling we next examined a role for this SR in LPS-induced cytokine production in bone marrow-derived mouse macrophages (BMDM). These cells express components of the LPS-TLR4 signaling apparatus, including CD14, MD2 and scavenger receptor A (SR-A) along with TLR4, TLR2 and SREC-I at physiological levels. We used both wild type bone marrow-derived macrophages as well as BMDM from TLR4 knockout and SREC-I knockout mice (Fig 7). BMDM were isolated and then separated from the total population of bone marrow derived cells using MAC-I and F4/80 macrophage specific antibodies (S2 Fig). We then measured the levels of interleukin-6 (IL-6, Fig 7A) and tumor necrosis factor α (TNF-α, Fig 7B) released by these macrophages. To examine a role for SREC-I expression in LPS-induced cytokine release, the BMDM were initially transfected with a SREC-I siRNA construct described previously [3]. As it was shown recently that LPS binding to scavenger receptor SR-A/CD204 could inhibit release of anti-inflammatory cytokines, we also assayed cytokine production either without or with (Fig 7A and 7B) blocking antibodies for this receptor [34]. LPS led to the induction of IL-6 (Fig 7A) and TNF-α (Fig 7C) in control cells and induction was markedly decreased by TLR4 KO. SREC-I knockdown (siRNA) also reduced the levels of LPS-mediated proinflammatory cytokine secretion in each case, while incubation with a control/scrambled RNA was ineffective (Fig 7A). Blocking antibodies for CD204/SR-A increased LPS-induced cytokine production in each case (IL-6 and TNF-α) (Fig 7A and 7B) [35]. In addition, IL-6 release was decreased in BMDM isolated from SREC-I knockout mice and further reduced by TLR4 siRNA (Fig 7C). We also assessed potential effects of SREC-I on LPS-induced TNF-α release in BMDM isolated from the SREC-I KO mice andsaw significant differences between WT and SREC-I KO mice (Fig 7D). TLR4 knockdown also reduced the levels of LPS-mediated IL-6 and TNF-α cytokine secretion in each case, while incubation with a control, scrambled RNA was ineffective (Fig 7C and 7D).

In addition to the inflammatory cytokine release, TLR4 has been shown to mediate induction of IFN expression in the presence of LPS. To determine a role for SREC-I we examined the release of IFN- β in BMDM taken from WT, SREC-I KO mice subjected to TLR4 knockdown with siRNA (Fig 7E). There was a sharp decrease in IFN-β release in the SREC-I KO/TLR4 knocked down BMDM (Fig 7F). Only low levels of IFN-β release were seen in cells taken from
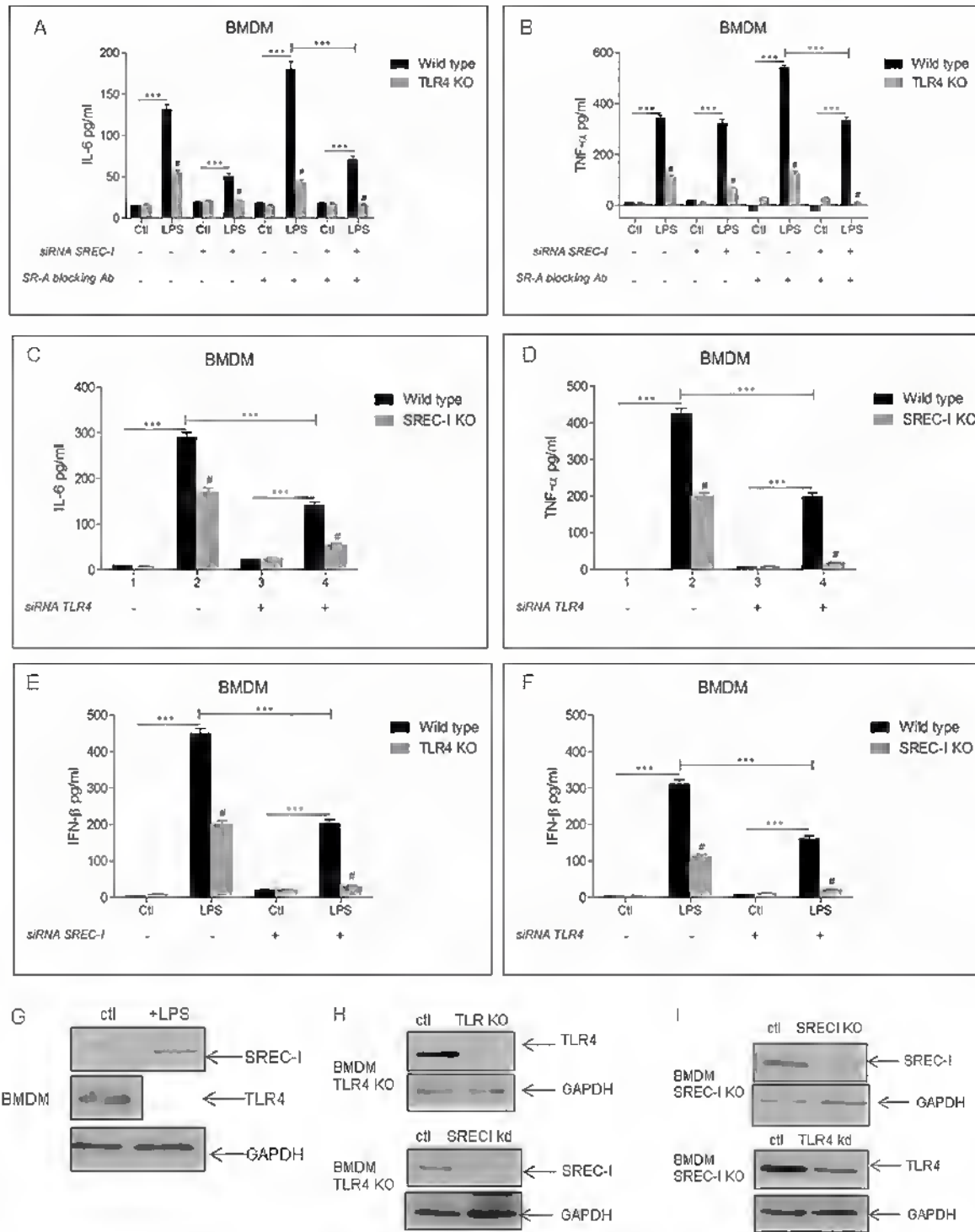
Fig 7. SREC-I inactivation reduced LPS-TLR4 mediated proinflammatory cytokine release in BMDM. A, TLR4 KO and SREC-I KD in macrophages led to reduced IL-6 release compared with WT cells. Primary macrophages from WT and TLR4 KO mice were transfected with siRNA-SREC-I or control hairpins for 72 hours and then incubated with LPS for 12 hours with or without SR-A blocking antibody. IL-6 release by cells was measured in the collected medium by ELISA. B, TLR4KO and SREC-I KD in BMDMs led to reduced TNF-α compared to WT cells. Primary macrophages from WT and TLR4 KO mice were transfected with siRNA-SREC-I or a control hairpin for 72 hours and then incubated with LPS for 12 hours with or without SR-A blocking antibody. TNF-α release was measured in medium by ELISA. C, SREC-I KO and TLR4KD in BMDM led to reduced IL-6 release compared with WT cells. Primary macrophages from WT and SREC-I KO mice were transfected with or without siRNA-TLR4 for 72 hours. IL-6 release into the medium was measured

according to manufacturer's instructions. **F,** SREC-I KO and TLR4 KD BMDMs led to reduced release of TNF-α compared to WT cells. Primary macrophages from WT and SREC-I KO mice were transfected with or without siRNA-TLR4 for 72 hours. TNF-α release by was then assayed as above. **E,F,** TLR4 KO and SREC-I KO BMDMs led to reduced release of IFN-β compared to WT cells. Primary macrophages from WT and TLR4 KO (E), SREC-I KO were transfected or not with SREC-I siRNA (E) and TLR4 siRNA (F) for 72 hours. IFN-β release in media was assayed as above. **G, H, I,** Primary BMDM cells (WT, TLR4/SREC-I KO mice, TLR4/SREC-I KO + SREC-I siRNA/TLR4 siRNA) were trypsinized and cell lysates were collected. Equal amount of protein was subjected to SDS-PAGE and Western blotting. All experiments were performedreproducibly 3 times. Error bars in graph show S.D. between three replicate experiments. ***$P<0.0001$ when compared to the control, and #$P<0.0001$ when compared to the WT. Values were generated by ANOVA using the Bonferroni post-test.

TLR4 KO-SREC-I knocked down BMDM indicating that SREC-I has a role in promoting LPS-TLR4 mediated IFN-β expression (Fig 7E).

Finally, we asked whether inhibiting the lipid microdomain formation/raft mediated internalization pathway for SREC-I localization could affect cytokine expression (Fig 8). Indeed, IL-6 release triggered by exposure to LPS was impaired when cells were treated with Toxin B, an inhibitor of the small GTPases (including Cdc42) required for the internalization pathway taken by SREC-I. The decrease in IL-6 expression was similar in magnitude to the decline in the cytokine observed when SREC-I was reduced in these cells by RNA interference (Figs 7 and 8). These results suggested that the nature of the lipid membrane microenvironment occupied by SREC-I after LPS treatment influenced TLR4 activity and downstream cytokine synthesis. To avoid the potential attenuation of cytokine release by SR-A, these experiments were performed in the presence of SR-A blocking antibody [35].
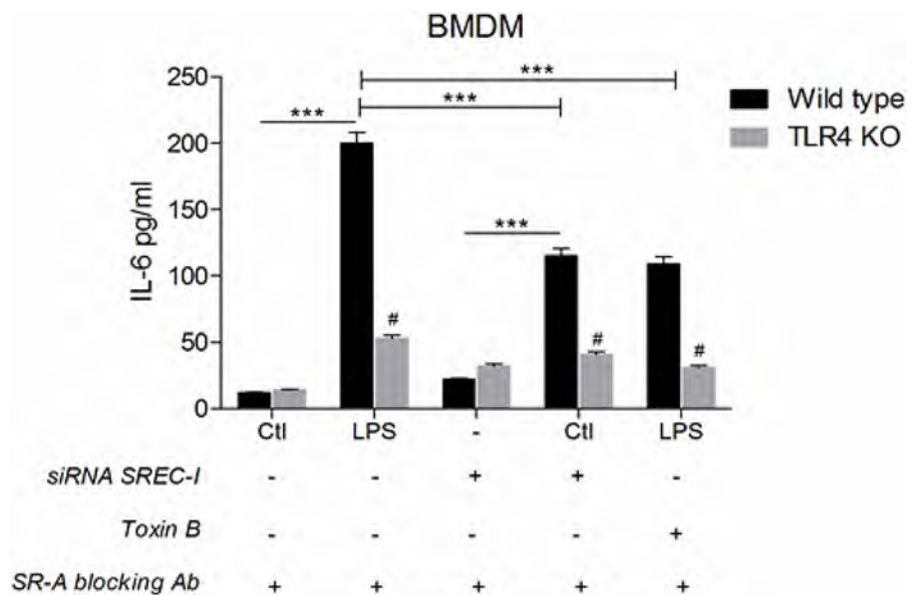


**Fig 8. Rho GTPase activity was required for LPS-SREC-I-TLR4 induced proinflammatory cytokine release.** BMDM cells from WT and TLR4 KO mice were transfected with siRNA SREC-I or control RNA. Cells were treated with or without Toxin B (2 ng/ml) and incubated withor without LPS. Experiments were performed in the presence of SR-A blocking antibodies. Cell media were collected, clarified by centrifugation and the IL-6 ELISA assay was performed. Experiments were repeated reproducibly 3 times. The height of the error bars represents the average of three independent measurements. The error bars represent one standard deviation from the mean. ***$P<0.0001$ when compared to the control, and #$P<0.0001$ when compared to the WT. Values were generated by ANOVA using the Bonferroni post-test.
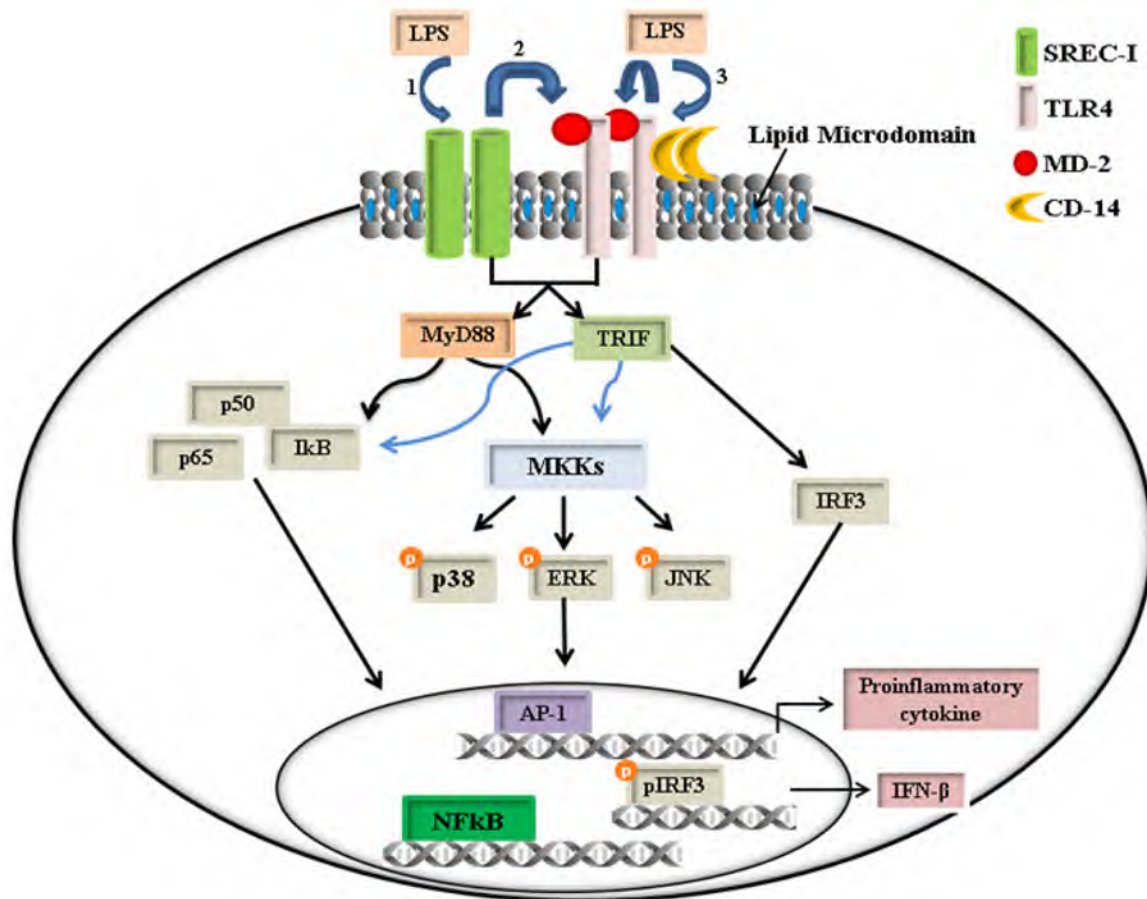
**Fig 9. Schematic diagram of the proposed pathway of LPS-SREC-I-TLR4 mediated activation of proinflammatory cytokine expression.** This cartoon depicts LPS binding to SREC-I (1) followed by LPS-SREC-I complex recruitment of TLR4 into discrete lipid microdomains (thick line) (2). Localization of LPS-SREC-I-TLR4 complexes to such lipid microdomains then led to activation of downstream proinflammatory cytokine release through adaptor proteins MyD88 and TRIF. LPS exposure could thus mediate activation of the NF-kB and MAPK pathways. In addition, LPS has been shown to be recognized by CD14, the primary responder to the endotoxin, which then bound to TLR4 and triggered proinflammatory signaling through NF-kB and MAPK (3). We have additionally shown that LPS-SREC-I-TLR4 signaling led to activation of IRF3. Engagement of these signaling pathways could then lead to activation of transcription factors NF-kB, AP-1 and IRF3 that have been shown to function combinatorially in cytokine gene transcription.

doi:10.1371/journal.pone.0122529.g009

## Discussion

Our experiments therefore have shown SREC-I to be a receptor capable of responding to LPS and interacting with TLR4 to trigger inflammatory signaling leading to enhancement of TNF-α, IFN-β and IL-6 expression (Fig 9). The mechanisms involved in the enhancement of cytokine secretion by SREC-I may involve sustained and stronger activation of the NF-kB and MAP kinase pathways that are known to function upstream of cytokine expression (Figs 2 and 3). Previous studies had suggested that SREC-I could interact with an extracellular protein-Tamm-Horsfall protein that may mediate TLR4 dependent inflammatory responses in dendritic cells [36]. Although SREC-I was shown to cooperate with TLR2 in recognition of hepatitis C virus N3 proteins in myeloid cells [37], we did not observe TLR2 involvement in LPS mediated TLR4 signaling by SREC-I (S3 Fig). We hypothesize that the mechanisms utilized for the mediation of TLR4 downstream signaling by SREC-I interaction appeared to involve LPS binding and recruitment of TLR4 into the GEEC pathway of internalization [32, 38] by ligand-bound

SREC-I, a process initiated by migration of the SREC-I into cholesterol rich lipid microdomains (Fig 6). Cholesterol-rich microdomains were shown to contain abundant levels of signaling molecules and indeed ligand binding to SREC-I promoted functional association with non-receptor tyrosine kinase Src and the small GTPase, Cdc42; these processes were shown to induce internalization in a dynamin-independent manner [2, 4, 33, 39]. Our experiments suggested that SREC-I might be able to function in some circumstances as a primary LPS receptor in a manner reminiscent of CD14, although the latter receptor has not been shown to assist in internalization of TLR4 into GEEC. Instead, CD14 appeared to promote TLR4 endocytosis via a dynamin-dependent pathway that was independent of Src and Cdc42 but dependent on another non-receptor tyrosine kinase, Syk [13, 40]. Our experiments therefore indicated that, as well as being involved in antigen cross presentation and adaptive immunity, SREC-I could stimulate innate immune processes by co-opting the activity of TLR4. So far the known regulators of TLR4 endocytosis include dynamin, clathrin and all other associated proteins. We cannot rule out however the possibility of other specialized means of microbial recognition by cells that are coupled to TLR4 signaling. In this regard, SREC-I mediated LPS-TLR4 binding and signaling involving insoluble lipid microdomains could be significant (Fig 5). SREC-I might be activated in this way by LPS (Figs 5 and 6), or any potentially by other microbial products, which are also involved in recognition microorganisms (A. Murshid, unpublished data).

CD14 was originally identified as a key factor in MyD88-dependent signal transduction at very low concentrations of LPS [41, 42]. Our findings suggested that SREC-I could supplement CD14 as a factor in MyD88-dependent signal transduction and it could also facilitate TRIF signaling at somewhat higher concentration of LPS both from plasma membrane and endosomes respectively in HEK 293 cells expressing SREC-I and TLR4. Earlier it was shown that the scavenger receptor CD36 and the mannose receptor could serve as alternatives to CD14 for TLR2 induced signaling [43]. In an analogous manner, SREC-I might participate in LPS-TLR4 signaling in addition to CD14 activity (Figs 2 and 7).

Structurally distinct SR family members, SREC-I and SR-A/CD204 have been ascribed number of properties in common in addition to binding LPS. These properties include the capacity to associate with modified proteins and to bind a number of heat shock proteins [44–47]. Both receptors were increased in expression in activated macrophages [48] (Calderwood SK, unpublished data). However, while SREC-I promoted antigen cross presentation, activation of CTL (cytotoxic T cell) and induction of innate immunity [2, 49] (Figs 3 and 7), the effects of SR-A/CD204 were anti-inflammatory and this receptor could inhibit a number of mechanisms in innate and adaptive immunity [50–52]. Some of these contrasting effects could involve the influence of SR expression on TLR4 activity; whereas SREC-I enhanced LPS-TLR4 signaling, at least partially through sequestration of the TLR in lipid microdomains (Figs 5 and 6), SR-A/CD204 was shown to inhibit the ubiquitinylation of the adaptor protein TRAF6, thus reducing levels of NF-kB signaling [53]

One unexplained finding in our studies was that Hsp90, although binding avidly to SREC-I and stimulating TLR4 association caused relatively low levels of inflammatory signaling. HSPs have been proposed as potential endogenous danger signals [54, 55]. One finding that could account for the paucity of Hsp90 induced inflammatory signals found here is that HSPs could interact with SR-A/CD204, a receptor that has been shown to inhibit TLR4 signaling [34]. However, SR-A also dampened LPS induce TLR4 signaling [34]. The differences between LPS and Hsp90 in terms of signaling through SREC-I were thus not certain. However, the extracellular component of SREC-I is a large multidomain structure and has been shown to contain numerous distinct potential sites for different ligands [4]. Future studies would address this question.

In conclusion therefore, we hypothesize that the Class F scavenger receptor SREC-I became associated with TLR4 within lipid microdomainsin Raw 264.7 macrophagesexposed to LPS, triggered inflammatory signaling and promoted sustained cytokine release (Fig 9). Earlier it has been shown that this receptor, expressed in both macrophages and DC, interacts with a range of ligands in addition to LPS and could thus participate in innate and adaptive responses to a range of endogenous or pathogenic immune challenges.

## Supporting Information

**S1 Fig. SREC-I expression led to enhanced ERK 2/1 activities in cells expressing TLR4 in the presence of LPS. A,** SREC-I could increase LPS-TLR4 activation of MAPK. HEK 293 cells expressing TLR4-MD2-CD14, TLR4-MD2-CD14-SREC-I were incubated with LPS (1 µg/ml) for 5 hours (CD14 neutralizing peptide added to SREC-I incubation). Cell lysates were collected and levels of phosphorylated ERK1/2 MAPK assayed.
(TIF)

**S2 Fig. BMDM were isolated from WT and KO mice. A,** Bone marrow cells were isolated and differentiated to macrophages. Cells were then stained with anti F4/80 antibody.
(TIF)

**S3 Fig. SREC-I supported LPS-TLR4 mediated NF-kB (phospho-p65). A,** HEK 293 cells expressing SREC-I and TLR4, TLR2 +SREC-I or TLR4 only were transfected with NF-kB-SEAP and incubated with LPS (1 µg/ml) or Pam3CSK4 (10 µg/ml) for 5 hours. NF-kB activity was measured as instructed by NF-kB-SEAporter assay kit.
(TIF)

## Author Contributions

Conceived and designed the experiments: SKC AM JG. Performed the experiments: AM TP. Analyzed the data: AM TJB SKC. Contributed reagents/materials/analysis tools: TP. Wrote the paper: SKC AM.

## References

1. Adachi H, Tsujimoto M. Characterization of the human gene encoding the scavenger receptor expressed by endothelial cell and its regulation by a novel transcription factor, endothelial zinc finger protein-2. J Biol Chem. 2002; 277(27):24014–21. PMID: 11978792

2. Murshid A, Gong J, Calderwood SK. Heat shock protein 90 mediates efficient antigen cross presentation through the scavenger receptor expressed by endothelial cells-I. J Immunol. 2010; 185(5):2903–17. doi: 10.4049/jimmunol.0903635 PMID: 20686127

3. Gong J, Zhu B, Murshid A, Adachi H, Song B, Lee A, et al. T cell activation by heat shock protein 70 vaccine requires TLR signaling and scavenger receptor expressed by endothelial cells-1. J Immunol. 2009; 183(5):3092–8. doi: 10.4049/jimmunol.0901235 PMID: 19641135

4. Murshid A, Gong J, Calderwood SK. Molecular chaperones and scavenger receptors: Binding and trafficking of molecular chaperones bu class F and class H scavenger receptors. Henderson B, Pockley AG, editors. Dordrecht: Springer; 2012. 215–28 p.

5. Means TK, Mylonakis E, Tampakakis E, Colvin RA, Seung E, Puckett L, et al. Evolutionarily conserved recognition and innate immunity to fungal pathogens by the scavenger receptors SCARF1 and CD36. J Exp Med. 2009; 206(3):637–53. doi: 10.1084/jem.20082109 PMID: 19237602

6. Tamura Y, Osuga J, Adachi H, Tozawa R, Takanezawa Y, Ohashi K, et al. Scavenger receptor expressed by endothelial cells I (SREC-I) mediates the uptake of acetylated low density lipoproteins by macrophages stimulated with lipopolysaccharide. J Biol Chem. 2004; 279(30):30938–44. PMID: 15145948

7. Akira S, Sato S. Toll-like receptors and their signaling mechanisms. Scand J Infect Dis. 2003; 35(9):555–62. PMID: 14620134

8.  Bianchi ME. DAMPs, PAMPs and alarmins: all we need to know about danger. J Leukoc Biol. 2007; 81(1):1–5. PMID: 17338044

9.  Takeuchi O, Akira S. Pattern recognition receptors and inflammation. Cell. 2010; 140(6):805–20. doi: 10.1016/j.cell.2010.01.022 PMID: 20303872

10. Hayden M, Ghosh S. Signaling to NFkB. Genes Dev. 2004; 18:2195–224. PMID: 15371334

11. Fenton MJ, Golenbock DT. LPS-binding proteins and receptors. J Leukoc Biol. 1998; 64(1):25–32. PMID: 9665271

12. Dunzendorfer S, Lee HK, Soldau K, Tobias PS. TLR4 is the signaling but not the lipopolysaccharide up-take receptor. J Immunol. 2004; 173(2):1166–70. PMID: 15240706

13. Zanoni I, Ostuni R, Marek LR, Barresi S, Barbalat R, Barton GM, et al. CD14 controls the LPS-induced endocytosis of Toll-like receptor 4. Cell. 2011; 147(4):868–80. doi: 10.1016/j.cell.2011.09.051 PMID: 22078883

14. Dziarski R, Gupta D. Role of MD-2 in TLR2- and TLR4-mediated recognition of Gram-negative and Gram-positive bacteria and activation of chemokine genes. J Endotoxin Res. 2000; 6(5):401–5. PMID: 11521063

15. Vogel SN, Perera PY, Detore GR, Bhat N, Carboni JM, Haziot A, et al. CD14 dependent and independent signaling pathways in murine macrophages from normal and CD14 "knockout" (CD14KO) mice stimulated with LPS or taxol. Prog Clin Biol Res. 1998; 397:137–46. PMID: 9575554

16. Bowdish DM, Sakamoto K, Kim MJ, Kroos M, Mukhopadhyay S, Leifer CA, et al. MARCO, TLR2, and CD14 are required for macrophage cytokine responses to mycobacterial trehalose dimycolate and Mycobacterium tuberculosis. PLoS Pathog. 2009; 5(6):e1000474. doi: 10.1371/journal.ppat.1000474 PMID: 19521507

17. Enomoto Y, Bharti A, Khaleque AA, Song B, Liu C, Apostolopoulos V, et al. Enhanced immunogenicity of heat shock protein 70 peptide complexes from dendritic cell-tumor fusion cells. J Immunol. 2006; 177(9):5946–55. PMID: 17056519

18. Murshid A, Gong J, Calderwood SK. Purification, preparation, and use of chaperone-Peptide complexes for tumor immunotherapy. Methods Mol Biol. 2013; 960:209–17. doi: 10.1007/978-1-62703-218-6_17 PMID: 23329490

19. Hu J, Nakano H, Sakurai H, Colburn NH. Insufficient p65 phosphorylation at S536 specifically contributes to the lack of NF-kappaB activation and transformation in resistant JB6 cells. Carcinogenesis. 2004; 25(10):1991–2003. PMID: 15192014

20. Tuyt LM, Dokter WH, Birkenkamp K, Koopmans SB, Lummen C, Kruijer W, et al. Extracellular-regulated kinase 1/2, Jun N-terminal kinase, and c-Jun are involved in NF-kappa B-dependent IL-6 expression in human monocytes. J Immunol. 1999; 162(8):4893–902. PMID: 10202034

21. Akira S, Takeda K. Toll-like receptor signalling. Nature reviews Immunology. 2004; 4(7):499–511. PMID: 15229469

22. Zietara N, Lyszkiewicz M, Gekara N, Puchalka J, Dos Santos VA, Hunt CR, et al. Absence of IFN-beta impairs antigen presentation capacity of splenic dendritic cells via down-regulation of heat shock protein 70. J Immunol. 2009; 183(2):1099–109. doi: 10.4049/jimmunol.0803214 PMID: 19581626

23. Wang S, Villablanca EJ, De Calisto J, Gomes DC, Nguyen DD, Mizoguchi E, et al. MyD88-dependent TLR1/2 signals educate dendritic cells with gut-specific imprinting properties. J Immunol. 2011; 187(1):141–50. doi: 10.4049/jimmunol.1003740 PMID: 21646294

24. O'Neill L. The Toll/interleukin-1 receptor domain: a molecular switch for inflammation and host defence. Biochem Soc Trans. 2000; 28(5):557–63. PMID: 11044374

25. Kawai T, Adachi O, Ogawa T, Takeda K, Akira S. Unresponsiveness of MyD88-deficient mice to endotoxin. Immunity. 1999; 11(1):115–22. PMID: 10435584

26. Watanabe S, Kumazawa Y, Inoue J. Liposomal Lipopolysaccharide Initiates TRIF-Dependent Signaling Pathway Independent of CD14. PLoS One. 2013; 8(4):e60078. doi: 10.1371/journal.pone.0060078 PMID: 23565187

27. Zhu Q, Egelston C, Vivekanandhan A, Uematsu S, Akira S, Klinman DM, et al. Toll-like receptor ligands synergize through distinct dendritic cell pathways to induce T cell responses: implications for vaccines. Proc Natl Acad Sci U S A. 2008; 105(42):16260–5. doi: 10.1073/pnas.0805325105 PMID: 18845682

28. Fitzgerald KA, Rowe DC, Barnes BJ, Caffrey DR, Visintin A, Latz E, et al. LPS-TLR4 signaling to IRF-3/7 and NF-kappaB involves the toll adapters TRAM and TRIF. J Exp Med. 2003; 198(7):1043–55. PMID: 14517278

29. Uto T, Wang X, Sato K, Haraguchi M, Akagi T, Akashi M, et al. Targeting of antigen to dendritic cells with poly(gamma-glutamic acid) nanoparticles induces antigen-specific humoral and cellular immunity. J Immunol. 2007; 178(5):2979–86. PMID: 17312143

30. Toshchakov VU, Basu S, Fenton MJ, Vogel SN. Differential involvement of BB loops of toll-IL-1 resistance (TIR) domain-containing adapter proteins in TLR4- versus TLR2-mediated signal transduction. J Immunol. 2005; 175(1):494–500. PMID: 15972684

31. Mayor S, Riezman H. Sorting GPI-anchored proteins. Nat Rev Mol Cell Biol. 2004; 5(2):110–20. PMID: 15040444

32. Sabharanjak S, Sharma P, Parton RG, Mayor S. GPI-anchored proteins are delivered to recycling endosomes via a distinct cdc42-regulated, clathrin-independent pinocytic pathway. Dev Cell. 2002; 2(4):411–23. PMID: 11970892

33. Lingwood D, Kaiser HJ, Levental I, Simons K. Lipid rafts as functional heterogeneity in cell membranes. Biochem Soc Trans. 2009; 37(Pt 5):955–60. doi: 10.1042/BST0370955 PMID: 19754431

34. Wang XY, Facciponte J, Chen X, Subjeck JR, Repasky EA. Scavenger receptor-A negatively regulates antitumor immunity. Cancer Res. 2007; 67(10):4996–5002. PMID: 17510431

35. Todt JC, Hu B, Curtis JL. The scavenger receptor SR-A I/II (CD204) signals via the receptor tyrosine kinase Mertk during apoptotic cell uptake by murine macrophages. J Leukoc Biol. 2008; 84(2):510–8. doi: 10.1189/jlb.0307135 PMID: 18511575

36. Pfistershammer K, Klauser C, Leitner J, Stockl J, Majdic O, Weichhart T, et al. Identification of the scavenger receptors SREC-I, Cla-1 (SR-BI), and SR-AI as cellular receptors for Tamm-Horsfall protein. J Leukoc Biol. 2008; 83(1):131–8. PMID: 17928461

37. Beauvillain C, Meloni F, Sirard JC, Blanchard S, Jarry U, Scotet M, et al. The scavenger receptors SRA-1 and SREC-I cooperate with TLR2 in the recognition of the hepatitis C virus non-structural protein 3 by dendritic cells. J Hepatol. 2010; 52(5):644–51. doi: 10.1016/j.jhep.2009.11.031 PMID: 20338659

38. Mayor S, Sabharanjak S, Maxfield FR. Cholesterol-dependent retention of GPI-anchored proteins in endosomes. Embo J. 1998; 17(16):4626–38. PMID: 9707422

39. Rajendran L, Simons K. Lipid rafts and membrane dynamics. J Cell Sci. 2005; 118(Pt 6):1099–102. PMID: 15764592

40. Husebye H, Halaas O, Stenmark H, Tunheim G, Sandanger O, Bogen B, et al. Endocytic pathways regulate Toll-like receptor 4 signaling and link innate and adaptive immunity. EMBO J. 2006; 25(4):683–92. PMID: 16467847

41. Gioannini TL, Teghanemt A, Zhang D, Coussens NP, Dockstader W, Ramaswamy S, et al. Isolation of an endotoxin-MD-2 complex that produces Toll-like receptor 4-dependent cell activation at picomolar concentrations. Proc Natl Acad Sci U S A. 2004; 101(12):4186–91. PMID: 15010525

42. da Silva Correia J, Soldau K, Christen U, Tobias PS, Ulevitch RJ. Lipopolysaccharide is in close proximity to each of the proteins in its membrane receptor complex. transfer from CD14 to TLR4 and MD-2. J Biol Chem. 2001; 276(24):21129–35. PMID: 11274165

43. Hoebe K, Georgel P, Rutschmann S, Du X, Mudd S, Crozat K, et al. CD36 is a sensor of diacylglycerides. Nature. 2005; 433(7025):523–7. PMID: 15690042

44. Berwin B, Delneste Y, Lovingood RV, Post SR, Pizzo SV. SREC-I, a type F scavenger receptor, is an endocytic receptor for calreticulin. J Biol Chem. 2004; 279(49):51250–7. PMID: 15371419

45. Berwin B, Hart JP, Rice S, Gass C, Pizzo SV, Post SR, et al. Scavenger receptor-A mediates gp96/ GRP94 and calreticulin internalization by antigen-presenting cells. Embo J. 2003; 22(22):6127–36. PMID: 14609958

46. Theriault JR, Adachi H, Calderwood SK. Role of scavenger receptors in the binding and internalization of heat shock protein 70. J Immunol. 2006; 177(12):8604–11. PMID: 17142759

47. Facciponte JG, Wang XY, Subjeck JR. Hsp110 and Grp170, members of the Hsp70 superfamily, bind to scavenger receptor-A and scavenger receptor expressed by endothelial cells-I. Eur J Immunol. 2007; 37(8):2268–79. PMID: 17615582

48. Chen Y, Wermeling F, Sundqvist J, Jonsson AB, Tryggvason K, Pikkarainen T, et al. A regulatory role for macrophage class A scavenger receptors in TLR4-mediated LPS responses. Eur J Immunol. 2010; 40(5):1451–60. doi: 10.1002/eji.200939891 PMID: 20162551

49. Murshid A, Gong J, Calderwood SK. The role of heat shock proteins in antigen cross presentation. Front Immunol. 2012; 3:63. doi: 10.3389/fimmu.2012.00063 PMID: 22566944

50. Yi H, Guo C, Yu X, Gao P, Qian J, Zuo D, et al. Targeting the immunoregulator SRA/CD204 potentiates specific dendritic cell vaccine-induced T-cell response and antitumor immunity. Cancer Res. 2013; 71(21):6611–20.

51. Zuo D, Yu X, Guo C, Wang H, Qian J, Yi H, et al. Scavenger receptor A restrains T-cell activation and protects against concanavalin A-induced hepatic injury. Hepatology. 2011; 57(1):228–38.

52. Guo C, Yi H, Yu X, Hu F, Zuo D, Subjeck JR, et al. Absence of scavenger receptor A promotes dendritic cell-mediated cross-presentation of cell-associated antigen and antitumor immune response. Immunol Cell Biol. 2012; 90(1):101–8. doi: 10.1038/icb.2011.10 PMID: 21383767

53. Yu X, Yi H, Guo C, Zuo D, Wang Y, Kim HL, et al. Pattern recognition scavenger receptor CD204 attenuates Toll-like receptor 4-induced NF-kappaB activation by directly inhibiting ubiquitination of tumor necrosis factor (TNF) receptor-associated factor 6. J Biol Chem. 2011; 286(21):18795–806. doi: 10.1074/jbc.M111.224345 PMID: 21460221

54. Calderwood SK, Murshid A, Gong J. Heat shock proteins: conditional mediators of inflammation in tumor immunity. Front Immunol. 2012; 3:75. doi: 10.3389/fimmu.2012.00075 PMID: 22566956

55. Asea A, Kraeft SK, Kurt-Jones EA, Stevenson MA, Chen LB, Finberg RW, et al. HSP70 stimulates cytokine production through a CD14-dependant pathway, demonstrating its dual role as a chaperone and cytokine. Nat Med. 2000; 6(4):435–42. PMID: 10742151